Membrane Trafficking Pathways in the Production and Clearance of the Alzheimer's Disease Aβ Peptide in Neurons and in Microglia

---

Dissertation

zur

Erlangung der naturwissenschaftlichen Doktorwürde

(Dr. sc. nat.)

vorgelegt der

Mathematisch-naturwissenschaftlichen Fakultät

der

Universität Zürich

von

Vinod Udayar

aus Indien

Promotionskommission

Prof. Dr. Lawrence Rajendran (Leitung der Dissertation)
Prof. Dr. Martin Schwab (Vorsitz)
Prof. Dr. Esther Stoeckli

Zurich, 2018

Membrane Trafficking Pathways in the Production and Clearance of the Alzheimer's Disease Aβ Peptide in Neurons and in Microglia

Dissertation

zur

Erlangung der naturwissenschaftlichen Doktorwürde

(Dr. sc. nat.)

vorgelegt der

Mathematisch-naturwissenschaftlichen Fakultät

der

Universität Zürich

von

Vinod Udayar

aus Indien

Promotionskommission

Prof. Dr. Lawrence Rajendran (Leitung der Dissertation)
Prof. Dr. Martin Schwab (Vorsitz)
Prof. Dr. Esther Stoeckli

Zurich, 2018

Summary

Alzheimer's Disease (AD) is the most common cause of dementia, accounting for as much as 80 % of all dementia cases, estimated to affect over 46 million people worldwide. AD is a disease that robs affected individuals of memory and cognition that affects both the individual and the family and friends – without any cure at sight, AD is also one of the most costliest and deadliest disease. It is characterized by progressive neurodegeneration which results in substantial neuron loss and brain atrophy explaining the cognitive decline and memory problems. Behavioral symptoms manifest as memory lapses and subtle personality changes in early-stage AD and progress to profound cognitive and memory decline in late-stage AD. Lack of curative therapy for AD after more than 100 years since its first description can at least in part be attributed to its complex etiology. In the last three decades, significant progress has been made in understanding the genetic, biochemical and molecular basis of the disease. These advancements have yielded a few therapeutic options that are under clinical trials, which are designed to delay progression and eventually cure the disease. Nevertheless, we still have not pinpointed the exact cause/causes for AD so that we can develop definitive cures for the disease. My thesis aims to understand the role of membrane trafficking pathways in regulation of Aβ levels and thereby the potential patho-mechanisms that underlie both the familial/early and late-onset AD (LOAD).

Studies on Familial AD (FAD) mutations have proven beyond doubt that excessive Aβ production is the driver of the pathogenesis observed in FAD. However, with an absence of such mutations, the causal factor of amyloid accumulation in LOAD has remained unidentified. Evidences suggest that impaired amyloid clearance could be the cause of amyloid build-up in LOAD. By applying cell and systems biology techniques I set out to investigate this at the cellular level. Using state-of-the-art screens, I identified Rab11 as a novel positive regulator of Aβ production through regulation of recycling endosomes. In addition, I also discovered a critical role for lysosomes in clearance of Aβ levels. Through the findings on Rab7 and Presenilin-2, I demonstrate that the lysosomal pathway is the major route for Aβ degradation. Based on this study, I propose that in LOAD the lysosomal pathway is critically vulnerable and that, environmental or genetic factors targeting the lysosomal pathway can significantly contribute to LOAD risk.

Rab11: a novel regulator for Aβ production

How neurons use their membrane trafficking to release neurotransmitters, growth factors or how they internalize nutrients is fairly well known. We hypothesized, that since most of the players in Aβ production are membrane associated, membrane trafficking in the cells should play an important role in Alzheimer's disease. To identify trafficking pathways that regulate Aβ, we performed a screen where we deleted all the Rab-GTPases in human genome and assessed their influence on the levels of Aβ. We identified Rab11 as the top positive regulators of Aβ levels. Mechanistic characterization revealed that Rab11 regulated the endosomal recycling of β-secretase, the first enzyme in the Aβ production pathway, to the plasma membrane without affecting APP trafficking. My results show that normally β-secretase is replenished to the cell-surface from where it is re-internalized for successive rounds of Aβ production in a Rab11 dependent manner. Absence of Rab11 thus impaired this cycle and reduced Aβ levels. Interestingly, exome sequencing revealed a significant genetic association of a Rab11A variant with late-onset AD patients, and protein interaction-network analysis identified Rab11 as a component of the late-onset AD risk network, suggesting a causal link between Rab11 and AD. By integrating these findings to existing literature on Rab function a "roadmap" for Aβ metabolism was created that illustrates that the membrane trafficking process is a complex process that regulates Aβ production.

Rab7: a novel regulator for Aβ clearance

Aβ levels are determined not just by production but through clearance mechanisms as well. In FAD, specific genetic mutations increase the production of Aβ peptide but in the late-onset AD, evidence suggests that its clearance may play the crucial role. So, what are the cellular mechanisms that affect clearance of Aβ? After having identified membrane trafficking regulators that are involved in Aβ production, I focussed on screening for trafficking regulators involved in Aβ clearance. An RNAi screen for all Rab-GTPases in a microglial cell line (BV2) identified Rab7 as a novel regulator of Aβ clearance. Microglia are resident macrophages of the brain and involved in the clearance of Aβ that is produced by neurons. Rab7 silencing in BV2 microglia led to a significant increase in Aβ uptake. Mechanistically, although Rab7 silencing increased Aβ uptake, the engulfed Aβ was shown to be accumulating in enlarged vesicles, reminiscent of lysosomes. Rab7 silencing perturbed the normal distribution of lysosomes and reduced lysosomal enzymatic activity, a key indicator of lysosomal function. Rab7 silencing impaired lysosomal clearance and thus increased overall protein aggregates in these cells. Interestingly, Rab7 silencing also increased total-tau

and phospho-tau levels in primary neurons. This indicates that both Aβ and tau can be degraded intracellularly by the lysosomal pathway and validates the relevance of this pathway in AD pathogenesis. Since the lysosomal pathway is linked to autophagy and nutrient sensing, our results suggest that nutrient intake and metabolism could affect Alzheimer's disease risk.

PS2: an unexpected negative regulator of Aβ levels

The role of the lysosomal degradation pathway in the regulation of Aβ levels and its importance in AD was further reinforced by findings on presenilin 2 (PS2), which constitutes one of the two possible catalytic subunits of the γ-secretase complex. In an unbiased genome-wide RNAi screen for human proteases, we unexpectedly identified PS2 as a negative regulator of Aβ levels. In the AD field, PS2 is often considered as the "insignificant cousin" of PS1, which is regarded as the main catalytic component of γ-secretase and which has over 200 mutations associated with FAD. Similarly, albeit in lower numbers, PS2 also has mutations that are associated with FAD, thus making PS1 and PS2 both positively involved in AD risk. However, my results now identify a completely novel function for PS2 in that it is involved in Aβ clearance through the lysosomal pathway. PS2 deficiency reduced both lysosomal number and function (increased lysosomal pH) and thus impaired Aβ degradation. We asked whether the increased lysosomal pH observed upon PS2 silencing was due to the dysregulation of lysosomal Ca^{2+} levels. Indeed, PS2 depletion reduced the lysosomal Ca^{2+} levels in a TRPML1-dependent manner and this led to an increase in lysosomal pH. Since, microglia are the main cell-type that degrade Aβ in the brain we next asked whether PS2 is also important in regulating lysosomal function and Aβ degradation in microglia. Indeed, PS2 depletion in BV2 microglia reduced lysosomal number and function and thus impaired Aβ degradation.

These results show, for the first time, that there is a functional dichotomy between the two presenilin paralogues, PS1 and PS2. While PS1 is largely responsible for Aβ production in the endosomes, PS2 controls Aβ clearance in lysosomes and thus contributes to homeostatic control of Aβ levels. Our results also suggest that disturbances in this homeostatic mechanism could affect Aβ accumulation and thus confer the risk to develop AD.

GSAP: a controversial regulator of Aβ production

A study in 2010 by He and colleagues reported the identification of a novel γ-secretase activating protein (GSAP). He and colleagues claimed that GSAP is processed from a holoprotein to a 16 kDa active form by a yet unidentified protease. They further observed that GSAP interacts with the γ-secretase complex to selectively regulate β-amyloid peptide generation from APP, without affecting Notch cleavage. This was an exciting finding in the field as inhibiting GSAP or the protease that cleaves full-length GSAP provided an opportunity to inhibit γ-secretase and Aβ production without interfering with Notch cleavage. Many of the side-effects observed in clinical trials for γ-secretase inhibitor were attributed to its inhibition of Notch cleavage. Thus, replicating this important finding about GSAP and identifying the protease that cleaves GSAP was an exciting opportunity.

To our surprise, I found that processing of GSAP is not required for Aβ production. In fact, I did not observe any cleaved GSAP product in multiple cell lines, including the ones tested by He and colleagues – thus we failed to replicate their main findings. Mechanistically, we found out that rather than specifically regulating γ-cleavage of APP, GSAP regulated the levels of full length APP. This was further supported from our observation that GSAP silencing affected APP processing by all three proteases, i.e., α, β- and γ-secretases. This effect on the processing is likely due to reduced APP levels and not because of GSAP's effect on the secretases. He and colleagues also showed that imatinib, an anti-cancer drug, reduced Aβ levels by inhibiting the GSAP-γ-secretase interaction. We on the other hand observed that imatinib reduced Aβ levels even in the absence of GSAP. Other studies that support our findings have also been published since then confirming our failure to replicate these. The exact mechanism of how GSAP regulates APP levels is not clear yet. Nevertheless, our results caution the validity of GSAP as a therapeutic target in Alzheimer's disease and reflect on the necessity of independent replication of scientific observations.

Collectively, our studies on membrane trafficking and Aβ metabolism have identified several novel regulators of Aβ levels both at the level of production as well as for clearance. These findings will help to bridge some of the knowledge gaps in AD pathogenesis and potentially open new therapeutic avenues and prevention strategies. Our studies also demonstrate the importance of systems cell biology-based investigation in unraveling the molecular complexity of AD. Lastly, the study on GSAP and Aβ reinforce the importance of robust validation and of reproducibility in science. As my personal contribution to enhance data

visibility and thereby facilitate reproducibility in science I have published all my articles in open access journals

Zusammenfassung

Die Alzheimer Krankheit (Alzheimer Demenz; AD) ist die häufigste Form der Demenz und umfasst ca. 80% aller Demenzfälle. Nach derzeitigen Schätzungen leben über 46 Millionen Menschen weltweit mit Demenz. AD ist gekennzeichnet durch eine fortschreitende Neurodegeneration, welche zu ausgeprägtem Hirnschwund und Verlust kognitiver Funktionen führt. Verhaltenstechnisch manifestiert sich die Krankheit in der frühen Phase in gelegentlichen Gedächtnisproblemen und leichten Persönlichkeitsänderungen, welche in der späteren Phase zu einem zunehmenden Verfall der kognitiven Fähigkeiten und der Gedächtnisleistung voranschreiten. Das Fehlen einer kurativen Therapie über 100 Jahre nach der ersten Beschreibung des Krankheitsbildes kann zumindest teilweise der komplexen Ätiologie der Alzheimer Krankheit zugeschrieben werden. In den vergangenen drei Jahrzehnten wurden bedeutende Fortschritte im Verständnis der genetischen, zellulären und molekularen Grundlagen der Krankheit gemacht. Diese Fortschritte haben bereits einige therapeutische Ansätze hervorgebracht, welche in klinischen Studien getestet wurden mit der Hoffnung, den Krankheitsverlauf zu verlangsamen und letztendlich die Krankheit zu heilen. Jedoch wurde die genaue Ursache für AD noch immer nicht identifiziert, auf deren Basis wir eine definitive Heilmethode entwickeln könnten. Meine Doktorarbeit hat zum Ziel, die Rolle der Signalwege des Membrantransports für die Regulierung der Aβ Mengen zu erforschen und darauf aufbauend die möglichen Pathomechanismen, welche der familiären/frühen Form von AD (FAD) und der sporadischen/späten Form (*late-onset* Alzheimer Demenz; LOAD) zugrunde liegen, besser zu verstehen.

Die Erforschung von Mutationen, welche die familiäre Form der Alzheimer Krankheit (FAD) verursachen, haben zweifelsfrei belegt, dass eine übermässige Produktion von Aβ der wichtigste Pathomechanismus in FAD ist. Solche Mutationen fehlen jedoch in LOAD und der kausale Faktor für die Akkumulation von Amyloid ist hier noch nicht identifiziert. Forschungsergebnisse deuten darauf hin, dass ein beeinträchtigter Abbau von Amyloid die Ursache für dessen Anhäufung in LOAD sein könnte. Mittels zellbiologischer und systembiologischer Techniken begann ich daher, dies auf zellulärer Ebene genauer zu untersuchen. In einem Screening für Proteine des Membrantransportes, welche Aβ regulieren, identifizierte ich Rab11 als einen neuen positiven Regulator der Aβ Produktion. Ergebnisse zu Rab7 und PS2 zeigen ausserdem, dass der lysosomale Verdau der Hauptweg für den intrazellulären Abbau von Aβ ist. Unsere Ergebnisse lassen vermuten, dass der lysosomale Signalweg in LOAD eine wichtige Rolle spielen könnte und dass Umweltfaktoren oder

genetische Faktoren, die den lysosomalen Abbauweg beeinträchtigen, signifikant zum LOAD Risiko beitragen könnten.

Rab11: Ein neuer Regulator der Aβ Produktion

Es ist bereits recht gut untersucht wie Nervenzellen ihren Membrantransport nutzen um Neurotransmitter und Wachstumsfaktoren freizusetzen oder um die Nährstoffaufnahme zu regulieren. Da die meisten Proteine, die an der Produktion von Aβ beteiligt sind, Membran-assoziiert sind, stellten wir die Hypothese auf, dass der Membrantransport in den Zellen eine wichtige Rolle in der Alzheimer Krankheit spielt.

Um Transportwege zu identifizieren welche Aβ regulieren führten wir in einem AD Zell-Modell ein RNAi-Screening für alle Rab-GTPasen im humanen Genom durch und analysierten deren Effekte auf die Aβ Menge. Wir identifizierten Rab11 als wichtigsten positiven Regulator des Aβ-Spiegels. Eine mechanistische Charakterisierung zeigte, dass Rab11 das endosomale Recycling der β-Sekretase, dem ersten Enzym in der Aβ Produktion, reguliert, ohne den Transport von APP zu beeinflussen. Meine Ergebnisse zeigen, dass die β-Sekretase normalerweise an die Zelloberfläche zurücktransportiert wird, von wo aus sie in einer Rab11-abhängigen Weise erneut internalisiert wird und für weitere Runden der Aβ-Produktion zur Verfügung steht. Der Knockdown von Rab11 beeinträchtigte diesen Zyklus und reduzierte somit den Aβ-Spiegel. Interessanterweise zeigte eine Exom-Sequenzierung eine signifikante genetische Assoziation einer Rab11A-Variante mit LOAD, und eine Proteininteraktions-Netzwerkanalyse identifizierte Rab11 als Bestandteil des LOAD-Risikonetzwerks, was auf einen kausalen Zusammenhang zwischen Rab11 und AD hindeutet. Durch Integration unserer Ergebnisse in die bestehende Literatur zur Funktion von Rab-Proteinen wurde eine "Roadmap" für den Aβ-Metabolismus erstellt in welcher ersichtlich wird, dass der Membrantransport zur Regulation von Aβ einem komplexen Wegenetz folgt.

Rab7: Ein neuer Regulator des Aβ Abbaus

Aβ-Spiegel werden nicht nur durch die Produktion, sondern auch durch Abbaumechanismen bestimmt. Bei der früh einsetzenden Form der AD erhöhen genetische Mutationen die Produktion des Aβ-Peptids, aber in der späten Form der AD gibt es Hinweise darauf, dass der Abbau eine entscheidende Rolle spielt. Welches sind also die zellulären Mechanismen, die

den Abbau von Aβ beeinflussen? Nachdem ich Regulatoren des Membrantransports identifiziert hatte, die an der Aβ Produktion beteiligt sind, konzentrierte ich mich auf das Screening von Regulatoren, die am Aβ-Abbau beteiligt sind. Ein RNAi-Screening für alle Rab-GTPasen in einer Mikroglia-Zelllinie (BV2) identifizierte Rab7 als wichtigen Regulator des Aβ Abbaus. Mikroglia sind die Makrophagen des Gehirns und sind dort am Abbau von Aβ beteiligt, welches von Neuronen produziert worden ist. Rab7-Silencing in BV2-Mikroglia führte zu einem signifikanten Anstieg der Aβ-Aufnahme. Mechanistisch zeigte sich, dass das aufgenommene Aβ sich in vergrösserten Vesikeln ansammelte, welche Ähnlichkeit mit Lysosomen hatten. Lysosomen. Rab7-Silencing störte die normale Verteilung von Lysosomen und reduzierte die lysosomale Enzymaktivität, ein wichtiger Indikator der lysosomalen Funktion. Rab7-Silencing beeinträchtigte auf diese Weise den lysosomalen Abbau und erhöhte die Menge an Proteinaggregaten in diesen Zellen. Interessanterweise erhöhte der Knockdown von Rab7 auch die Menge an Tau-Protein und die Phospho-Tau-Konzentration in primären Neuronen. Dies deutet darauf hin, dass sowohl Aβ als auch Tau via den lysosomalen Weg intrazellulär abgebaut werden können, und bestätigt die Relevanz dieses Abbaumechanismus für die AD Pathogenese. Da der lysosomale Stoffwechselweg eine wichtige Rolle bei der Autophagie spielt und auch eng an die Nährstoffaufnahme gekoppelt ist legen unsere Ergebnisse nahe, dass Nährstoffaufnahme und Stoffwechsel das Alzheimer-Risiko beeinflussen könnten.

PS2: Ein unerwarteter negativer Regulator des Aβ-Spiegels

Die Bedeutung des lysosomalen Abbauweges für die Regulation des Aβ-Spiegels und seine Rolle in AD wurde weiter verdeutlicht durch Befunde zu Presenilin 2 (PS2), eine von zwei möglichen enzymatischen Untereinheiten des γ-Sekretase-Komplexes. In einem Genom-weiten RNAi-Screening für Proteasen identifizierte ich unerwarteterweise PS2 als einen negativen Regulator von Aβ. Im AD Forschungsfeld wird PS2 oft als "unbedeutender Cousin" von PS1 wahrgenommen, welches als funktionell bedeutendere katalytische Komponente der γ-Sekretase betrachtet wird, die über 200 mit FAD assoziierte Mutationen aufweist. Jedoch gibt es auch FAD Mutationen in PS2, wenn auch in geringerer Anzahl. Meine Ergebnisse zeigen nun eine völlig neue Funktion von PS2 in der Regulation von Aβ unter Beteiligung der Lysosomen. PS2-Silencing verringerte sowohl die Anzahl an Lysosomen als auch ihre Funktionstüchtigkeit (erhöhter lysosomaler pH-Wert) und beeinträchtigte damit den Abbau von Aβ. Ich untersuchte als nächstes, ob der erhöhte lysosomale pH-Wert, der beim PS2-Silencing beobachtet wurde, auf eine Dysregulation des

lysosomalen Ca^{2+}-Spiegels zurückzuführen sei. Tatsächlich reduzierte die PS2-Depletion die lysosomale Ca^{2+}-Konzentration in TRPML1-abhängiger Weise und dies führte zu einem Anstieg des lysosomalen pH-Wertes. Da der zelluläre Abbau von Aβ im Gehirn vor allem durch Mikroglia durchgeführt wird, untersuchte ich als nächstes, ob PS2 auch in Mikroglia für die Regulierung der lysosomalen Funktion und den Aβ Abbau wichtig ist. Tatsächlich reduzierte die PS2-Depletion auch in BV2-Mikroglia die lysosomale Zahl und Funktion und somit den Aβ Abbau. Diese Ergebnisse zeigen zum ersten Mal, dass es eine funktionelle Dichotomie zwischen den beiden Presenilin-Paralogen PS1 und PS2 gibt. Während PS1 hauptsächlich für die Aβ Produktion in den Endosomen verantwortlich ist, kontrolliert PS2 den Aβ Abbau in Lysosomen und trägt somit zur homöostatischen Kontrolle des Aβ-Spiegel bei. Unsere Ergebnisse deuten auch darauf hin, dass Störungen in diesem homöostatischen Mechanismus die Aβ Akkumulation beeinflussen könnten und somit ein Risiko für die Entwicklung von AD bergen.

GSAP: ein umstrittener Regulator der Aβ Produktion

Eine Studie von He und Kollegen aus dem Jahr 2010 berichtete über die Identifizierung eines neuen γ-Sekretase-aktivierenden Proteins (GSAP). Er und seine Kollegen behaupteten, dass GSAP von einer noch nicht identifizierten Protease aus einem Holoprotein zu einer aktiven 16 kDa-Form prozessiert wird. Sie beobachteten ferner, dass GSAP mit dem γ-Sekretase Komplex interagiert, um selektiv die Produktion von β-Amyloid Peptid aus APP zu regulieren, ohne die Prozessierung von Notch zu beeinflussen. Dies war ein spannender Befund, da die Hemmung von GSAP oder der Protease, welche das Holoprotein spaltet, eine Möglichkeit versprach, γ-Sekretase und damit die Aβ Produktion zu inhibieren, ohne die Spaltung von Notch zu stören. Viele der Nebenwirkungen, die in klinischen Studien für den γ-Sekretase-Inhibitor beobachtet wurden, wurden seiner hemmenden Wirkung auf die Notch-Spaltung zugeschrieben. Daher erschien die Replikation dieses wichtigen Befundes über GSAP und die Identifizierung der Protease, die GSAP spaltet, eine wichtige und spannende Aufgabe.

Zu meiner Überraschung zeigten meine Ergebnisse jedoch, dass die Spaltung von GSAP für die Aβ Produktion nicht erforderlich ist. Auch konnte ich kein GSAP-Spaltprodukt identifizieren, obwohl ich mehrere Zelllinien getestet habe, einschliesslich der von He und Kollegen verwendeten Linie. Ihre Haupterkenntnisse waren also nicht reproduzierbar.

Mechanistisch zeigte sich, dass GSAP nicht wie ursprünglich berichtet spezifisch die Spaltung von APP durch γ-Sekretase reguliert, sondern die Menge an APP selbst beeinflusste. Dies wurde zudem durch unsere Beobachtung gestützt, dass GSAP-Silencing die APP-Verarbeitung durch alle drei Proteasen, d.h. α-, β- und γ-Sekretasen, beeinflusste. Dieser Effekt auf die Verarbeitung ist höchstwahrscheinlich auf die verringerten APP-Level zurückzuführen und nicht auf die Wirkung von GSAP auf die Sekretasen. He und seine Kollegen zeigten auch, dass Imatinib, ein Anti-Krebs-Medikament, Aβ-Spiegel durch Hemmung der GSAP-γ-Sekretase-Interaktion reduzierte. Wir haben jedoch beobachtet, dass Imatinib die Aβ-Spiegel sogar in Abwesenheit von GSAP reduziert. In der Zwischenzeit wurden weitere Studien veröffentlicht, welche unsere Ergebnisse stützen. Der genaue Mechanismus, über welchen GSAP den APP-Spiegel reguliert, ist noch nicht klar. Nichtsdestotrotz lassen unsere Ergebnisse Zweifel an der Validität von GSAP als therapeutisches Target für die Alzheimer Krankheit aufkommen und sie verdeutlichen die Notwendigkeit einer unabhängigen Replikation von wissenschaftlichen Beobachtungen.

Zusammenfassend haben unsere Studien zum Membrantransport und zum Aβ-Metabolismus mehrere neue Regulatoren von Aβ identifiziert, sowohl auf Ebene der Produktion als auch beim Abbau. Diese Ergebnisse tragen dazu bei einen Teil der Wissenslücke hinsichtlich der Pathogenese von AD zu schliessen und eröffnen möglicherweise neue therapeutische Targets und Präventionsstrategien. Unsere Studien zeigen auch, wie wichtig Systembiologie-basierte Untersuchungen zur Aufklärung der molekularen Komplexität von AD sind. Weiterhin verdeutlichen die Studien zu GSAP und Aβ die Bedeutung einer robusten Validierung wissenschaftlicher Ergebnisse. Als persönlichen Beitrag zur Verbesserung der Datensichtbarkeit und zur Erleichterung der Reproduzierbarkeit in der Wissenschaft habe ich alle meine Artikel in Open-Access-Zeitschriften veröffentlicht.

Table of Contents

Summary……III

Zusammenfassung……...VIII

1. Introduction……1
1.1 Introduction to Alzheimer's disease (AD)……...1
1.2 Anatomical and pathological characteristics of the disease……1
1.3 Molecular basis of the disease……..2
1.3.1 Amyloid pathology……...2
1.3.2 Amyloid production…….....2
1.3.2.1 Amyloid precursor protein…….3
1.3.2.2 β-Secretase…….4
1.3.2.3 γ –Secretase……5
1.3.3 Amyloid Clearance……...5
1.3.3.1 Enzymatic degradation of Aβ……...6
1.3.3.2 Efflux mechanisms to clear Aβ out of the brain……...7
1.3.3.2.1 Efflux across the blood brain barrier……7
1.3.3.2.2 Efflux through the interstitial fluid bulk-flow……..8
1.3.4 Tau pathology……...8
1.3.4.1 Structure and function……..8
1.3.4.2 Phosphorylation and de-phosphorylation mechanisms……9
1.3.4.3 Tau mutations…….10
1.3.4.4 Homeostatic control of Tau levels……..10
1.4 Cellular basis of the disease…….11
1.4.1 Neuronal contribution…….11
1.4.1.1 Production pathways…….11
1.4.1.1.1 Role of membrane trafficking in production of Aβ…….11
1.4.1.1.2 Early and recycling endosomes in the production of Aβ…….12
1.4.1.1.3 Aβ release mechanisms……13
1.4.1.2 Clearance pathways – Intracellular lysosomal proteolysis in amyloid clearance…….13
1.4.2 Microglial contribution……14

1.4.2.1 Role of phagocytosis in the removal of amyloid……....14
1.4.2.2 Role of phagocytosis in synaptic pruning and synapse loss……...15
1.4.2.3 Regulation of microglial clearance mechanisms……15
1.4.3 Synaptic pathology……16
1.5 Genetic basis of the disease……..16
1.5.1 Familial AD……16
1.5.1.1 APP mutations……..17
1.5.1.1.1 Disease causing mutations……..17
1.5.1.1.2 Protective mutations……....17
1.5.1.2 Presenilin mutations……..18
1.5.2 Late-onset AD……18
1.5.2.1 Genome Wide Association Studies (GWAS) on LOAD……..19
1.5.2.2 Mutations in the neuroinflammation/microglial function-related genes..19
1.5.2.3 Mutations in the membrane trafficking related genes……...20
1.6 Biomarkers of AD……20
1.6.1 Aβ and Tau-based biomarkers……20
1.6.2 Synaptic markers……21
1.6.3 Systems biology-driven biomarker profiles……22
1.7 Therapeutic strategies……....23
1.7.1 Current status……..23
1.7.2 Therapies based on novel insights into membrane trafficking in AD……24
1.8 Systems biology approaches to understand membrane trafficking complexity in AD….25
1.8.1 Rabs GTPase……26
1.8.2 RNAi-screens……27
1.8.3 Multiplexing assays to screen for regulators of Aβ production and clearance….28

2. Objectives of the thesis……...29

3. Chapter 1: A paired RNAi and RabGAP overexpression screen identifies Rab11 as a regulator of β-amyloid production.
(Udayar et al., Cell Reports, 2013)……30

4. Chapter 2: RNAi screen of genome wide Rab-GTPases identifies Rab7 as a novel regulator of Aβ clearance……...80

5. Chapter 3: The Alzheimer's disease Presenilin-2 regulates lysosomal degradation pathway and Aβ clearance…….95

6. Chapter 4: γ-Secretase Activating Protein (GSAP) does not specifically regulate γ-cleavage of APP but regulates APP levels in HeLa cells.
(Udayar & Rajendran, Matters, 2016; Udayar & Rajendran, Matters Select, 2016)……..137

7. Outlook……..165

8. Abbreviations……169

9. References…….171

10. Originality report…….....195

11. Acknowledgements…….196

12. Curriculum vitae…….……..……..197

1. Introduction

1.1 Introduction to Alzheimer's disease (AD)

Alzheimer's disease (AD) is the most prevalent form of dementia. It is a progressive neurodegenerative disorder that is characterized by significant loss in cognition and intellectual capacity and affects millions of people the world over. In 1906, Alois Alzheimer, the German psychiatrist after whom the disease is named, first described the disease based on his observation of a 55-year old female patient (Alzheimer et al., 1995). AD has become one of the most pressing health issues in western countries and, as life expectancy continues to rise, the number of people affected by this devastating disease is poised to increase significantly in the near future (Pfeil et al., 2012; Prince et al., 2016). More than 5% of the elderly population aged 65 years or above suffer from AD. In the year 2000, this level of prevalence represented a total of 4.5 million affected individuals in the US alone (Hebert et al., 2003). According to more recent findings, in 2011, prevalence of AD in Switzerland in people above the age of 64 was almost 8% (Pfeil et al., 2012). The likelihood of developing AD rises sharply with increasing age, doubling approximately every 5 years over the age of 65 and affecting almost one fifth of elderly people aged 85 years or above (Prince et al., 2016). Early symptoms of AD are frequently hard to distinguish from normal age-related cognitive dysfunction and include memory loss and problems in retaining and recalling recently acquired information. Transition from mild to moderate AD is characterized by an increase in severity of existing symptoms that includes progressive memory impairment, cognitive dysfunction and a progressive deterioration of language function. In the terminal stages of the disease, the decline in cognitive performance is so severe that patients need assistance even for the most routine activities (Winblad et al., 2016). The diagnosis for AD is based on a detailed analysis of the clinical history along with physical (including neuroimaging) and neuropsychological analysis of the patient. Although, in recent years there has been a vast improvement in the accuracy of diagnosis, a definitive diagnosis for AD is only possible upon analysis of post-mortem brain tissue. Since the exact etiology of AD is currently unknown, curative drugs are difficult to develop. The current focus of treatment for AD is to slow the progression of symptoms and improve cognition.

1.2 Anatomical and pathological characteristics of the disease

AD is characterised by the selective damage in brain areas important for cognition and memory. Earliest alterations in AD affect the regions involved in episodic memory, specifically, in the hippocampus and entorhinal cortex (Braak and Braak, 1991). In the

damaged areas of an AD brain, the dysfunction and loss of neurons is associated with characteristic pathological hallmarks that increases the vulnerability of these regions. These pathological hallmarks are presence of extracellular proteinaceous deposits called amyloid plaques and intraneuronal cytoskeletal structures known as neurofibrillary tangles (NFTs) (Braak and Braak, 1991; Rogers and Friedman, 2008; Serrano-Pozo et al., 2011). Specifically, amyloid deposition is observed in the regions of the default mode network, regions thought to be active in terms of basal synaptic activity, thus tying synaptic activity and amyloid deposition (Sperling et al., 2009).

1.3 Molecular basis of the disease

1.3.1 Amyloid pathology

Amyloid pathology is characterized by the presence of extracellular neuritic plaques composed predominantly of amyloid β (Aβ). It is found abundantly in the amygdala, hippocampus and neocortex in AD brain. Apart from extracellular plaques, amyloid deposition in AD also occurs frequently within cerebral vessels and is known as cerebral amyloid angiopathy (CAA) (Selkoe, 2001). Based on analysis of post-mortem brains it was observed that more than 80% of AD patients have Aβ within blood vessel. Specifically, small arterioles, capillaries and venules in the cerebral cortex often contain amyloid deposits (Serrano-Pozo et al., 2011).

1.3.2 Amyloid production

Amyloid plaques predominantly consist of a peptide termed β-amyloid (Aβ). It is present either in its soluble monomeric/oligomeric conformation or in the insoluble plaque form and is causally associated to the neurodegeneration observed in AD. Therefore, studying the processes that regulate amyloid peptide formation is critical for our understanding of AD. Aβ is produced from a membrane protein called Amyloid precursor protein (APP) by the action of two secretases. During the production of Aβ, APP is first cleaved by β-site amyloid precursor protein cleaving enzyme 1 (BACE1), also known as β-secretase. This is followed by cleavage by another secretase complex known as the γ-secretase (Figure1).

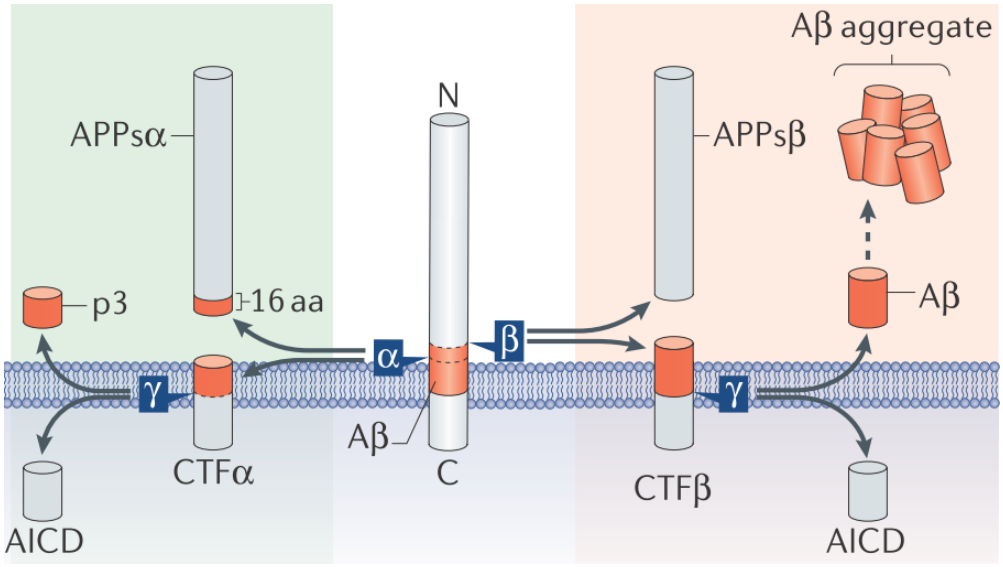

Figure 1: APP processing. APP undergoes cleavage by α-secretase to release sAPPα and αCTF, in the non-amyloidogenic pathway (left, in green). APP undergoes cleavage by β-secretase to generate sAPPβ and βCTF in the amyloidogenic pathway (right, in red). In the amyloidogenic pathway, βCTF is cleaved by γ-secretase to generate Aβ peptide (adapted from Müller et al., 2017).

1.3.2.1 Amyloid precursor protein

Amyloid precursor protein (APP) is a type 1 transmembrane protein, with a large extracellular domain, and is widely expressed in the brain at high levels. APP mRNA can undergo alternative splicing to generate many isoforms, of which the 695 amino acid form (APP695) is the predominant isoform in the brain (Bayer et al., 1999). APP is involved in a diverse range of biological functions that include nervous system development, synaptic function and plasticity, and cell survival among others (Muller et al., 2017). APP is produced in the endoplasmic reticulum (ER) and it undergoes maturation (glycosylation) in the Golgi complex. It is then routed to the plasma membrane from where it is endocytosed into endosomes (Small and Gandy, 2006). Several studies have shown that APP gets cleaved by β-secretase predominantly in endosomes and that endocytosis of APP and β-secretase is a key determinant for Aβ production (Kinoshita et al., 2003; Rajendran et al., 2006; Sannerud et al., 2011). The endosome with its low pH (pH 5.0-6.0) provides an optimal environment for β-secretase activity, which reflects the dependence of Aβ production on endocytosis. APP can also be cleaved by another secretase, known as α-secretase. α-secretase cleavage of APP prevents the production of the toxic Aβ peptide and the cleavage has been shown to occur at the plasma membrane (Lichtenthaler, 2011).It is generally accepted that APP cleavage by γ-secretase to generate Aβ also occurs in post-golgi compartments, i.e in endosomes.

1.3.2.2 β-secretase

In 1999, some years after APP processing was characterized, several groups independently discovered that the β-secretase activity for APP cleavage is conferred by the β-site amyloid precursor protein cleaving enzyme 1 (BACE1) (Sinha et al., 1999; Vassar et al., 1999; Yan et al., 1999). BACE1 is a transmembrane protein that belongs to the pepsin-like family of aspartyl proteases. BACE1 exhibits all the properties of a luminal protease that can cleave APP at the extracellular ectodomain and cleavage of APP by BACE1 was found necessary for the generation of Aβ peptide (Vassar et al., 2009). BACE1 is ubiquitously expressed even though its activity is highest in the brain. In vivo studies with APPTg/BACE1KO bigenic mice provided further proof that BACE1 activity is indeed necessary for Aβ production and development of amyloid pathology in the APPTg mice (Luo et al., 2001; Ohno et al., 2004). Identification of a familial AD associated mutation, known as the Swedish mutation (APPsw), that results in massive increase in the affinity of APP to BACE1 further cemented BACE1's status as the major β-secretase involved in Aβ production and AD (Citron et al., 1992). BACE1 is localized in many different organelles, but its activity is reported to be highest in Golgi and endosomes, organelles that have an acidic pH and thus provide optimal environment for BACE1 activity. This organelle-dependent variation in BACE1 activity can be regulated by pathways that regulate BACE1 trafficking. Interestingly, BACE1 has a dileucine motif in its transmembrane domain, which is crucial for its internalization into endosomes. BACE1 trafficking and subcellular localization via its dileucine binding motif is regulated by proteins belonging to the GGA family (He et al., 2005; von Arnim et al., 2006).Due to is central role in Aβ production, contribution of BACE1 to amyloid pathology in AD has been intensely studied. Studies have shown that BACE1 levels in the brain increase with age and stress (Fukumoto et al., 2004; Velliquette et al., 2005). It is important to note that aging is the biggest risk factor for sporadic AD and hence elevated BACE1 levels during aging might be an important mediator of amyloid pathology in AD. Moreover, Aβ itself is thought to initiate a positive feedback loop that increases BACE1 levels (Zhao et al., 2007). Whether this increase in BACE1 levels also increases the cleavage of other BACE1 substrates and contribute to the AD pathogenesis is not yet clear.

1.3.2.3 γ-secretase

The C-terminal fragments that are produced upon the cleavage of APP by either α- or β-secretase are subsequently cleaved by γ-secretase, a large protein complex composed of four subunits: Aph-1, Nicastrin, Presenilin-1 and -2 (PS1, PS2) and Pen2. Sequential cleavage of APP first by β-secretase and then by γ-secretase generates Aβ. Like β-secretase, γ-secretase also cleaves many substrates other that APP. For example, Notch cleavage by γ-secretase is a very well established signaling process that plays an important role during and after development (Selkoe and Kopan, 2003). Hence, therapeutic strategies involving inhibition of β- or γ-secretase need to take this into account. Despite these constraints, γ-secretase has been considered a promising therapeutic target and several drugs have undergone clinical trials albeit with no clear beneficial effects. In fact, results from clinical trials have shown γ-secretase inhibition to cause considerable side effects and even worsening of cognition and behavior. For instance, in 2012 a phase III clinical trial for Semagacestat was halted due to adverse side effects such as skin cancer and infection coupled with no clinical benefit. Phase II clinical trial with Avagacestat, another γ-secretase inhibitor, was also stopped due to reports of cerebral microbleeds and skin cancer (Hung and Fu, 2017).These side effects of γ-secretase inhibition can be attributed to the fact that γ-secretase activity is also important for the cleavage of several physiological substrates such as Notch, Ephrin, Cadherin etc. The take home message from these studies is that we need to understand the biology of γ-secretase and its functions much better to be able to design better/specific therapeutic strategies. For example, one aspect of γ-secretase complex that warrants deeper understanding is the heterogeneity of the complex that can result from the presence of two homologs of Presenilin (PS1 and PS2) and two homologs of Aph1 (Aph1a and Aph1b). In vitro evidence for presence of spatially distributed γ-secretase heterogeneity further cements the idea that such a heterogeneity could also exist at the organismal level (Hebert et al., 2004). Yet another study suggested that γ-secretase heterogeneity at the level of Aph1 is important for target specificity (Acx et al., 2017; Dejaegere et al., 2008). What remains poorly understood is the biological consequence of γ-secretase heterogeneity at the level of PS1 and PS2. Thus, continued studies to understand the cellular biology of the individual components of APP processing machinery are much needed.

1.3.3 Amyloid Clearance

β-amyloid (Aβ) is a physiological product of cellular metabolism and like many other cellular metabolites its systemic level is regulated by both pathways that produce and pathways that

clear Aβ. Clearance of Aβ is mediated by several processes that occur parallelly. These include enzymatic degradation of Aβ, efflux of Aβ from the brain and cell-mediated clearance. I will discuss cell-mediated clearance at a later stage in this chapter.

1.3.3.1 Enzymatic degradation of Aβ

Enzymatic degradation of Aβ is carried out by a varied group of proteases that act in concert to counterbalance the production of Aβ by degrading it. These proteases can be broadly classified in the following categories: metallo proteases, serine proteases, aspartyl proteases, cysteine proteases and threonine proteases (Leissring, 2016). Several studies have demonstrated that enzymatic degradation of Aβ contributes significantly to the determination of cerebral Aβ levels (Eckman and Eckman, 2005; Farris et al., 2007; Leissring, 2008; Turner and Nalivaeva, 2007). To give an example, Farris and colleagues measured brain interstitial fluid (ISF) in mice lacking Neprilysin (NEP), one of the key metalloproteases involved in Aβ degradation. Deletion of NEP led to doubling of steady-state Aβ levels and a significant increase in the half-life of Aβ in ISF (Farris et al., 2007). Additionally, studies have reported NEP overexpression to reduce monomeric Aβ levels and Aβ plaques in the J20 line of APP transgenic mice by as much as 90 % (Leissring et al., 2003; Meilandt et al., 2009). Although, NEP overexpression did not reverse the learning and memory deficits observed in the J20 APP transgenic mice (Meilandt et al., 2009). This was attributed to the finding that though NEP overexpression reduced monomeric Aβ and Aβ plaques, there were no changes in the level of oligomeric Aβ after NEP overexpression (Meilandt et al., 2009). Endothelin-converting enzyme 1 and 2 (ECE1 and ECE2) are also metalloproteases that have been shown to degrade Aβ. A key difference though is that unlike NEP, ECE1 and ECE2 have an acidic pH optimum and thus function primarily in intracellular acidic organelles (Eckman et al., 2003). Matrix-metalloproteinases (MMPs), specifically MMP2 and MMP9, are bona fide Aβ degrading enzymes and have been shown to be degrading both monomeric as well as fibrillar Aβ (Yan et al., 2006). Insulin-degrading enzyme (IDE) is another metalloprotease that has been extensively studied for its role as an Aβ degrading enzyme. IDE has been shown to degrade exclusively the monomeric forms of Aβ and is predominantly present in the cytosol (Falkevall et al., 2006). Additionally, in vivo deletion of IDE have shown to substantially increase cerebral Aβ levels in APP transgenic mice (Farris et al., 2003). Plasmin, a serine protease has been shown to degrade Aβ, both monomeric as well as fibrillar (Tucker et al., 2000). Cathepsin B (CatB), is the only cysteine protease that has been shown to degrade Aβ in vivo (Mueller-Steiner et al., 2006). CatB is highly enriched in the

endolysosomal degradation pathway and shows optimal activity at acidic pH. Another protease that efficiently degrades Aβ at acidic pH is Cathepsin D, an aspartyl protease. Like CatB, it is also highly enriched in the acidic endolysosomal degradation pathway. CatD KO mice show an increase in steady-state Aβ levels as well as accelerated onset of plaque formation (Saido and Leissring, 2012). Altogether, the presence of a wide range of proteases capable of degrading Aβ suggests that maintenance of systemic Aβ levels is not only a function of its production but also its degradation.

1.3.3.2 Efflux mechanisms to clear Aβ from the brain

1.3.3.2.1 Efflux across the blood brain barrier

A key process of amyloid clearance is its efflux out of the brain parenchyma into the blood across the blood brain barrier (BBB). Endothelial cells connected by tight junctions form the critical barrier component in the BBB. These endothelial tight junctions prevent passive diffusion of Aβ into the blood. Specialized transporters at the BBB are required for the efflux of Aβ out of the brain. Lipoprotein receptor-related protein 1 (LRP1), a low-density lipoprotein receptor (LDLR) family protein, has been shown to be the main transporter for the efflux of Aβ across the BBB (Bell et al., 2007; Deane et al., 2004; Shibata et al., 2000). There are other studies that dispute the significance of LRP1 as a predominant transporter for Aβ efflux from the brain (Ito et al., 2010). Nevertheless, several studies have shown that LRP1 levels in brain microvessels are reduced, along with an increase in cerebral and brain amyloid in aging, both in mouse models and patients with AD (reviewed in Zlokovic, 2011) (Zlokovic, 2011). There is thus a strong indication for a link between reduced efflux of Aβ by LRP1 and increased amyloid accumulation in the brain. Lipoprotein receptor-related protein 2 (LRP2), another member of the LDLR family, associates with Clusterin (also known as ApoJ) to efflux Aβ across the BBB into circulation (Pascale et al., 2011). Apart from the LDLR family proteins, ATP-binding cassette (ABC) transporters, specifically ABCA1 and ABCB1, have also been shown to be involved in Aβ efflux from the brain. Unlike ABCB1, which directly transports Aβ from the brain into circulation, ABCA1 is thought to aid Aβ efflux by regulating ApoE lipidation. Lipidated ApoE binds Aβ efficiently which can then be transported from the brain by LRP1 or ABCB1 (Fitz et al., 2012; Tarasoff-Conway et al., 2015).

1.3.3.2.2 Efflux through the interstitial fluid bulk-flow

Interstitial fluid (ISF) bulk-flow into the lymphatic system is another important route for Aβ efflux from the brain. Earlier studies in mice had posited efflux across the BBB to be the main route for Aβ efflux from the brain (Shibata et al., 2000; Zlokovic, 2004). More recent studies have disputed this earlier claim and attribute a much larger contribution for ISF bulk-flow in Aβ efflux from the brain (Iliff et al., 2012; Kress et al., 2014). Aβ in the ISF is drained into the cerebrospinal fluid (CSF) sink and the perivascular space by bulk-flow. Several factors affect perivascular drainage pathways that clear Aβ from the brain, specifically, ApoE isoform status, arterial age and arterial pulsation. These mechanisms in turn can also be regulated by the body's homeostatic mechanisms, particularly, those that are active during sleep. Sleep has been shown to be a positive regulator of amyloid clearance from the brain by the virtue of its influence on ISF bulk flow (Xie et al., 2013). Perivascular drainage of Aβ has been shown to be impaired in AD (Weller et al., 2008). Another critical route for interstitial Aβ is its drainage via the glymphatic system, a process where astroglial channel proteins along the lymphatic system regulate the ISF bulk-flow. The astroglial Aquaporin4 (AQP4) channel has been shown to be vital in regulating glymphatic ISF bulk-flow. Aβ clearance along the perivascular pathway was reduced by as much as 65 % in Aqp4 knockout mice (Iliff et al., 2012). Interestingly, glymphatic clearance has been shown to be reduced upon aging, thus suggesting a role for this route of Aβ clearance in late-onset AD (LOAD) (Kress et al., 2014). As mentioned earlier, ISF bulk-flow also drains Aβ into the CSF sink. Aβ in CSF can then be absorbed either into blood circulation through the arachnoid villi and Blood CSF Barrier (BCB) or into the lymphatic system, through the perineuronal spaces (Pascale et al., 2011; Silverberg et al., 2003). The recently discovered meningeal lymphatic system might provide another route for Aβ ISF bulk-flow, though the exact contribution of this pathway is yet to be determined (Louveau et al., 2015).

1.3.4 Tau pathology

1.3.4.1 Structure and function

Tau is a microtubule associated protein found abundantly in mature neurons. In humans, Tau exists as six molecular isoforms and is encoded on chromosome 17 (Neve et al., 1986). The tau isoforms occur as a result of alternative splicing of the tau pre-mRNA. The six isoforms differ molecularly at two levels. First, in the presence of either three (3R) or four (4R) microtubule binding repeats (R) in the carboxy-terminal region. Second, in the presence of one (1N), two (2N) or zero repeats (0N) at the amino-terminal. This gives rise to the six tau

isoforms, three types of 3R tau (1N3R, 2N3R, 0N3R) and three types of 4R tau (1N4R, 2N4R, 0N4R). Tau is a natively unfolded protein with very little secondary structure, mostly composed of random coil with short hydrophobic motifs forming β-sheet structures in the microtubule binding repeats (Gustke et al., 1994; Mukrasch et al., 2009; Schweers et al., 1994). The aggregation property of tau is attributed to these β-sheet structure-forming motifs. The most well-established role for tau is its interaction with tubulin, which promotes the assembly of tubulin into microtubules. Moreover, tau interaction with the microtubules also helps to stabilize the structure (Weingarten et al., 1975). Some of the other functions attributed to tau are dependent on its primary role in promoting and stabilizing microtubules. Tau depletion in cultured neurons suppressed neurite outgrowth (Caceres et al., 1991), a finding that was also reproduced in tau knockout mice (Dawson et al., 2001). Tau was also shown to regulate axonal transport in cultured cells and mouse models (Ebneth et al., 1998; Probst et al., 2000).

1.3.4.2 Phosphorylation and de-phosphorylation mechanisms

Tau is a phosphoprotein and its microtubule assembly promoting activity is modulated by the degree of its phosphorylation. There are 85 potential phosphorylation sites in the longest isoform of tau (2N4R) and for roughly half the number of sites phosphorylation has been demonstrated experimentally (Hanger et al., 2009a). The most abundant phosphorylation sites in tau are serine/threonine sites that are flanked by proline sites. Specifically, there are 17 such sites that have also been shown to be abnormally hyperphosphorylated in AD by proline-directed Ser/Thr kinases. These kinases include extracellular-signal-regulated kinase 2 (Erk2), a Mitogen-activated protein kinase, glycogen synthase 3 (GSK3) and cyclin dependent protein kinase (CDK5) (Hanger et al., 2009b). Other Ser/Thr kinases include Prader-Willi/Angelman region 1 (PAR1) kinase, protein kinase A (PKA) and calcium/calmodulin-dependent protein kinase II (CaMK II). Tau can also be phosphorylated by tyrosine kinases such as LCK, FYN and ABL1. Interestingly, excessive phosphorylation of tau at the threonine position has been shown to promote tau aggregation (Rosseels et al., 2015). Phosphorylation of tau regulates tau function by several different mechanisms. Phosphorylation of tau at the KXGS motif reduces its affinity to microtubules, whereas phosphorylation at the flanking region of tau can result in detachment of tau from microtubules. Hyperphosphorylation of tau can also result in tau mis-trafficking from axons to the somatodendritic compartment, leading to synaptic dysfunction (Hoover et al., 2010; Thies and Mandelkow, 2007). Tau phosphorylation can also affect its degradation by the

proteasome complex or authophagy (Dickey et al., 2007). The levels of phosphorylated tau are not only regulated by the kinases that phosphorylate tau but also the phosphatases that directly interact with tau and dephosphorylate it. Ser/Thr protein phosphatases are abundant in the brain and thus they have a critical role in regulating tau function. Protein phosphatases 1, 2A, 2B, 2C and 5 (PP1, PP2A, PP2B, PP2C and PP5) are the phosphatases involved in tau dephosphorylation. PP2A is the predominant tau dephosphatase as it accounts for almost 70% of the tau phosphatase activity in humans. Moreover, activity of PP2A has been shown to be reduced in AD brains (Gong et al., 1993). PP2A activity reduction in AD has been attributed to several reasons, including reduced protein levels, increased inhibition and perturbation of subcellular localization (Gong et al., 1993; Sontag et al., 2004).

1.3.4.3 Tau mutations

The identification of mutations in tau that cause Frontotemporal dementia with parkinsonism linked to chromosome 17 (FTDP-17) provided the first evidence that mutated tau alone can lead to neurodegeneration (Hutton et al., 1998). Since then several mutations in tau have been identified in both the exonic and in the intronic region of the human tau gene, with some mutations also implicated in Corticobasal degeneration (CBD) and Progressive supranuclear palsy (PSP) (Coppola et al., 2012; Kouri et al., 2014). Almost all the mutations linked to FTDP-17 are missense or splicing mutations that are clustered in or around the microtubule binding domain. Tau proteins with mutations in these regions have reduced affinity for microtubules and have an increased propensity to form aggregates. Mechanistic characterization of some of these mutations revealed that mutations such as R406W, V337M and G272V make the tau protein a more favorable substrate for the phosphorylating kinases and hence lead to hyperphosphorylation (Alonso Adel et al., 2004). Many of the silent mutations in tau result in alternative splicing of the exon 10 and consequently increase the 4R/3R ratio (Lee et al., 2001). However, how these altered ratio leads to increased tau aggregation is still not clear.

1.3.4.4 Homeostatic control of tau levels

Homeostatic control of tau levels is achieved by maintaining a balance between tau synthesis, processing and degradation. Tau is an intracellular protein and hence intracellular protein degradation pathway play an important role in maintaining tau levels. Nevertheless, tau can be released in the extracellular space, particularly during neuronal death and neuronal activation (Avila et al., 2014; Yamada et al., 2014). Degradation of intracellular tau is

mediated mostly by the autophagy-lysosome pathway and the proteasome pathway (Avila et al., 2014). Impairment of the autophagy-lysosome pathway by addition of chloroquine leads to increased levels of full-length tau (Bednarski and Lynch, 1996). Conversely, stimulation of autophagy by rapamycin treatment or serum starvation led to reduction in tau levels and tau aggregates (Wong et al., 2008). Tau is a small, unfolded and cytosolic protein and hence it is an ideal cargo for proteasomal degradation. Indeed, studies have shown that tau can be degraded by the both the ubiquitin-dependent as well as the ubiquitin-independent proteasomal pathway (David et al., 2002; Hamano et al., 2009). To date no specific transporter for tau efflux across the BBB has been identified, suggesting that clearance of extracellular tau from the brain happens predominantly via ISF bulk flow and CSF absorption. Tau clearance from ISF and CSF is thought to follow the same routes as Aβ. Nevertheless, the processes that regulate extracellular tau clearance warrant further studies to further our understanding of AD.

1.4 Cellular basis of the disease

1.4.1 Neuronal contribution

Neurons are the most profoundly affected cell type in AD brains. Neuronal dysfunction and its gradual degeneration is directly linked to the cognitive and memory deficits observed in AD. However, it is important to note that neurons are not innocuous bystanders that are targeted by Aβ. In fact, in the brain neurons are the chief source of Aβ. The core components necessary for Aβ production, i.e, APP, BACE1 and γ-secretase, are highly expressed in neurons. All the components involved in Aβ production are membrane proteins and hence, regulation of membrane trafficking pathways is thought to be intimately linked with regulation of Aβ levels. The focus of this thesis is to understand the role of membrane trafficking pathways in the maintenance of amyloid levels. Below, I will briefly discuss our current understanding in this regard.

1.4.1.1 Production pathways

1.4.1.1.1 Role of membrane trafficking in production of Aβ

APP is a transmembrane protein that is cleaved by β- and γ-secretase, which are also membrane proteins, to generate Aβ. Apart from β-secretase, α-secretase can also cleave APP and since the α-cleavage is within the Aβ region, α-cleavage prevents the formation of Aβ. Whether APP is cleaved by α- or β-secretase depends on the localization of APP. α-secretase can cleave APP already at the plasma membrane. β-secretase on the other hand cleaves APP

predominantly in the endosomes as it needs the acidic pH of the endosomes to be optimally active. Studies have convincingly shown that endocytosis is necessary for β-secretase cleavage of APP and Aβ production and that redirecting APP from the membrane to endosomes influences the relative α- and β-cleavage of APP (Daugherty and Green, 2001; Ehehalt et al., 2003; Kinoshita et al., 2003; Refolo et al., 1995). APP and BACE1, the bona fide β-secretase, both need to be endocytosed from the plasma membrane for them to interact with each other. We know that APP from the cell membrane is internalized by both clathrin-dependent as well as raft-dependent endocytosis (Koo and Squazzo, 1994; Schneider et al., 2008). On the other hand, BACE1 is internalized through an ADP ribosylation factor 6 (ARF6) dependent pathway (Sannerud et al., 2011). This indicates that after endocytosis, APP and BACE1 must meet each other in a compartment within the cell. It is now clear that APP and BACE1, though internalized separately, meet and interact with each other in early endosomes.

1.4.1.1.2 Early and recycling endosomes in the production of Aβ

Once endocytosed APP can be trafficked to different intracellular routes which include early endosomes, recycling endosomes, late endosomes, lysosomes or even back to the golgi. In the search for the precise subcellular compartment where APP is cleaved by β-secretase our lab analyzed the site of maximal interaction between them by Fluorescence resonance energy transfer (FRET). The maximum intermolecular interaction between APP and β-secretase was shown to occur in the early endosomes. Additionally, data from live imaging of surface labeled APP and β-secretase confirmed that early endosomes are the major site of β-cleavage of APP (Rajendran et al., 2006). After β-cleavage of APP, the liberation of Aβ peptide from β-C terminal fragment (CTF) requires an additional cleavage by the γ-secretase complex. Localization studies with GFP fused β-CTF showed that γ-secretase cleavage of β-CTF also occurs in early endosomes (Kaether et al., 2006). From the above-mentioned studies we can conclude that early endosomes are the major cellular site for Aβ production. A more recent study on understanding the mechanism of APP and BACE1 localization and interaction posited the recycling endosomes as the intracellular compartment where APP and BACE1 meet (Das et al., 2013). Recycling endosomes are elongated structures that deliver cargoes from early endosomes back to the plasma membrane. Das and colleagues showed that in cultured hippocampal neurons APP is normally present in golgi-derived vesicles whereas BACE1 is present in recycling endosomes. Upon neuronal activation, APP is traffickedby a clathrin-dependent mechanism into recycling endosomes where it meets BACE1 (Das et al.,

2013). They further showed that APP and BACE1 also interact with each other in these recycling endosomes and that this interaction is significantly attenuated when APP carries the protective Icelandic mutation, A673T (Das et al., 2016). Thus it is evident that Aβ is produced in intracellular organelles (early/recycling endosomes) and that regulators of their residence in these structures are potential modifiers of Aβ levels.

1.4.1.1.3 Aβ release mechanisms

Aβ is produced in endosomes and rapidly released into the extracellular space. Much of the Aβ that is generated in endosomes can be sorted to multivesicular bodies (MVBs). It was shown that Aβ is released from these MVBs via its fusion with the plasma membrane. It was shown that through MVB fusion only a fraction of the Aβ is released in association with exosomes (Rajendran et al., 2006), with the bulk being released as soluble Aβ. Nevertheless, there is evidence that this released exosomal Aβ could contribute to amyloid plaque formation (Yuyama et al., 2008). A more recent study suggested that autophagy, apart from its role in degradation, also plays a role in secretion of Aβ. Though the exact mechanism by which autophagy leads to Aβ secretion is not clear (Nilsson et al., 2013). Though not much is known about the regulators of Aβ release, intracellular cholesterol accumulation has been implicated in Aβ secretion. Increased cholesterol accumulation leads to decreased Aβ secretion and consequently increased intracellular Aβ (Runz et al., 2002). Further investigation to understand the regulation of Aβ secretion is much needed.

1.4.1.2 Clearance pathways - intracellular endo-lysosomal proteolysis in amyloid clearance

Neurons are the major cell type that produce Aβ in the brain. Nevertheless, neurons also have the machinery that can degrade the Aβ produced in intracellular compartments. The endo-lysosomal pathway is the major pathway by which neurons are thought to degrade Aβ. Lysosomes are the cells major degradative organelle and are ubiquitously present in all cell types. Lysosomes are the terminal degradative organelle for both, cargoes that are routed via the endocytic pathway as well as the ones that are routed via the autophagic pathway. Aβ is produced in the endosomes and hence can be trafficked to the lysosomes via the endocytic pathway. In the endocytic pathway, the cargoes are endocytosed from the extracellular lumen and lead to formation of early endosomes (EE), site of Aβ production, which then mature to late endosomes (LE). Both autophagosome (from the autophagic pathway) and LE finally deliver their contents to lysosomes, where they are degraded by the proteases present in them.

Lysosomes are characterized by a lower pH compared to other cellular organelles and the lower pH facilitates the lysosomes to digest the cargoes with the help of pH dependent hydrolases. As mentioned earlier, autophagy also depends on functional lysosomes to regulate degradation of cargoes. Autophagy also has been shown to be a key regulator of Aβ clearance (Nilsson and Saido, 2014). Aβ has been shown to be present in autophagosomes which eventually depend on lysosomes to degrade their cargo (Yu et al., 2005). Moreover, β-CTF has also been shown to be targeted to degradation via autophagy in AP2/PICALM dependent manner (Tian et al., 2013). Thus, a functional autophagic pathway must at least in part regulate Aβ metabolism in neurons.

1.4.2 Microglial contribution

1.4.2.1 Role of phagocytosis in the removal of amyloid

Microglia are the resident brain macrophages that have critical roles in maintenance of CNS homeostasis during development and later stages in life. Microglial phagocytosis is called upon in several physiological and pathophysiological situations such as synapse elimination, axonal and myelin debris removal and clearance of potentially toxic peptides such as Aβ (Paolicelli et al., 2011; Sierra et al., 2013). Once phagocytosed, the cargoes are eventually degraded in lysosomes. Data from both human patients and AD mouse models suggests that microglia are present in the immediate vicinity of amyloid plaques and are often found surrounding them (Lai and McLaurin, 2012). Since microglia are not major contributors of Aβ production, their presence around plaques was proposed to be for the phagocytosis of these plaques. Indeed, in vitro evidence indicates that microglia can efficiently phagocytose fibrillar Aβ through many different receptors, including Toll-like receptor 2 and 4 (TLR2 and TLR4) and Scavenger receptor A1 (SCARA1) (Frenkel et al., 2013; Liu et al., 2012; Paresce et al., 1996). However, the role of microglia as scavengers of Aβ in vivo is disputed. Studies from AD mouse models have shown that though microglial cells were associated with plaques, they do not phagocytose Aβ from these plaques (Stalder et al., 2001). A possible explanation for this is that in aging AD mice there is a marked decrease in phagocytic genes compounded with an increase in pro-inflammatory cytokines (Hickman et al., 2008). More recent evidence indicates that microglia do have the capacity to phagocytose Aβ in vivo and that there must be cell intrinsic and extrinsic factors which influence the microglial phagocytic capacity (Paolicelli et al., 2017).

1.4.2.2 Role of phagocytosis in synaptic pruning and synapse loss

Conventionally, microglia were considered as scavenger cells that are active only during injury or pathological manifestations. However, our current understanding of the role of microglia in the brain is constantly evolving. Studies indicate that microglial processes actively contact synapses and survey the environment even in an uninjured brain (Nimmerjahn et al., 2005; Wake et al., 2009). Microglia were found to actively phagocytose synapses during normal brain development. In fact, microglial phagocytosis of synapses was shown to be an essential part of synaptic pruning, a process that is vital in efficient brain connectivity (Paolicelli et al., 2011). Microglial synaptic pruning is a highly regulated process that is mediated by the complement system, specifically complement receptor 3 (CR3) and its ligand C3. Mice lacking either CR3 or C3 show decreased microglial synaptic pruning, increase in synaptic density and behavior deficits (Schafer et al., 2012). Decreased synaptic pruning due to impaired microglial phagocytosis also has disease relevance. Reduced synaptic pruning in mice lacking chemokine receptor Cx3cr1 led to decreased synaptic transmission and connectivity and the behavioral changes were reminiscent of autism-spectrum disorder (Zhan et al., 2014). It is plausible that hyperactive microglia due to amyloid accumulation may lead to indiscriminate synapse loss and thus add to the pathological mechanisms of amyloid aggregation/plaques. Further studies in this direction could provide vital clues into the complex mechanism of amyloid pathology in AD.

1.4.2.3 Regulation of microglial clearance mechanisms

Microglial cells are the professional phagocytes of the brain both in physiological and pathological situations. The process of microglial phagocytosis can be categorized into three basic steps. These are Step 1: Find the target, Step 2: Eat the target and Step 3: Digest the target. Regulation of microglial clearance can occur at any of these steps, although the threshold for whether microglia should phagocytose a target or not is established in the first two steps. Microglial processes are very dynamic and they continuously survey the environment around them. Microglia can either by chance or in response to a chemoattractant find a target that carries the so called ‘eat me’ signal (Sierra et al., 2013). One type of signaling molecule that regulate microglial clearance are nucleotides such as ATP and UDP, which are released by apoptotic cells (Elliott et al., 2009). Another type of signal that microglial cells recognize are ligands called fractalkine which are also released by apoptotic cells (Truman et al., 2008). Yet another type of signal are cannabinoids that are secreted by neurons in pathological conditions. These are recognized by cannabinoid receptors on

microglial membranes and leads to their migration towards the target (Walter et al., 2003). Much of the regulation of microglial clearance occurs at step 2, i.e. Eat the target. Here, microglia engage with their target by means of tethering and engulfing, a process that is regulated by receptor-ligand interactions. For instance, Aβ phagocytosis depends on the interaction of Aβ with receptors like SCARA1 and TLR2 that are present on microglia. These receptors recognize the 'eat me' signal exhibited by the target cell or molecule and thus initiate the process of phagocytosis. The triggering receptor expressed on myeloid cells 2 (TREM2) is another example of receptor that has been shown to trigger phagocytosis. Variants of TREM2 have been identified as risk factors for AD (Guerreiro et al., 2013; Jonsson et al., 2013). Interestingly, a recent study reported that TREM2 promotes Aβ phagocytosis by upregulating CD36 receptors on microglia and it is plausible that AD variants of TREM2 are inefficient in promoting Aβ phagocytosis (Kim et al., 2017).

1.4.3 Synaptic pathology

Synaptic loss is the best neuropathological correlate to the degree of cognitive decline observed in AD (Terry et al., 1991). Synapse loss is also a relatively early phenomenon in AD progression. Markers of synapse pathology or loss are potential biomarkers for early diagnosis of AD and I will discuss them later in this chapter. Compared to amyloid plaques, oligomeric species of Aβ correlate better with cognitive decline due to AD. In fact, Aβ oligomers have been shown to induce synaptic dysfunction and degeneration. Since synapses are an indispensable unit of neuronal communication, it is plausible that loss of synapses trigger a cascade of events that lead to neuron loss and cognitive decline. The mechanisms by which Aβ affects synaptic function and integrity are thought to be related to its effect on N-Methyl-D-aspartate (NMDA) receptor functioning and thereby on inhibition of long term potentiation (LTP) (De Felice et al., 2007). Though, the effect of Aβ oligomers on NMDARs is thought to require several other participating receptor proteins like p75 neurotrophin receptor (p75NTR), frizzled etc. Elucidating the precise molecular events that lead to synaptic dysfunction and synapse loss is an active area of research in AD.

1.5 Genetic basis of the disease

1.5.1 Familial AD

Aging and familial history of AD are the biggest risk factors for AD. More than 95% of all AD cases occur in individuals above the age of 60 years and are classified as late-onset AD (LOAD). The remaining 5% of cases are classified as familial AD (FAD) and patients can be

as young as 30 years old. Several genes implicated in FAD have been reported and all of them are involved in Aβ processing. These include mutations in the amyloid precursor protein (APP), the substrate, and in presenilins (PS1 and PS2), the catalytic units of the γ-secretase complex. Most of the FAD mutations lead to increased production of Aβ, with a shift towards Aβ42 peptide, which is the most toxic species of Aβ. These findings emphasize that the amyloid cascade hypothesis is central to the pathogenesis observed in FAD.

1.5.1.1 APP mutations

1.5.1.1.1 Disease causing mutations

The human APP gene is located on the chromosome 21. Duplications of chromosomal region containing the APP gene have been reported to cause an autosomal-dominant form of AD and CAA (Rovelet-Lecrux et al., 2006; Sleegers et al., 2006). Moreover, 26 pathogenic missense mutations of APP have been reported (Tcw and Goate, 2017). A double mutation (K670N/M671L) located at the N-terminus of Aβ and the β-secretase, respectively, was identified in a Swedish family with familial AD (Mullan et al., 1992) and was shown to increase production of total Aβ in vitro. Ten pathogenic mutations have been identified within the Aβ sequence, including D678N, E682K (Leuven mutation), A692G (Flemish mutation) and E693G (Arctic mutation). The different mutations within the Aβ domain have been shown to have a varied effect on APP processing and Aβ itself (Haass et al., 1994; Wisniewski et al., 1997). Fourteen mutations have been reported in the C-terminal Aβ domain and these mutations affect the activity of the secretases, resulting in pathological processing of APP.

1.5.1.1.2 Protective mutation

The A673T mutation in APP is the only protective mutation that was reported after a whole-genome sequencing analysis of an Icelandic cohort. The mutation was shown to be protective against AD and age-related cognitive decline (Jonsson et al., 2012). The A673 residue is located close to the primary β-secretase cleavage site and is within the Aβ region. In a cellular model, the A673T mutation was shown to reduce Aβ production by approximately 40 % compared to wild-type APP (Jonsson et al., 2012). Further evidence of a specific reduction in β-secretase cleavage in the A673T variant of APP in primary neurons substantiated the Aβ reducing effect of this protective mutation (Benilova et al., 2014; Maloney et al., 2014).

1.5.1.2 Presenilin mutations

According to 'www.alzforum.org', more than 200 mutations in PS1 and PS2 among FAD patients have been identified. The majority of the presenilin mutations are located in and around the transmembrane domain of the protein. FAD PS1/2 mutations are some the most devastating mutations as the age of disease onset ranges between 35 to 55 years. It has been reported that at least some presenilin mutations alter the interaction of APP and presenilin such that they increase production of Aβ42 compared to other Aβ species (Szaruga et al., 2017). The increased ratio of Aβ42/Aβ40 then leads to an increase in aggregation of the Aβ peptides due to the high aggregation propensity of Aβ42. This mechanism of action of the mutations fit well with the amyloid cascade hypothesis. Since presenilin is required for Aβ production, it was initially thought that most of the presenilin mutations must be toxic gain-of-function mutations. However, several studies in cell lines reported that presenilin mutations decrease the cleavage of notch, cadherin and syndecan and thus reflect loss of function of the γ-secretase complex (Baki et al., 2001; Bentahir et al., 2006; De Strooper, 2007; Schroeter et al., 2003). In fact, a recent study analyzed 138 pathogenic PS1 mutations in a γ-secretase cell-free assay and showed that about 90 % of the mutations lead to reduced Aβ42 as well as Aβ40 levels (Sun et al., 2017). This further confirms that most of the presenilin mutations are indeed loss of function mutations. Then how does this relate to the clinical findings that FAD patients with PS mutations have an increased amyloid load? The general consensus is that the loss-of-function mutations of presenilins lead to incomplete digestion of APP-CTFs, leading to relative increase in longer isoforms of Aβ. Since the relative increase in Aβ42 and not the total increase of Aβ is the driving force behind amyloid aggregation, FAD PS mutations can therefore lead to increased amyloid load despite a loss of function at the γ-secretase activity level. An alternative amyloid-independent explanation for the FAD PS1 mutations and their pathogenicity is the fact that presenilins are implicated in a diverse range of functions in the brain and loss of these functions triggers neurodegeneration (Shen and Kelleher, 2007). More research in this direction, especially studies towards understanding the presenilin1/2-dependent γ-secretase heterogeneity, are much needed.

1.5.2 Late-onset AD

Unlike FAD, late-onset AD (LOAD) cannot be attributed to mutations in a single gene and hence the amyloid cascade hypothesis is not the default hypothesis that can explain the etiology of LOAD. Nevertheless, LOAD has a big genetic component and it is likely that the risk is distributed over many genes and hence many cellular pathways. Genetic risk factors

for LOAD have been identified through GWAS (see the following section). However, not much is known about the possible mechanisms of action of these risk genes. More studies are needed to determine how amyloid aggregation occurs in LOAD despite the absence of disease-causing mutations in the APP processing machinery.

1.5.2.1 Genome-wide association studies (GWAS) on LOAD

APOE (Apolipoprotein E) was the first identified susceptibility gene for LOAD. Compared to other APOE alleles, the ε4 allele (APOE4) is associated with an increased risk for LOAD (Pericak-Vance et al., 1991). Studies have shown that ApoE4 contributes to LOAD risk by negatively regulating Aβ clearance from the brain. More than a decade after the identification of APOE4, additional risk genes for LOAD were identified through GWAS. In GWAS, single nucleotide polymorphisms (SNPs) are sequenced in LOAD patients and controls. The frequencies of SNP variants are correlated with the phenotype and risk loci are identified (Lambert et al., 2009). More recent studies include additional strategies such as chromosomal microarrays or whole-exome sequencing (Guerreiro et al., 2013; Sims et al., 2017) to identify novel risk variants. Although the first generation of GWAS identified some new risk genes for LOAD, the variants were not replicated to be associated with risk in independent studies. The European Alzheimer Disease Initiative (EADI) led the second generation of GWAS that examined a much larger number of LOAD patients and identified risk genes that were replicated in independent studies (Lambert et al., 2009; Lambert et al., 2013; Naj et al., 2017). Since then, other GWAS and meta-analysis of multiple GWAS have yielded, verified and replicated lists of LOAD risk genes. Although many of these genes could be linked to Aβ**,** evidences suggest that these mutations do not confer AD risk by skewing the ratio of Aβ species in favor of the more toxic ones (Bali et al., 2012). The finding that several of these genes are involved in the immune system (CLU, CR1, ABCA7 and CD33), in synaptic function and endocytosis (PICALM, CD33, CD2AP and BIN1), and lipid transport and metabolism (CLU and ABCA7) further emphasize the molecular complexity that underlie LOAD (Tosto and Reitz, 2013).

1.5.2.2 Mutations in the neuroinflammation/microglial function-related genes

Neuroinflammation, including microglial response to amyloid, was since long believed to play an important role in the pathogenesis of AD (McGeer et al., 1989). In accord, several of the risk genes associated with LOAD have been shown to be important in neuroinflammation pathways. Of these genes, CR1, CD33, and TREM2 have been studied in some detail.

Antibody mediated blockage of CR1 inhibits activation of microglia and decreases microglial phagocytosis of Aβ (Crehan et al., 2013). Another study demonstrated that CD33 levels in microglia is increased in AD patients and that CD33 inhibits uptake and clearance of Aβ42 in vitro (Griciuc et al., 2013). Wang and colleagues showed that TREM2 deficiency increases Aβ accumulation, which can be attributed to dysfunctional microglia that do not respond to amyloid plaques (Wang et al., 2015). Thus, these studies highlight the relevance of neuroinflammation and microglial function/dysfunction in the pathogenesis of AD.

1.5.2.3 Mutations in the membrane trafficking related genes

The importance of membrane trafficking in AD has been discussed in the earlier sections. It is hence not surprising that many LOAD risk genes were found to be involved in trafficking processes like endocytosis and lysosomal degradation. Earlier in the chapter we have seen that SorLA1, a LOAD risk gene, is involved in APP trafficking from endosomes to golgi and thus affects Aβ levels. PICALM, another LOAD risk gene, was shown to be involved in the endosomal trafficking of APP and possibly transport of brain Aβ across the blood brain barrier (Kanatsu et al., 2014; Zhao et al., 2015). In a study that is part of this thesis, we identified a mutation in Rab11 that significantly associates Rab11 function with LOAD, possibly through its regulation of BACE1 recycling (Udayar et al., 2013). BIN1, the risk gene only second to APOE4 in its risk for LOAD has diverse functions that include actin dynamics and clathrin-mediated endocytosis (Pant et al., 2009) and clathrin-mediated endocytosis is a crucial pathway for APP endocytosis and Aβ production. Thus, a critical role for membrane trafficking genes in AD is predicted by these genetic and cell biology studies in AD.

1.6 Biomarkers of AD

1.6.1 Aβ and Tau-based biomarkers

The diagnostic criteria for AD are primarily based on biomarkers and neuropsychological testing. The same criteria are used to classify patients as preclinical AD, mild cognitive impairment (MCI) associated with AD and clinical AD (Albert et al., 2011; Sperling et al., 2011). For AD, biomarkers that are currently under use can be broadly classified into either brain imaging-based markers or CSF-based markers. Biomarker changes, specifically low cerebrospinal fluid (CSF) Aβ42 and positive amyloid-PET scans precede all other AD-related alterations. According to a hypothetical temporal model based on existing AD biomarker data, the chronological order of biomarker changes in AD is as follows, i) lower CSF Aβ42 ii) increased CSF tau iii) decrease in cerebral glucose metabolism and brain atrophy (detected

by MRI) and iv) cognitive impairment (Selkoe and Hardy, 2016). In fact, studies in familial AD patients suggested that decreased levels of Aβ42 in CSF can be detected 25 years before any cognitive symptoms are manifested (Bateman et al., 2012). The decrease in CSF Aβ42 is thought to be due to its decreased clearance from the brain into the CSF sink and /or its increased aggregation in the brain as amyloid plaques (Stefani et al., 2005; Zetterberg et al., 2010). Aβ also serves as a brain imaging marker for AD as brain amyloid load can be visualized by positron emission tomography (PET) scans of Pittsburg compound-B (PiB), a ^{11}C-labelled dye that binds amyloid (Klunk et al., 2004). Total tau and phospho-tau are two other validated markers for diagnosis of AD. Total tau levels in CSF increase during normal aging, though this increase is significantly higher in AD patients (Sjogren et al., 2001). Increase in total tau levels in CSF can also be used to classify MCI patients as MCI-stable or MCI-to-AD (Blennow, 2004). Tau can be hyperphosphorylated at many different sites and often the phosphorylated tau species are dysfunctional. Tau phosphorylation at position 181 (pTau181) is significantly higher in AD patients compared to control (Hampel et al., 2010). The general consensus is that only with a combination of Aβ42 and total/phospho-tau (pTau181) measurement in CSF can sporadic AD be diagnosed with a sensitivity of more than 95 % and specificity of more than 85 % (Blennow, 2004; Blennow et al., 2010; Marksteiner et al., 2007).

1.6.2 Synaptic biomarkers

Loss of synapses is the best correlate to the cognitive deficits observed in AD. Synapse loss occurs relatively early in the disease, much before neurodegeneration and cognitive decline. Thus, indicators of synapse dysfunction or loss could be used as potential biomarkers for early diagnosis of AD. Improvements in ELISA based assays to detect synaptic proteins with high sensitivity has led to several studies that have measured the changes in levels of different synaptic proteins in CSF from AD patients. Currently, there is no validated biomarker of synaptic dysfunction/loss that is sensitive and specific enough to be used as diagnostic marker in AD. Nevertheless, there are some very interesting candidate biomarkers. Meta-analysis of synaptic pathology reported in 417 publications confirmed that synapse loss in specific brain regions is indeed an early event in AD and that presynaptic markers were affected more than postsynaptic markers in AD (de Wilde et al., 2016). The presynaptic protein synaptosomal-associated protein 25 (SNAP25) is one such marker. SNAP25 is involved in vesicle fusion at the synapsis and are important for proper synapse functioning. In three separate cohorts, CSF levels of SNAP25 were found to be higher in AD compared to

controls (Brinkmalm et al., 2014). CSF levels of synaptotagmin 1, another presynaptic protein, was shown to be higher in AD patients as well as in patients with MCI. Interestingly, synaptotagmin 1 levels in CSF correlated with both total-tau and phospho-tau levels in AD patients and thus can be a potential addition to the CSF biomarker profile in AD (Ohrfelt et al., 2016). Studies have shown that CSF levels of neurogranin, a postsynaptic protein involved in synaptic plasticity, is increased in AD patients and that it can be used to predict MCI to AD conversion (Kester et al., 2015; Kvartsberg et al., 2015; Thorsell et al., 2010). A recent large cohort study confirmed that CSF neurogranin levels are indeed increased in AD patients. The study reported that high CSF neurogranin levels correlated with brain atrophy in AD and with amyloid plaque load in preclinical AD. Moreover, high CSF neurogranin level could predict rates of cognitive decline in patients with early symptomatic AD (Tarawneh et al., 2016). Another study reported that high CSF levels of neurogranin appeared to be specific for AD when compared to other neurodegenerative diseases such as frontotemporal dementia and Parkinson's disease (Wellington et al., 2016). Addition of CSF neurogranin levels to existing repertoire of AD biomarkers promises to complement and further increase the sensitivity of the diagnosis.

1.6.3 Systems biology-driven biomarker profiles

AD is a complex disease that entails the convergence of a complex maze of cellular pathways and processes that eventually lead to neurodegeneration and memory loss. The ideal systems biology-based biomarker profiling for AD would involve integrating mRNA, non-coding RNA, proteins and metabolites changes over a period. Biomarker profiles generated from such an approach have the potential to be more robust and sensitive compared to conventional biomarkers that are based on isolated pathways or processes. Due to the nature of the disease, generating such a biomarker profile based on affected tissues is an inherent limitation. In AD, tissues that are used for studying disease pathogenesis come from post-mortem brain samples and hence do not reflect the early stages of disease. An alternative approach to circumvent this issue would be to develop biomarker profiles based on analysis of blood or plasma samples. This approach has its own limitations as blood carries the molecular signatures from all the different tissues. Any such biomarker profiling study would require a combination of sophisticated computational tools along with sensitive and specific measurement assays (Lausted et al., 2014).

1.7 Therapeutic strategies

1.7.1 Current status

The main goal of therapeutic strategies for AD is to improve cognition and slow the progression of disease. The treatments available at present do not cure the disease per se. In recent years, significant efforts and resources have been devoted to the development of better treatment strategies, which may eventually lead to a cure. According to 'www.alz.org', there are currently five drugs approved by the U.S. Food and Drug Administration (FDA) for the treatment of AD. These are donepezil, galantamine, rivastigmine, memantine and combination of donepezil and memantine. The first three drugs are cholinesterase inhibitors that increase the levels of acetylcholine by inhibiting cholinesterase. Memantine is a NMDA receptor antagonist that is believed to protect cells from excess glutamate by partially blocking the NMDA receptor. All these drugs are symptomatic as without knowing the definitive cause it is difficult to design drugs that cure the disease. Because of the significant progress in our understanding of amyloid and its metabolism, anti-amyloid strategies are on the rise. Aβ is causally associated with the neurodegeneration observed in AD and hence, anti-Aβ therapies that either inhibit the production (by inhibiting β- or γ-secretase) or clear the amyloid load via Aβ immunotherapy offer an exciting possibility to reduce the amyloid load and improve the cognitive function (Selkoe and Hardy, 2016). One of the major hurdles in developing an effective therapy involving β- or γ-secretase inhibitor is that both the secretases cleave many other substrates and thereby play an important role in many physiological processes during development and beyond (Hemming et al., 2009; Kuhn et al., 2012; Willem et al., 2006; Wolfe, 2008). Our lab has addressed this issue by developing a modified version of β-secretase inhibitor that is more specific and efficient compared to the unmodified version of the inhibitor. The strategy behind the development of the inhibitor is explained in the following section. Aβ immunotherapy offers an exciting opportunity to target amyloid directly and slow the progression or possibly cure AD. A big advantage for Aβ immunotherapy is that compared to β- or γ-secretase inhibitors, antibodies against Aβ specifically target Aβ without interfering with other physiologically relevant substrates. Aducanumab, a human monoclonal antibody that targets aggregated Aβ, has emerged as one of the most promising immunotherapy candidate at present. After demonstrating its efficacy in AD mouse models, the antibody was used in a Phase 1b trial in a small cohort of 165 patients with prodromal or mild AD. Monthly intravenous infusions of aducanumab for a year reduced brain Aβ and slowed cognitive decline in the treated patients. This antibody is

currently under Phase 3 trials. Nevertheless, keeping in mind the complexity of the disease, new therapeutic approaches and strategies need to be pursued.

1.7.2 Therapies based on novel insights into membrane trafficking in AD

The absence of effective therapies for AD is primarily due to the complex nature of the disease. Much of the therapeutic interventions tested in the recent past included inhibitors against either γ-secretase or β-secretase. These inhibitors proved to be ineffective and several of them caused major side-effects. Some of the reasons for these failures are delayed therapeutic intervention, inefficient drug targeting strategies and pan-inhibition of the secretase functions. Understanding the trafficking pathways involved in regulation of Aβ production offers the possibility to address some of above mentioned limitations. For instance, the knowledge that β-secretase cleaves APP in early endosomes was ingeniously used by Rajendran and colleagues to design a novel therapeutic strategy for efficient inhibition of β-secretase (Ben Halima et al., 2016; Rajendran et al., 2008). Rajendran and colleagues began with a transition-state inhibitor against β-secretase which binds and inactivates only the active conformation of β-secretase. Since β-secretase is active in endosomes they reasoned that targeting the inhibitor to these endosomes will make them inhibit β-secretase more efficiently. They designed a membrane-tethered version of the originally free and soluble inhibitor to target it to the intracellular compartments, in this case endosomes. They linked the inhibitor to a sterol moiety to create a membrane-anchored β-secretase inhibitor that readily partitioned into cholesterol-rich domains on endosomal membrane. β-secretase is also known to be enriched in these cholesterol-rich domains. As predicted, the membrane-anchored β-secretase inhibitor was shown to be more potent in inhibiting β-secretase both in flies and in mice (Rajendran et al., 2008).

Another approach stemming from membrane trafficking studies that was demonstrated to be a viable therapeutic option for AD is boosting the level/function of the endocytic pathway. Mecozzi and colleagues demonstrated that stabilizing the retromer complex by novel pharmacological chaperones, R33 or R55, lowers Aβ level in mouse primary neurons (Mecozzi et al., 2014). The Aβ lowering effect of the drugs was attributed to the reduced endosomal residence time of APP. The rationale behind the explanation is that reduced endosomal residence time will lower the rate of Aβ production and consequently lower Aβ levels. Recently, retromer stabilization with R33 was shown to also reduce pathogenic tau phosphorylation in human stem cell models of AD (Young et al., 2018). These studies are

particularly interesting as retromer deficiency, specifically that of vacuolar protein sorting-associated protein 26 and 35 (VPS26 and VPS35) has been reported in late-onset AD patients (Small et al., 2005; Wen et al., 2011). Thus, furthering our understanding of membrane trafficking processes involved in AD promises novel therapeutic avenues to fight this complex and devastating disease.

1.8 Systems biology approaches to understand membrane trafficking complexity in AD

The basic components that generate Aβ in vitro comprise APP, β-secretase and the γ-secretase complex in a lipid vesicle with optimal pH (Edbauer et al., 2003). In intact cells and organisms these basic components are dependent and regulated by many processes and signaling pathways. Therefore, a systems biology approach that integrates information about the role of different genes, signaling and metabolic pathways that regulate APP processing and Aβ levels is crucial in our understanding of the complex cellular events that underlie AD.

Our lab has previously shown that internalization of APP to early endosomes is necessary for it's processing by β- and γ-secretases and that these occur predominantly in early endosomes (Rajendran et al., 2008). Hence, membrane trafficking to and away from early endosomes must have a critical role in determining the residency of these components and hence Aβ levels. In support of this rationale is the fact that trafficking regulators that retrieve Aβ relevant cargoes from early endosomes to the Golgi are implicated in AD Proteins belonging to the GGA family have been shown to retrieve β-secretase from endosomes to Golgi and their depletion leads to increased amyloidogenic processing of APP (Tesco et al., 2007). Interestingly, mutations in SorLA 1 (a sortilin related receptor 1) that causes failure in retrieving APP from early endosomes and leads to an increase in Aβ production has been found to confer risk for late-onset AD (Andersen et al., 2005; Rogaeva et al., 2007). It is likely that there are many other proteins that regulate the trafficking of APP processing machinery along the biosynthetic/endocytic pathway and thereby potentially modify the risk for AD. The aim of this thesis is to identify all the essential trafficking pathways that are involved at various stages in APP metabolism.

1.8.1 Rab GTPase

Rab proteins are small GTPases belonging to the Ras superfamily. They are monomeric G proteins that regulate vesicular trafficking in the biosynthetic, endocytic and degradation routes in the cell. Thus, they enable cargo sorting and distribution to the different subcellular

compartments. Rab GTPases are reversibly attached to cell membranes by hydrophobic geranylgeranyl group. They can switch between the inactive GDP-bound form to the active GTP-bound form and thus mediate vesicular fusion or fission. GDP to GTP exchange is achieved by Rab-specific GTP exchange factors called GEFs whereas the hydrolysis of GTP to GDP is achieved by the GTPase activating proteins, called GAPs (Fig. 3). There are about 60 Rab proteins and about 40 Rab-GAPs in the human proteome. These diverse Rabs also serve as membrane identity markers, as specific Rabs are involved in specific trafficking route. For example, Rab3 is a very well established regulator in the biosynthetic pathway and exocytosis and mediates trafficking from the Golgi-ER to plasma membrane (Zahraoui et al., 1989). Interestingly, Rab3A, one of the Rab3 isoform was shown to be involved in anterograde transport of APP (Szodorai et al., 2009).

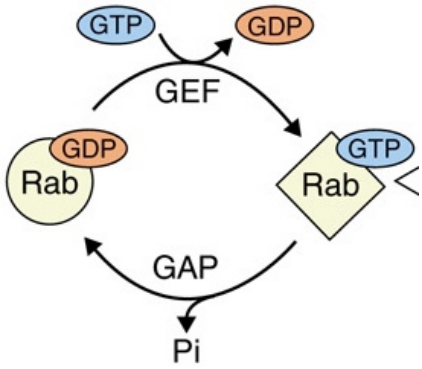

Figure 3: The Rab GTPase cycle. Rab proteins can be converted into GTP-bound form by GEFs and are the active form in most cases. Rab-GTP can be converted to the Rab-GDP form by the action of GAPs, which is in most cases the inactive form (adapted from Stenmark and Olkonen, 2001) (Stenmark and Olkkonen, 2001).

The biology of Rab proteins provide multiple ways to study its function. Like for most genes, siRNA targeting specific Rab mRNA can be used to deplete mRNA and subsequently protein levels of the particular Rab. Additionally, overexpression of Rab-GAP plasmids can deplete the active form of Rab proteins and increases the inactive, GDP-bound form, thereby preventing their normal function (Fig. 3). Such Rab-GAP screens have been performed to identify regulators of several cellular processes such as cilia formation, toxin uptake and endocytosis. Yet another way to study Rab function is to use mutant Rab plasmids where the Rabs are either locked in its GTP-bound form (dominant active) or GDP-bound form (dominant-inactive). Overexpression of the dominant active or dominant negative form leads to specific Rab activation or inactivation respectively. Thus, using Rab siRNA library, Rab-

GAP library and mutant Rab proteins plasmids, we aimed to study APP processing and create a “road map” for β-amyloid production and degradation.

1.8.2 RNAi screens

RNA interference (RNAi) is an endogenous process in cells by which small RNA molecules prevent gene expression by targeting the corresponding mRNA molecule. It is known to exist in many eukaryotes, including plants and animals. Since its discovery, RNAi has developed rapidly into a valuable tool for genetic studies that does not require alterations at the genomic level. The small interfering RNA molecule (so called siRNA) can be introduced into cells by techniques such as electroporation, microinjection and liposome transfection. Due to the relative ease and efficiency of the system RNAi screens have been successfully performed in many model systems, for instance, Caenorhabditis elegans, drosophila embryos and several mammalian cell lines. These studies have led to significant advancement in our understanding of processes such as embryonic development, cell signaling, aging and viral infection mechanisms (Mohr et al., 2010; Prudencio and Lehmann, 2009; Seyhan and Rya, 2010). RNAi screens in mammalian cultured cells are carried out predominantly by using liposome-mediated transfection to introduce the siRNA in these cells. Several companies provide customizable or off-the-shelf siRNA libraries that can be readily transfected into cells. Combined with a faster, efficient and robust sample analysis platform (like the multiplexing assay introduced below), RNAi screens provide a powerful yet simple method to perform genome-wide analysis in cells. One noticeable limitation of the RNAi screens are the potential false-positives due to siRNA off-target effects. In recent times, there has been a vast improvement in the design of individual siRNA molecules to minimize or practically eliminate off-target effects. In our RNAi screens, we use a pool of 3-4 different siRNAs to target a particular gene to achieve efficient knockdown. After carefully selecting our hit candidates we deconvolute the analysis by performing the knockdown with individual analysis separately. We then look at the result of each of the individual knockdown and only when the results are consistent across the different siRNAs we proceed with further characterization. This approach further minimizes any potential false-positives in our RNAi screen. A robust and efficient RNAi screen depends as much on the sample assaying techniques as it does on the knockdown method itself. Below, I will introduce the multiplexing assay system that we have developed in our lab.

1.8.3 Multiplexing assays to screen for regulators of Aβ production and clearance

As mentioned above, one of the key components of the RNAi-screens is a medium to high-throughput ELISA assay that can measure Aβ and other relevant metabolites efficiently. In the past, our lab has successfully established and used an efficient high-throughput ELISA assay to study the effect of genes (by RNAi) and cellular pathways (by chemical inhibitors) on the production of Aβ (Rajendran et al., 2006; Rajendran et al., 2008). Our lab further extended this approach to generate a high-throughput multiplexing assay (Udayar et al., 2013). This assay parallelly measures the different Aβ species as well as the β-cleaved ectodomain of APP (sAPPβ). A major advantage of this assay is that we get insights into the possible role of the gene/small inhibitor under study. Parallel measurement of Aβ and sAPPβ provides information whether a gene affects β-cleavage of APP (cases where sAPPβ levels is affected) or γ-cleavages (cases where Aβ levels is affected but not sAPPβ levels). This information helps in designing the further experiments for mechanistic characterization more efficiently. We can categorize the hits as either β-cleavage affecting or γ-cleavage affecting. For the ones that fall in the β-cleavage category we can design experiments to analyze APP or BACE1 levels, their localization, BACE1 activity etc. For the ones that fall in the γ-cleavage category we can analyze the levels of the different components of the γ-secretase, γ-secretase assembly, its activity and so on. Another major advantage of the multiplexing assay is that it measures Aβ and sAPPβ from a single sample and hence greatly minimizes sample and assay induced variations. In this multiplexing assay system, we can also combine the measurement of Aβ and sAPPα (product of α-cleavage of APP) or any desired combination of metabolites. This gives us a powerful tool to dissect the role of genes in the maintenance of Aβ levels more efficiently.

2. Objectives of the thesis

To study the membrane trafficking pathways involved in the production and clearance of Aβ peptides in neurons and microglia.

Recent advances suggest that cell biological knowhow is vital in understanding the etiology of AD and for therapeutic interventions. By curating a "road map" for Aβ metabolism, this study contributes significantly to our understanding of AD.

Chapter 1

A paired RNAi and RabGAP overexpression screen identifies Rab11 as a novel regulator of β-amyloid production

Vinod Udayar[a,b,c,d], Virginie Buggia-Prévot[f], Rita L. Guerreiro[g,m], Gabriele Siegel[a,b], Naresh Rambabu[h], Amanda L. Soohoo[i], Moorthi Ponnusamy[h], Barbara Siegenthaler[a,b], Jitin Bali[a,b,c], AESG[g], Mikael Simons[j,k], Jonas Ries[l], Manojkumar A. Puthenveedu[i], John Hardy[g,m], Gopal Thinakaran[f] and Lawrence Rajendran[a,b,c,e]

[a]*Systems and Cell Biology of Neurodegeneration,* [b]*Division of Psychiatry Research,* [c]*Graduate program of the Zurich Neuroscience Center,* [d]*Erasmus Mundus Joint Doctorate program,* [e]*Graduate program of the Zurich Center for Integrative Human Physiology, University of Zurich, August-Forel Str. 1, 8008, Zurich, Switzerland;* [f]*Departments of Neurobiology, Neurology and Pathology, The University of Chicago, Chicago, IL 60637,* [g]*Alzheimer's Exome Sequencing Group, University College London, UK,* [h]*Raise.Rural Foundation for promoting research awareness in Student Environment in Rural India,* [i]*Department of Biological Sciences, Carnegie Mellon University, Pittsburgh, PA 15213,* [j]*Department of Neurology, University of Göttingen, 37075, Göttingen Germany,* [k]*Max-Planck Institute for Experimental Medicine, 37075, Göttingen Germany,* [l]*Cell Biology and Biophysics, European Molecular Biology Laboratory, 69117, Heidelberg, Germany,* [m]*Reta Lila Weston Research Laboratories, Department of Molecular Neuroscience, UCL Institute of Neurology, London WC1N 3BG, UK*

Published in Cell Reports:

Cell Reports, 2013 Dec; 5:1536–1551, doi: 10.1016/j.celrep.2013.12.005

Author contributions

L.R designed research; V.U performed all the RNAi, RabGAP screens and validation experiments. G.S. performed the optimization of siRNA transfection in mouse primary neurons. B.S and J.B performed the ECL optimization assays. V.B-P and G.T performed plasmid cloning and live cell imaging experiments. M.S provided reagents. N.R performed the PPI network analysis of GWAS AD gene products. M.P integrated all the data to curate the roadmap for APP processing. A.L.S and M.A.P performed and analyzed the recycling experiments. R.L.G, J. H and the AESG group provided the exome sequencing data on Rab11. L.R, V.U, V.B-P and G.T analyzed the data. L.R wrote the paper and all the authors participated in the editing of the manuscript.

Abstract

Alzheimer's disease (AD) is characterized by cerebral deposition of β-amyloid (Aβ) peptides, which are generated from amyloid precursor protein (APP) by β- and γ-secretases. APP and the secretases are membrane-associated, but whether membrane trafficking controls Aβ levels is unclear. Here, we performed an RNAi screen of all human Rab-GTPases, which regulate membrane trafficking, complemented with a Rab-GTPase-activating protein screen, and present a roadmap of the membrane trafficking events regulating Aβ production. We identify Rab11 and Rab3 as key players. While retromers and retromer-associated proteins control APP recycling, we show that Rab11 controlled β-secretase endosomal recycling to the plasma membrane and thus affected Aβ production. Exome sequencing revealed a significant genetic association of a Rab11A variant with late-onset AD patients, and network analysis identified Rab11A and Rab11B as components of the late-onset AD risk network, suggesting a causal link between Rab11 and AD. Our results reveal new trafficking pathways that regulate Aβ levels, and show how systems biology approaches can unravel the molecular complexity underlying AD.

Introduction

Alzheimer's disease (AD) is the most common form of dementia and is characterized by the cerebral deposition of Aβ peptides in the form of amyloid plaques (De Strooper, 2010; Frisoni et al., 2011). The amyloid cascade hypothesis postulates that Aβ peptides trigger a series of pathological events leading to neurodegeneration (Huang and Mucke, 2012; Selkoe, 2011b). Aβ-peptides are liberated from the transmembrane amyloid precursor protein (APP) by the sequential actions of β-secretase and γ-secretase (Thinakaran and Koo, 2008; Willem et al., 2009). β-secretase activity is conferred by a transmembrane aspartyl protease, also termed BACE1 (β-site APP cleaving enzyme 1) (Vassar et al., 1999) whereas γ-secretase is a multimeric transmembrane protein complex composed of Presenilin-1 (PS1)/ Presenilin-2 (PS2), Nicastrin, Aph-1 and PEN-2 (Annaert and De Strooper, 2002; Selkoe and Wolfe, 2007). Familial mutations in APP, PS1 or PS2 that increase the production of the amyloidogenic Aβ42 peptide, have been associated with early-onset AD (Borchelt et al., 1996; Duff et al., 1996). However, there is only limited insight into the cause of late onset AD, which contributes to more than 95% of cases. Genetic modifiers of late onset AD may also regulate Aβ production, raising the possibility that genes regulating APP metabolism might impact the risk for AD (Andersen et al., 2005; Rogaeva et al., 2007; Selkoe, 2011a).

Several lines of evidence support an important role for membrane trafficking in the amyloidogenic processing of APP and hence in AD pathogenesis (Rajendran and Annaert, 2012; Thinakaran and Koo, 2008). APP and BACE1 are transmembrane proteins that are synthesized in the endoplasmic reticulum (ER), matured in the Golgi complex and then transported to the plasma membrane and into endosomes via endocytosis (Small and Gandy, 2006; Thinakaran and Koo, 2008). The endolysosomal compartment has been implicated as one of the major sites for Aβ generation (Cataldo et al., 2000; Haass et al., 1992; Koo and Squazzo, 1994). Recent work has revealed that BACE1 cleavage of APP occurs predominantly in early endosomes, and endocytosis of APP and BACE1 is essential for β-cleavage of APP, and Aβ production (Kinoshita et al., 2003; Rajendran et al., 2006; Sannerud et al., 2011). The pH of endosomes (pH 4.0-5.0) is optimal for BACE1 activity, which also explains the requirement for endocytosis (Kalvodova et al., 2005; Vassar et al., 2009). In contrast, α-secretase cleavage of APP, which precludes Aβ production, occurs at the plasma membrane (Lichtenthaler, 2011). Components of the γ-secretase complex are also synthesized in the ER, but their assembly and maturation requires the coordinated regulation of the ER-Golgi recycling circuit (Spasic and Annaert, 2008).

We previously showed that β-cleavage of APP occurs in a Rab5-EEA1 positive membrane compartment and that endocytosis is essential for Aβ generation (Rajendran et al., 2006). Targeting a transition-state BACE1 inhibitor to endosomes inhibited Aβ production in cultured cells and mice (Rajendran et al., 2008). Interestingly, proteins that belong to the retromer family, which transport cargo from early endosomes to the Golgi, have also been implicated in AD (Rogaeva et al., 2007; Small et al., 2005). These AD risk genes regulate the residency of APP and BACE1 in the early endosomal compartment therefore regulating Aβ generation (Siegenthaler and Rajendran, 2012). Similarly, proteins of the GGA family have been shown to traffic BACE1 from endosomes to the Golgi, and their depletion led to increased amyloidogenic processing of APP (He et al., 2005; Tesco et al., 2007; von Arnim et al., 2006). While APP is known to be routed from endosomes to golgi via the retromer- and retromer associated proteins including SORL1 and VPS26 proteins (Andersen et al., 2005; Morel et al., 2013; Small and Gandy, 2006; Rogaeva et al., 2007; Small et al., 2005; Siegenthaler and Rajendran, 2012), nothing much is known about BACE1 recycling from endosomes. A better understanding of the specific trafficking mechanisms involved in Aβ production will thus provide further insights into disease pathogenesis and potentially provide novel therapeutic strategies for treating this currently untreatable disease.

Rab GTPases regulate many aspects of membrane protein trafficking, acting as membrane organizers on cellular compartments that mediate vesicular trafficking and aid in vesicle fusion (Seabra et al., 2002). They regulate vesicular trafficking both in the biosynthetic and endocytic routes, enabling cargo sorting within the different membrane compartments (Zerial and McBride, 2001). Rab GTPases switch between an inactive GDP-bound form and an active GTP-bound form, which enables vesicular fusion (Stenmark and Olkkonen, 2001). While GDP-GTP exchange is mediated by Rab-specific GTP exchange factors (GEFs), GTP hydrolysis is achieved by the GTPase activating proteins, (GAPs) (Barr and Lambright, 2010). In humans, there are 60 Rab proteins and 39 RabGAPs. Overexpression of RabGAPs depletes the active form of Rab proteins and increases the inactive, GDP-bound form, thereby preventing their normal function (Yoshimura et al., 2007).

Here, we systematically analyzed the role of the cell's major membrane trafficking processes in Aβ production by the combined use of RNA interference (RNAi)-mediated silencing of all Rab GTPase proteins and an overexpression screen of the RabGAPs.

Results

Development of a multiplexing platform to quantitatively assay sAPPβ and Aβ levels

We first developed a multiplexing assay to quantitatively screen for Aβ and sAPPβ, the two products of the amyloidogenic processing of APP (Figure 1A), from a single sample. Simultaneous measurements of Aβ and sAPPβ from a single sample in the same well would indicate whether a 'hit' affected the β-cleavage of APP (changing sAPPβ levels) or the γ-cleavage/ fate of Aβ (changing Aβ levels) (Figure 1B). Thus, inter-measurement variations are avoided, which increases the sensitivity and signal-to-noise ratio allowing high-throughput measurements. We used an electrochemi-luminescence (ECL) assay platform as it provides high sensitivity and robust signal detection. In each well of a 384-well plate, one spot of anti-Aβ40 and one of anti-sAPPβ antibodies were separately spotted (Figure 1C). Two other spots were coated with BSA for background and non-specific binding controls. Upon binding to the analytes in the samples, electrochemical signals from the ruthenium-labeled respective secondary antibodies were detected through an image-based capture. Since the captured antibodies are spatially positioned at distinct spots in the well, the values corresponded to the amount of the analyte bound to the specific capture antibody. As a proof of principle, we studied the binding of synthetic Aβ40 and recombinant sAPPβ in the same well. We incubated different concentrations of synthetic Aβ peptides in the assay plate and found a linear dependency of the signal to the amount of peptide used at concentrations lower than 50ng/ml. At concentrations above 50ng/ml, we observed saturation (Figure 1D). Similar saturation kinetics were observed with recombinant sAPPβ protein, suggesting that this system perfectly recapitulates binding reactions. When only Aβ was added to the well, background signals were observed for sAPPβ, and vice versa. When both Aβ and sAPPβ were added in the same well, specific signals were detected (Figure 1D), demonstrating a high degree of specificity and no cross-reactivity between the two analytes. In addition, electrochemiluminescence detection allowed us to detect concentrations as low as 10-100 picograms of Aβ and sAPPβ.

We then proceeded to see if Aβ and sAPPβ could be measured from cultured cells and neurons from transgenic mice. Both Aβ and sAPPβ could be measured from HEK and HeLa cells stably expressing the pathogenic Swedish mutant of APP, which causes familial early onset AD (Figure 1E). Conditioned medium collected at different times shows that both Aβ and sAPPβ gradually accumulated in a time-dependent manner (Figure 1E). Increase in the volume of the conditioned supernatants produced a linear increase in the measurements

demonstrating assay robustness (Figure S1). We could also quantify sAPPβ and Aβ in cortical neurons from mice expressing human APP with Arctic/Swedish (Arc/Swe) mutations (Figure 1E). Sample swapping (Figure 1F) experiments showed that no significant signal was observed for the β-cleaved ectodomain of Swedish APP (sAPPβsw) when measured with the plate coated in capture antibodies, which recognized the β-cleaved ectodomain of wild-type APP (sAPPβwt). Similarly, no signal was obtained for sAPPβ when we swapped the sAPPβwt supernatants on the sAPPβsw-coated plates. However, robust signals for Aβ were detected in all conditions. Thus, the assay is highly specific for both Aβ and sAPPβ.

RNAi screen of human Rab proteins identifies novel proteins involved in Aβ and sAPPβ production

To study the role of all human Rab proteins in the regulation of amyloidogenic APP-processing, we first performed an RNAi screen in cells that robustly produce Aβ and sAPPβ (Rajendran 2006, Rajendran 2008), and assayed these products using the multiplexing electrochemiluminescence assay system (Figure 2A, 2B). We included APP, BACE1 and Pen2 (a subunit of the γ-secretase) as positive controls. As expected, silencing of APP and BACE1 decreased both Aβ and sAPPβ levels, whereas silencing of Pen2 decreased Aβ levels, but not sAPPβ levels (Figure 2A, 2B), further validating the assay. Quantification was based on the electrochemiluminescence counts, normalized to the cell viability counts and relative to that of the scrambled control (medium GC containing siRNA oligo (MedGC)). Apart from Rab36, silencing of the other Rab proteins did not significantly alter cell viability (Figure S1B). The screen identified Rabs that significantly decreased both Aβ and sAPPβ (Figure 2A and B), including Rab3A, Rab11A, Rab36 and Rab17 (Figure S2A, B). Rab36, a GTPase involved in late endosome positioning, was a top hit in the screen, decreasing both Aβ and sAPPβ (Figure 2C). A secondary validation screen reproduced all the selected hits (Figure S2C). Knockdown efficiency of the relevant genes was confirmed by RT-PCR (Figure S2D). Though our analysis accounts for toxicity, and quantifies Aβ and sAPPβ as a relative count of viable cells, Rab36 depletion was consistently toxic in all the screens (Figure S1B). Therefore, we removed it from further analysis.

Rab11A, the major Rab protein involved in the slow recycling of cargo proteins from early endosomes to the cell surface (Sonnichsen et al., 2000), was the second top hit in our analysis. In addition, silencing of the isoform, Rab11B, also reduced Aβ levels (Figure 2A). Interestingly, all the isoforms of Rab3, except Rab3C, decreased both Aβ and sAPPβ levels.

Rab3 proteins are involved in synaptic function (Schluter et al., 2004) and in the fast axonal transport of APP (Szodorai et al., 2009). Silencing of Rab3A and 3B decreased overall APP levels, suggesting that Rab3 plays a role in the trafficking and maintenance of APP levels (Figure S2E).

Silencing of Rab44, Rab6A and Rab10 decreased Aβ levels without affecting sAPPβ (Figure 2C), implying that these GTPases affect either γ-secretase cleavage or the fate of Aβ. Interestingly, knockdowns of several Rabs also increased both sAPPβ and Aβ levels. To understand how these trafficking pathways contributed to both Aβ and sAPPβ levels, we plotted the normalized values of Aβ and sAPPβ values from the screen in a 2-dimensional plot and observed a largely correlative curve for both the values, indicating that the Rab proteins responsible for regulating β-cleavage are also responsible for controlling Aβ levels and that any perturbation at the level of BACE1 cleavage of APP is the rate-limiting step in Aβ production (Figure 2D).

RabGAP overexpression screen identifies overlapping hits with the Rab RNAi screen

As RNAi can have off-target effects leading to false positive results, we complemented our RNAi screen with an overexpression screen of all 39 RabGAPs in the human genome, which suppress Rab function by accelerating the hydrolysis of GTP. In this screen, we overexpressed each RabGAP in the same cellular system used for the RNAi screen and quantitatively measured Aβ, sAPPβ levels and cell viability (Figure 3; Figure S1). Many RabGAPs were found to affect sAPPβ and Aβ levels (Figure 3). RN-TRE, a GAP which has previously been shown to affect amyloidogenic processing of APP (Ehehalt et al., 2003) reduced both Aβ and sAPPβ. TBC1D10B, a GAP for Rab35, Rab27A, Rab22A, Rab31 and Rab3A, decreased both Aβ and sAPPβ (Frasa et al., 2012). However, only Rab3A silencing via RNAi decreased Aβ and sAPPβ (Figure 2, 3). EVI5, a RabGAP for Rab11 (Frasa et al., 2012; Laflamme et al., 2012), decreased both Aβ and sAPPβ. In addition, one other RabGAP for Rab11, namely TBC1D15, decreased both Aβ and sAPPβ. Intriguingly, TBC1D14, which alters Rab11 localization and subsequently delays recycling of Transferrin to the plasma membrane (Longatti et al., 2012), decreased Aβ levels (Figure 3C). These results independently identified Rab11 as an important regulator of sAPPβ and Aβ production.

Epistasis mini-array profiling identifies distinct trafficking routes

We next analyzed whether the identified Rabs regulated Aβ production through the same trafficking pathway or through distinct mechanisms. To this end, we performed an epistasis mini array profiling (EMAP) screen (Schuldiner et al., 2005) wherein we silenced all the hits against all the hits in a 14 x 14 matrix, to determine whether a combined knockdown gives rise to an aggravating (non-interacting) or alleviating (interacting) phenotype (i.e. β-cleavage of APP). Here again, single knockdowns of either Rab3A or Rab11A decreased sAPPβ levels (Figure S3). However, when they were silenced together, a further decrease (an aggravating phenotype) was observed, which indicates that Rab3A and Rab11A act independently and contribute to β-cleavage via distinct trafficking routes. Most of the genes that were identified as hits did not interact with each other, with the exception that a double knockdown of Rab10/ Rab23 or Rab10/ Rab25 showed an alleviating phenotype, suggesting that these Rabs regulate the same membrane trafficking pathways.

Validation of Rab11A as a hit

Since Rab11A was identified as one of the strongest hits in both the RNAi screen and the RabGAP screen, we independently validated this finding in a different cellular model. siRNA mediated silencing of Rab11A in HEK cells stably expressing wtAPP led to a strong reduction of both Aβ and sAPPβ levels (Figure S4A), similar to the effect observed upon silencing of Rab11A in HeLa cells stably expressing sweAPP (Figure 4A). Consistent with this, Western blotting analysis with anti-APP C-terminus antibodies revealed a strong reduction in β-C-terminal fragment (CTF) levels (C99) with increase in α-CTF levels (Figure 4B). This suggests that Rab11A silencing markedly affected β-cleavage of APP and also Aβ levels. Western blotting with anti-Rab11A antibodies showed that Rab11A silencing efficiently knocked down the protein (Figure 4B) (with > 90% efficiency). In addition, Rab11A silencing led to a decrease in all three species of Aβ (Aβ38, 40 and 42) (Figure 4C), and reduced amyloid levels in the cell lysates suggesting that Rab11A regulates Aβ production rather than secretion (Figure S4B). Silencing of Rab11A using 4 different siRNAs singly also led to a decrease in Aβ without affecting cell viability, thus demonstrating the specificity of the observed effect (Figure 4D). All siRNAs against Rab11A also silenced Rab11A expression (Figure 4D inset).

To further validate these results, we employed a different strategy to interfere with Rab11 function. Since Rab-proteins exist in both a GTP-bound and GDP-bound form, we

overexpressed the GDP-locked (dominant negative; DN) mutant forms of Rab11A (the ubiquitously expressed isoform) and Rab11B (the isoform highly expressed in neurons) in cells to phenocopy the effect of Rab11 silencing. Similar to silencing of Rab11A, overexpression of Rab11A-DN reduced Aβ and sAPPβ levels significantly. Overexpression of Rab11B-DN (which would also interfere with the function of WT-Rab11) also significantly reduced Aβ and sAPPβ levels (Figure 4E).

Finally, we assessed the effect of silencing the expression of evolutionarily conserved Rab11 family-interacting proteins on β-cleavage of APP in the cells (Lindsay and McCaffrey, 2002). Knock down of four of the five FIP family proteins (Shiba et al., 2006), with the exception of Rab11FIP1 (retromer-like), decreased sAPPβ levels (Figure 4F). Thus, not only Rab11 but also Rab11-interacting proteins, which were identified as Rab11-effector proteins, reduced β-cleavage of APP.

Rab11 silencing in primary neurons from WT and APP transgenic mice reduce Aβ levels

We next studied if Rab11 also regulated Aβ production in the neuronal context. Silencing Rab11A and Rab11B in primary neurons isolated from APP transgenic mice significantly decreased both sAPPβ and Aβ levels (Figure 4G). Both RT-PCR and Western blotting analysis show efficient silencing of Rab11A and 11B (Figure S4C, D and Figure 4H). Knockdown of Rab11A and Rab11B in primary neurons isolated from WT mice again reduced Aβ (both Aβ40 and Aβ42) levels (Figure 4I-J). Moreover, silencing either Rab11A or Rab11B also significantly decreased Aβ levels (Figure S4E). Thus, Rab11 is crucial for β-cleavage and Aβ generation.

Rab11 controls membrane trafficking of BACE1

We hypothesized that Rab11 must regulate either at the level of APP or at the level of BACE1. Rab11 silencing or Rab11A DN expression did not affect the total cellular levels of APP or BACE1 (Figure 4B and Figure S4F respectively). To analyze protein localization, we performed live cell imaging of cells transfected with either APP-YFP or BACE1-YFP using a wide-field microscope maintained under a temperature-controlled environment. BACE1-YFP prominently localized to the perinuclear endocytic recycling compartment (ERC), and was also found in numerous highly motile vesicular and tubular structures dispersed throughout the cell (Figure 5A). Inspection of individual carriers revealed rapid transport of tubulo-

vesicular structures along a curvy linear trajectory, suggesting active transport along microtubules. Indeed, brief treatment of cells with the microtubule disrupting reagent nocodazole inhibited dynamic transport of BACE1, and induced the formation of enlarged immobile vesicles (not shown). The distribution and dynamics of BACE1 trafficking, but not of APP, was markedly altered by expression of $Rab11A_{S25N}$, the dominant negative mutant of Rab11 (Rab11A DN) (Figure 5A). The length of the BACE1-positive tubular carriers emanating from the ERC was significantly enhanced by Rab11A DN overexpression, but remained highly dynamic, suggesting that GTPase activity of Rab11 is involved in the fission of BACE1 tubular carriers and/or their tethering and fusion with the target.

Rab11 GTPase is involved in recycling many cargos from the ERC, including the recycling endosome marker transferrin receptor (TfR) (Sonnichsen et al., 2000). TfR as well as internalized transferrin becomes associated with a distinct tubular network in cells expressing Rab11 DN (Choudhury et al., 2002; Wilcke et al., 2000). To address whether BACE1 follows the recycling route from recycling endosomes, we first checked whether BACE1 colocalizes with TfR. BACE1 significantly co-localized with TfR (Figure 5B). Not only the steady state levels of TfR, but also internalized transferrin colocalized with BACE1 in Rab11 compartments (data not shown). In control cells and those transfected with Rab11A WT, BACE1-YFP colocalized with TfR in the ERC as well as in numerous vesicles and short tubulo-vesicular carriers (Figure 5B). However, in cells expressing Rab11A DN, BACE1 and TfR were found in elongated tubular structures that emanated from the ERC (Figure 5B). Neither the prominent perinuclear localization of APP in the TGN nor the dynamics of APP-positive structures was disturbed by Rab11A DN expression (Figure 5A). Thus, BACE1 localization and trafficking is akin to that of TfR, which requires recycling via the Rab11-mediated pathway for transferrin internalization. Since Rab11 regulates the recycling of TfR through the slow recycling route, it may also regulate the recycling of BACE1 thus affecting both the cell surface as well as the early-endosomal trafficking of BACE1.

Rab11 affects the recycling of BACE1

Since BACE1 accumulated in elongated tubulo-vesicular structures in cells expressing Rab11A DN, we hypothesized that under these conditions, BACE1 is unable to be trafficked to the plasma membrane and thus is unavailable for re-internalization to early endosomes, the site of β-amyloid production. To test this, we performed two different experiments. First, we tested if Rab11A regulated cell surface levels of BACE1 using FLAG-tagged BACE1 (Figure

S5A). Here we used both FACS (Fluorescent Activated Cell Sorting) as well as immunofluorescence on cells transfected with either control or Rab11A DN expressing plasmids. Cells expressing Rab11A DN indeed displayed reduced cell surface levels of BACE1 (Figure 6A and B). Similar results were obtained using imaging of cell surface labeled BACE1 in HeLa (Figure 6C) and primary neurons (Figure 6D). Rab11A DN did not reduce the total levels of BACE1 (Figure S4F) in line with the observations that under Rab11A DN expressing conditions, BACE1 accumulates in the tubulo-vesicular compartments and is not re-routed to degradative compartments.

Next, we specifically looked at the effect of Rab11A in the recycling pool of BACE1 using a quantitative ratiometric assay to measure recycling by differential labeling. To this end, cells were labeled with Alexa 647-conjugated M1 anti-FLAG for 30 min at 37˚C, to allow antibodies to bind surface BACE1 and be internalized. After internalization, cells were incubated with Alexa 488-conjugated secondary antibodies for 30 min at 37˚C, to detect internalized anti-FLAG-bound receptors that recycled to the surface. In the Rab11A DN expressing cells, BACE1 recycling was significantly decreased, confirming that Rab11 functions to recycle BACE1 from the endosomes to the plasma membrane (Figure 6E). Quantitation of the fluorescence signal clearly revealed that the recycling pool of BACE1 is markedly decreased in cells expressing Rab11A DN. Two parallel controls were used: a surface control, where cells both incubations were performed at 4˚C, and an endocytosis control, where the first incubation was at 37˚C and the second at 4˚C (Figure S5B). Cells without BACE1 did not show any labeling under these conditions.

Together these results suggest that vesicular trafficking regulated by Rab11 GTPase is critically important for the homeostatic regulation of BACE1 trafficking and Aβ production in endocytic organelles.

Rab11 genetic variability in Late-onset Alzheimer's disease

We used exome sequencing data from 170 neuropathologically assessed controls and 185 late-onset AD patients to study if variants in Rab11A were associated with disease risk. Our results revealed a significant association of a variant in Rab11A (rs117150201, uncorrected p value = 0.01), thus establishing a potential association between Rab11 and AD (Table 1).

Network analysis of GWAS genes linked to late-onset AD identifies Rab11A and Rab11B as interacting proteins

To determine whether other genes linked with late onset AD (LOAD) risk also acted via Rab11, we used protein-protein interaction (PPI) network analysis to study the interaction partners of proteins linked to LOAD risk. We used the protein products of top 10 genes linked to LOAD (Alzgenes; www.alzgene.org) and created a two-level depth interactome of these proteins. In the cluster with Bin1, a risk gene that is strongly associated with LOAD risk, we identified both Rab11A and Rab11B and their interacting proteins, Rab11FIP1-5 (Fig. S6). In our RNAi-based screen, Rab11A, Rab11B and all the FIPs (except for FIP1) regulated β-amyloid levels further supporting the findings that the LOAD risk gene, Bin1 could contribute to amyloid production via Rab11. Interestingly the Bin1 cluster also included Arf6, a known player in BACE1 endocytosis to early endosomal compartments (Sannerud et al., 2011) and GGA3, which regulates early endosomal residency of BACE1 (Tesco et al., 2007), further supporting the link between Bin1, Rab11 and BACE1 endocytosis and recycling. These results from this unbiased network analysis strongly link Rab11 to late-onset AD risk.

New Rabs and membrane trafficking pathways in amyloid secretion

Using a systems approach, our screen also identified other regulatory active Rabs and provides new insights into membrane trafficking pathways that play crucial roles in amyloid production and secretion. This allowed us to present the first comprehensive roadmap for APP processing (Figure 7). Most of the hits were Rabs involved in the regulation of the trafficking either to or from early endosomes (Galvez et al., 2012), confirming the critical role of early endosomes in β-amyloid generation (Kinoshita et al., 2003; Koo and Squazzo, 1994; Rajendran et al., 2006; Small and Gandy, 2006). In addition to Rab11, several other Rabs were identified to also regulate β-amyloid levels. Silencing of Rab2A, for instance, increased Aβ and sAPPβ levels (Figure 2), and the cognate GAP, TBC1D11, showed a similar effect (Figure 3). Rab2A is involved in the maintenance of Golgi structure and function. It interacts with the atypical protein kinase C (aPKC) (Tisdale, 2003) that positively regulates α-cleavage of APP via α-secretase (Nitsch et al., 1993).

On the other side, Rab5C silencing significantly increased sAPPβ and Aβ, while the other Rab5 isoforms did not. Rab5C is involved in the endocytosis and recycling of cell surface

molecules (Onodera et al., 2012). Silencing of Rab5C dramatically increased the cellular levels of APP (Figure S2E), which explains the increase in sAPPβ and Aβ.

The Rab proteins that have been implicated in exosome release, namely Rab27 and Rab35 (Hsu et al., 2010; Ostrowski et al., 2010), negatively regulated Aβ and sAPPβ levels (Figure 2). This is consistent with our previous work showing that very small amounts of Aβ can be released via exosomal vesicles, and suggests that the exosomal pathway is connected to an intracellular degradation mechanism and that inhibition of the exosomal pathway re-routes the cargo for effective secretion.

Discussion

To rule out potential off-target effects of the RNAi screen, we complemented it with 5 independent experimental conditions: 1) an unbiased Rab-GAP overexpression screen. To our knowledge, this is the first time a paired RNAi screen (of all human Rab GTPases) and an overexpression screen (of Rab GTPase activating proteins (RabGAPs)) was performed. 2) Rab11 DN phenocopied the effect of RNAi of Rab11, 3) All 4 different siRNAs against Rab11 decreased Aβ levels, 4) Rab11 RNAi had the same effect in many different cells including primary neurons, and finally 5) silencing Rab11-associated proteins such as EHD or FIPs produced similar effect.

The results from our RNAi, RabGAP and EMAP screens provide a valuable list of all the human Rab proteins that affect Aβ and sAPPβ levels and their nature of interaction. We also silenced different isoforms of a particular Rab by means of RNAi and indeed, in many cases, we found isoform specific effects on Aβ levels.

Silencing of Rab4A, Rab6A and Rab10 decreased only Aβ. Conversely, silencing of Rab8A, Rab25, Rab14 and Rab34 significantly increased only Aβ. Such Aβ specific effects are likely the result of either an altered γ-secretase cleavage of APP or a change in secretion and/or degradation of the produced Aβ. Of particular interest is Rab8, which increased Aβ levels when depleted in cells. Rab8 is involved in various physiological functions such as exocytosis and cilia formation. Interestingly, expression of a mutant Presenilin-1 (A260V) in PC12 cells dramatically decreased Rab8 levels thus affecting trafficking via Golgi (Kametani et al., 2004). We also identified some hits that specifically decreased sAPPβ levels without affecting Aβ. While this at first seems counter-intuitive, it implies the possibility that specific

Rabs play a role in the release/secretion of sAPPβ without affecting the processing of APP. However, we see a clear overall correlation of sAPPβ and Aβ which suggests two things: a) β-cleavage is rate-limiting and thus determines cellular and secreted Aβ levels, or b) compartments that define β-cleavage are also involved in γ-cleavage of APP to generate Aβ (Kaether et al., 2006; Rajendran et al., 2006).

We identified Rab11 as a main regulator of APP processing. Both by ECL assays and through Western blotting to study APP processing, we show that BACE1-mediated processing of APP is affected in Rab11-silenced cells. Interestingly, while we see a significant reduction in C99 levels, C83 levels are increased. This could be due to an increased α-cleavage of APP or C99 or could also represent a defect in γ-secretase cleavage demonstrating that Rab11 recycling endosomes play a crucial role in APP processing and Aβ production. Indeed, Rab11 has been shown to interact with γ-secretase component, Presenilin (Dumanchin et al., 1999; Wakabayashi et al., 2009). However, we did not observe any influence of Rab11A on the activity or localization of γ-secretase (data not shown).

APP endocytosis is mediated by the YENPTY cytosolic motif and is regulated by both cholesterol-dependent and clathrin-mediated endocytic pathways (Perez et al., 1999; Schneider et al., 2008). Similarly, endocytosis of BACE1 has been shown to be both clathrin-dependent and clathrin-independent via the ADP-ribosylation factor 6 pathway (Prabhu et al., 2012; Sannerud et al., 2011). So far, early endosomes, TGN and the plasma membrane have been suggested to contribute to β-amyloid production (Choy et al., 2012; Chyung and Selkoe, 2003; Rajendran et al., 2006; Sannerud et al., 2011). While APP is known to be routed from endosomes to Golgi via the retromer and associated proteins (Andersen et al., 2005; Morel et al., 2013; Small and Gandy, 2006; Rogaeva et al., 2007; Small et al., 2005; Siegenthaler and Rajendran, 2012), nothing much is known about BACE1 recycling from endosomes.

Our results now identify the Rab11-dependent slow recycling pathway as a novel trafficking route involved in Aβ generation. A recent study showed that synaptic activity mediates the convergence of APP and BACE1 in acidic microdomains that colocalize with Transferrin receptor (TfR)(Das et al., 2013). Since this study did not look at co-localization of APP and BACE1 in Rab11 compartments and that a significant proportion of TfR is also found in early endosomes (Sonnichsen et al., 2000), the interaction most likely occurs in early endosomes as TfR is internalized from the plasma membrane to early endosomes and then is

recycled to the plasma membrane via Rab11-positive vesicles. Several studies suggest that early endosomes are the compartments where BACE1 cleaves APP, also in the neuronal context (Choy et al., 2012; Chyung and Selkoe, 2003; Rajendran et al., 2006; Sannerud et al., 2011). The fact that retromer-associated proteins or GGA3 regulate Aβ levels is due to their involvement in sorting of APP or BACE1 respectively, from early endosomes and not recycling endosomes (Andersen et al., 2005; Morel et al., 2013; Siegenthaler and Rajendran, 2012; Tesco et al., 2007). Furthermore, early endosomes are acidic (Maxfield and Yamashiro, 1987) and recycling endosomes are not as they lack functional vacuolar ATPase (Gagescu et al., 2000; Schmidt and Haucke, 2007). In addition, we do not observe the β-cleaved ectodomain of APP in Rab11-positive compartments (Rajendran et al. 2006), suggesting that the compartments that Das et al., observed as stations where APP and BACE1 meet are most likely to be early endosomes and not recycling endosomes. So, how do recycling endosomes contribute to β-amyloid generation? Our results now clearly show that mechanistically, Rab11-containing recycling endosomes mediate the recycling of BACE1 to replenish the pool of BACE1 in early endosomes. In support of this latter notion, our time-lapse analysis shows dramatic alteration of BACE1 dynamics in cells expressing Rab11A DN mutant. In addition, we could clearly demonstrate that recycling of BACE1 from endosomes to the plasma membrane (for subsequent re-internalization) is severely impaired in the absence of functional Rab11 using both FACS and recycling assays. In addition, Rab17, another protein involved in the recycling of internalized cargo also regulated sAPPβ and Aβ levels thus underscoring the importance of recycling endosomes in APP processing.

Our screen and validation results uncover a new trafficking route involved in Aβ production. Since BACE1 cleavage of APP is critically involved in the pathogenesis of early onset AD (Yang et al., 2003) and in certain forms of sporadic AD (Jonsson et al., 2012), we propose that Rab11-mediated recycling route represents a novel drug target for AD, which is supported by our exome sequencing results and the unbiased protein-protein interaction network analysis. Interestingly, Eps15 homology domain-containing (EHD) proteins, which form complexes with Rab11 via Rab11FIP2, were independently identified as critical regulators of dynamic BACE1 trafficking and axonal sorting in hippocampal neurons. Moreover, knockdown of EHD1 or EHD3 significantly reduced Aβ levels in primary neurons [Buggia-Prévot et al., in press]. The network model suggests that the interaction of Bin1 with Rab11 is via Arf6, a known player in BACE1 endocytosis to early endosomal compartments (Sannerud et al., 2011) and GGA3, a protein that regulates early endosomal residency of

BACE1 (Tesco et al., 2007) is also involved in the network, further supporting the link between Alzheimer's disease risk and Rab11-mediated BACE1 endocytosis and recycling.

Taken together, our results clearly establish a novel link for recycling endosomes in BACE1 recycling, Aβ generation and AD and underscore the importance of systems level analysis in understanding the complexity of AD.

Materials and Methods

cDNA constructs

Plasmids encoding DsRed-tagged human WT Rab11A and DN mutant (S25N) (Choudhury et al 2002) were purchased from Addgene. C-terminally EYFP-tagged mouse BACE1 was generated by subcloning BACE1 cDNA (provided by Nabil G. Seidah), in-frame into the pEYFP-N1 vector. HA-tagged Rab11A constructs have been described (Ren et al., 1998). The sequence corresponding to the Flag epitope in the BACE1-FLAG construct was introduced after the pro-peptide cleavage site within the lumenal domain of mouse BACE1 using the following primers:
5'- CCGGGAGACCGACTACAAGGACGATGATGACAAGGGGGGAGGATC and 5'-CCGGGATCCTCCCCCCTTGTCATCATCGTCCTTGTAGTCGGTCTC.

siRNA

siRNAs were purchased from Invitrogen (stealth siRNA).

RNAi screen

RNAi screen was performed using HeLa cells expressing the Swedish APP mutation (HeLa-sweAPP). siRNA were transfected with a final concentration of 5nM using Oligofectamine (Invitrogen) as transfection reagent at a concentration of 0.3µl in a total volume of 100µl following manufacturer's instructions. Each siRNA transfection was performed in quadruplicate. After 24 hr the transfection mix on the cells was replaced with fresh culture medium. 69 hr after transfection, medium was again replaced with 100 µl fresh medium containing 10 % Alamar blue (AbD Serotec). 72 hr after transfection, Alamar blue measurements were taken using SpectraMAX GeminiXS (Molecular Devices) at an excitation wavelength of 544nm and emission at 590nm. Supernatant was collected and assayed for Aβ and sAPPβ. The cells in the transfected plate were lysed with 50 µl of lysis buffer for 20 min on ice.

RabGAP screen

The RabGAP screen was performed in HeLa-sweAPP cells. Cells were seeded in 96-well plates at a density of 6000 cells/well one day before transfection. Effectene (Qiagen) was used as transfection reagent following manufacturer's instruction using 2.5 µl of Effectene and 0.8 µl of Enhancer in a total volume of 100µl. Transfection mix was replaced with fresh

medium after 3.5 hr. 24 hr after transfection, medium was again replaced with fresh medium containing 10 % Alamar blue (AbD Serotec). 27 hr after transfection, Alamar blue measurements were taken using SpectraMAX GeminiXS (Molecular Devices) at an excitation wavelength of 544nm and emission at 590nm. Supernatant was collected and assayed for Aβ and sAPPβ using the Electrochemiluminescence assay (see Extended Methods section). The cells in the transfected plate were lysed with 30 µl of lysis buffer, incubated for 20 min on ice and stored at -20°C.

Live cell image acquisition and processing

Images were acquired on a motorized NikonTe2000 microscope equipped with a Cascade II:512 CCD Camera (Photometrics) using a 100X objective (NA 1.4). During live imaging, cells were maintained at 37°C in imaging medium [140 mM NaCl, 5 mM KCl, 3 mM $CaCl_2$, 2 mM $MgCl_2$, 1.5mM D-glucose, and 10 mM HEPES (pH 7.4)] in a custom-designed environment chamber. Time-lapse images were acquired at the rate of 2 frames/sec. Images of fixed cells were acquired as 200 nm z-stacks, deconvolved using Huygens software (Scientific Volume Imaging). Extended Depth of Field plugin of ImageJ software was used to generate single plane projections from processed z-stacks (Rasband, 1997-2012; Forster et al., 2004).

Recycling assay

Cells were labeled with Alexa 647-conjugated M1 anti-FLAG for 30 min at 37˚C, to allow antibodies to bind surface BACE1 and be internalized. Cells were washed twice in media, and incubated with Alexa 488-conjugated secondary antibodies for 30 min at 37˚C, to detect labeled internalized receptors that recycled to the surface. Cells were fixed in 4% paraformaldehyde for 15 min, washed, mounted, and imaged. Cells were imaged using an Andor Revolution XD spinning disk system with a Nikon Eclipse Ti automated inverted microscope, using a 60x TIRF 1.49 NA objective. Images were acquired using an Andor iXon+ EM-CCD camera using Andor IQ with 488, 561, and 647 nm solid state lasers as light sources, using identical parameters for all images. Confocal images were collected as tiff stacks and analyzed in ImageJ (National Institutes of Health, Bethesda, MD). All fluorescence quantitations were performed on images directly acquired from the camera with no manipulation or adjustments. To measure fluorescence, a region of interest was drawn around each cell, and the mean fluorescence in each channel recorded. In each field, a region of the field without cells was chosen to estimate background. Percent recycling was

calculated as the ratio of 488 to 647 fluorescence, after background correction. Statistical analyses were done using Microsoft Excel or Graphpad Prism (Graphpad Software, La Jolla, CA).

Epistasis mini-array profiling

Epistasis mini-array profiling (EMAP) was performed keeping the general siRNA transfection method the same as the one followed for the RNAi screen except that a final siRNA concentration of 10nM was used (5nM siRNA for each targeted gene). For the single knockdowns, 5 nM of the specific siRNA pool was combined with 5 nM of Scrambled (MedGC) siRNA. In the EMAP screen, we silenced hit 1-14 Rabs (indicated in Figure S6) vs. 1-14 Rabs.

siRNA transfection for HEK-wtAPP cells

Lipofectamine RNAiMAX (Invitrogen) was used as transfection reagent. 24hr prior to transfection, cells were seeded at an initial seeding density of 3500 cells per well in a 96-well plate pre-coated with Poly D lysine (Sigma Aldrich). siRNAs were transfected at a final concentration of 5 nM by using 0.3 μl of Lipofectamine RNAiMAX(Invitrogen) in a total volume of 100μl. Each siRNA transfection was performed in quadruplicates. After 48 hr the transfection mix was replaced with fresh medium containing 10 % Alamar blue (AbD Serotec). 60 hr after transfection, Alamar blue measurements were taken using SpectraMAX GeminiXS (Molecular Devices) at an excitation wavelength of 544nm and emission at 590nm. Supernatant was collected and assayed for Aβ and sAPPβ as described in the ECL section. The cells in the transfected plate were lysed with 35 μl of lysis buffer for 20 min on ice.

Off-Target prediction of the siRNAs

For Stealth siRNAs, the off-target effects are determined using the Smith-Waterman alignment methods. These off-target effects are associated with the presence of one or more perfect 3' untranslated region (UTR) matches with the hexamer or heptamer seed region (positions 2-12) of the antisense strand of the Stealth siRNA. We screen the 5', 3' and CDS sequence for any potential off target effects. In case there is a positive alignment this is listed as potential off-target effect. (Smith and Waterman, Journal of Mol. Biol. 147:195:7).

Plasmid transfection

The plasmid transfection for Rab11 DN was performed in HeLa-sweAPP cells. Lipofectamine 2000 (Invitrogen) was used as transfection reagent. Cells were seeded in a 96-well plate at an initial seeding density of 6000 cells per well 24h prior to the transfection. 0.3 μg of plasmid DNA was was transfected using 0.3 μl of Lipofectamine 2000 in a total volume of 100μl. Transfection mix was replaced after 3 hr by fresh culture medium. 21 hr after transfection, medium was again replaced with fresh medium containing 10 % Alamar blue (AbD Serotec). 60 hr after transfection, Alamar blue measurements were taken. Supernatant was collected and assayed for Aβ and sAPPβ. The cells in the transfected plate were lysed with 35 μl of lysis buffer, incubated for 20 min on ice and stored at -20°C.

siRNA transfection in primary neurons

Mouse primary cortico/hippocampal neuronal cultures were prepared from embryos (E16) from either wildtype mice or transgenic mice expressing the human APP with the Swedish mutation. siRNAs were transfected at a final concentration of 100nM using 0.45 μl of Lipofectamine RNAiMAX (Invitrogen) as transfection reagent in a total volume of 100μl.

Electrochemiluminescence detection of human Aβ 38, 40 and 42 and mouse Aβ

For the measurement of Aβ38, 40 and 42, Aβ triplex plates were used. For the measurement of mouse Aβ, mouse Aβ specific ECL assay plates were used with 4G8 antibodies as detection antibodies enabling the detection of Aβx-38;-40,42 peptides. Pre-coated plates were blocked with TBST (Tris Buffered Saline containing Tween), containing 1% Blocker A, for 1 hr at room temperature on a shaker at 750rpm. After washing, 25 μl of the cell culture supernatant was added to each well along with 25 μl of detection antibody followed by incubation for 2 hr at room temperature on a shaker at 750rpm. After washing detection was performed in 35 μl of 2X MSDT read buffer and read with the Sector Imager 6000.

Real-time RT-PCR

Total RNA from cultured cells or Primary neurons was isolated using TRIzol (Invitrogen) according to manufacturer's instructions. 1 μg of total RNA was used to prepare cDNA using the iScript cDNA synthesis kit (BIO-RAD) according to the manufacturer's recommended protocol. Real-time PCR was performed using iTaq Universal SYBR Green Supermix (BIO-RAD) according to manufacturer's instructions. Relative gene expression levels were calculated with the ΔΔCt method using GAPDH for normalization.

Cell culture and transfection

HeLa cells expressing the Swedish mutant of APP (HeLa-swAPP) were grown as previously described (Bali et al., 2012). HEK-293 cells were obtained from ATCC and maintained in HyClone DMEM (Fisher Scientific) supplemented with 10% FBS. Cells were plated in 24-well plates and co-transfected with FLAG-BACE1 and wild type or S25N Rab using Effectene (Qiagen), using 0.2 μg plasmid DNA and according to manufacturer's instructions. They were passed onto 25mm coverglass 24 hr after transfection and imaged after 48 hours. COS-7 cells were cultured in DMEM 10% bovine growth serum (HyClone), supplemented with 2 mM L-Glutamine and Penicillin/Streptomycin (Gibco). Cells were plated on poly-L-lysine-coated 35 mm glass bottom dishes (MatTek) for live imaging or on 18 mm microscope coverglass for immunofluorescence staining. Cells were transfected overnight with 1μg total of DNA using Fugene (Roche), according to the manufacturer's instructions.

Immunofluorescence

Cells were fixed using 4% paraformaldehyde and permeabilized for 5 min at room temperature, with 0.2%Triton X-100 in PBS. The coverslips were then blocked with PBS containing 3% BSA, 50 mM NH_4Cl, and 10 mM glycine for 1 hr. Human anti-transferrin receptor antibody (Invitrogen) diluted in PBS 3% BSA 0.2% Tween20, was added and incubated for 1 hr at room temperature. Subsequently, the coverslips were incubated with Cy5-conjugated goat anti-mouse antibody (Invitrogen) for 1 hr at room temperature and mounted using Permafluor (Thermo Fisher Scientific).

Alamar Blue assay

69 hr post-transfection, the medium of transfected cells was replaced with normal medium containing 10% Alamar blue. The final volume in each well was 100 μL. 3 hr after the medium change, cell viability was monitored using Fluoroscan Ascent Cf (Labsystems), with excitation wavelength 544nm and emission at 590nm. The cell viability was measured using the Alamar blueTM assay (Serotec Ltd., Kidlington, Oxford, UK), where the absorbance was monitored at the end of the reaction (after 3 hr) (Labsystems Multiscan MS UV visible spectrophotometer).

Protein-Protein Interaction Analysis of Proteins linked to late-onset Alzheimer's disease

The ID of the risk genes *(Bertram L, McQueen M, Mullin K, Blacker D, Tanzi R. The AlzGene Database. Alzheimer Research Forum. Available at: http://www.alzgene.org)* were used as input to query the String database (ww.string-db.org, University of Zurich, Switzerland) against the Homo sapiens datasets and the protein-protein interactome was visualized using cytoscape (Cytoscape™, Seatle, US). Since our study is focused on finding how the genes interact with each other at different levels/depth of the network, only the data from Experiments, Databases & Text mining were taken into consideration. The confidence score was set to highest confidence to minimize the possibility of false positives. The number of interactors was limited to a maximum of 50. The AD risk genes were used as core nodes to initialize the network construction. STRING database was queried with the individual core nodes to retrieve the primary nodes (First level of network construction). Later the STRING database is queried with the primary nodes to extract the respective secondary nodes (second level of network construction). The RAB11FIP3 node is extended to one more level to have a better understanding on its role in the whole interactome. All the data were downloaded as tab delimited text files from the STRING database and imported to cytoscape for data integration, visualization and analysis. The data integration is carried out with the aid of Advanced Network Merge plugin *[http://cbio.mskcc.org/~jgao/]*. The organic layout is generated to have a better visual on the clustered structure of the graph.

Western Blotting

After 72 hr of siRNA transfection or 24 hr after plasmid transfection, cells were lysed in buffer containing 2% NP-40 and 0.2% SDS and protease inhibitors (Roche). Equal amounts of the lysate (according to the protein content quantified by BCA assay (Pierce) were run on 4-12% BIS-TRIS gels (Invitrogen). The gel was blotted onto a nitrocellulose membrane (BioRad) and probed with the respective antibodies.

Anti-APP, C-Terminal antibody: SIGMA (F3165-1MG), Anti-BACE1 antibody: Prosci incorporation (2253), Anti-Rab11A antibody: Abcam (ab128913), GAPDH antibody: Meridian Science.

Author contributions

L.R designed research; V.U performed all the RNAi, RabGAP screens and validation experiments. G.S. performed the optimization of siRNA transfection in mouse primary neurons. B.S and J.B performed the ECL optimization assays. V.B-P and G.T performed

plasmid cloning and live cell imaging experiments. M.S provided reagents. N.R performed the PPI network analysis of GWAS AD gene products. M.P integrated all the data to curate the roadmap for APP processing. A.L.S and M.A.P performed and analyzed the recycling experiments. R.L.G, J. H and the AESG group provided the exome sequencing data on Rab11. L.R, V.U, V.B-P and G.T analyzed the data. L.R wrote the paper and all the authors participated in the editing of the manuscript.

AESG (Alzheimer's Exome Sequencing Group):
Rita Guerreiro[1,2]
José Brás[1]
Celeste Sassi[1,2]
J. Raphael Gibbs[1,2]
Dena Hernandez[1,2]
Michelle K. Lupton[3]
Kristelle Brown[4]
Kevin Morgan[4]
John Powell[3]
Andrew Singleton[2]
John Hardy[1]

1. Department of Molecular Neuroscience, UCL Institute of Neurology, London WC1N 3BG, UK.
2. Laboratory of Neurogenetics, National Institute on Aging, National Institutes of Health, Bethesda, Maryland, United States of America
3. Institute of Psychiatry, King's College London, London, UK
4. Human Genetics and Cellular Pathology, School of Molecular Medical Sciences, University of Nottingham, Nottingham, NG7 2UH, UK

Acknowledgements

We thank G. Yu for the HeLa-swAPP cells, We thank T.C. Südhof for the generous gifts of Rab11 constructs and F. Barr for the generous gift of the RabGAP library. We thank M. Schwab, W. Annaert, H. Mohler, R. Nitsch, C. Hock and the members of the Rajendran Lab for critical input into the study. We thank R. Paolicelli for the help with statistics and E. Schwarz for help with the editing of the manuscript. L.R acknowledges the financial support from the Swiss National Science Foundation grant, the Novartis Foundation grant, the Velux

Foundation, Bangerter Stiftung, Baugarten Stiftung and the Synapsis Foundation. L.R and V. U acknowledge the funding support from the European Neuroscience Campus of the Erasmus Mundus Program. G.S. was supported by an EMBO long-term fellowship and is a recipient of a Postdoc-Forschungskredit of the University of Zurich. G.T. acknowledges the grant support from the National Institutes of Health (AG019070 and AG021495) and Cure Alzheimer's Fund. V.B-P. was partially supported by a fellowship from Alzheimer's Disease Research Fund of Illinois Department of Public Health. This Exome sequencing work was supported in part by the Alzheimer's Research UK (ARUK), by an anonymous donor, by the Wellcome Trust/MRC Joint Call in Neurodegeneration award (WT089698) to the UK Parkinson's Disease Consortium (UKPDC) whose members are from the UCL/Institute of Neurology, the University of Sheffield and the MRC Protein Phosphorylation Unit at the University of Dundee, by the Big Lottery (to Dr. Morgan) and by a fellowship from ARUK to Dr. Guerreiro. The Exome Sequencing part was also supported in part by the Intramural Research Programs of the National Institute on Aging and the National Institute of Neurological Disease and Stroke, National Institutes of Health, Department Of Health and Human Services Project number ZO1 AG000950-10. Some samples and pathological diagnoses were provided by the MRC London Neurodegenerative Diseases Brain Bank and the Manchester Brain Bank from Brains for Dementia Research, jointly funded from ARUK and AS via ABBUK Ltd.

References

Andersen, O.M., Reiche, J., Schmidt, V., Gotthardt, M., Spoelgen, R., Behlke, J., von Arnim, C.A., Breiderhoff, T., Jansen, P., Wu, X.*, et al.* (2005). Neuronal sorting protein-related receptor sorLA/LR11 regulates processing of the amyloid precursor protein. Proc Natl Acad Sci U S A *102*, 13461-13466.

Annaert, W., and De Strooper, B. (2002). A cell biological perspective on Alzheimer's disease. Annu Rev Cell Dev Biol *18*, 25-51.

Barr, F., and Lambright, D.G. (2010). Rab GEFs and GAPs. Curr Opin Cell Biol *22*, 461-470.

Borchelt, D.R., Thinakaran, G., Eckman, C.B., Lee, M.K., Davenport, F., Ratovitsky, T., Prada, C.M., Kim, G., Seekins, S., Yager, D.*, et al.* (1996). Familial Alzheimer's disease-linked presenilin 1 variants elevate Abeta1-42/1-40 ratio in vitro and in vivo. Neuron *17*, 1005-1013.

Buggia-Prévot et al., A Novel Function for EHD Family Proteins in Unidirectional Retrograde Dendritic Transport of BACE1 and Alzheimer's disease Aβ production. Cell Reports, this issue.

Cataldo, A.M., Peterhoff, C.M., Troncoso, J.C., Gomez-Isla, T., Hyman, B.T., and Nixon, R.A. (2000). Endocytic pathway abnormalities precede amyloid beta deposition in sporadic Alzheimer's disease and Down syndrome: differential effects of APOE genotype and presenilin mutations. Am J Pathol *157*, 277-286.

Choudhury, A., Dominguez, M., Puri, V., Sharma, D.K., Narita, K., Wheatley, C.L., Marks, D.L., and Pagano, R.E. (2002). Rab proteins mediate Golgi transport of caveola-internalized glycosphingolipids and correct lipid trafficking in Niemann-Pick C cells. J Clin Invest *109*, 1541-1550.

Choy, R.W., Cheng, Z., and Schekman, R. (2012). Amyloid precursor protein (APP) traffics from the cell surface via endosomes for amyloid beta (Abeta) production in the trans-Golgi network. Proc Natl Acad Sci U S A.

Chyung, J.H., and Selkoe, D.J. (2003). Inhibition of receptor-mediated endocytosis demonstrates generation of amyloid beta-protein at the cell surface. J Biol Chem *278*, 51035-51043.

Das, U., Scott, D.A., Ganguly, A., Koo, E.H., Tang, Y., and Roy, S. (2013). Activity-Induced Convergence of APP and BACE-1 in Acidic Microdomains via an Endocytosis-Dependent Pathway. Neuron *79*, 447-460.

De Strooper, B. (2010). Proteases and proteolysis in Alzheimer disease: a multifactorial view on the disease process. Physiol Rev *90*, 465-494.

Duff, K., Eckman, C., Zehr, C., Yu, X., Prada, C.M., Perez-tur, J., Hutton, M., Buee, L., Harigaya, Y., Yager, D.*, et al.* (1996). Increased amyloid-beta42(43) in brains of mice expressing mutant presenilin 1. Nature *383*, 710-713.

Dumanchin, C., Czech, C., Campion, D., Cuif, M.H., Poyot, T., Martin, C., Charbonnier, F., Goud, B., Pradier, L., and Frebourg, T. (1999). Presenilins interact with Rab11, a small GTPase involved in the regulation of vesicular transport. Hum Mol Genet *8*, 1263-1269.

Ehehalt, R., Keller, P., Haass, C., Thiele, C., and Simons, K. (2003). Amyloidogenic processing of the Alzheimer beta-amyloid precursor protein depends on lipid rafts. J Cell Biol *160*, 113-123.

Frasa, M.A., Koessmeier, K.T., Ahmadian, M.R., and Braga, V.M. (2012). Illuminating the functional and structural repertoire of human TBC/RABGAPs. Nat Rev Mol Cell Biol *13*, 67-73.

Frisoni, G.B., Hampel, H., O'Brien, J.T., Ritchie, K., and Winblad, B. (2011). Revised criteria for Alzheimer's disease: what are the lessons for clinicians? Lancet Neurol *10*, 598-601.

Gagescu, R., Demaurex, N., Parton, R.G., Hunziker, W., Huber, L.A., and Gruenberg, J. (2000). The recycling endosome of Madin-Darby canine kidney cells is a mildly acidic compartment rich in raft components. Mol Biol Cell *11*, 2775-2791.

Galvez, T., Gilleron, J., Zerial, M., and O'Sullivan, G.A. (2012). SnapShot: Mammalian Rab proteins in endocytic trafficking. Cell *151*, 234-234 e232.

Haass, C., Koo, E.H., Mellon, A., Hung, A.Y., and Selkoe, D.J. (1992). Targeting of cell-surface beta-amyloid precursor protein to lysosomes: alternative processing into amyloid-bearing fragments. Nature *357*, 500-503.

He, X., Li, F., Chang, W.P., and Tang, J. (2005). GGA proteins mediate the recycling pathway of memapsin 2 (BACE). J Biol Chem *280*, 11696-11703.

Hsu, C., Morohashi, Y., Yoshimura, S., Manrique-Hoyos, N., Jung, S., Lauterbach, M.A., Bakhti, M., Gronborg, M., Mobius, W., Rhee, J.*, et al.* (2010). Regulation of exosome secretion by Rab35 and its GTPase-activating proteins TBC1D10A-C. J Cell Biol *189*, 223-232.

Huang, Y., and Mucke, L. (2012). Alzheimer mechanisms and therapeutic strategies. Cell *148*, 1204-1222.

Jonsson, T., Atwal, J.K., Steinberg, S., Snaedal, J., Jonsson, P.V., Bjornsson, S., Stefansson, H., Sulem, P., Gudbjartsson, D., Maloney, J.*, et al.* (2012). A mutation in APP protects against Alzheimer's disease and age-related cognitive decline. Nature.

Kaether, C., Schmitt, S., Willem, M., and Haass, C. (2006). Amyloid precursor protein and notch intracellular domains are generated after transport of their precursors to the cell surface. Traffic *7*, 408-415.

Kalvodova, L., Kahya, N., Schwille, P., Ehehalt, R., Verkade, P., Drechsel, D., and Simons, K. (2005). Lipids as modulators of proteolytic activity of BACE: involvement of cholesterol, glycosphingolipids, and anionic phospholipids in vitro. J Biol Chem *280*, 36815-36823.

Kametani, F., Usami, M., Tanaka, K., Kume, H., and Mori, H. (2004). Mutant presenilin (A260V) affects Rab8 in PC12D cell. Neurochem Int *44*, 313-320.

Kinoshita, A., Fukumoto, H., Shah, T., Whelan, C.M., Irizarry, M.C., and Hyman, B.T. (2003). Demonstration by FRET of BACE interaction with the amyloid precursor protein at the cell surface and in early endosomes. J Cell Sci *116*, 3339-3346.

Koo, E.H., and Squazzo, S.L. (1994). Evidence that production and release of amyloid beta-protein involves the endocytic pathway. J Biol Chem *269*, 17386-17389.

Laflamme, C., Assaker, G., Ramel, D., Dorn, J.F., She, D., Maddox, P.S., and Emery, G. (2012). Evi5 promotes collective cell migration through its Rab-GAP activity. J Cell Biol *198*, 57-67.

Lichtenthaler, S.F. (2011). Alpha-secretase in Alzheimer's disease: molecular identity, regulation and therapeutic potential. J Neurochem *116*, 10-21.

Lindsay, A.J., and McCaffrey, M.W. (2002). Rab11-FIP2 functions in transferrin recycling and associates with endosomal membranes via its COOH-terminal domain. J Biol Chem *277*, 27193-27199.

Longatti, A., Lamb, C.A., Razi, M., Yoshimura, S., Barr, F.A., and Tooze, S.A. (2012). TBC1D14 regulates autophagosome formation via Rab11- and ULK1-positive recycling endosomes. J Cell Biol *197*, 659-675.

Maxfield, F.R., and Yamashiro, D.J. (1987). Endosome acidification and the pathways of receptor-mediated endocytosis. Adv Exp Med Biol *225*, 189-198.

Nitsch, R.M., Slack, B.E., Farber, S.A., Borghesani, P.R., Schulz, J.G., Kim, C., Felder, C.C., Growdon, J.H., and Wurtman, R.J. (1993). Receptor-coupled amyloid precursor protein processing. Ann N Y Acad Sci *695*, 122-127.

Onodera, Y., Nam, J.M., Hashimoto, A., Norman, J.C., Shirato, H., Hashimoto, S., and Sabe, H. (2012). Rab5c promotes AMAP1-PRKD2 complex formation to enhance beta1 integrin recycling in EGF-induced cancer invasion. J Cell Biol *197*, 983-996.

Ostrowski, M., Carmo, N.B., Krumeich, S., Fanget, I., Raposo, G., Savina, A., Moita, C.F., Schauer, K., Hume, A.N., Freitas, R.P.*, et al.* (2010). Rab27a and Rab27b control different steps of the exosome secretion pathway. Nat Cell Biol *12*, 19-30; sup pp 11-13.

Perez, R.G., Soriano, S., Hayes, J.D., Ostaszewski, B., Xia, W., Selkoe, D.J., Chen, X., Stokin, G.B., and Koo, E.H. (1999). Mutagenesis identifies new signals for beta-amyloid precursor protein endocytosis, turnover, and the generation of secreted fragments, including abeta42 [In Process Citation]. J Biol Chem *274*, 18851-18856.

Pfeffer, S., and Aivazian, D. (2004). Targeting Rab GTPases to distinct membrane compartments. Nat Rev Mol Cell Biol *5*, 886-896.

Prabhu, Y., Burgos, P.V., Schindler, C., Farias, G.G., Magadan, J.G., and Bonifacino, J.S. (2012). Adaptor protein 2-mediated endocytosis of the beta-secretase BACE1 is dispensable for amyloid precursor protein processing. Mol Biol Cell *23*, 2339-2351.

Rajendran, L., and Annaert, W. (2012). Membrane trafficking pathways in Alzheimer's disease. Traffic *13*, 759-770.

Rajendran, L., Honsho, M., Zahn, T.R., Keller, P., Geiger, K.D., Verkade, P., and Simons, K. (2006). Alzheimer's disease beta-amyloid peptides are released in association with exosomes. Proc Natl Acad Sci U S A *103*, 11172-11177.

Rajendran, L., Schneider, A., Schlechtingen, G., Weidlich, S., Ries, J., Braxmeier, T., Schwille, P., Schulz, J.B., Schroeder, C., Simons, M.*, et al.* (2008). Efficient inhibition of the Alzheimer's disease beta-secretase by membrane targeting. Science *320*, 520-523.

Ren, M., Xu, G., Zeng, J., De Lemos-Chiarandini, C., Adesnik, M., and Sabatini, D.D. (1998). Hydrolysis of GTP on rab11 is required for the direct delivery of transferrin from the pericentriolar recycling compartment to the cell surface but not from sorting endosomes. Proc Natl Acad Sci U S A *95*, 6187-6192.

Rogaeva, E., Meng, Y., Lee, J.H., Gu, Y., Kawarai, T., Zou, F., Katayama, T., Baldwin, C.T., Cheng, R., Hasegawa, H., *et al.* (2007). The neuronal sortilin-related receptor SORL1 is genetically associated with Alzheimer disease. Nat Genet *39*, 168-177.

Sannerud, R., Declerck, I., Peric, A., Raemaekers, T., Menendez, G., Zhou, L., Veerle, B., Coen, K., Munck, S., De Strooper, B., *et al.* (2011). ADP ribosylation factor 6 (ARF6) controls amyloid precursor protein (APP) processing by mediating the endosomal sorting of BACE1. Proc Natl Acad Sci U S A *108*, E559-568.

Schluter, O.M., Schmitz, F., Jahn, R., Rosenmund, C., and Sudhof, T.C. (2004). A complete genetic analysis of neuronal Rab3 function. J Neurosci *24*, 6629-6637.

Schmidt, M.R., and Haucke, V. (2007). Recycling endosomes in neuronal membrane traffic. Biol Cell *99*, 333-342.

Schneider, A., Rajendran, L., Honsho, M., Gralle, M., Donnert, G., Wouters, F., Hell, S.W., and Simons, M. (2008). Flotillin-dependent clustering of the amyloid precursor protein regulates its endocytosis and amyloidogenic processing in neurons. J Neurosci *28*, 2874-2882.

Schuldiner, M., Collins, S.R., Thompson, N.J., Denic, V., Bhamidipati, A., Punna, T., Ihmels, J., Andrews, B., Boone, C., Greenblatt, J.F., *et al.* (2005). Exploration of the function and organization of the yeast early secretory pathway through an epistatic miniarray profile. Cell *123*, 507-519.

Seabra, M.C., Mules, E.H., and Hume, A.N. (2002). Rab GTPases, intracellular traffic and disease. Trends Mol Med *8*, 23-30.

Selkoe, D.J. (2011a). Alzheimer's disease. Cold Spring Harbor perspectives in biology *3*.

Selkoe, D.J. (2011b). Resolving controversies on the path to Alzheimer's therapeutics. Nat Med *17*, 1060-1065.

Selkoe, D.J., and Wolfe, M.S. (2007). Presenilin: running with scissors in the membrane. Cell *131*, 215-221.

Shiba, T., Koga, H., Shin, H.W., Kawasaki, M., Kato, R., Nakayama, K., and Wakatsuki, S. (2006). Structural basis for Rab11-dependent membrane recruitment of a family of Rab11-interacting protein 3 (FIP3)/Arfophilin-1. Proc Natl Acad Sci U S A *103*, 15416-15421.

Siegenthaler, B.M., and Rajendran, L. (2012). Retromers in Alzheimer's disease. Neurodegener Dis *10*, 116-121.

Small, S.A., and Gandy, S. (2006). Sorting through the cell biology of Alzheimer's disease: intracellular pathways to pathogenesis. Neuron *52*, 15-31.

Small, S.A., Kent, K., Pierce, A., Leung, C., Kang, M.S., Okada, H., Honig, L., Vonsattel, J.P., and Kim, T.W. (2005). Model-guided microarray implicates the retromer complex in Alzheimer's disease. Ann Neurol *58*, 909-919.

Sonnichsen, B., De Renzis, S., Nielsen, E., Rietdorf, J., and Zerial, M. (2000). Distinct membrane domains on endosomes in the recycling pathway visualized by multicolor imaging of Rab4, Rab5, and Rab11. J Cell Biol *149*, 901-914.

Spasic, D., and Annaert, W. (2008). Building gamma-secretase: the bits and pieces. J Cell Sci *121*, 413-420.

Stenmark, H., and Olkkonen, V.M. (2001). The Rab GTPase family. Genome Biol *2*, REVIEWS3007.

Szodorai, A., Kuan, Y.H., Hunzelmann, S., Engel, U., Sakane, A., Sasaki, T., Takai, Y., Kirsch, J., Muller, U., Beyreuther, K.*, et al.* (2009). APP anterograde transport requires Rab3A GTPase activity for assembly of the transport vesicle. J Neurosci *29*, 14534-14544.

Tesco, G., Koh, Y.H., Kang, E.L., Cameron, A.N., Das, S., Sena-Esteves, M., Hiltunen, M., Yang, S.H., Zhong, Z., Shen, Y.*, et al.* (2007). Depletion of GGA3 stabilizes BACE and enhances beta-secretase activity. Neuron *54*, 721-737.

Thinakaran, G., and Koo, E.H. (2008). Amyloid precursor protein trafficking, processing, and function. J Biol Chem *283*, 29615-29619.

Tisdale, E.J. (2003). Rab2 interacts directly with atypical protein kinase C (aPKC) iota/lambda and inhibits aPKCiota/lambda-dependent glyceraldehyde-3-phosphate dehydrogenase phosphorylation. J Biol Chem *278*, 52524-52530.

Vassar, R., Bennett, B.D., Babu-Khan, S., Kahn, S., Mendiaz, E.A., Denis, P., Teplow, D.B., Ross, S., Amarante, P., Loeloff, R.*, et al.* (1999). Beta-secretase cleavage of Alzheimer's amyloid precursor protein by the transmembrane aspartic protease BACE. Science *286*, 735-741.

Vassar, R., Kovacs, D.M., Yan, R., and Wong, P.C. (2009). The beta-secretase enzyme BACE in health and Alzheimer's disease: regulation, cell biology, function, and therapeutic potential. J Neurosci *29*, 12787-12794.

von Arnim, C.A., Spoelgen, R., Peltan, I.D., Deng, M., Courchesne, S., Koker, M., Matsui, T., Kowa, H., Lichtenthaler, S.F., Irizarry, M.C.*, et al.* (2006). GGA1 acts as a spatial switch altering amyloid precursor protein trafficking and processing. J Neurosci *26*, 9913-9922.

Wakabayashi, T., Craessaerts, K., Bammens, L., Bentahir, M., Borgions, F., Herdewijn, P., Staes, A., Timmerman, E., Vandekerckhove, J., Rubinstein, E.*, et al.* (2009). Analysis of the gamma-secretase interactome and validation of its association with tetraspanin-enriched microdomains. Nat Cell Biol *11*, 1340-1346.

Wilcke, M., Johannes, L., Galli, T., Mayau, V., Goud, B., and Salamero, J. (2000). Rab11 regulates the compartmentalization of early endosomes required for efficient transport from early endosomes to the trans-golgi network. J Cell Biol *151*, 1207-1220.

Willem, M., Lammich, S., and Haass, C. (2009). Function, regulation and therapeutic properties of beta-secretase (BACE1). Semin Cell Dev Biol *20*, 175-182.

Yang, L.B., Lindholm, K., Yan, R., Citron, M., Xia, W., Yang, X.L., Beach, T., Sue, L., Wong, P., Price, D.*, et al.* (2003). Elevated beta-secretase expression and enzymatic activity detected in sporadic Alzheimer disease. Nat Med *9*, 3-4.

Yoshimura, S., Egerer, J., Fuchs, E., Haas, A.K., and Barr, F.A. (2007). Functional dissection of Rab GTPases involved in primary cilium formation. J Cell Biol *178*, 363-369.

Zerial, M., and McBride, H. (2001). Rab proteins as membrane organizers. Nat Rev Mol Cell Biol *2*, 107-117.

Figure 1

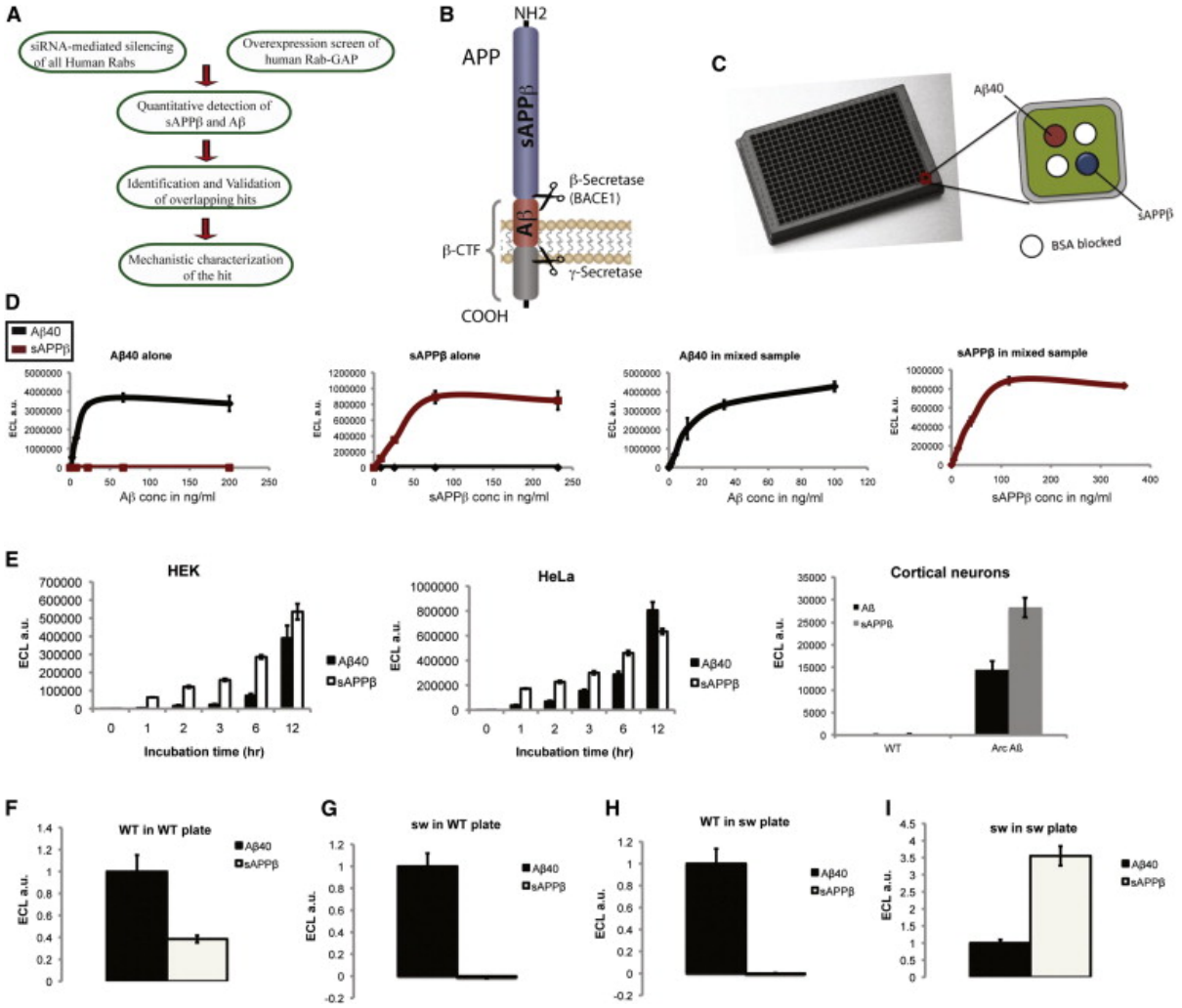

Figure 1: A multiplexing platform for the detection of amyloidogenic processing of Amyloid precursor protein (APP)

A. Schematic of the screen. B. Cartoon of APP cleavage by β-and γ-secretases. C. Cartoon of Electrochemiluminescence (ECL) detection system. D. Incubation of synthetic Aβ (Aβ40, black) and recombinant sAPPβ (red) either individually or together gives specific signals. E. Supernatants from HEK (HEK-sweAPP) or HeLa cells overexpressing the Swedish mutant of APP (HeLa-sweAPP) and primary cortical neurons from Arc/sweAPP Tg analyzed for Aβ (black) and sAPPβ (white for HEK and HeLa; grey for the cortical neurons) levels (error bars indicate SD). F & G. Specificity of the ECL-multiplex assay platform. Signals for Aβ40 (black) and wt-sAPPβ (grey) from conditioned medium HEK-wtAPP (F) or HEK-sweAPP (G) analyzed with capture antibodies specific for Aβ and wt sAPPβ. H & I. Signals for Aβ40 (black) and swe-sAPPβ (grey) from conditioned medium of HEK-wtAPP cells (H) or HEK-sweAPP cells (I). (Error bars indicate SD.)

Figure 2

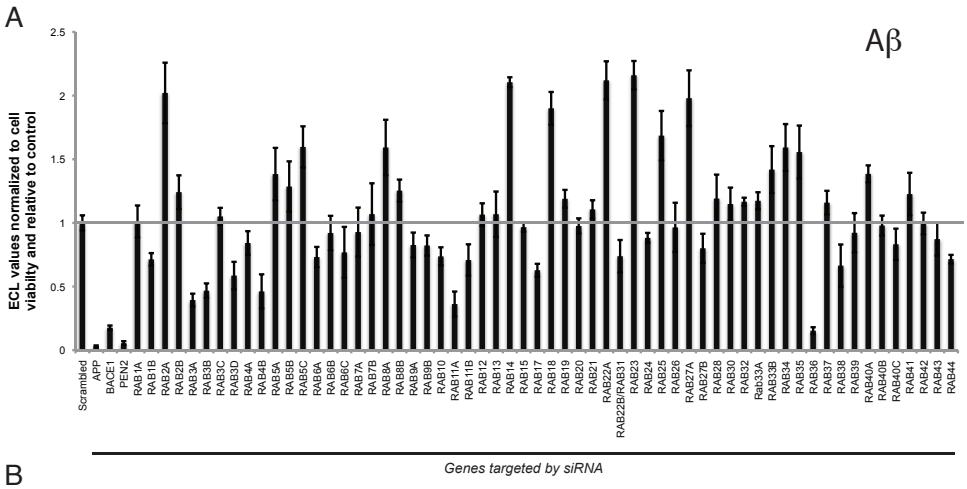

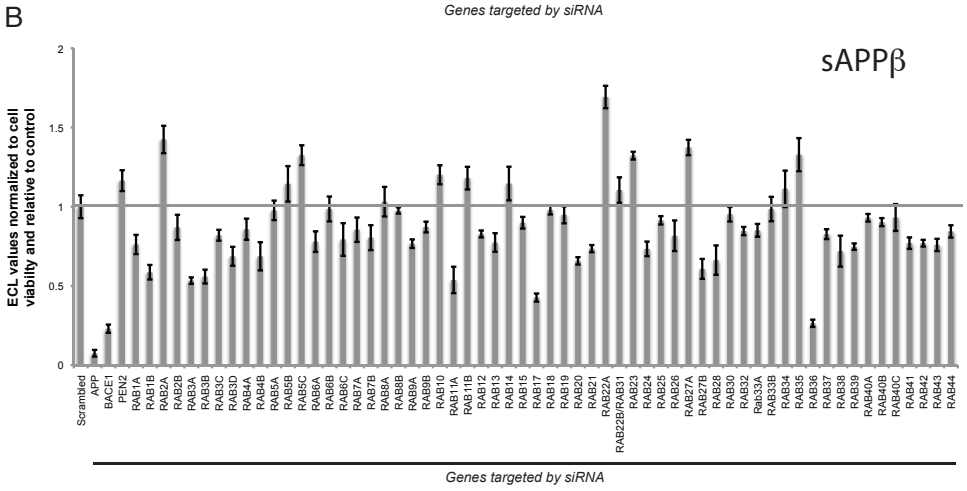

C

Decreased both Aβ and sAPPβ

Aβ			sAPPβ		
	zscore	ttest		zscore	ttest
APP	-2.0455	3.6E-06	APP	-2.8368	1.8E-05
PEN2	-1.9924	4.8E-06	BACE	-2.2829	5.8E-05
RAB36	-1.7957	1.3E-05	RAB36	-2.1609	6.9E-05
BACE	-1.7484	1.1E-05	RAB17	-1.5814	0.0003
RAB11A	-1.3747	0.00143	RAB3A	-1.2001	0.00081
RAB3A	-1.312	0.00023	RAB11A	-1.1845	0.00577
RAB4B	-1.1755	0.01045	RAB3B	-1.1082	0.00199
RAB3B	-1.1644	0.00066	RAB1B	-1.0105	0.00294
RAB3D	-0.9259	0.01521	RAB3D	-0.6524	0.01578
RAB17	-0.8419	0.00309	RAB4B	-0.6514	0.0345
RAB1B	-0.6711	0.01004			

Increased both Aβ and sAPPβ

Aβ			sAPPβ		
	zscore	ttest		zscore	ttest
RAB23	2.23546	9.7E-05	RAB22A	2.93728	0.00048
RAB22A	2.15526	0.00044	RAB2A	1.97984	0.00939
RAB2A	1.95641	0.00593	RAB27A	1.79941	0.00517
RAB27A	1.87374	0.00499	RAB35	1.63803	0.04164
RAB35	1.82537	0.02946	RAB5C	1.6263	0.01461
RAB5C	1.10419	0.01356	RAB23	1.61606	0.00559

Decreased only Aβ

Aβ		
	zscore	ttest
RAB44	-0.6669	0.00587
RAB6A	-0.6338	0.03545
RAB10	-0.6232	0.02997

Increased only Aβ

Aβ		
	zscore	ttest
RAB34	1.80169	0.01666
RAB18	1.71446	0.0007
RAB14	1.59769	0.02098
RAB25	1.28256	0.0149
RAB8A	1.09556	0.03933

Decreased only sAPPβ

sAPPβ		
	zscore	ttest
RAB27B	-0.9354	0.00642
RAB20	-0.7548	0.00413
RAB28	-0.7374	0.02872
RAB24	-0.4841	0.02109
RAB21	-0.479	0.01295
RAB39	-0.4339	0.01538
RAB43	-0.3958	0.0259
RAB1A	-0.3852	0.04499

Increased only sAPPβ

None

D

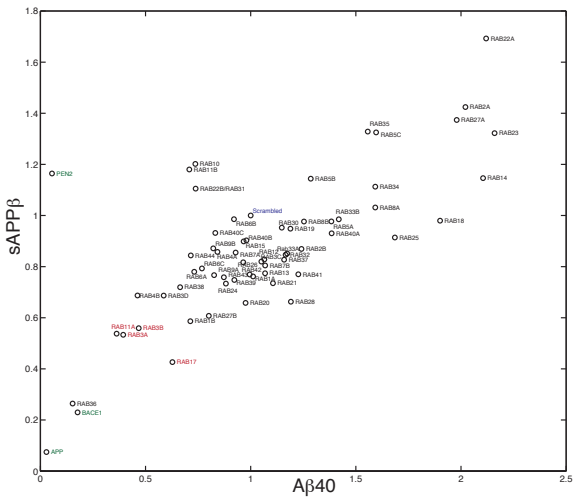

Figure 2: RNAi screen of genome wide Rabs identify Rabs involved in regulating the levels of Aβ and sAPPβ.

A & B. Graph showing the levels of Aβ (A) and sAPPβ (B) from the Rab siRNA screen. HeLa-sweAPP cells were transfected with Scrambled oligo (negative control), or pooled siRNA against APP, BACE1, PEN2 and the 60 Rabs and assayed for Aβ and sAPPβ (error bars indicate SEM). C. List of genes that had the strongest effect on Aβ and sAPPβ levels after siRNA mediated silencing along with the Z-score and t-test values. D. Two-dimensional plot representing the levels of Aβ and sAPPβ from the Rabs siRNA screen. Positive controls APP, BACE1 and PEN2 are indicated in green, and negative control Scrambled is indicated in blue. Rabs silencing that led to the strongest decrease in both Aβ and sAPPβ are indicated in red. All statistics were performed using the 2 tailed *t*-tests and using one way ANOVA.

Figure 3

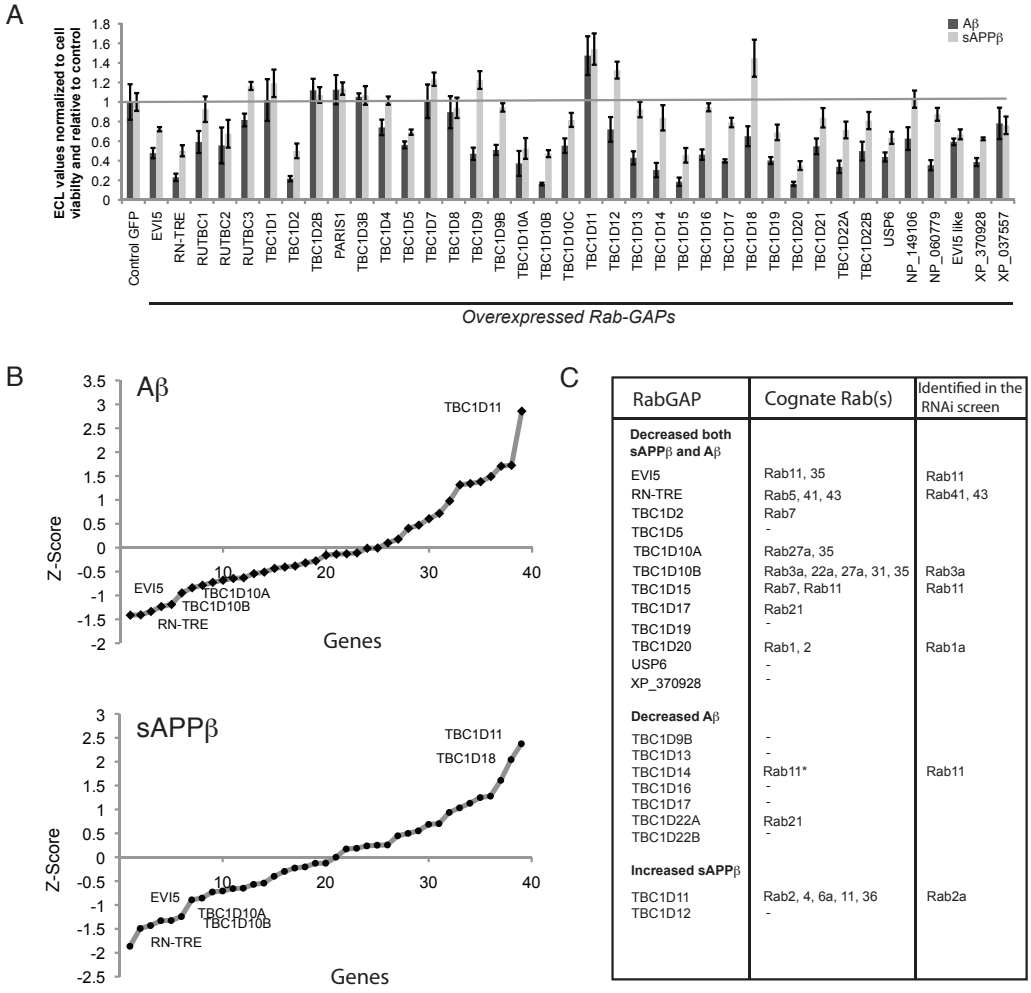

RabGAP	Cognate Rab(s)	Identified in the RNAi screen
Decreased both sAPPβ and Aβ		
EVI5	Rab11, 35	Rab11
RN-TRE	Rab5, 41, 43	Rab41, 43
TBC1D2	Rab7	
TBC1D5	-	
TBC1D10A	Rab27a, 35	
TBC1D10B	Rab3a, 22a, 27a, 31, 35	Rab3a
TBC1D15	Rab7, Rab11	Rab11
TBC1D17	Rab21	
TBC1D19	-	
TBC1D20	Rab1, 2	Rab1a
USP6	-	
XP_370928	-	
Decreased Aβ		
TBC1D9B	-	
TBC1D13	-	
TBC1D14	Rab11*	Rab11
TBC1D16	-	
TBC1D17	-	
TBC1D22A	Rab21	
TBC1D22B	-	
Increased sAPPβ		
TBC1D11	Rab2, 4, 6a, 11, 36	Rab2a
TBC1D12	-	

Figure 3: RabGAP screen identifies novel GAPs and Rabs in the regulations of Aβ and sAPPβ levels.

A. Graph showing the levels of Aβ (black) and sAPPβ (grey) after RabGAP plasmid overexpression. HeLa-sweAPP cells were transfected with plasmid expressing RabGAP fused with GFP or a plasmid expressing GFP (negative control) and assayed for Aβ and sAPPβ (error bars indicate SEM). B. Graphs showing Z-scores of the effects on sAPPβ and Aβ levels after RabGAP overexpression. C. Table showing RabGAPs that had the strongest effect on Aβ and/or sAPPβ levels along with its cognate Rab(s). * indicates that the TBC1D14 is not a GAP for Rab11 but has been shown to perturb the localization and function of Rab11 (Longatti et al., 2012).

Figure 4:

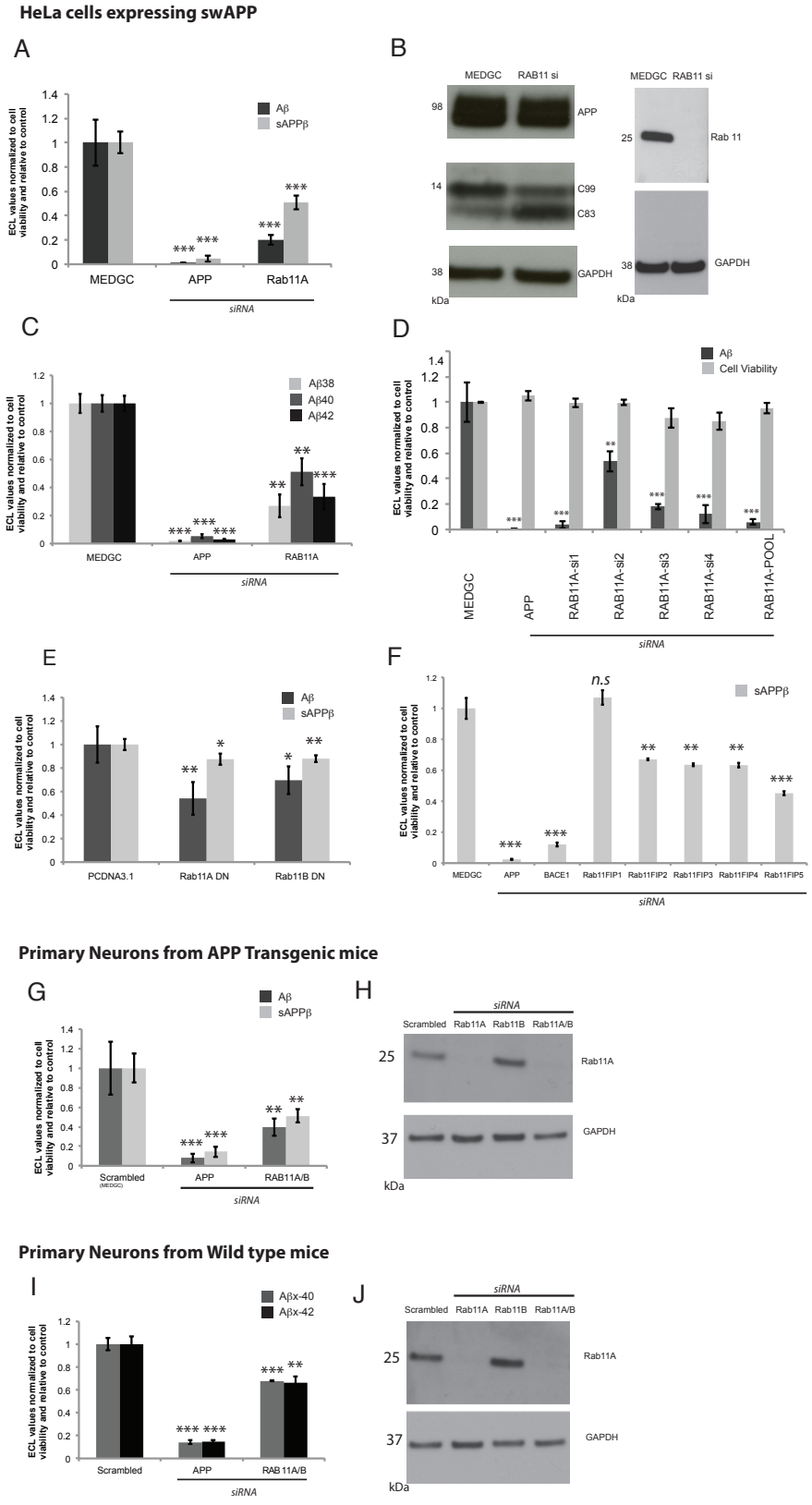
HeLa cells expressing swAPP
A
B
C
D
E
F
Primary Neurons from APP Transgenic mice
G
H
Primary Neurons from Wild type mice
I
J
ECL values normalized to cell viability and relative to control
Aβ
sAPPβ
Aβ38
Aβ40
Aβ42
Cell Viability
Aβx-40
Aβx-42
MEDGC
APP
Rab11A
RAB11A
RAB11A si
Rab 11
C99
C83
GAPDH
kDa
siRNA
RAB11A-si1
RAB11A-si2
RAB11A-si3
RAB11A-si4
RAB11A-POOL
PCDNA3.1
Rab11A DN
Rab11B DN
n.s
BACE1
Rab11FIP1
Rab11FIP2
Rab11FIP3
Rab11FIP4
Rab11FIP5
Scrambled
Rab11B
Rab11A/B
RAB11A/B

Figure 4: Rab11 regulates BACE1 cleavage of APP in model cell lines and primary neurons from wild type and APP transgenic mice

A. HeLa-sweAPP cells were transfected with Scrambled oligo (MEDGC, negative control) or pooled siRNA against APP and Rab11A and assayed for Aβ (dark grey) and sAPPβ (light grey). (Error bars indicate SD). B. HeLa-sweAPP cells were transfected with scrambled oligo or pooled siRNA against Rab11A and the lysates were assayed by Western blotting as indicated. C. HeLa-sweAPP cells were transfected with scrambled oligo or pooled siRNAs against APP and Rab11A and assayed for Aβ38 (light grey), Aβ40 (dark grey), and Aβ42 (black). (Error bars indicate SEM). D. HeLa-sweAPP cells were transfected with scrambled oligo or pooled siRNA against APP, single siRNA (si1-4) against Rab11A and pooled siRNA against Rab11A and assayed for Aβ40 (dark grey) and cell viability (light grey) and the lysates were assayed by Western blotting as indicated (Inset). (Error bars indicate SD). E. HeLa-sweAPP cells were transfected with PCDNA 3.1 (negative control), Rab11ADN and Rab11BDN and assayed for Aβ40 (dark grey) and sAPPβ (light grey). (Error bars indicate SEM). F. HeLa-sweAPP cells were transfected with scrambled oligo or pooled siRNA against APP, BACE1 and Rab11FIP1-5 and assayed for sAPPβ (Error bars indicate SEM). G-J: Silencing of Rab11 in primary neurons from APP transgenic and wildtype mice reduces β-cleavage of APP and Aβ levels: G. Rab11A and B were silenced in primary cortical and hippocampal neurons isolated from APP transgenic mice expressing the Swedish mutation in APP and the secreted levels of Aβ and sAPPβ were measured. The scrambled oligo was used as a negative control and siRNA targeting APP as positive control. H. Western blotting with anti-Rab11A and anti-GAPDH antibodies from control and Rab11-silenced primary neurons. I. Rab11A and B were silenced in primary cortical and hippocampal neurons isolated from wildtype (WT) mice and the secreted levels of endogenous Aβ40 and Aβ42 were measured. The scrambled oligo was used as a negative control and siRNA targeting APP as positive control. J. Western blotting with anti-Rab11A and anti-GAPDH antibodies from control and Rab11-silenced primary WT neurons. * $P < 0.05$, ** $P < 0.01$, *** $P < 0.001$ compared with scrambled MEDGC or PCDNA3.1. All statistics were performed using the 2 tailed t-tests. Similar significance was also observed with one-way ANOVA analysis (Dunnett's a posteriori analysis)(Supplementary Figure 14).

Figure 5

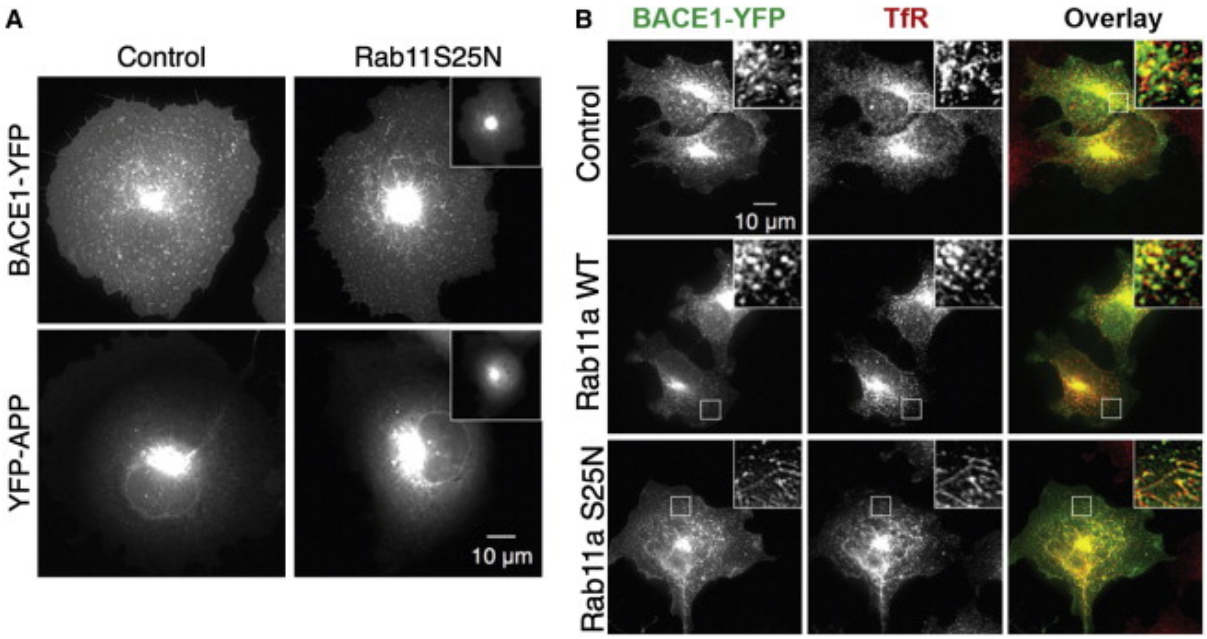

Figure 5: BACE1 colocalizes with Rab11 compartments and its trafficking is altered upon Rab11 dysfunction

A. Live-cell images of COS cells transfected with BACE1-YFP or YFP-APP along with empty vector (control) or Rab11A DN. Expression of Rab11A DN protein is shown in the insets. B. COS cells were transiently co-transfected with BACE1-YFP (green) and empty vector, HA-tagged Rab11A WT or S25N dominant negative mutant and fixed and stained with anti-HA (not shown) and TfR antibodies (red) to label recycling endosomes. The colors in the first two panels are green for BACE1-YFP and red for TfR.

Figure 6

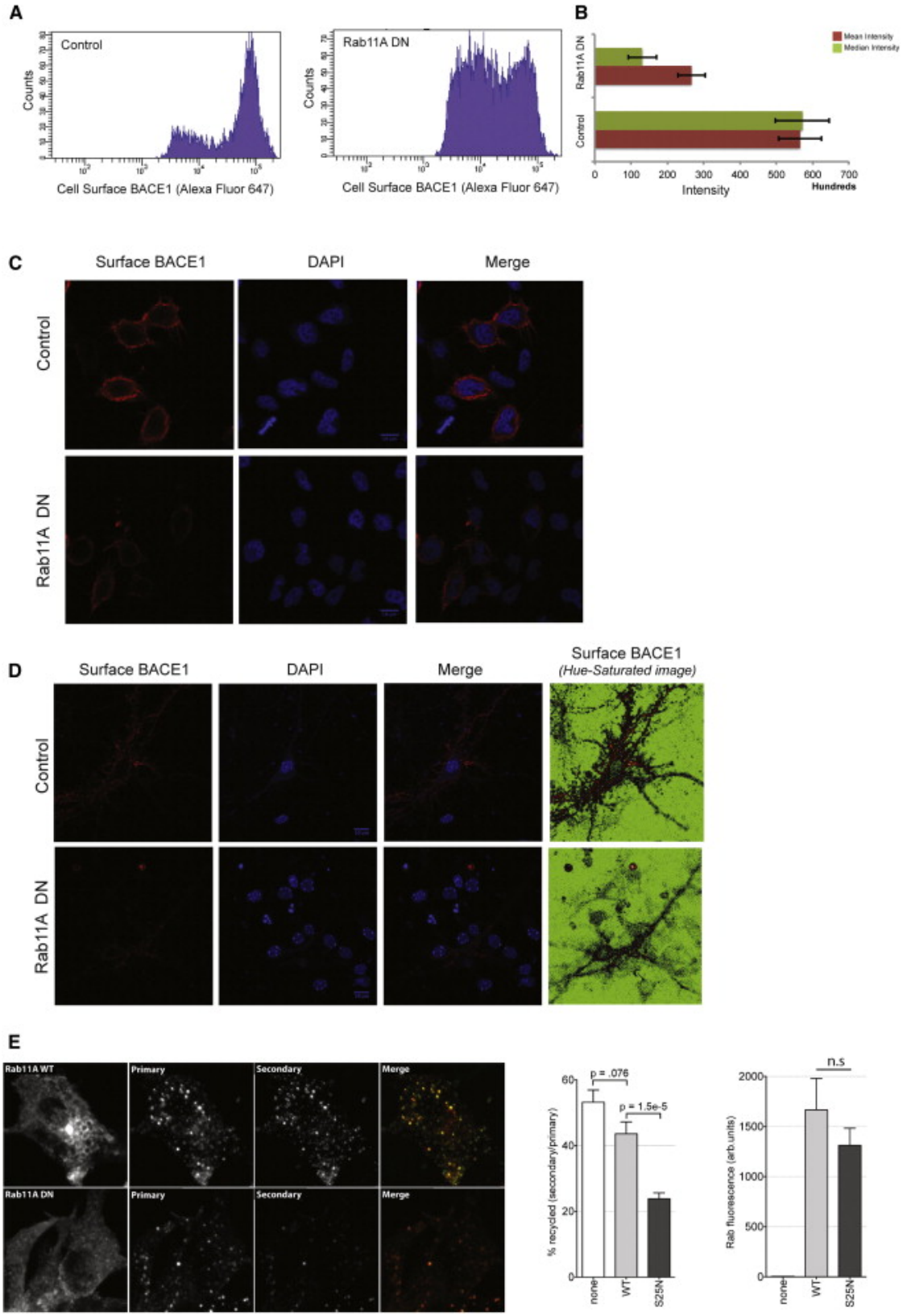
A
Control
Counts
Cell Surface BACE1 (Alexa Fluor 647)
Rab11A DN
Counts
Cell Surface BACE1 (Alexa Fluor 647)
B
Mean Intensity
Median Intensity
Rab11A DN
Control
0
100
200
300
400
500
600
700
Intensity
Hundreds
C
Surface BACE1
DAPI
Merge
Control
Rab11A DN
D
Surface BACE1
DAPI
Merge
Surface BACE1
(Hue-Saturated image)
Control
Rab11A DN
E
Rab11A WT
Primary
Secondary
Merge
Rab11A DN
Primary
Secondary
Merge
p = .076
p = 1.5e-5
% recycled (secondary/primary)
60
40
20
0
none
WT
S25N
n.s
Rab fluorescence (arb.units)
2000
1500
1000
500
0
none
WT
S25N

Figure 6: Rab11 regulates the surface recycling of BACE1 and is essential for maintenance of BACE1 cell surface levels

A. HeLa-swAPP cells were transfected with either control plasmids or the dominant negative mutant of Rab11A and Flag-tagged BACE1. Cell surface levels of BACE1 were determined via FACS on non-permeabilized cells using anti-FLAG antibodies and Alexa-647 coupled secondary antibodies. B. The mean and the median intensity of the cell surface levels of BACE1 are lower in Rab11A DN expressing cells. C. Microscopy of cell surface BACE1 on non-permeablized HeLa cells expressing BACE1-Flag. Rab11A DN expressing cells have marked decrease in cell surface BACE1. D. Immunofluorescence of cell surface BACE1 on non-permeablized primary neurons transfected with BACE1-Flag. Also in neurons, Rab11A DN expressing cells have a marked decrease in cell surface BACE1. E. Recycling of BACE1 is significantly decreased in Rab11A DN expressing cells. Cells were transfected with BACE-FLAG /Rab11A constructs (WT and DN) and incubated with Alexa647-conjugated M1 anti-FLAG primary antibodies for 30 min at 37°C, followed by washing and incubation with Alexa-488 secondary antibodies at 37°C for 30 min. This allows the primary antibody to bind the surface/cycling BACE1 and label the endosomal BACE population, and the secondary antibody to only bind the BACE1 that recycled to the surface. A ratio of the secondary to the primary gives the amount recycled in this time.

Figure 7

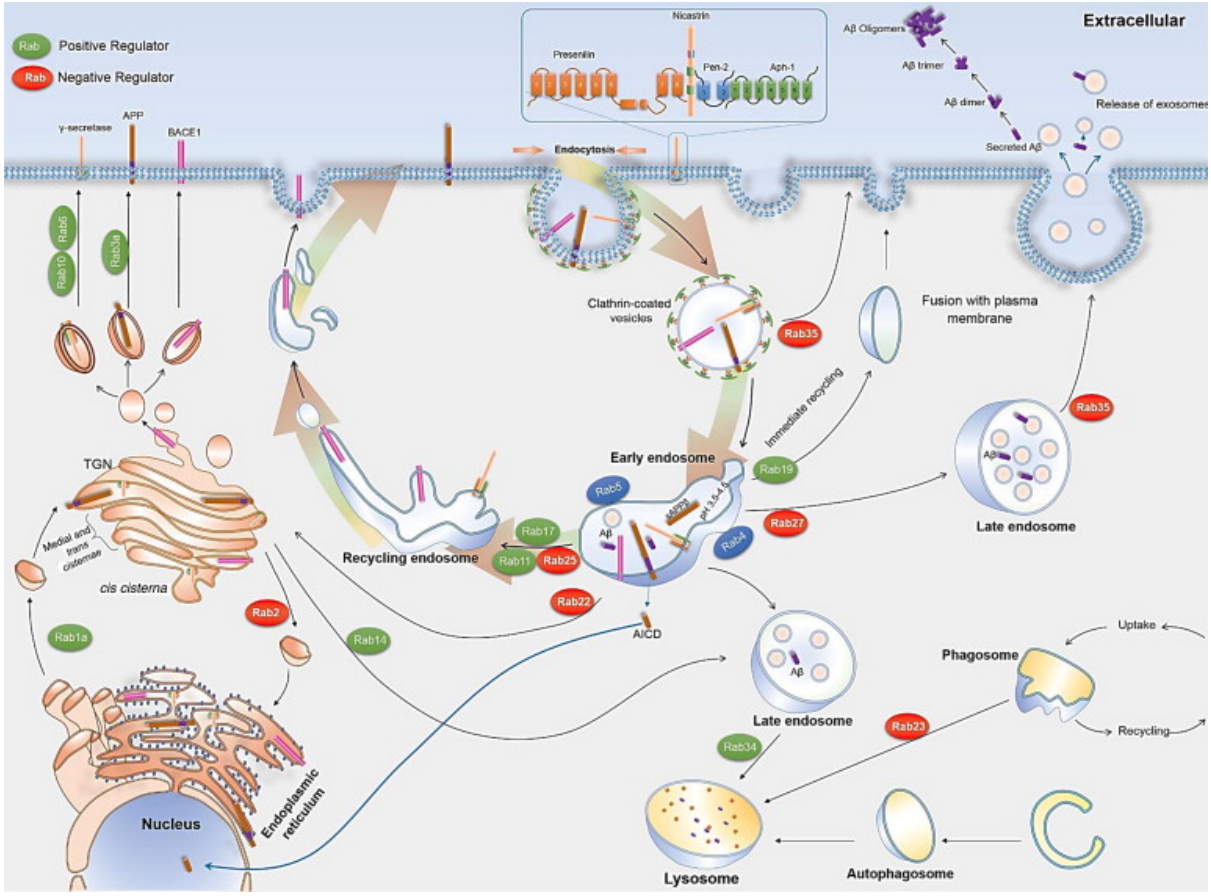

Figure 7: A Roadmap of APP processing and Aβ production

Integrated map of the Rabs identified in the screen as regulators of APP processing and Aβ production/secretion. Rabs indicated in green positively regulate Aβ levels and those indicated in red are negative regulators. Note that the majority of the Rabs regulate trafficking to and from early endosomes.

Supplementary Figure 1

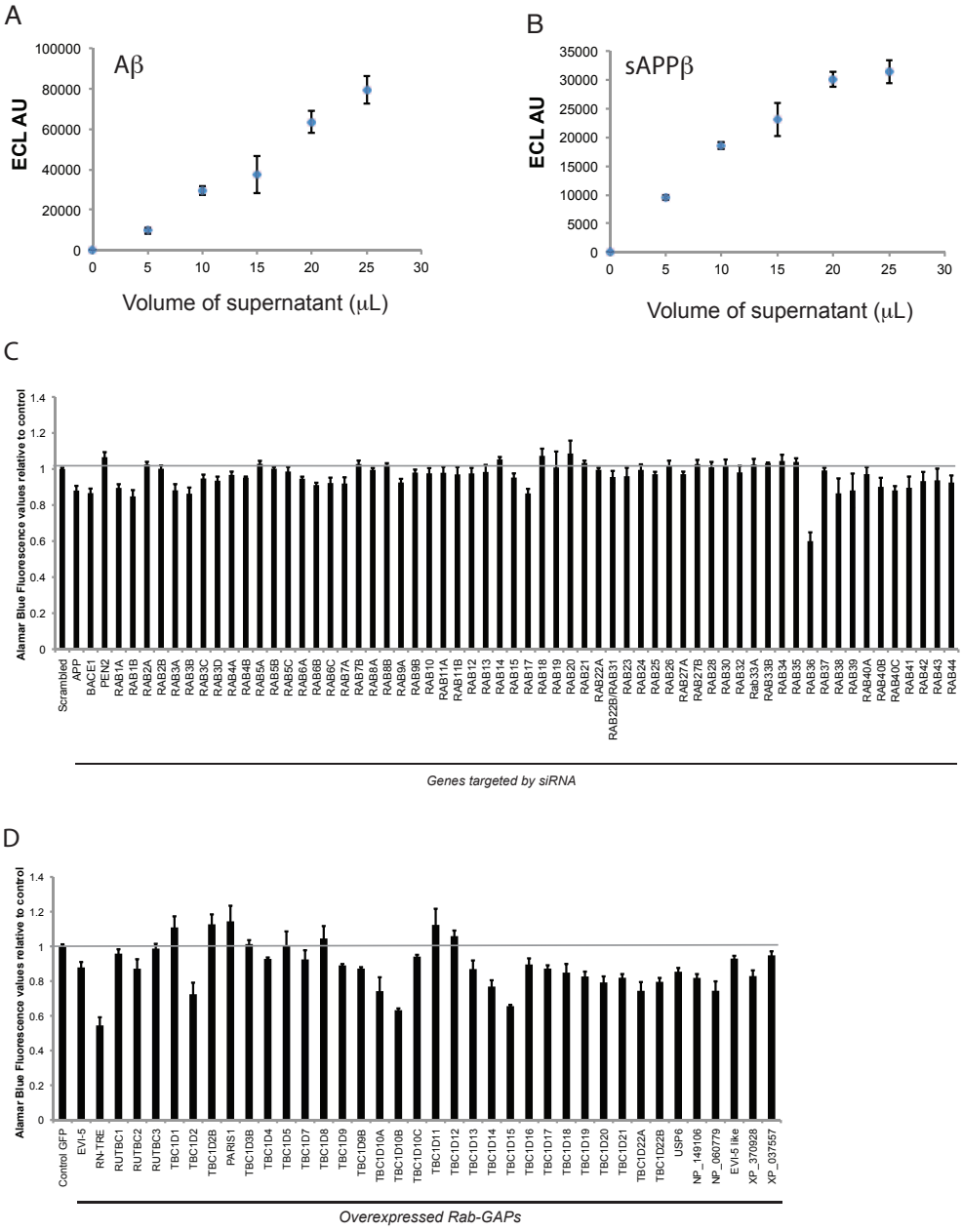

Supplementary Figure 1: Linearity of Aβ and sAPPβ detection and cell viability assay after RNAi and Rab-GAP screen. (Related to Figure 1, 2 & 3) A & B. Different volumes of cell culture supernatants from HeLa-sweAPP cells were assayed for Aβ40 (A) and sAPPβ (B) by ECL-multiplex assay. C & D. Cells from RNAi screen (C) and cells from Rab-GAP screen (D) were assayed for fluorescence intensity after incubation with Alamar Blue® to estimate cell viability. (Error bars indicate SD).

Supplementary Figure 2

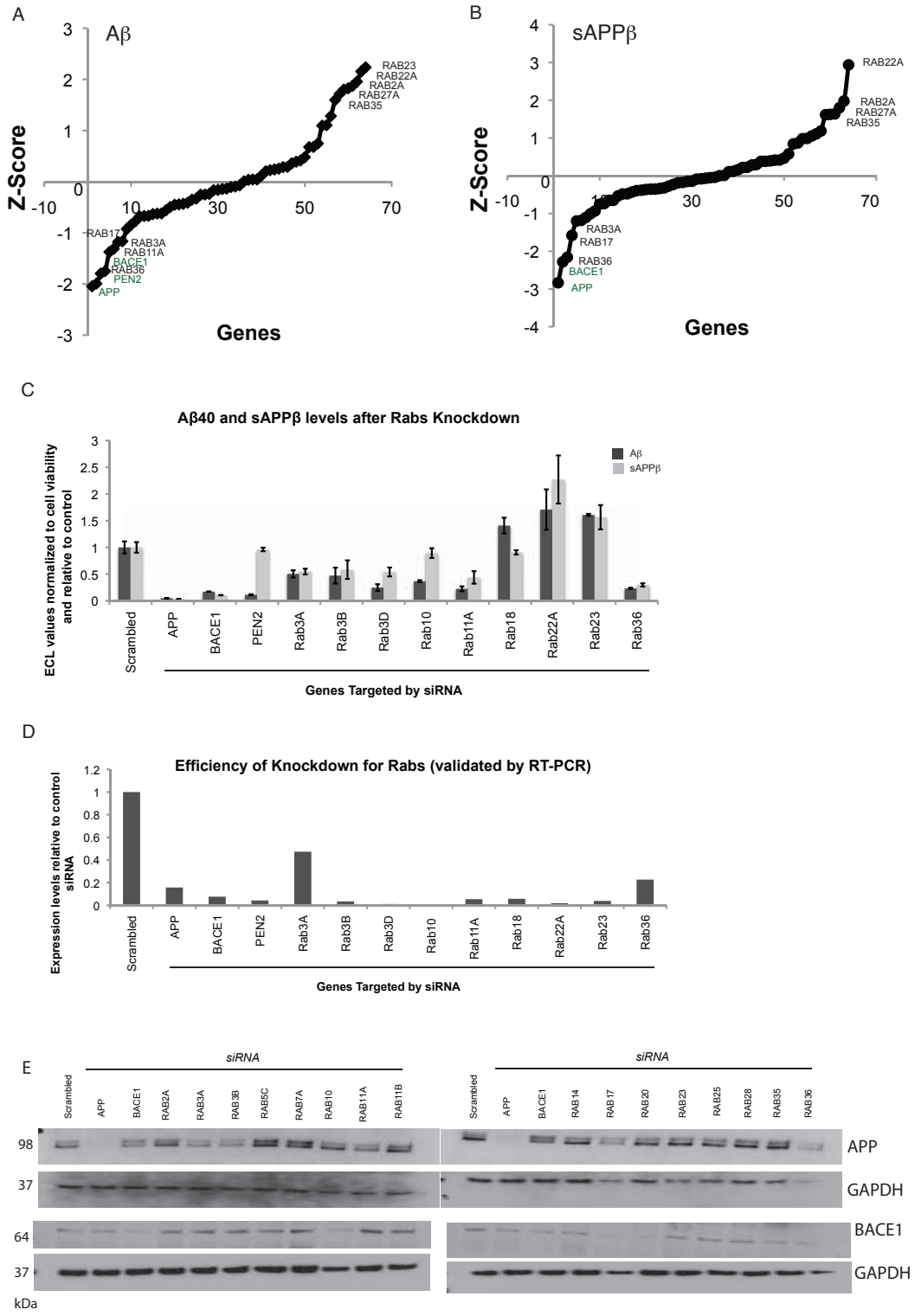

Supplementary Figure 2: Z score of the RNAi screen and validation of top hits. (Related to Figure 2 & 4)

A & B. Graphs showing Z-scores of the effects on Aβ (A) and sAPPβ (B) levels after RNAi screen in HelasweAPP cells. C & D. HeLa-sweAPP cells were transfected with siRNA pool against Scrambled (Negative control), APP, BACE1, PEN2 and the top hit Rabs and assayed for Aβ (black) and sAPPβ (grey) levels (C) and the knockdown efficiency was estimated by RT-PCR (D). E. HeLa-sweAPP cells were transfected with Scrambled (Negative control) or pooled siRNA against APP, BACE1 and the top hits of the Rab RNAi screen and the cell lysates were run on SDS-PAGE, blotted either with anti-APP c-terminus antibody or anti-BACE1. Both blots were reprobed with anti-GAPDH for loading control.

Supplementary Figure 3

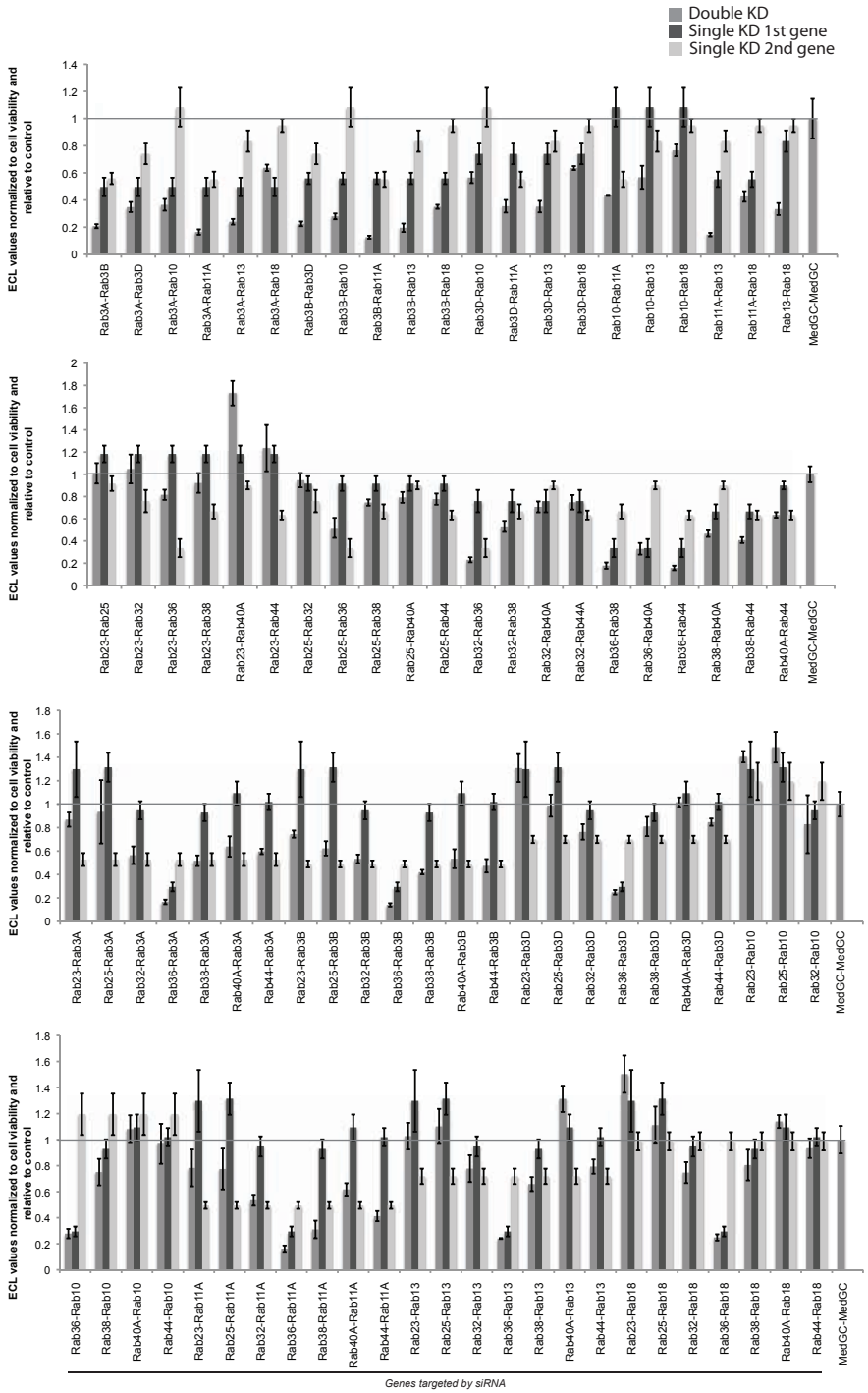

Supplementary Figure 3: Epistasis mini array profiling (EMAP) of the hit Rabs from the RNAi screen. (Related to Figure 2)

The 14 hits identified form the RNAi screen were silenced either alone (single knockdown) or in the combination (double knockdown) indicated in the graph and the supernatant were assayed for sAPPβ levels (Error bars indicate SEM). All statistics are performed using the 2 tailed t-tests.

Supplementary Figure 4

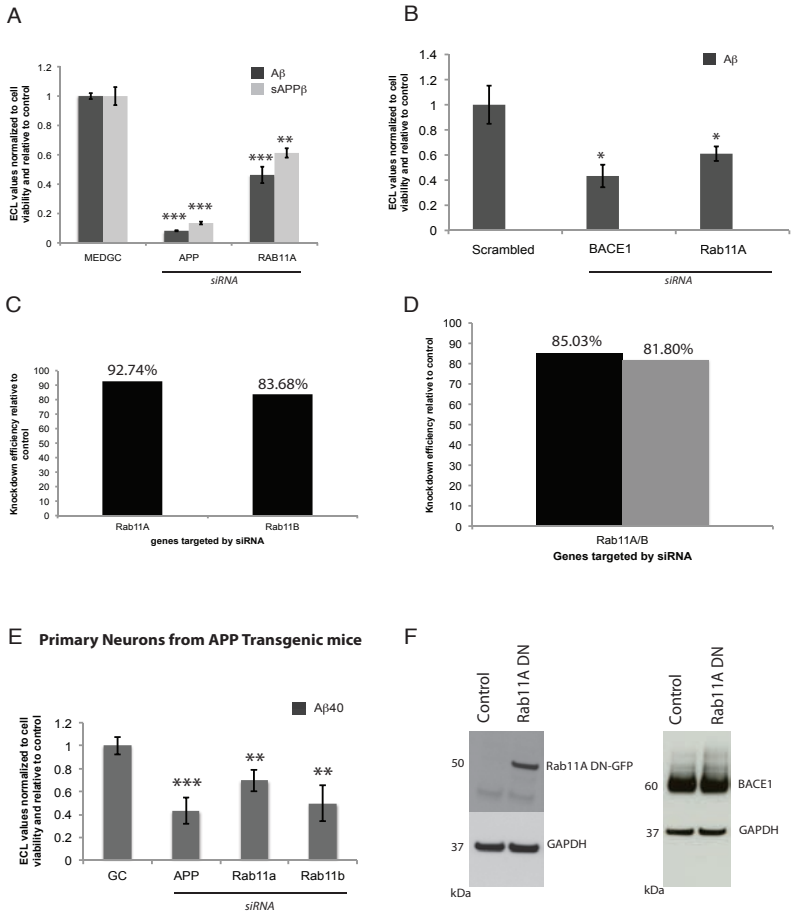

Supplementary Figure 4. Validation of the effects of Rab11 (Related to Figure 4& 6)

A. HEK-wtAPP cells were transfected with Scrambled (MEDGC) or pooled siRNA against APP and Rab11A and the cell lysates were assayed for Aβ and sAPPβ levels. B. HeLa-sweAPP cells were transfected with Scrambled (Negative control) or pooled siRNA against BACE1 and Rab11A and the cell lysates were assayed for Aβ levels. C, D & E. Primary cortical and hippocampal neurons from transgenic mice expressing the human APP with the Swedish mutation were transfected with Scrambled (Negative control) or pooled siRNA against Rab11A and Rab11B singly (C) or together (D) and the knockdown efficiency was estimated by RT-PCR. Silencing of Rab11A or Rab11B reduced Aβ levels (E). F. HeLa-sweAPP cells were cotransfected with Control or Rab11ADN plasmids and the lysates were assayed by western blot and protein levels of Rab11A and BACE1 was estimated using anti-Rab11A and BACE1 antibodies respectively. * $P < 0.05$, ** $P < 0.01$, *** $P < 0.001$compared with Scrambled (MEDGC). All statistics are performed using the 2 tailed ttests.

Supplementary Figure 5

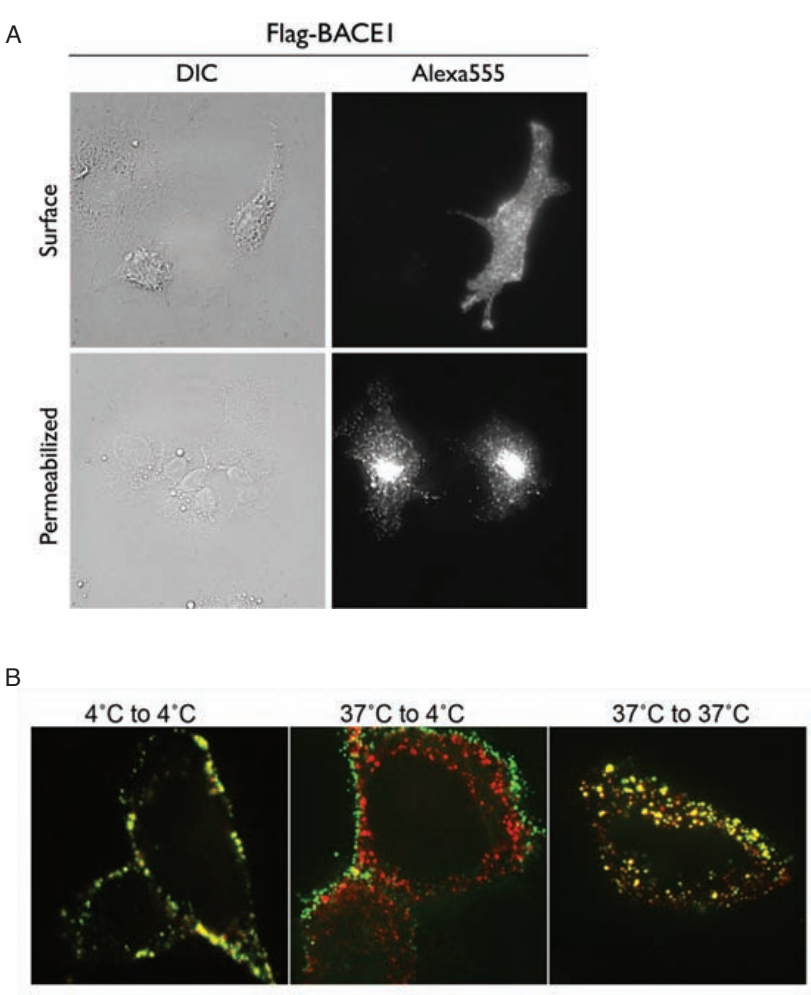

Supplementary Figure 5: Validation of BACE1-Flag tagged construct and recycling assay. (Related to Figure 5 & 6)

A. COS cells cultured on small glass coverslips were transfected with psport6Flag- BACE1 and cell surface (surface) and intracellular (permeabilized) BACE1 were detected by anti-FLAG antibody. B. Cells were transfected with FLAG-tagged BACE1 and three different antibody incubation conditions were used to validate the assay system. The primary antibody used was an Alexa647 conjugated anti-FLAG antibody and the secondary antibody was Alexa488 conjugated. The following three incubation conditions were followed:i) Incubation of both anti-FLAG and the secondary antibody at 4°C. ii) Incubation of anti-FLAG antibody at 37°C and secondary antibody at 4°C. iii) Incubation of both anti-FLAG and the secondary antibody at 37°C.

Supplementary Figure 6

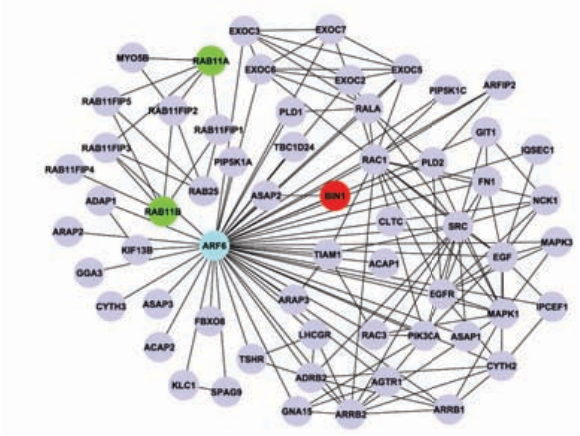

Supplementary Figure 6: Protein-Protein interaction network analysis of the AD risk gene products identifies Rab11A and Rab11B as interacting partners of Bin1.

The top Alzgenes were seeded using the multi-protein search field in STRING database and the clusters were analyzed. In the Bin1 containing cluster, Rab11FIPs, Rab11A and Rab11B were identified as interacting partners. Note that Bin1 connects to Rab11 via Arf6, a BACE1 trafficking regulator and Rab11FIP3. GGA3, another protein that regulates BACE1 trafficking is also present in the network.

Table 1

Chr	Pos	dbSNP	Ref	Alt	AA_CHANGE	CODON	LOCATION/EFFECT	P	OR
15	66161839		C	T	NA	NA	START_GAINED	0.49	0.32
15	66161849		G	C	NA	NA	UTR_5_PRIME	1.00	2.81
15	66170080	rs74845010	A	G	NA	NA	INTRON	0.26	1.34
15	66170121		T	C	G86	ggT/ggC	SYNONYMOUS_CODING	0.48	0.31
15	66170128	rs11556462	T	C	L89	Ttg/Ctg	SYNONYMOUS_CODING	0.48	0.31
15	66180298	rs75724883	C	T	NA	NA	UTR_3_PRIME	0.67	0.58
15	**66181143**	**rs117150201**	**T**	**G**	**NA**	**NA**	**UTR_3_PRIME**	**0.01**	**0.47**
15	66181154	rs77317331	C	T	NA	NA	UTR_3_PRIME	0.78	1.11
15	66181246		C	CTTAA	NA	NA	UTR_3_PRIME	1.00	2.82

Details of the cohorts:

Cohort	Control	AD
Number of Samples analysed	170	185
Gender (%F)	45%	53%
Mean age at onset in years (±SD)	NA	71.3 (10.1)
Mean age in years (±SD)	78.4 (9.7)	81.2 (10.8)

Table 1: Details of the cohort used for Exome Sequencing in this study.

Chapter 2

RNAi screen of genome-wide Rab-GTPases identifies Rab7 as a novel regulator of Aβ clearance in microglia

Vinod Udayar*[,a,b,c], Rosa Paolicelli[a,d], Gabriele Siegel[a,d], and Lawrence Rajendran[a,d]

[a] *Systems and Cell Biology of Neurodegeneration,* [b] *Erasmus Mundus Neuroscience program,* [c] *Graduate programs of the Zurich Neuroscience Center, University of Zurich, Switzerland,* [d] *IREM, University of Zurich, Wagistrasse 12, 8952, Schlieren, Switzerland,*

Correspondence to: rajendran@bli.uzh.ch

Keywords:

Alzheimer's disease, APP, RNAi, Rab7, amyloid, tau, lysosomes, Lamp2, microglia.

Abstract

Presence of amyloid plaques in the brain is one of the main hallmarks of Alzheimer's disease (AD). Amyloid plaques are mostly composed of β-amyloid (Aβ) peptides that initially aggregate into oligomers and subsequently into higher order fibrillar structures. Production and clearance of β-amyloid (Aβ) are both determinants of amyloid build-up in the brain. Cellular trafficking pathways that could potentially regulate Aβ production and clearance are not well understood. Here, we performed an RNAi screen of all Rab-GTPases in BV2 microglia cells and performed an Aβ uptake assay to assess the effects of loss of function of Rab-GTPases on Aβ clearance. We identified Rab7 a novel regulator of Aβ clearance. Although Rab7 silencing increased the uptake of Aβ, the engulfed Aβ was shown to be accumulating in Rab7 silenced cells compared to control condition. In depth analysis of lysosomal degradation revealed significant defects in lysosomal pathway upon Rab7 silencing. Rab7 silencing led to altered distribution of degradative acidic organelles, reduced cathepsin B activity, impaired clearance of EGF and increased general protein accumulation. Rab7 silencing also impaired Aβ clearance and increased Aβ levels in neurons and Hela cells. Rab7 silencing also increased total-tau and phospho-tau levels in primary neurons. Taken together, our results identify a novel role for Rab7 in clearance of Aβ both in neurons and microglia and thus could play a crucial role in late-onset AD.

Introduction

Alzheimer's disease (AD) is the most common cause of dementia, accounting for more than 40 million patients worldwide. AD is characterized by progressive neurodegeneration and result in significant neuron loss, cerebral atrophy and cognitive decline (Selkoe and Hardy, 2016). Behavioral symptoms manifest as memory lapses and subtle personality disorders in early-stage AD, which then progress to significant cognitive and memory impairment in late-stage AD. Cerebral deposition of β-amyloid (Aβ) and tau, which are also the clinical hallmarks of the disease, are believed to play a causative role in AD. Findings from Familial AD (FAD) mutations studies have implicated excessive Aβ production to be the cause of the pathogenesis observed in FAD. Due to absence of such mutations, the causal factor of amyloid accumulation in LOAD has not yet been determined. Evidences suggest that impaired amyloid clearance in and from the brain could be the cause of amyloid build-up in LOAD.

Microglia are the brain's resident macrophages and are the chief phagocytic cells in the brain. Microglial phagocytosis is involved in several processes such as synapse elimination, myelin debris removal and clearance of toxic peptides such as Aβ (Paolicelli et al., 2011 and Sierra et al., 2013). In vitro evidence indicates that microglia can efficiently phagocytose fibrillar Aβ through different receptors, such as Toll-like receptor 2 (TLR2) and Scavenger receptor A1 (SCARA1) (Paresce et al., 1996 and Frenkel et al., 2013). However, not much is known about the cellular regulators of Aβ uptake and degradation in microglia. Identification and characterization of regulators of Aβ clearance in microglia will allow us to establish the molecular etiology of AD in greater detail. Membrane trafficking regulators are interesting candidates in this regard as degradation pathways in the cell rely on membrane trafficking to move cargoes from one compartment to the other. Rab-GTPases are master regulators of membrane trafficking in the cell. Manipulation of their level or function provides us a valuable tool to study the role of membrane trafficking in Aβ clearance.

Here, we performed an RNAi screen of all Rab-GTPases in BV2 microglia cells to identify regulators of Aβ uptake and clearance. We identified Rab7 as a novel regulator of Aβ clearance. Rab7 silencing increased the uptake of Aβ, but impaired the degradation of the uptaken Aβ. The impairment in degradation of Aβ was due to disrupted lyosomal function in the absence of Rab7.

Results and Discussion

RNAi screen of Rab proteins identifies Rab7 as a novel regulator of Aβ clearance in BV2 microglia.

To understand the role of the distinct Rab proteins that regulate β-amyloid clearance, we performed an RNA interference (RNAi)-mediated silencing screen of all the Rab-GTPases of the genome in a BV2 microglia cells, followed by overnight (20 h) incubation of conditioned medium containing Aβ and analyzed the levels of residual Aβ using electrochemiluminescence (ECL) platform (Rajendran et al., 2008; Udayar et al., 2013). We identified Rab7 a novel regulator of Aβ clearance. Silencing of Rab7 in BV2 microglia led to the increased uptake of Aβ from the extracellular space as evident by the lowest level of residual Aβ upon measurement by ECL assay (Figure 1). Though the residual Aβ level indicates clearance from the conditioned medium, the fate of the engulfed Aβ needed to be investigated. To validate this finding, we used another technique to analyze Aβ uptake. We visualized the increased uptake of Aβ by employing TAMRA labeled Aβ for the assays. We clearly see that Rab7 silencing leads to an increase in uptake of Aβ (Figure 2A). Moreover, in an independent RNAi screen for regulators of lysosomes we found that Rab7 silencing showed increased levels and altered distribution of LysoTracker stained acidic organelles (late-endosome/lysosome) (Figure 2B). This prompted us to further investigate the mehanisms involved in the increased clearance of Aβ upon Rab7 sliencing.

Rab7 silencing leads to impairment of lysosomal degradation pathway and impacts steady state Aβ levels.

To investigate whether this increased and altered distribution of the acidic organelles had an impact on lysosomal function we performed cathepsin B activity assay on intact and living cells. We employed Magic Red assay to monitor cathepsin B activity. After 72 hours siRNA transfection cells were incubated with Magic Red cathepsin B substrate for 1 hour. Cleavage of substrate by active cathepsin B leads to accumulation of fluorescent signal. Interestingly, cathepsin B activity was significantly reduced upon Rab7 silencing (Figure 3A). Since cathepsin B is active in lysosomes, the reduced cathepsin B activity indicates a possible impairment in lysosomal degradation pathway. To investigate if Rab7 silencing led to a general impairment in lysosomal degradation, we analyzed EGF/EGFR degradation upon Rab7 silencing. We used TAMRA labeled EGF and performed a pulse-chase experiment to investigate the fate of engulfed EGF. In line with the cathepsin B activity assay, EGF/EGFR degradation was severely impaired upon Rab7 silencing (Figure 3B). This prompted us to

investigate whether general protein accumulation was affected upon Rab7 depletion. ThioS staining revealed a significant accumulation of β-sheet rich-aggregates in the absence of Rab7, indicating an increase in general protein load (Figure 3C). Moreover, steady-state Aβ levels were significantly increased upon Rab7 silencing in HeLa cells expressing swedish APP. This suggests that steady-state Aβ levels depend on lysosomal pathway and that Rab7 could regulate this aspect of Aβ metabolism.

Rab7 silencing does not alter the sensitivity of primary neurons to exogenous Aβ42.

Since Rab7 silencing impaired lysosomal function and led to an increase in Aβ levels, we wondered whether Rab7 silencing also affects the level of Tau, another important player in Alzheimer's Disease. We investigated if the levels of Tau, is also affected upon Rab7 silencing. Indeed, the levels of total and phospho-Tau were significantly increased upon Rab7 silencing in primary neurons (Figure 4A). This is particulary interesting as Tau is a microtubule associated cytosolic protein. It is plausible that the increased Tau levels could be as a result of impaired autophagosome-lysosome fusion. Tau levels have shown to be dependent on autophagy (Inoue et al., 2012, Chesser et al., 2013). Moreover, Rab7 has been shown to be involved in the late maturation of autophagosomes (Gutierrez et al., 2004, Jäger et al., 2004). Thus, the increased Tau levels observed upon Rab7 silencing could be due to impaired late maturation of Tau containing autophagic vacuoles. Next, we asked if the observed lysosomal defects and increased Tau levels upon Rab7 silencing render the neurons more sensitive to insults from exogenously added Aβ42. Neurons showed a dose-dependent response to the exogenously added Aβ42 evident from the reduced cell viability (Alamar Blue) and increased LDH release upon increasing concentration of exogenously added Aβ42 (Figure 4B and 4C). This response was comparable between the control and Rab7 depleted condition (Figure 4B and 4C). We analyzed levels of synaptic protein synaptophysin and ER stress marker, GRp78 from primary neurons treated with exogenously added Aβ42 upon Rab7 silencing. Though, we observed a dose-dependent response to the exogenously added Aβ42 on the levels of these two proteins the effect was comparable in the Rab7 depleted and control conditions (Figure 4D). This suggests that exogenously added Aβ42 mediates neuronal toxicity independent of the lysosomal status or intracellular levels of Tau. It will be interesting to study whether endogenously produced Aβ, particularly Aβ42, would be more neurotoxic in Rab7 depleted conditions.

Conclusion:

In all, we show that Rab7 silencing increases uptake of Aβ in BV2 microglia but the cells do not degrade the enguled Aβ as efficiently as in the control conditions. Moreover, Rab7 silencing impairs lysosomal degradation pathway, increased steady-state Aβ and total-Tau/phospho-Tau levels. Our study suggests that both Aβ and tau can be degraded intracellularly by the lysosomal pathway and its disruption could contribute significantly to the pathogenesis observed in AD.

ACKNOWLEDGEMENTS

We thank G. Yu for the HeLa-swAPP cells. We thank M. Schwab, E. Stoeckli and the members of the Rajendran Lab for critical input into the study. L.R acknowledges the financial support from the Swiss National Science Foundation grant, Sinergia grant, the Velux Foundation, Bangerter Stiftung, Baugarten Stiftung, Cure Alzheimer's Fund and the Synapsis Foundation. L.R and V. U acknowledge the funding support from the European Neuroscience Campus of the Erasmus Mundus Program.

Materials and Methods

Cell culture

BV2 microglia cells were cultured in Dulbecco's modified Eagle's medium (Invitrogen) at 37°C and 5% CO_2 in a humidified incubator. Media were supplemented with 10% (v/v) fetal calf serum (Invitrogen), 1% (v/v) penicillin/streptomycin. HeLa cells expressing the Swedish mutant of APP (HeLa swAPP) cells were cultured in Dulbecco's modified Eagle's medium (Invitrogen) at 37°C and 5% CO_2 in a humidified incubator. Media were supplemented with 10% (v/v) fetal calf serum (Invitrogen), 1% (v/v) penicillin/streptomycin (Gibco) 0.1%(v/v) G418 antibiotic (Carl Roth) and 0.1%(v/v) selective antibiotic Zeocin (Invitrogen). Primary neurons isolated from E-16 embryos were cultured in NBM (Invirtogen) supplemented with B27 (Invitrogen)

siRNAs

All siRNAs are chemically synthesized stealth^{TM} siRNAs from Invitrogen. A pool of 4 different siRNA against all the proteases were transfected into HeLa swAPP cells, BV2 microglia cells and primary neurons.

siRNA Reverse Transfection (HeLa and BV2 microglia)

For HeLa cells, transfection complexes in quadruplicates were prepared in Opti-mem serum-free medium (Invitrogen) by mixing 0.3 µL of Oligofectamine (Invitrogen) and 5 nM of siRNA. Cells were seeded at a density of 3500 cells/well in 96-well format after addition of transfection complexes. For BV2 microglia cells, cells were seeded at a density of 4500 cells/well in 96-well format the day before transfection (minimum 20 hours before transfection). On the day of transfection, complexes in quadruplicates were prepared in Opti-mem serum-free medium (Invitrogen) by mixing 0.27 µL of Lipofectamine 2000 (Invitrogen) and 10 nM of siRNA. After 25 minutes of incubation transfection complexes were added on to the cells.

siRNA Forward Transfection in primary neurons

Transfection complexes in quadruplicates were prepared in NBM medium (Invitrogen) by mixing 0.35 µL of RNAi max (Invitrogen) and incubated for 5 mins (Reagent 1). 50 nM of siRNA was mixed in 10 ul of NBM medium (Invitrogen) and also incubated for 5 mins (Reagent 2). Both the reagents were mixed and incubated for 20 minutes followed by addition on primary neurons. Primary neurons were 5-6 days in culture before transfections.

Aβ clearance assay with BV2 microglia

BV2 microglia cells were transfected with the respective siRNAs. After 48 hours, Aβ containing conditioned medium from HeLa sweAPP were placed on the BV2 microglia. After 16 hours, supernatant was collected and assayed for Aβ40 levels by ECL ELISA.

Cell proliferation assay

69 h after siRNA transfection cell viability was analyzed with an alamar blue cell proliferation assay (AbD Serotec BUF012B) using a Plate reader with excitation at 544nm and emission at 590nm (Molecular Devices Spectramax Gemini XS) according to the manufacturer's recommended protocol.

SDS-PAGE and Immunoblotting

For detection of intracellular proteins, whole cell extracts were prepared using a lysis buffer (1%NP40 and 0.1% SDS) supplemented with proteinase inhibitors. Extracts were subjected to SDS-PAGE using pre-cast gels (Invitrogen). In all cases, gel loading was normalized to total protein content in the cell extract (Using BCA assay). Proteins were transferred onto nitrocellulose membranes, which were then blocked with PBS containing 5% (w/v) dry skim milk for at least 1 h at room temperature. The membranes were then incubated with different primary antibody followed by the appropriate horseradish peroxidase-conjugated secondary antibody for at least 1 h at room temperature. Both antibodies were diluted in 5% milk/PBS 0.05% Tween-20. Immunoblotted proteins were detected using an enhanced chemiluminescence kit (Pierce).

Electrochemiluminescence (ECL) Assay

MSD 96-Well MULTI-ARRAY Human Multiplex Kits were used (Meso Scale Discovery) to measure the level of Aβ38, Aβ40 and Aβ42. For the measurment of Aβ40 and sAPPβ 384 well MULTI-ARRAY Human Electrochemiluminescence plate was used following the instructions of the manufacturer.

Aβ42 toxicity assay on neurons

48 hours after siRNA transfection, primary neurons were treated with different concentrations of Aβ42 which were freshly prepared by separating aggregated proteins

through column chromatography. Only monomeric/oligomeric Aβ42 were added on the primary neurons.

Cathepsin B assay

Magic Red Cathepsin B assay kit from Immunochemistry Technologies (Cat no. 937) was used to perform cathepsin B assay according to the manufacturer's protocol.

References:

Chesser A.S., Pritchard S.M., and Johnson G. V. W. (2013). Tau Clearance Mechanisms and Their Possible Role in the Pathogenesis of Alzheimer Disease. Front Neurol. 4:122.

Frenkel, D., Wilkinson, K., Zhao, L., Hickman, S.E., Means, T.K., Puckett, L., Farfara, D., Kingery, N.D., Weiner, H.L., and El Khoury, J. (2013). Scara1 deficiency impairs clearance of soluble amyloid-b by mononuclear phagocytes and accelerates Alzheimer's-like disease progression. Nat. Commun. 4, 2030.

Gutierrez M.G., Munafó D.B., Berón W., Colombo M.I. (2004). Rab7 is required for the normal progression of the autophagic pathway in mammalian cells. J Cell Sci. 2687-97

Inoue K., Rispoli J., Kaphzan H., Klann E., Chen E. I., Kim J., Komatsu M., Abeliovich A. (2012). Macroautophagy deficiency mediates age-dependent neurodegeneration through a phospho-tau pathway. Molecular Neurodegeneration 1750-1326-7-48

Jäger S., Bucci C., Tanida I., Ueno T., Kominami E., Saftig P., Eskelinen E.L. (2004). Role for Rab7 in maturation of late autophagic vacuoles. J Cell Sci. 4837-48.

Paolicelli,R.C., Bolasco, G., Pagani, F., Maggi, L., Scianni, M., Panzanelli, P., et al.(2011). Synaptic pruning by microglia is necessary for normal brain development. *Science* 333, 1456–1458.

Paresce, D.M., Ghosh, R.N., and Maxfield, F.R. (1996). Microglial cells internalize aggregates of the Alzheimer's disease amyloid beta-protein via a scavenger receptor. Neuron 17, 553–565.

Rajendran, L., Schneider, A., Schlechtngen, G., Weidlich, S., Ries, J., Braxmeier, T., Schwille, P., Schulz, J.B., Schroeder, C., Simons, M.*, et al.* (2008). Efficient inhibition of the Alzheimer's disease beta-secretase by membrane targeting. Science *320*, 520-523.

Selkoe DJ, Hardy J. (2016) The amyloid hypothesis of Alzheimer's disease at 25 years. *EMBO Molecular Medicine*. ;8(6):595-608.

Sierra A, Abiega O, Shahraz A, Neumann H. (2013). Janus-faced microglia: beneficial and detrimental consequences of microglial phagocytosis. Frontiers in Cellular Neuroscience 7:6.

Udayar, V., Buggia-Prevot, V., Guerreiro, R.L., Siegel, G., Rambabu, N., Soohoo, A.L., Ponnusamy, M., Siegenthaler, B., Bali, J., Aesg*, et al.* (2013). A paired RNAi and RabGAP overexpression screen identifies Rab11 as a regulator of beta amyloid production. Cell Rep *5*, 1536-1551.

Willem, M., Lammich, S., and Haass, C. (2009). Function, regulation and therapeutic properties of beta-secretase (BACE1). Semin Cell Dev Biol *20*, 175-182.

Figure 1

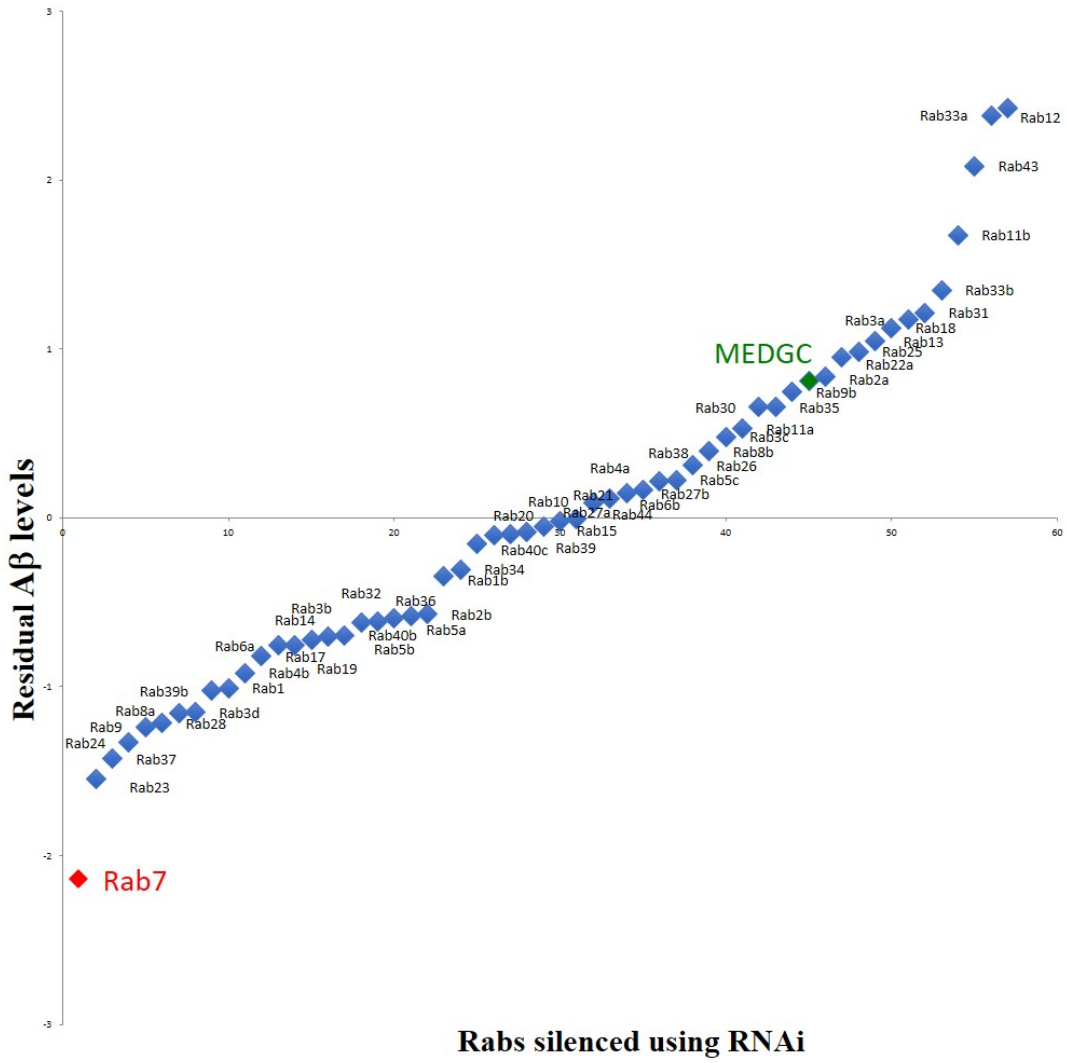

Figure 1: RNAi screen for genome-wide Rabs to identify Aβ clearance regulators

Z-score of Rab-GTPase RNAi screen for residual Aβ after Aβ uptake/clearance assay. BV2 microglia cells transfected with siRNA for all the Rab-GTPases and incubated overnight (20 h) with conditioned medium containing Aβ. Graph shows Z-scores of residual Aβ levels (Y axis) after all the mouse Rabs were knocked down (x-axis) and the Aβ uptake/clearance assay performed on these cells. Rab7 KD (knockdown) (red) shows the lowest level of residual Aβ compared to control (MEDGC, green) suggesting an increase uptake.

Figure 2

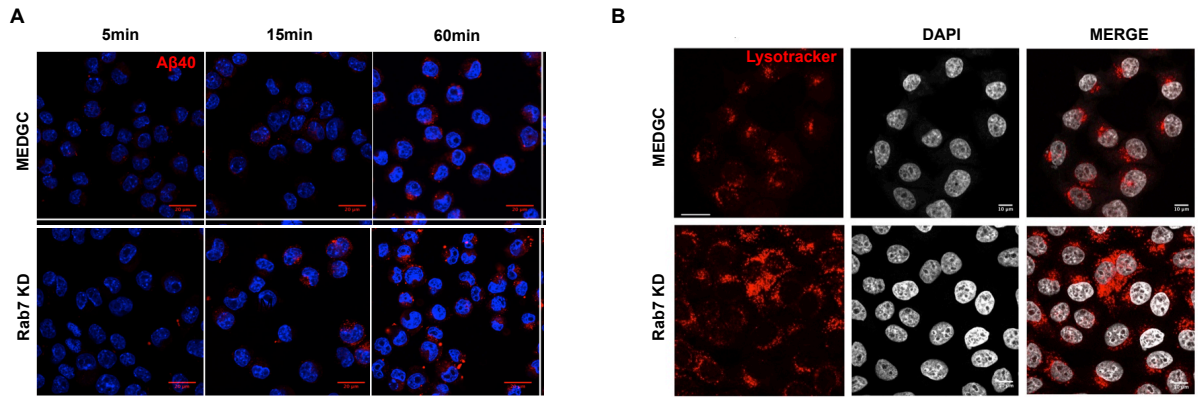

Figure 2: Fluorescent Aβ uptake in BV2 microglia upon Rab7 depletion

A. BV2 microglia cells transfected with siRNA for Rab7 and incubated with Aβ40-TAMRA (5, 15, 60 min). Rab7 KD leads to increased uptake of Aβ40-TAMRA. B. Hela cells transfected with siRNA for Rab7 and incubated with LysoTracker for 1.15 h to stain acidic organelles. Rab7 KD leads to altered distribution and increased levels of LysoTracker positive organelles.

Figure 3

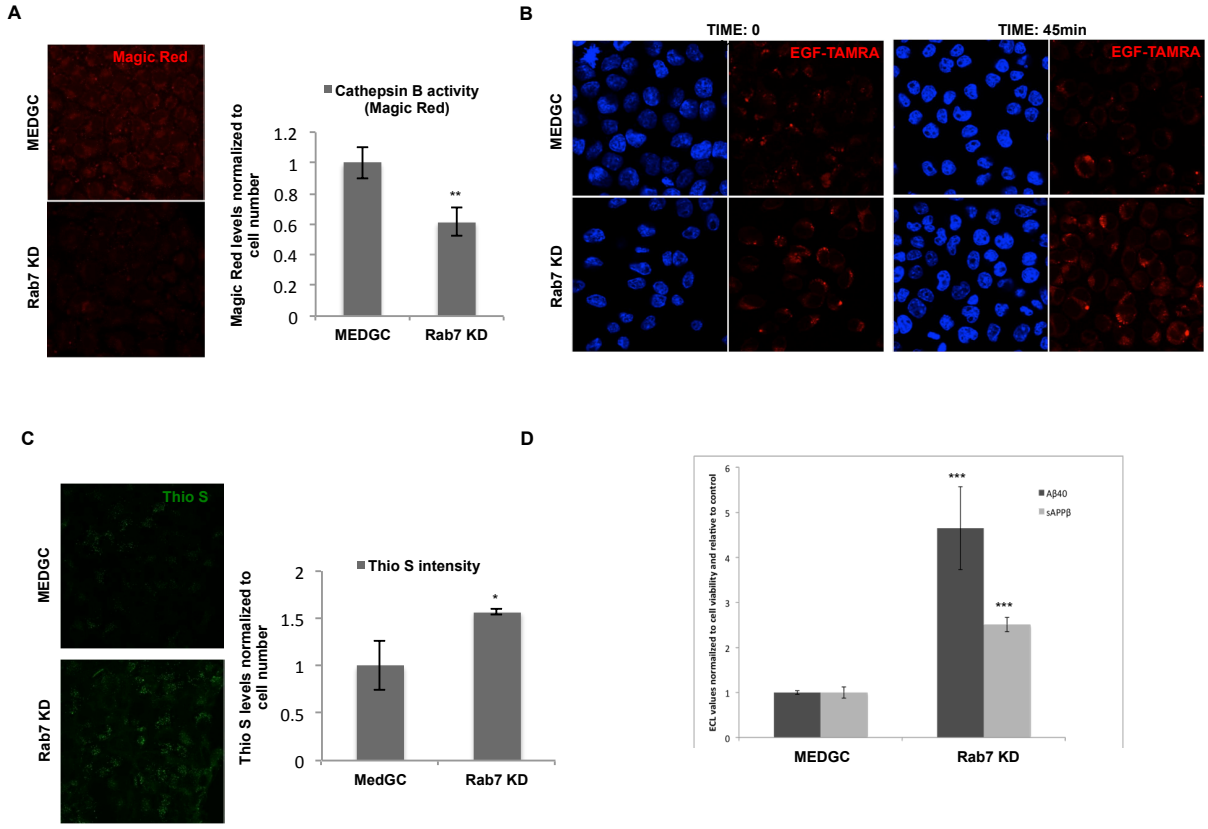

Figure 3: Effect of Rab7 depletion on lysosomal function

A. Hela cells were transfected with siRNA for Rab7 and incubated with Magic Red for 1 hour. Rab7 KD leads to reduced cathepsin B activity. B. Hela cells transfected with siRNA for Rab7 and pulse-chased with EGF-TAMRA. Rab7 KD leads to increased accumulation of EGF-TAMRA upon 45 minutes of chase indicating decreased degradation of EGF-TAMRA. C. Hela cells were transfected with siRNA for Rab7 and fixed and stained with Thio S dye. Rab7 KD leads to increase in general protein accumulation as evident by increased Thio S signal. D. HeLa cells expressing Swedish APP were transfected with siRNA for Rab7 and after 69 hours conditioned medium was collected. Aβ and sAPPβ in the conditioned medium was analyzed by ECL assay. Rab7 KD led to an increase in Aβ and sAPPβ levels. All statistics were performed using the 2 tailed *t*-tests. * $p<0.05$, ** $p<0.01$, *** $p<0.001$.

Figure 4

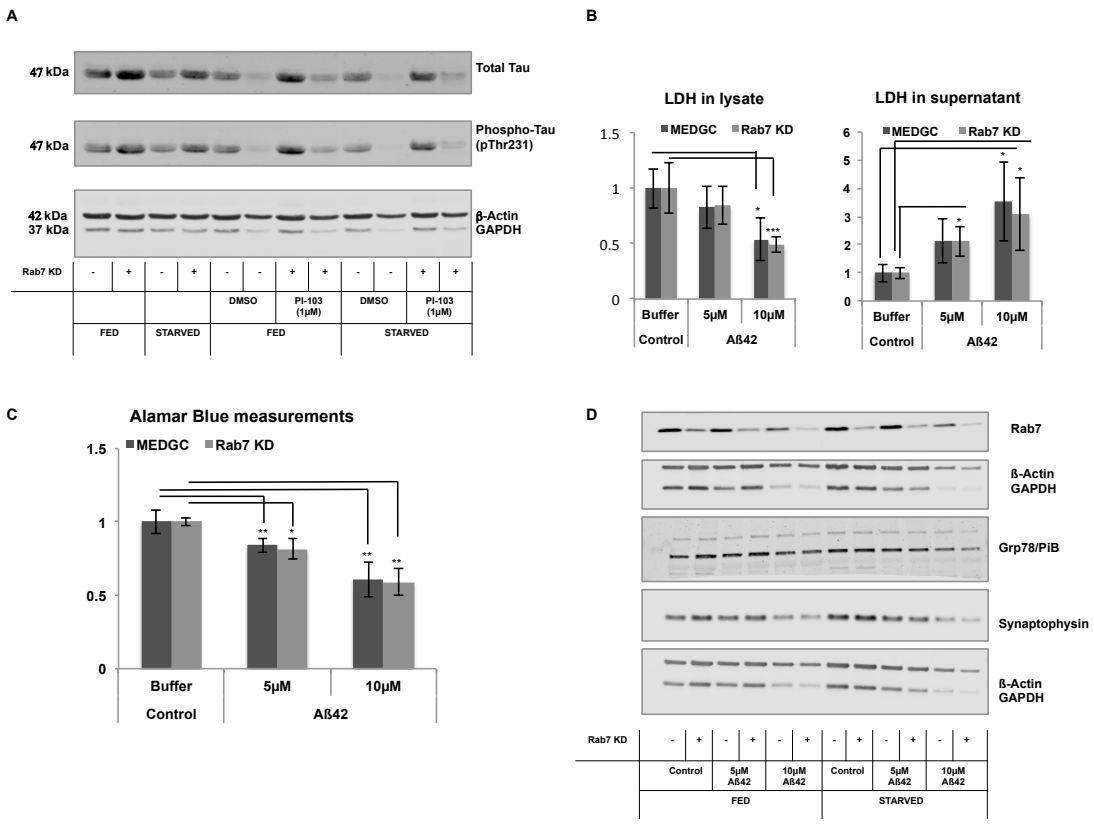

Figure 4: Effect of Rab7 depletion on neuronal tau levels

A. Mouse primary neurons were transfected with siRNA against Rab7 and the lysates were processed for western blotting to analyze the levels of total-Tau/phospho-Tau. Rab7 silencing led to an increase in both total-Tau and phosphor-Tau. B. Mouse primary neurons were transfected with siRNA against Rab7 and after 60 hours the neurons were treated with Aβ42. LDH levels were measured in cell lysates and supernatant from the treated neurons. C. Mouse primary neurons were transfected with siRNA against Rab7 and after 60 hours the neurons were treated with Aβ42. Cell viability was analyzed by monitoring metabolism of Alamar Blue dye. D. Mouse primary neurons were transfected with siRNA against Rab7. After 60 hours the neurons were treated with Aβ42 and the lysates were processed for western blotting to analyze the levels of different proteins. * $p<0.05$, ** $p<0.01$, *** $p<0.001$.

Chapter 3

The Alzheimer's disease Presenilin-2 negatively regulates β-amyloid levels by modulating lysosomal function

Vinod Udayar*[,a,b,c], Rosa Paolicelli*[,a,d], Jitin Bali*[g], Mrityunjoy Mondal*[,a,c,], Ju-Hyun Lee[e], Andrea Valeri[a,d], Gabriele Siegel[a,d], Ralph Nixon[e], Wim Annaert[f], and Lawrence Rajendran[a,d]

[a] *Systems and Cell Biology of Neurodegeneration,* [b] *Erasmus Mundus Neuroscience program,* [c] *Graduate programs of the Zurich Neuroscience Center and IMMED,* [d] *IREM, University of Zurich, Wagistrasse 12, 8952, Schlieren, Switzerland.* [e] *Center for Dementia Research, Nathan S Kline Institute, 140 Old Orangeburg Road, Orangeburg, NY 10962, USA.* [f] *VIB Center for the Biology of Disease, KU Leuven, 3000 Leuven, Belgium; Department of Human Genetics, KU Leuven, 3000 Leuven, Belgium.* [g]*Max Planck Institute for Biology of Ageing, Joseph-Stelzmann-Str. 9b D-50931 Cologne, Germany.*

* Contributed equally to this work

(Parts of this chapter were submitted in the PhD thesis of Dr. Jitin Bali to the University of Zurich)

Correspondence to: rajendran@bli.uzh.ch

Keywords:
Alzheimer's disease, PS2, PS1, RNAi, APP, amyloid, lysosomes, neurons, Lamp2, microglia.

Author contributions: L.R designed research; V.U, R.P, and M.M performed experiments for validations and mechanistic characterizations in cell lines, neurons, microglia and animal tissues. J.B performed the initial RNAi screen and experiments in cell lines. A.V provided technical assistance with animal work, G.S. performed the siRNA transfection in mouse primary neurons. J.H.L and R.N provided the data on calcium efflux and PS2. W.A provided AD-PS2KO mice tissues and samples for analysis. L.R, V.U, R.P and M.M co-wrote the paper and all the authors participated in the editing of the manuscript.

Abstract

β-Amyloid (Aβ) peptide, causatively linked to Alzheimer's disease (AD), is generated from amyloid precursor protein (APP) by the β-and γ-secretases. γ-Secretase activity is conferred by an intramembrane protease complex, which contains either Presenilin-1 (PSEN1) or Presenilin-2 (PSEN2) as its catalytic component. While autosomal dominant mutations in both presenilins cause early onset AD, the functional origin of the existence of these paralogues is not yet known. In an unbiased genome-wide human protease siRNA screen, we identified PSEN2 as an unprecedented negative regulator of Aβ levels as opposed to PSEN1, whose silencing strongly reduced Aβ levels as previously reported. Mechanistically, PSEN2, unlike PSEN1, is localized in late-endosomes/ lysosomes and impacts the functionality of degradative lysosomal structures. PSEN2 deficiency reduced both lysosomal number and function and thus impaired Aβ degradation in neurons and microglia. PSEN2 knockout mice crossed with an AD mouse model showed exacerbated amyloid pathology. Our study, for the first time, shows a functional dichotomy between PSEN1 and PSEN2: while PSEN1 is largely responsible for Aβ production, PSEN2 controls Aβ clearance in lysosomes thus effecting homeostatic control in the process. Our results imply that disturbances in this balance could affect Aβ accumulation and thus confer the risk to develop AD.

Introduction

Alzheimer's disease (AD) is the most common form of neurodegenerative disease (De Strooper; Hardy and Higgins, 1992). A characteristic feature of the disease is the presence of amyloid-β (Aβ) containing plaques in the brain (Hardy, 1996). The soluble oligomeric form as well as the plaque-associated form of Aβ peptide is believed to cause the neurodegeneration observed in AD. Aβ is liberated from the amyloid precursor protein (APP) via proteolytic processing by β- and γ-secretases (Thinakaran and Koo, 2008). β-Secretase activity is conferred by a transmembrane aspartyl protease, also termed BACE1 (β-amyloid cleaving enzyme 1) and catalyzes the rate limiting reaction in the generation of Aβ (Haass and Selkoe, 2007; Vassar et al., 2009). γ-Secretase is a multi-component complex that is composed of presenilin (PSEN1/PSEN2), Nicastrin, APH-1 (APH1A/ APH1B) and PEN-2 (De Strooper, 2003; Hartmann et al., 1997; Vetrivel et al., 2004). Familial mutations in APP or in the components of the γ-secretase complex that increase the production of a longer version of Aβ, Aβ42, have been associated with the early onset of the disease (Hardy and Crook, 2001; Tanzi and Bertram, 2005). All these data suggest amyloid-dependent mechanisms in the pathogenesis of familial AD (Borchelt et al., 1996; Hardy and Selkoe, 2002). However, the cause of the late onset AD, which contributes 95% of the total AD cases, is still not understood (Hardy, 2006). Several lines of evidence suggest that genetic modifiers of late onset AD (the case of APOe4) also regulate Aβ metabolism, raising the possibility that genes regulating APP processing might influence the risk for AD (Harold et al., 2009)(Bali et al, PNAS, 2012). Therefore, identification of genes involved in the regulation of Aβ level constitutes a necessary step towards understanding the pathogenesis of late onset AD and for designing effective therapy. In particular, not much is known about the proteases that regulate the key secretases in the amyloidogenic processing of APP. In addition, while mutations in both PSEN1 and PSEN2 cause early onset AD, not much is known about the functional distinction between these two paralogues. Here, through an RNAi screen of genome-wide proteases and an independent epistasis screen of all the γ-secretase components, we identify PSEN2 as a negative regulator of Aβ levels.

Results and Discussion

RNAi screen for genome-wide proteases identifies PSEN2 as a major negative regulator of Aβ *(This section was part of Dr. Jitin Bali's PhD thesis)*

To understand the role of the distinct proteases that regulate β-amyloid production, we performed an RNA interference (RNAi) screen of all the proteases of the human genome in a human cell model of AD (Rajendran et al, Science, 2008; Udayar et al, Cell reports, 2013), and analyzed the levels of Aβ using an electrochemiluminescence (ECL) assay (Fig.1A). Depletion of the β-secretase (BACE1; β-site APP cleaving enzyme 1) induced one of the strongest depletion of Aβ confirming that BACE1 is the β-secretase in the amyloidogenic processing of APP. Since presenilins (PSENs) are also critically involved in the production of Aβ (Annaert et al., 1999; De Strooper et al., 1998; Hartmann et al., 1997), we used both PSEN1 and PSEN2 as positive controls (Borchelt et al., 1996; Tomita et al., 1997). While PSEN1 silencing led to a significant decrease in Aβ levels, PSEN2 silencing had the opposite effect, resulting in a significant increase in Aβ levels (Fig.1A). In another set of experiments where we only silenced the different components of γ-secretase (PSEN1, PSEN2 and PEN-2) to study specifically the functional consequences of the two presenilin paralogues (PSEN1 and PSEN2) on γ-secretase heterogeneity (Serneels et al., 2009), we again found that PSEN2 silencing increased Aβ levels while PSEN1 silencing reduced Aβ levels (Fig.1B). On the other hand, silencing of PEN-2 completely abolished Aβ production which was similar to silencing both PSEN1 and PSEN2 together (Fig.1B,C). Importantly, the opposite effects of PSEN1 and PSEN2 silencing on Aβ levels were present for all major Aβ species (Aβ38, Aβ40 and Aβ42) (Sup Fig.1). In order to rule out that the observed effect of PSEN2 silencing was an ECL measurement artifact, we investigated whether a similar increase in Aβ levels could be detected by conventional western blotting from the plain conditioned medium or after immunoprecipitation (IP) of Aβ from conditioned medium. As shown in Fig. 1D, upon PSEN2 silencing an increase in Aβ was visible in the supernatant even without any IP required (4kDa band). After IP using 6E10 antibody, we could clearly detect an increase in Aβ levels upon PSEN2 silencing but not PSEN1/2 or PSEN1. To investigate whether PSEN2 silencing would increase the levels of any secreted molecule, we analyzed secreted alkaline phosphatase (SEAP) in the different conditions and found that PSEN2 removal did not affect its secretion (Sup Fig.2).

To rule out any siRNA mediated off-target effects, we performed three different validation experiments. First we used two different siRNA oligonucleotide sequences against PSEN2

and both of these increased Aβ levels independently (Sup Fig.1). As controls, we used two different sequences targeting PSEN1 and both of them significantly decreased Aβ levels. We then independently verified the findings through enzymatically produced RNAi, esiRNA (Kittler et al 2006). Consistently, we found that PSEN2 silencing induced a significant increase in Aβ levels, while PSEN1, as expected, lead to a reduction (Fig.1E). To validate these findings in the WT APP context, we silenced PSEN2 in HEK cells expressing the human WT APP and found that PSEN2 silencing dramatically increased Aβ levels (Sup Fig.3). Finally, we performed rescue experiments wherein we overexpressed the murine PSEN2 (mPSEN2), resistant to human siRNA, in cells depleted of the endogenous PSEN2. *mPSEN2* overexpression clearly rescued Aβ levels in the PSEN2 silencing condition (Fig.1F). Interestingly, mPSEN2 overexpression also significantly reduced Aβ in the control condition (Fig.1F). All these results conclusively demonstrate that PSEN2 negatively regulates Aβ levels.

PSEN2 deletion exacerbates amyloid pathology in AD transgenic mice

(data from fig.2A-C was part of Dr. Jitin Bali's PhD thesis)

To validate our initial observations in the neuronal context, we silenced PSEN2 in primary mouse cortical neurons overexpressing human APP carrying the Arctic and Swedish mutations (Fig.2A). Consistent with the results from human cell lines, PSEN2 silencing significantly increased Aβ levels also in primary neuronal cultures (Fig.2A). Western blotting and immuno-fluorescence staining with anti-PSEN2 antibodies confirmed the efficiency of the knockdown (Fig.2A, B). We further validated our finding in primary neurons prepared from APP (arc/swe) transgenic mice crossed with PSEN2 deficient mice. We observed that PSEN2 (-/-) and to a lesser extent PSEN2 (+/-) neurons have higher Aβ levels compared to PSEN2 (+/+) neurons (Fig.2C). These results support that PSEN2 negatively regulates Aβ levels. To investigate whether PSEN2 regulates amyloid levels in an *in vivo* setting, we crossed AD transgenic mice co-expressing APP KM670/671NL and PSEN1 L166P (APPPS1 mice, Radde et al., 2006) to PSEN2 knockout mice, to generate APPPS1 mice deficient for PSEN2. Thioflavin S (ThioS) staining, routinely employed to determine the presence of β-sheet rich protein aggregates, revealed significantly increased amyloid plaque load in the brain of 6 months old APPPS1 mice lacking PSEN2, as compared to their PSEN2(+/+) littermates (Fig.2D). Detailed morphometric analysis of plaques by 3D reconstruction showed increased plaque number, volume and average size in PSEN(-/-) APPPS1 mice compared to PSEN2 (+/+) controls (Fig. 2D-H). Size distribution analysis of the plaques also

showed a specific increase in medium to large plaques (5000-40000 μm^3), in APPPS1 mice lacking PSEN2 (Fig. 2I). The mean intensity of ThioS signal between the two groups was not changed, indicating no alterations of amyloid binding property of ThioS (Sup Fig.4). Overall, these findings provided *in vivo* evidence for a novel role for PSEN2 in regulating amyloid burden.

Increased Aβ upon PSEN2 silencing is not due to increased γ-secretase activity

(This section was part of Dr. Jitin Bali's PhD thesis)

To study the mechanism through which PSEN2 regulates Aβ levels, we first assessed whether silencing of PSEN2 increased PSEN1 levels or its activity in a compensatory way, thereby leading to an increase in Aβ production. Quantitative mRNA analysis (Fig. 3A-C) showed that PSEN2 knockdown did not significantly affect PSEN1 mRNA levels, however we see a slight increase in protein levels by Western blotting (Fig. 3D).

Considering previous studies showing that PSEN2 provided only minimal contribution to APP cleavage (Franberg et al., 2011), we pondered over the attractive hypothesis that γ-secretase complexes containing PSEN2 outnumber complexes containing PSEN1, which are more efficient in cleaving APP and thus producing Aβ.

If this hypothesis were to be correct, PSEN2 depletion would increase PSEN1-complexes and hence Aβ production. To test whether PSEN1 activity is increased, we employed two independent approaches. In the first set of experiments, we studied the amyloidogenic processing of APP and found, as expected, that it was significantly impaired by depletion of PSEN1, as seen by the accumulation of the CTFs (Fig. 3E). Contrary to the hypothesis, a similar impairment was also observed when PSEN2 was silenced (Fig.3E), suggesting that PSEN2 also contributes to the cleavage of APP-CTFs and Aβ generation (Sannerud et al, 2016). We cannot still rule out a possibility that PSEN2 determines the half-life of PEN2, which can in turn affect both presenilins/ γ-secretase activity. Silencing of PSEN1 and PSEN2 together further increased the accumulation of the APP-CTFs suggesting that γ-secretase activity is fully abolished (Fig.3E). This showed that PSEN2, like PSEN1, could efficiently process APP in the cellular context. In a second set of experiments, we studied whether PSEN2 loss affected the γ-secretase activity by using a fluorescently labeled inhibitor (GSI) that specifically labeled active γ-secretase complexes (Fig.3F). Validation experiments confirmed that GSI was indeed able to prevent Aβ production in a cellular

context, leaving unaltered sAPPβ levels (Fig.3G). Mouse embryonic fibroblasts from wildtype mice showed labeling with the fluorescent GSI in punctate and diffuse structures, while the signal was massively reduced in fibroblasts deficient for both PSEN1 and PSEN2, thus demonstrating the specificity of the inhibitor (Fig.3H). Notably, cells that lacked either PSEN1 or PSEN2 showed decreased fluorescent GSI labeling compared to the WT, indicating that both PSEN1 and PSEN2 contribute to the cellular pool of active γ-secretase complexes (Fig.3H). This clearly suggests that the increased Aβ observed upon PSEN2 silencing cannot be attributed to increased overall γ-secretase activity. All these results demonstrated that PSEN2 indeed contributes to the cleavage of APP similar to PSEN1 in the cellular context but nevertheless negatively regulates total Aβ levels.

PSEN2 silencing impairs starvation-induced lysosomal pathway, Aβ clearance and leads to general protein accumulation

Having ruled out an increased γ-secretase activity as the cause for increased Aβ production upon PSEN2 silencing, we investigated whether PSEN2 regulates Aβ clearance. Recently, we identified nutrient sensing mechanisms as a novel way that regulates lysosomal degradation of Aβ (Mondal and Bali et al., to be submitted). To test the possibility that PSEN2 plays a role in regulating nutrient signaling dependent degradation of Aβ, we measured Aβ levels in nutrient rich (Fed) and nutrient limiting (Starved) conditions, upon PSEN2 depletion. We observed that in fed conditions, PSEN2 silencing led to a significant increase in Aβ compared to control, confirming the results from our screen. When analyzing the effects of starvation, we observed a massive reduction (58.66 %, MEDGC FED vs MEDGC Starved) in Aβ levels compared to fed control (Fig.4A). However, in cells lacking PSEN2, nutrient limitation reduced Aβ only by 30.19 % (Fig.4A). This suggests that PSEN2 contributes to the regulation of nutrient signaling-mediated clearance of Aβ. Additionally, when we analyzed APP and APP-CTF levels upon PSEN2 silencing under different nutrient conditions, we observed that not only Aβ, but also APP levels were increased upon PSEN2 silencing (Fig.4B). In line with this, APP levels were shown to be regulated by the lysosomal degradation pathway (Xiao et al., 2015). Thus, we hypothesized that PSEN2 most likely regulates lysosomal function.

Since our findings pointed towards a general rather than an Aβ-specific degradative impairment, we hypothesized that PSEN2 regulates the whole lysosomal protein degradation process. We therefore investigated whether general amyloid load was altered upon PSEN2

silencing. To this end we used ThioS staining and optimized the use of ThioS to detect amyloid in the cellular context (Mondal, Bali et al, *under revision*). Though there was not a significant difference in ThioS signal between PSEN2-depleted cells and control in fed condition, significantly higher ThioS-positive structures were detected upon PSEN2 silencing in the absence of nutrients (Fig.4C), again supporting a critical role for PSEN2 in modulating nutrient signaling-mediated protein degradation. Intracellular protein clearance driven by nutrient limitation is thought to occur through the autophagy-lysosomal pathway, and thus we asked whether PSEN2 has a role in its regulation (Lee et al, Cell, 2010 for PSEN1 role in autophagy). First, we investigated the status of LC3I-to-LC3II conversion, as index of autophagosomes maturation, eventually degraded in lysosomes. In presenilins depleted cells, we observed accumulation of LC3II in baseline conditions (in the absence of chloroquine), indicative of impairment in the autophagic pathway (Fig. 4D). As autophagic cargo degradation requires functional lysosomes, and considering that lysosomal pathway is also the major degradative pathway for luminal cargoes, we investigated the lysosomal status of cells lacking PSEN2. Since lysosomal acidification is linked to its function, we first assessed the state of acidic organelles in the cells (late endosomes and lysosomes), by using the pH-sensitive dye LysoTracker-DND-99. No significant differences in LysoTracker levels were found upon PSEN2 silencing in fed conditions (Fig.4E). However, upon nutrient depletion, cells lacking PSEN2 completely failed to show the starvation-induced increase in LysoTracker levels that can be observed in control cells (Fig.4E). Consistent with our previous results, these data suggest that PSEN2 critically regulates nutrient sensing-mediated lysosomal degradation.

Under nutrient deprivation, lysosomal levels can be transcriptionally regulated by activation of the Coordinated Lysosomal Expression and Regulation (CLEAR) genes. Analysis of mRNA levels of CLEAR genes-network after PSEN2 silencing, in fed or starved conditions did not reveal major changes of the whole network. However, we observed a significant decrease specifically in the mRNA levels of ATP6V0E1, one of the subunits of the v-ATPase complex, required for lysosomal acidification, specifically under nutrient deprivation (Sup Fig.5). This finding could explain the reduction in LysoTracker positive structures in starved PSEN2-depleted cells. To verify the lysosomal status further, we analyzed the lysosomal marker Lysosomal Associated Membrane Protein 2 (LAMP2) by immunofluorescence and found that, while starvation strongly induced LAMP2 levels in scrambled condition, this was

not the case for PSEN2 depleted cells (Fig.4F), indicating that PSEN2 is required to mediate lysosomal function upon nutrient deprivation.

Lysosomal acidification and Ca^{2+} efflux impairment upon deletion of PSEN2

To understand the molecular mechanisms underlying lysosomal dysfunction in PSEN2 depleted cells, we performed another set of focused experiments in mouse embryonic fibroblast (MEF) cells. First, we conducted lysosomal acidity analyses using LysoTracker and quantified lysosomal pH using fluorometric analysis with LysoSensor blue/yellow dextran. We observed a marked reduction in numbers of LysoTracker positive puncta in PSEN2 KO cells although the intensity of some of the remaining puncta achieved a normal LysoTracker signal intensity (Fig.5A). To confirm acidification impairment more directly, we assessed lysosomal pH using Lysosensor and observed a significantly increased lysosomal pH in PSEN2 KO cells (pH 5.20) compared to WT cells (pH 4.87) (Fig.5B). In addition, we found the v-ATPase activity to be markedly reduced in PS2KO MEF cells (Fig 5C). Furthermore, CTSD activity as assessed by Bodipy-FL-Pepstatin A assay was significantly reduced compared to that in WT cells (Fig. 5D). Increased lysosomal pH upon PSEN1 deletion was shown to cause decreased lysosomal Ca^{2+} levels due to increased lysosomal Ca^{2+} efflux in a TRPML1 dependent manner (Lee et al., 2015). We investigated if PSEN2 loss also leads to a similar effect on Ca^{2+} homeostasis. Indeed, the abnormally elevated pH led to a significant reduction in lysosomal Ca^{2+} levels, as measured by low-affinity rhod-dextran (Fig.5E). This lysosomal Ca^{2+} decrease was associated with an elevation of cytosolic Ca^{2+} levels, as measured by Fura-2 (Fig.5E). We further investigated if, similar to PSEN1 deletion, loss of PSEN2 also led to decreased lysosomal Ca^{2+} levels due to hyperactive calcium channel, TRPML1. To this end, we tested if blocking the lysosomal NAADP dependent calcium channels by Ned-19 could prevent the increased cytosolic Ca^{2+} levels upon PSEN2 deletion. The cytosolic Ca^{2+} elevation observed by OGB-AM (Oregon-Green 488 Bapta-1 AM) in untreated PS2KO MEF cells was now corrected back to WT levels in the lysosomal NAADP dependent calcium channel inhibitor, Ned-19 treated PS2KO MEF cells (Fig.5F). Since TRPML1 is the main lysosomal NAADP dependent calcium channel, our data indicate that the increased cytosolic Ca^{2+} levels in PSEN2 KO are due to hyperactive TRPML1 channel. Overall, we provide mechanistic evidence for a critical role of PSEN2 in regulating lysosomal Ca^{2+} in a TRPML1 dependent manner.

Dysfunctional lysosomes in mice lacking PSEN2

Since APPPS1;PSEN2 KO mice displayed a significantly higher amyloid load than APPPS1;PSEN2 WT littermates, and having shown in a cellular context that PSEN2 critically regulates lysosomes, we hypothesized that the augmented plaque pathology in the AD mouse model lacking PSEN2 could originate from defective lysosomal function.

To our surprise, when assessed by western blotting, brain homogenates from APPPS1 mice lacking PSEN2 exhibited significantly higher levels of lysosomal proteins LAMP1 and LAMP2, as compared to APPPS1 PSEN2 WT littermates (Fig.6A-C). These findings were in apparent contrast with the decrease in LAMP2 observed upon PSEN2 silencing *in vitro*. However, further immunofluorescence examinations on APPPS1 mice brain slices revealed that conspicuous lysosomal structures (LAMP2 positive) were deposited around amyloid plaques (Fig.6D). It was previously shown that the majority of lysosomes surrounding plaques reside within swollen neuronal axons and lack functional proteases (Gowrishankar et al., 2015). Indeed, we found significantly higher amount of such plaque-associated LAMP2-positive organelles in PSEN2 KO mice (Fig.6E, F).

Of note, when we examined cortical areas devoid of plaques, we found that not only perinuclear levels of LAMP2 were significantly lower in neurons of PSEN2 KO mice, but were also associated with increased intraneuronal amyloid (Fig.6G-I), supporting defective intracellular Aβ clearance. We further validated this finding in primary neurons, where siRNA mediated silencing of PSEN2 led to decrease in LAMP2 protein levels (Sup Fig.6. Overall, these data indicate an impaired lysosomal function in the absence of PSEN2. We further looked at microglia specific lysosomal marker in these brain slices and found PSEN2 KO mice have significantly lower level of CD68 compared to PSEN2 WT mice (Fig.6J). This result infers that microglia lacking PSEN2 have lower lysosomal levels.

Impaired microglial clearance of amyloid upon PSEN2 depletion

Microglia are the resident brain macrophages and represent the major phagocytes of the CNS. Once phagocytosed, the cargoes are eventually degraded in lysosomes. Hence, a functional lysosomal degradation pathway is crucial for the maintenance of microglial phagocytosis. Since PSEN2 has been shown to be the predominant presenilin in microglia we hypothesized that depletion of PSEN2 could impair lysosomal pathway and thereby its phagocytic capacity (Jayadev et al., 2010). To understand whether presenilin depletion in microglia affects lysosomal function and if this has an impact on its amyloid clearance capacity, we performed

siRNA-mediated silencing of PSEN1, PSEN2 or PEN2 in BV2-microglia cells. The efficiency of the knockdown was confirmed by Western blotting (Fig. 7A, B).

Consistently with our previous data, depletion of either PSEN1 or PSEN2 led to a significant decrease in LAMP2 immunoreactivity (Fig.7C, D) as well as LysoTracker- signal (Fig. 7E, F). Of note, 3D reconstruction and quantification of the LysoTracker puncta confirmed the reduction in number of lysotracker-positive organelles upon PSEN1 and PSEN2 depletion (Fig.7G), but not upon other γ-secretase components, such as PEN2, APH1 and NCT (Sup Fig.7). We also validate our findings in primary microglia from WT and PSEN2 KO mice and found primary microglia lacking PSEN2 to have significantly less LysoTracker signal (Fig.7H, I). Importantly, interference with γ-secretase enzymatic activity without altering PSEN levels does not impair lysosomal acidification, as demonstrated by the treatment of BV2 cells with the γ-secretase inhibitor DAPT which even led to a slight increase in LysoTracker signal compared to controls (Fig.7J, K).These finding indicate that, apart from their well-documented role in the production of Aβ through the γ-secretase complex, presenilins have additional γ-secretase independent roles in maintaining the cells' degradative organelles.

Next, we investigated whether the impaired lysosomal state observed upon PSEN2 depletion would affect the microglial phagocytic capacity. To this end, we assessed microglia-mediated Aβ clearance by measuring residual levels of Aβ upon overnight incubation (Sup Fig.8). Interestingly, depletion of PSEN2 significantly reduced the microglial phagocytic capacity, as evidenced by the increase in residual Aβ in the assay medium as compared to control condition (Fig.7L). PSEN1 silencing also impaired Aβ clearance albeit to a much lesser extent as compared to PSEN2, whereas silencing of other γ-secretase components, such as PEN2, APH1 and NCT did not alter Aβ clearance (Fig.7L). In addition, BV2 microglia treated with DAPT also showed normal Aβ clearance rates (Fig.7M), again supporting a γ-secretase independent mechanism for presenilin-mediated control of lysosomal function.

Taken together our results demonstrate for the first time, that PSEN2, unlike PSEN1, negatively regulates Aβ levels. Till this date, no specific function of PSEN2 in APP cleavage is assigned. Our results, for the first time, demonstrate that these paralogues have diametrically opposite function – antagonizing each other- not at the catalytic level of the γ-secretase cleavages but at the regulation of the end product, namely, Aβ. It was demonstrated

recently by Sannerud et al., that PSEN2 localization is majorly restricted to late endosomes/lysosomes whereas PSEN1 is more broadly distributed in the cell (Sannerud et al., 2016). Taking into account our present data on the effect of PSEN2 silencing on lysosomal function and our recent finding linking nutrient sensing and lysosomal degradation we propose the following model to explain the functional dichotomy of the two presenilins. According to this model, PSEN1 is predominantly located in organelles in the biosynthetic pathway and is mainly involved in the production of Aβ. PSEN2 on the other hand is located in late endosome/lysosomes where it regulates lysosomal degradation pathway by possibly integrating nutrient signaling. Presenilin double knock-out cells have been shown to have dysfunctional nutrient sensing ability along with an impaired lysosomal degradation pathway which were rescued by expressing PSEN1 or PSEN2 (Reddy et al., 2016). Though the authors imply functional redundancy for the two presenilins, we believe that in homeostatic conditions, PSEN2, by virtue of its presence on late endosomes/lysosomes, regulates nutrient signaling and lysosomal degradation pathway.

Transcription factor TFEB is one of the major regulators of lysosomal biogenesis upon nutrient deprivation and was shown to be involved in mediating presenilin-loss induced lysosomal dysfunction (Reddy et al., 2016). We investigated whether starvation-induced nuclear translocation of TFEB, required for its transcriptional activity, was impaired in PSEN2 depleted cells. By using HeLa cells stably expressing GFP-tagged TFEB, we found that TFEB nuclear translocation was not significantly affected upon PSEN2 depletion (Sup Fig. 9A, B). This is in line with our data from the analysis of TFEB-mediated CLEAR network genes activation, which was not altered upon PSEN silencing. These data so far seem to exclude an impairment of TFEB-mediated lysosomal biogenesis, however the contribution of other transcription factors (such as TFE3, MITF and FOXO3), either individually or in concert, might explain the observed decrease in lysosomal markers. One of the upstream signaling cascades that could link nutrient signaling, lysosomal function and protein level is the mTOR signaling pathway. mTOR is the central kinase, which regulate protein synthesis and higher mTOR activity suppresses protein clearance. To investigate mTOR activity, we looked at 1) phosphorylation status of downstream substrate of mTOR and 2) mTOR/LAMP2 localization. We found no significant changes in mTOR activity assessed by phosphorylation status of its downstream substrates (S6K, Ulk1, 4EBP1), suggesting that mTOR signaling does not mediate the lysosomal dysfunction observed upon nutrient deprivation in PSEN2 depletion (Sup Fig.9C). Additionally, we also did not observe

any significant difference in mTOR/LAMP2 localization between control and PSEN2 depleted condition (Sup Fig.9D). Considering that mTOR pathway also regulates TFEB-mediated lysosomal biogenesis, we could rule out a direct involvement of TFEB/mTOR pathway in the PS2 depletion-induced lysosomal defects.

We observed the effect of PSEN2 deficiency on Aβ clearance both in neuronal as well as microglial cells. Neurons are generally thought to be involved in Aβ generation and microglia in Aβ clearance. Our results, however, show the existence of an intracellular lysosomal Aβ degradation pathway in both neurons and microglia and a crucial role for PSEN2 in the regulation of this pathway. We believe that our results also suggest that inhibition of γ-secretase should be carried out not on PSEN2-containing γ-secretase but on PSEN1-containing complexes. Interestingly, PSEN2-sparing inhibitors are available (Borgegård et al., 2012). Since γ-secretase inhibitors (GSIs) produced adverse effects on cognition in the recent clinical trials (Karran et al., 2011; Sambamurti et al., 2011; Schor, 2011) and also that GSIs are potentially toxic compounds, our results caution that specific or more PSEN2-inhibition could cause adverse effects or even worsen the pathology.

Materials and Methods

Cell culture and AD mouse model

HeLa cells expressing the Swedish mutant of APP (HeLa swAPP) cells were cultured in Dulbecco's modified Eagle's medium (Invitrogen) at 37°C and 5% CO_2 in a humidified incubator. Media were supplemented with 10% (v/v) fetal calf serum (Invitrogen), 1% (v/v) penicillin/streptomycin (Gibco) 0.1%(v/v) G418 antibiotic (Carl Roth) and 0.1%(v/v) selective antibiotic Zeocin (Invitrogen).Primary neurons isolated from E-16 embryos were cultured in NBM (Invirtogen) supplemented with B27 (Invitrogen). Mouse Embryonic Fibroblasts lines (MEFs), acquired from Dr. Bart De Strooper (Leuven Institute for Neurodegenerative Disease, Belgium), and Murine neuroblastoma (N2a) were maintained in DMEM (Invitrogen, 11995-073) with 10% FBS (Hyclone,), and penicillin/streptomycin (Invitrogen) at 37°C and 5% CO2. AD transgenic PS2 knockout mice were generated from B6-Tg (Thy1-APP KM670/671NLjuc; Thy1-PS1 L166Pjuc) mice (Radde et al., 2006)

siRNAs

All siRNAs are chemically synthesized stealth^{TM} siRNAs from Invitrogen. A pool of 4 different siRNA against all the proteases were transfected into HeLa swAPP cells.

siRNA Reverse Transfection

Transfection complexes in quadruplicates were prepared in Opti-mem serum-free medium (Invitrogen) by mixing 0.3 µL of Oligofectamine (Invitrogen) and 5 nM of siRNA. HeLa sw APP cells at a density of 3500 cells/well were seeded in 96-well format after addition of transfection complexes.

siRNA Forward Transfection in primary neurons

Transfection complexes in quadruplicates were prepared in NBM medium (Invitrogen) by mixing 0.35 µL of RNAi max (Invitrogen) and incubated for 5 mins (Reagent 1). 50 nM of siRNA was mixed in 10 ul of NBM medium (Invitrogen) and also incubated for 5 mins (Reagent 2). Both the reagents were mixed and incubated for 20 minutes followed by addition on primary neurons. Primary neurons were 5-6 days in culture before transfections.

Cell proliferation assay

69 h after siRNA transfection cell viability was analyzed with an alamar blue cell proliferation assay (AbD Serotec BUF012B) using a Plate reader with excitation at 544nm and emission at 590nm (Molecular Devices Spectramax Gemini XS) according to the manufacturer's recommended protocol.

Treatment with γ-Secretase inhibitors

10,000 HeLa-swe APP cells were seeded in each well of a 96 well plate (Nunc) a day prior to inhibitor treatment. On the day of inhibitor treatment medium was replaced with fresh medium containing DAPT (Sigma) or fluorescent γ- secretase inhibitor . Cells were incubated with these inhibitors for 3 hours. Alamar blue measurements were taken to determine cell viability using SpectraMAX GeminiXS (Molecular Devices) at an excitation wavelength of 544nm and emission at 590nm. Supernatant was collected and frozen at -20°C. Electrochemiluminescence assay was performed to determine the amount of Aβ and sAPPβ secreted by these cells.

SDS-PAGE and Immunoblotting

For detection of intracellular proteins, whole cell extracts were prepared using a lysis buffer (1%NP40 and 0.1% SDS) supplemented with proteinase inhibitors. Extracts were subjected to SDS-PAGE using pre-cast gels (Invitrogen). In all cases, gel loading was normalized to total protein content in the cell extract (Using BCA assay). Proteins were transferred onto nitrocellulose membranes, which were then blocked with PBS containing 5% (w/v) dry skim milk for at least 1 h at room temperature. The membranes were then incubated with different primary antibody 6E10 (Covance), APP C terminal antibody (Sigma), BACE1 (Prosci), PSEN1 (Epitomics), PSEN2 (Epitomics), GAPDH (Meridian life sciences) followed by the appropriate horseradish peroxidase-conjugated secondary antibody for at least 1 h at room temperature. Both antibodies were diluted in 5% milk/PBS 0.05% Tween-20. Immunoblotted proteins were detected using an enhanced chemiluminescence kit (Pierce).

Electrochemiluminescence (ECL) Assay

MSD 96-Well MULTI-ARRAY Human Multiplex Kits were used (Meso Scale Discovery) to measure the level of Aβ38, Aβ40 and Aβ42. For the measurment of Aβ40 and sAPPβ 384 well MULTI-ARRAY Human Electrochemiluminescence plate was used following the instructions of the manufacturer.

Plasmid Transfection

HeLa swAPP cells were transfected with mock plasmid (pCDNA), or plasmid expressing mouse wild type Presenilin2 (PSEN2) using Lipofectamine 2000 reagent (Invitrogen), according to the manufacturer's protocol. 24 h after transfection the medium exchanged and conditioned medium was collected for 3 h and this was analyzed for Aβ40 using the Meso Scale Discovery Electrochemiluminescence (ECL) platform as described in the previous section.

RT-PCR analysis

72 h after transfection, RNA was prepared using the RNeasy Plus Mini kit (Qiagen cat. 74136). Purity of RNAs (A260/A280 , A260/A230) and concentration was measured using Nanodrop spectrophotometer. 2 μg of total RNA was used for reverse transcription with oligo-dT primer using Superscript first-strand synthesis system for RT-PCR (Invitrogen) according to the manufacturer's recommended protocol. RT-PCR analysis was performed uing Taq man probes following manufacturer's instructions using a 7900HT Fast Real-Time PCR system (Applied Biosystems).

Assays were performed in Quadruplicates and expression levels of genes were normalized against GAPDH controls. Levels of Med-GC cDNA as an internal control were normalized to GAPDH cDNA according to the ΔΔCt method.

Localization of active γ-secretase complexes by fluorescently tagged γ-secretase inhibitor.

Mouse embryonic fibroblast cells with Presenilin 1 KO, Presenilin 2 KO, Presenilin 1/2 KO or Wild-type were treated with the γ-secretase inhibitor derivative L-685,458 tagged with Quasar 670 at a final concentration of 1 μM for 10 minutes. The cells were fixed, stained with DAPI and mounted. The cells were visualized using the Confocal Laser Scanning Microscope Leica TCS SP8.

LysoTracker and active CTSD imaging

Immunocytochemistry was performed as previously described (Lee et al 2010). Organelles with low internal pH were labeled by LysoTracker DND-99 dye at a final concentration of 100 nM for 60 min. Active CTSD was labeled by adding Bodipy-FL-pepstatin A directly to

the medium at a final concentration of 1 mg/ml for 1 hr. Following wash with PBS, add new medium for live imaging.

Lysosomal pH measurement

Cells (2 x 10^3) were plated in 96well-plate for 48 hrs. Lysosensor yellow/blue-dextran (250 mg) was incubated for 24 hrs. Un-uptaken Lysosensor were washed with PBS then read in a Wallac Victor 2 fluorimeter (Perkin Elmer) with Ex. 355nm and Em. 440nm/535nm. The pH values were determined from the standard curve generated via the pH calibration samples.

Vacuolar-type H^+-ATPase activity assay

Activities were measured by v-ATPase assay kit (Novus Bio, 601-0120) base on manufactures manual. 4 mg of microsomal proteins were used for each ATPase assay. Assay samples were incubated with ATP contained substrate buffer mix and after 30 min incubation, ATP hydrolysis activity was measured with 650 nm.

Ca^{2+} Measurements

Cells were plated on glass bottom dishes the night before treatment. For baseline calcium measurements, cells were incubated with 25mg/mL rhod-dextran for 12 hrs before imaging. After incubation, cells were chased for 30 mins in complete media before it was exchanged for calcium-free HBSS (Invitrogen) and then cells were imaged. The mean intensity of the rhod signal of single cells was analyzed using ImageJ (NIH). For all cytosolic measurements, cells were incubated with 2μM Fura-2 AM (Life Technologies) for 1 hour and then chased with complete medium for 30 minutes. Cells were washed with HBSS (Invitrogen) and imaged and analyzed using ImageJ (NIH).

Acknowledgements:

We thank G. Yu for the HeLa-sweAPP cells. We thank Dr. S. Ferguson for the generous support with TFEB-GFP constructs and cell lines. We thank K. Simons, K. Beyreuther and C. Haass for critical input in the study and the manuscript. We thank B. Siegenthaler, M. Schmitz and F. Kivrak-Pfiffner for the technical help. L.R acknowledges the Professorship Grant and financial support from the Velux Foundation. Swiss National Science Foundation grant, the Novartis Foundation grant, Bangerter Stiftung, Baugarten Stiftung and the Synapsis Foundation are acknowledged. L.R and V.U acknowledge the funding support from the European Neuroscience Campus of the Erasmus Mundus Program.

References

Annaert, W.G., Levesque, L., Craessaerts, K., Dierinck, I., Snellings, G., Westaway, D., George-Hyslop, P.S., Cordell, B., Fraser, P., and De Strooper, B. (1999). Presenilin 1 controls gamma-secretase processing of amyloid precursor protein in pre-golgi compartments of hippocampal neurons. J Cell Biol *147*, 277-294.

Borchelt, D.R., Thinakaran, G., Eckman, C.B., Lee, M.K., Davenport, F., Ratovitsky, T., Prada, C.M., Kim, G., Seekins, S., Yager, D.*, et al.* (1996). Familial Alzheimer's disease-linked presenilin 1 variants elevate Abeta1-42/1-40 ratio in vitro and in vivo. Neuron *17*, 1005-1013.

De Strooper, B. Proteases and Proteolysis in Alzheimer Disease: A Multifactorial View on the Disease Process. Physiol Rev *90*, 465-494.

De Strooper, B. (2003). Aph-1, Pen-2, and Nicastrin with Presenilin generate an active gamma-Secretase complex. Neuron *38*, 9-12.

De Strooper, B., Saftig, P., Craessaerts, K., Vanderstichele, H., Guhde, G., Annaert, W., Von Figura, K., and Van Leuven, F. (1998). Deficiency of presenilin-1 inhibits the normal cleavage of amyloid precursor protein. Nature *391*, 387-390.

Franberg, J., Svensson, A.I., Winblad, B., Karlstrom, H., and Frykman, S. (2011). Minor contribution of presenilin 2 for gamma-secretase activity in mouse embryonic fibroblasts and adult mouse brain. Biochem Biophys Res Commun *404*, 564-568.

Haass, C., and Selkoe, D.J. (2007). Soluble protein oligomers in neurodegeneration: lessons from the Alzheimer's amyloid beta-peptide. Nat Rev Mol Cell Biol *8*, 101-112.

Hardy, J. (1996). New insights into the genetics of Alzheimer's disease. Ann Med *28*, 255-258.

Hardy, J. (2006). A hundred years of Alzheimer's disease research. Neuron *52*, 3-13.

Hardy, J., and Crook, R. (2001). Presenilin mutations line up along transmembrane alpha-helices. Neurosci Lett *306*, 203-205.

Hardy, J., and Selkoe, D.J. (2002). The amyloid hypothesis of Alzheimer's disease: progress and problems on the road to therapeutics. Science *297*, 353-356.
Hardy, J.A., and Higgins, G.A. (1992). Alzheimer's disease: the amyloid cascade hypothesis. Science *256*, 184-185.

Harold, D., Abraham, R., Hollingworth, P., Sims, R., Gerrish, A., Hamshere, M.L., Pahwa, J.S., Moskvina, V., Dowzell, K., Williams, A.*, et al.* (2009). Genome-wide association study identifies variants at CLU and PICALM associated with Alzheimer's disease. Nat Genet *41*, 1088-1093.

Hartmann, T., Bieger, S.C., Bruhl, B., Tienari, P.J., Ida, N., Allsop, D., Roberts, G.W., Masters, C.L., Dotti, C.G., Unsicker, K.*, et al.* (1997). Distinct sites of intracellular production for Alzheimer's disease A beta40/42 amyloid peptides. Nat Med *3*, 1016-1020.

Karran, E., Mercken, M., and De Strooper, B. (2011). The amyloid cascade hypothesis for Alzheimer's disease: an appraisal for the development of therapeutics. Nat Rev Drug Discov *10*, 698-712.

Sambamurti, K., Greig, N.H., Utsuki, T., Barnwell, E.L., Sharma, E., Mazell, C., Bhat, N.R., Kindy, M.S., Lahiri, D.K., and Pappolla, M.A. (2011). Targets for AD treatment: conflicting messages from gamma-secretase inhibitors. J Neurochem *117*, 359-374.
Schor, N.F. (2011). What the halted phase III gamma-secretase inhibitor trial may (or may not) be telling us. Ann Neurol *69*, 237-239.

Serneels, L., Van Biervliet, J., Craessaerts, K., Dejaegere, T., Horre, K., Van Houtvin, T., Esselmann, H., Paul, S., Schafer, M.K., Berezovska, O.*, et al.* (2009). gamma-Secretase heterogeneity in the Aph1 subunit: relevance for Alzheimer's disease. Science *324*, 639-642.

Tanzi, R.E., and Bertram, L. (2005). Twenty years of the Alzheimer's disease amyloid hypothesis: a genetic perspective. Cell *120*, 545-555.

Thinakaran, G., and Koo, E.H. (2008). Amyloid precursor protein trafficking, processing, and function. J Biol Chem *283*, 29615-29619.

Tomita, T., Maruyama, K., Saido, T.C., Kume, H., Shinozaki, K., Tokuhiro, S., Capell, A., Walter, J., Grunberg, J., Haass, C.*, et al.* (1997). The presenilin 2 mutation (N141I) linked to familial Alzheimer disease (Volga German families) increases the secretion of amyloid beta protein ending at the 42nd (or 43rd) residue [see comments]. Proc Natl Acad Sci U S A *94*, 2025-2030.

Vassar, R., Kovacs, D.M., Yan, R., and Wong, P.C. (2009). The beta-secretase enzyme BACE in health and Alzheimer's disease: regulation, cell biology, function, and therapeutic potential. J Neurosci *29*, 12787-12794.

Vetrivel, K.S., Cheng, H., Lin, W., Sakurai, T., Li, T., Nukina, N., Wong, P.C., Xu, H., and Thinakaran, G. (2004). Association of gamma-secretase with lipid rafts in post-Golgi and endosome membranes. J Biol Chem *279*, 44945-44954.

Figure 1

(This figure was part of Dr. Jitin Bali's PhD thesis)

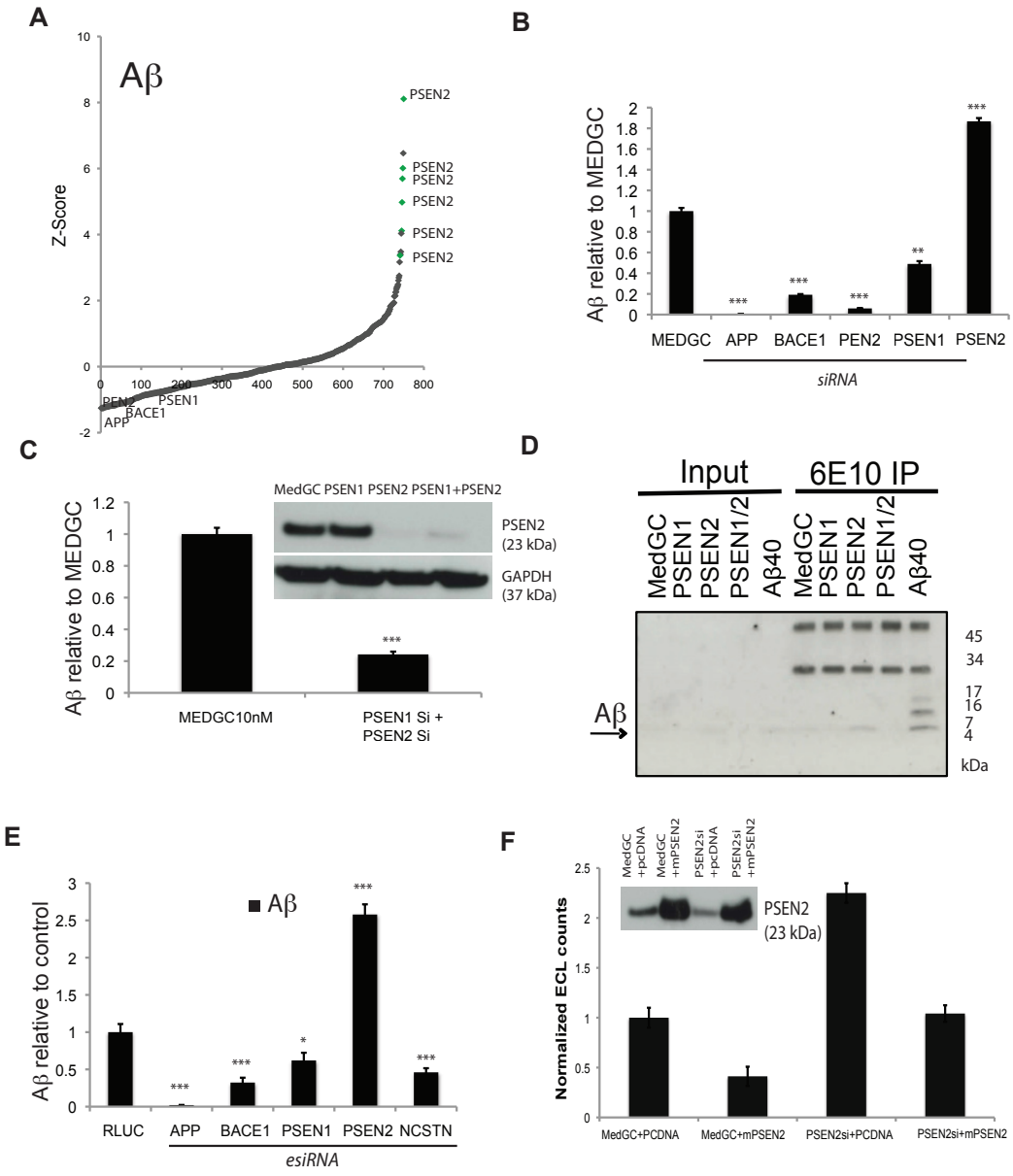

Figure 1: RNAi of human proteases identify PSEN2 as a negative regulator of Aβ levels

A) Scheme of the protease screen. B) HeLa-swe APP cells transfected with all the proteases present in human genome and graph showing Z-scores of Aβ levels from the siRNA protease screen. PSEN2 KD leads to an increase in Aβ levels. C) HeLa-swe APP cells transfected with siRNA against APP, BACE1, PSEN1, PSEN2 and PSEN1+2 show an increase in Aβ only in PSEN2 knock down cells. Western blot probed against PSEN2 show effective knockdown. GAPDH was used as a loading control. D) Increased Aβ upon PS2 silencing detected in conditioned medium by blotting with 6E10 antibody. HeLa cells stably expressing swe-APP were transfected with siRNA against PSEN1, PSEN2 or PSEN1/2. Conditioned medium were used to perform immunoprecipitation with 6E10 antibody followed by western blot analysis. E) HeLa-swe APP cells transfected with esiRNA against APP, BACE1, PSEN1, PSEN2, NCT and probed for Aβ level. F) HeLa-swe APP cells transfected with siRNA against PSEN2 and rescued with mice PSEN2 leads to the reduction of Aβ levels. MEDGC and PCDNA were used as controls. * $p<0.05$, ** $p<0.01$, *** $p<0.001$.

Figure 2
(sub-figures A, B and C were part of Dr. Jitin Bali's PhD thesis)

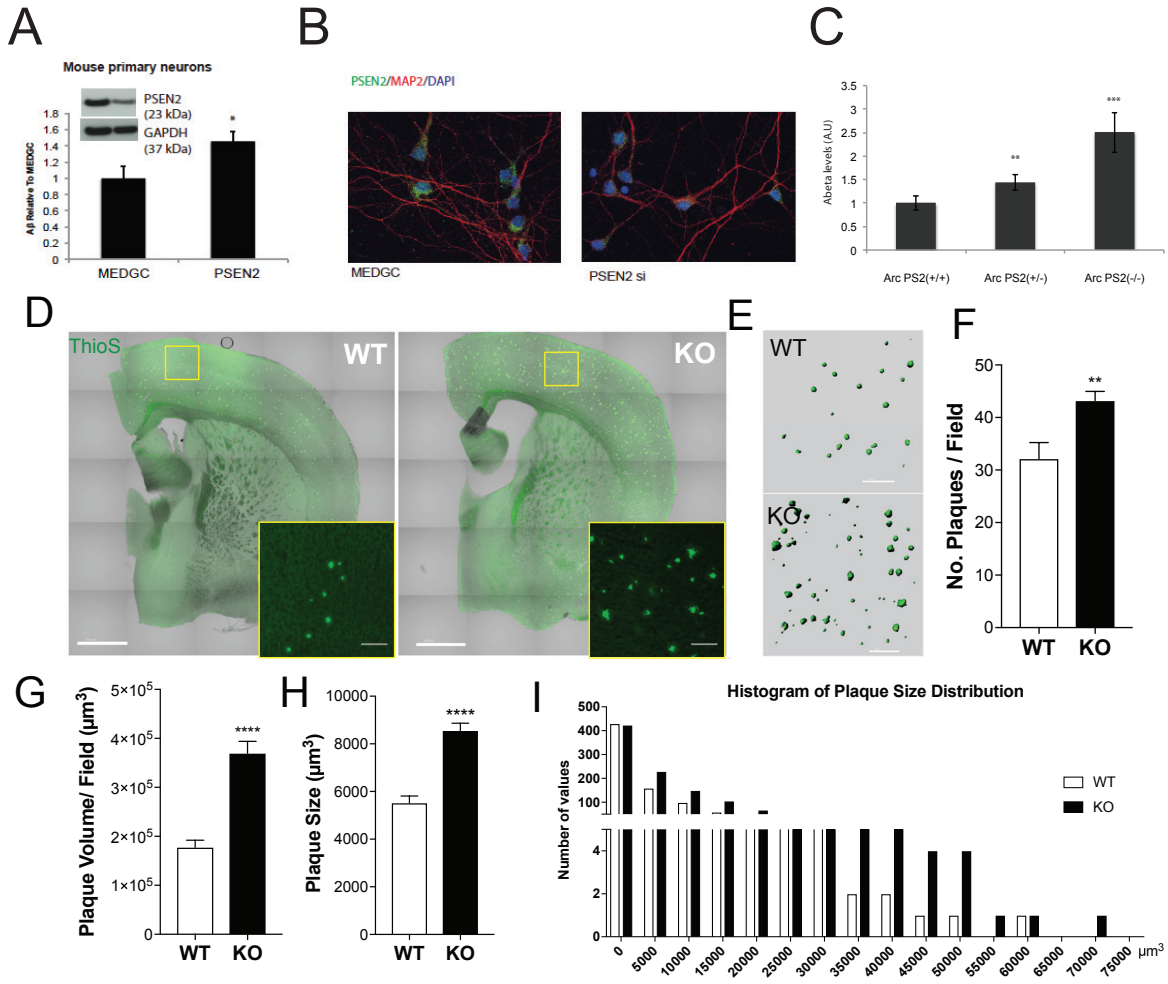

Figure 2: PSEN2 deletion aggravates amyloid pathology in AD transgenic mice

A) PSEN2 knockdown leads to an increase in Aβ level in mouse primary neurons. Mouse primary neurons were transfected with siRNA against PSEN2. Aβ was measured in conditioned medium from the neurons and the neuronal lysates were used for western blotting. B) Immunostaining was performed to further validate the knockdown efficiency C) Aβ levels in Arc AD mice with heterozygous or homozygous PS2 deletion D) Thioflavin S staining in brain slices. Thioflavin S (Thio S) staining was performed to stain for amyloid plaques in brain slices from 6 month old AD PSEN2 WT (WT) and AD PSEN2 KO (KO) mice. E and F) 3D reconstruction of amyloid plaques from the brain slices. 3D reconstruction of amyloid plaques in brain slices from 6-month-old AD PSEN2 WT (WT) and AD PSEN2 KO (KO) mice was performed by Imaris software. G and H) Amyloid plaque volume and size from the brain slices in brain slices from 6 month old AD PSEN2 WT (WT) and AD PSEN2 KO (KO) mice. I) Amyloid plaque mean intensity in brain slices from 6 month old AD PSEN2 WT (WT) and AD PSEN2 KO (KO) mice. I) Histogram depicting amyloid plaque size distribution in brain slices from 6 month old AD PSEN2 WT (WT) and AD PSEN2 KO (KO) mice. * $p<0.05$, ** $p<0.01$, *** $p<0.001$.

Figure 3

(This figure was part of Dr. Jitin Bali's PhD thesis)

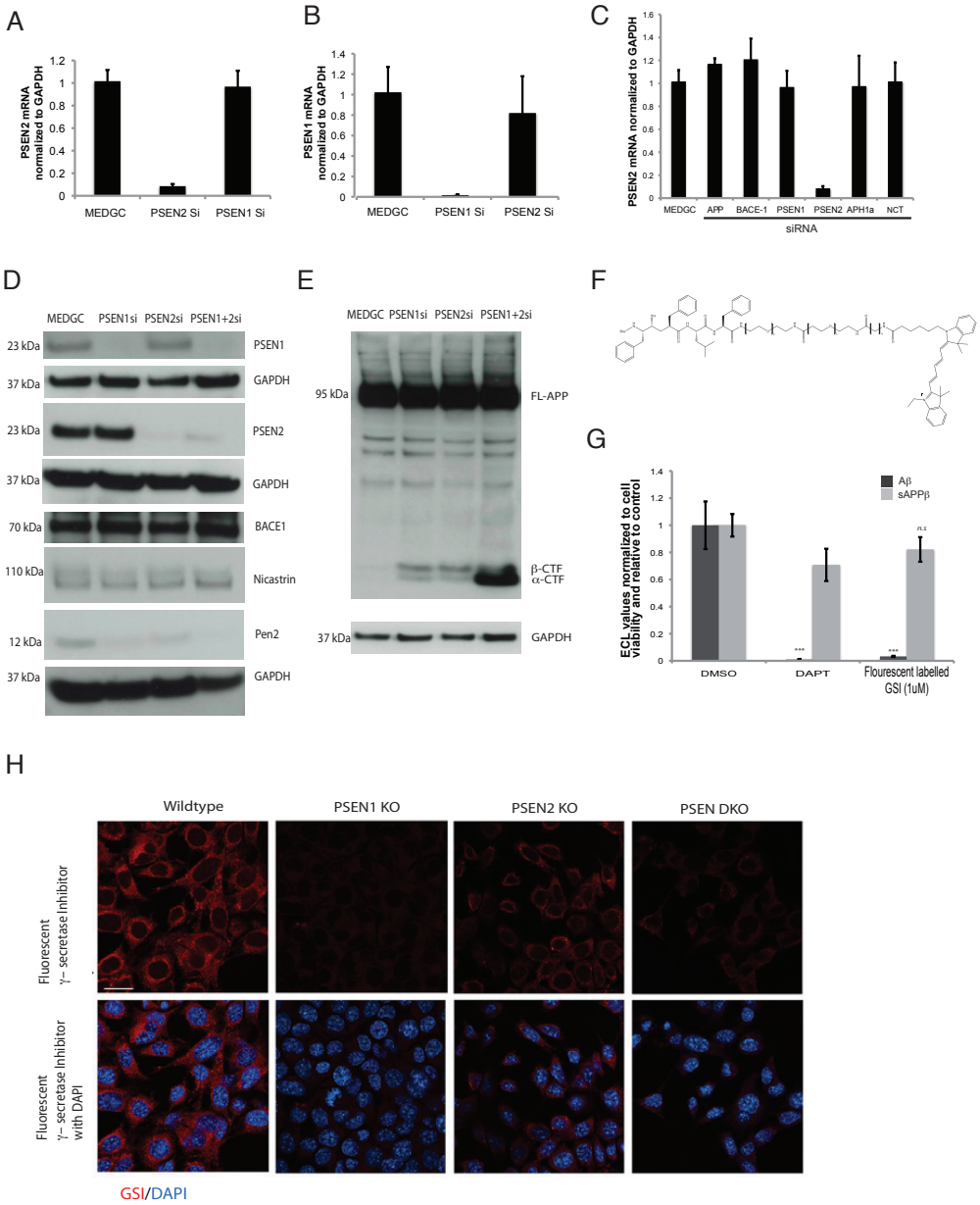

Figure 3: Increased Aβ upon PSEN2 silencing is not due to increased γ-secretase activity
A) Efficient knockdown of mRNA levels revealed by real-time RT-PCR showing a reduction in PSEN2 mRNA level only in PSEN2 knockdown condition. MEDGC was used as a transfection control and mRNA levels were normalized to GAPDH. B) Efficient knockdown of mRNA levels revealed by real-time RT-PCR showing a reduction in PSEN1 mRNA level only in PSEN1 knockdown condition. MEDGC was used as a transfection control and mRNA levels were normalized to GAPDH. C) Efficient knockdown of mRNA levels revealed by real-time RT-PCR showing a reduction in PSEN2 mRNA level in PSEN2 knockdown condition. No change in PSEN2 mRNA was observed in APP, BACE1, PS1, APH1a and NCT knock down cells. MEDGC was used as a transfection control and mRNA levels were normalized to GAPDH. D) HeLa-sweAPP cells were transfected with pooled siRNAs (4 different siRNAs) against PSNE1, PSEN2 or PSEN1+2 or a control-siRNA (MEDGC) and cell lysates were analyzed by Western Blot using the respective antibodies. GAPDH was used as a protein loading control. E) HeLa-sweAPP cells were transfected with pooled siRNAs (4 different siRNAs) against PSNE1, PSEN2 or PSEN1+2 or a control-siRNA (MEDGC) and cell lysates were analyzed by Western Blot using APP C terminal specific antibody. GAPDH was used as a protein loading control. F) HeLa-sweAPP cells treated with γ-secretase inhibitors (DAPT and fluorescent labelled γ-secretase inhibitor) and probed for Aβ (black) and sAPPβ (grey) levels. G) MEF cells treated with fluorescent labelled γ-secretase inhibitor (red). DAPI (blue) was used to stain nucleus. H) HeLa Kyoto BAC-Nicastrin cells were transfected with pooled siRNAs (4 different siRNAs) against PSEN2 or control-siRNA (MEDGC). Cell lysates were used for immnuoporecipitation followed by Western Blot analysis using PSEN1 and PSEN2 specific antibody. * $p<0.05$, ** $p<0.01$, *** $p<0.001$.

Figure 4

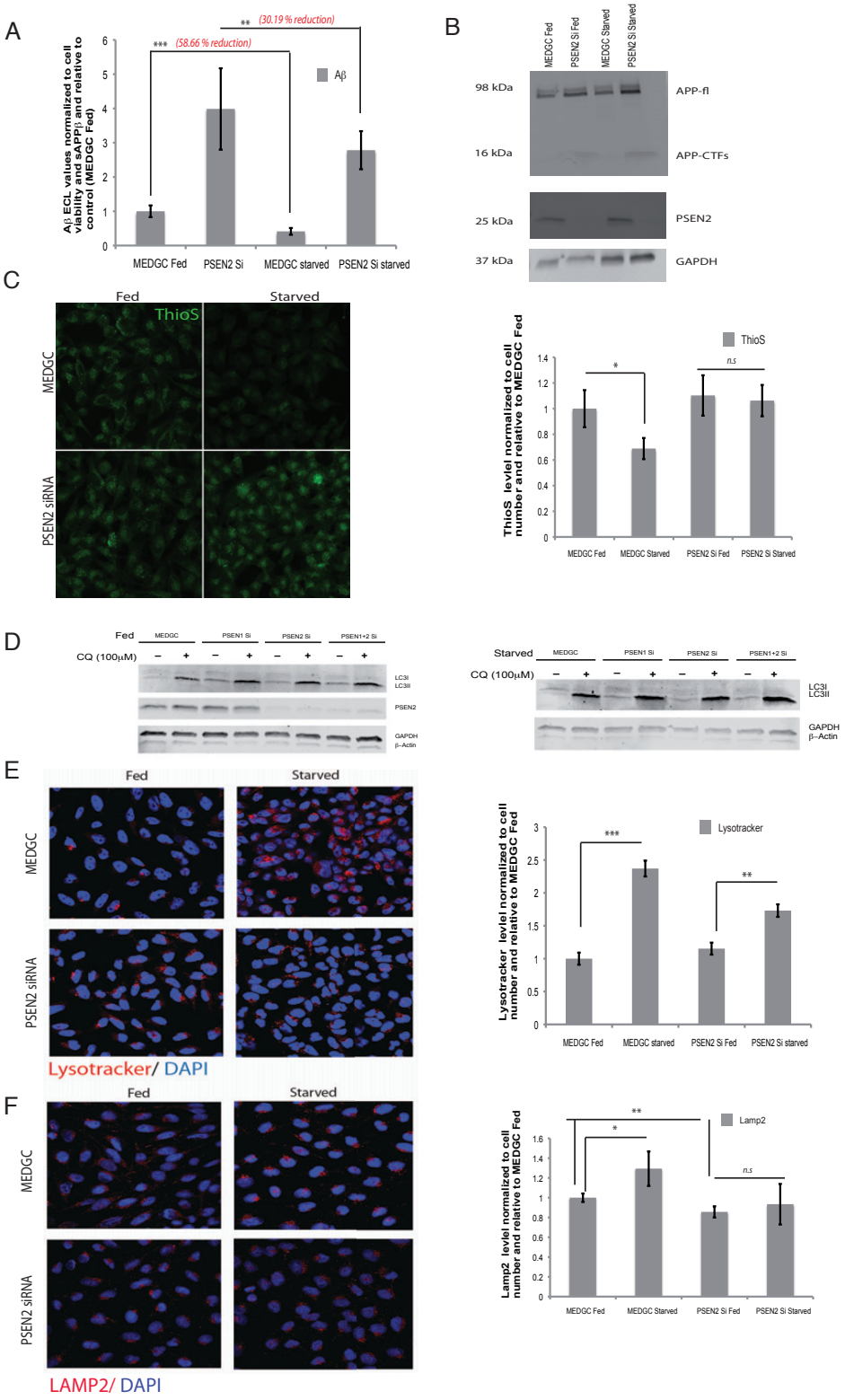
A
Aβ ECL values normalized to cell viability and sAPPβ and relative to control (MEDGC Fed)
*** (58.66 % reduction)
** (30.19 % reduction)
Aβ
MEDGC Fed
PSEN2 Si
MEDGC starved
PSEN2 Si starved
B
MEDGC Fed
PSEN2 Si Fed
MEDGC Starved
PSEN2 Si Starved
98 kDa
APP-fl
16 kDa
APP-CTFs
25 kDa
PSEN2
37 kDa
GAPDH
C
Fed
Starved
ThioS
MEDGC
PSEN2 siRNA
ThioS levlel normalized to cell number and relative to MEDGC Fed
ThioS
n.s
MEDGC Fed
MEDGC Starved
PSEN2 Si Fed
PSEN2 Si Starved
D
Fed
Starved
MEDGC
PSEN1 Si
PSEN2 Si
PSEN1+2 Si
CQ (100μM)
LC3I
LC3II
PSEN2
GAPDH
β–Actin
E
Fed
Starved
MEDGC
PSEN2 siRNA
Lysotracker/ DAPI
Lysotracker levlel normalized to cell number and relative to MEDGC Fed
Lysotracker
MEDGC Fed
MEDGC starved
PSEN2 Si Fed
PSEN2 Si starved
F
Fed
Starved
MEDGC
PSEN2 siRNA
LAMP2/ DAPI
Lamp2 levlel normalized to cell number and relative to MEDGC Fed
Lamp2
n.s
MEDGC Fed
MEDGC Starved
PSEN2 Si Fed
PSEN2 Si Starved

Figure 4: PSEN2 silencing impairs starvation induced lysosomal pathway, Aβ clearance and leads to general protein accumulation

A) HeLa-Swe APP cells were transfected with siRNA against PSEN1 or PSEN2. After 69 hours the medium was replaced with either nutrient rich (fed) or nutrient deprived (starved) medium for 3 hours. Aβ levels in the conditioned medium were analyzed by an ECL assay. B) HeLa-Swe APP cells were transfected with siRNA against PSEN1 or PSEN2. After 69 hours the medium was replaced with either nutrient rich (fed) or nutrient deprived (starved) medium for 3 hours. Cell lysates were analyzed by Western Blot using APP C terminal specific antibody and PSEN2 antibody. GAPDH was used as a loading control. C) HeLa-Swe APP cells were transfected with siRNA against PSEN1 or PSEN2. After 69 hours the medium was replaced with either nutrient rich (fed) or nutrient deprived (starved) medium for 3 hours. Cells were fixed and stained with ThioS (green) and processed for confocal imaging. D) PSEN silencing leads to impaired Autophagic flux. HeLa-Swe APP cells were transfected with siRNA against PSEN1, PSEN2 or PSEN1/2. After 69 hours the medium was replaced with either nutrient rich (fed) or nutrient deprived (starved) medium for 3 hours with or without chloroquine (CQ). Cell lysates were analyzed by Western Blot using antibody against LC3 and PSEN2. GAPDH and β-actin were used as loading control. E) HeLa-Swe APP cells were transfected with siRNA against PSEN1 or PSEN2. After 69 hours the medium was replaced with either nutrient rich (fed) or nutrient deprived (starved) medium for 3 hours. Cells were incubated with LysoTracker Red DND-99 (red) for 1.5 hours and processed for confocal imaging. F) HeLa-Swe APP cells were transfected with siRNA against PSEN1 or PSEN2. After 69 hours the medium was replaced with either nutrient rich (fed) or nutrient deprived (starved) medium for 3 hours. Cells were fixed and probed with anti-Lamp2 antibody (red) and processed for confocal imaging. * $p<0.05$, ** $p<0.01$, *** $p<0.001$.

Figure 5

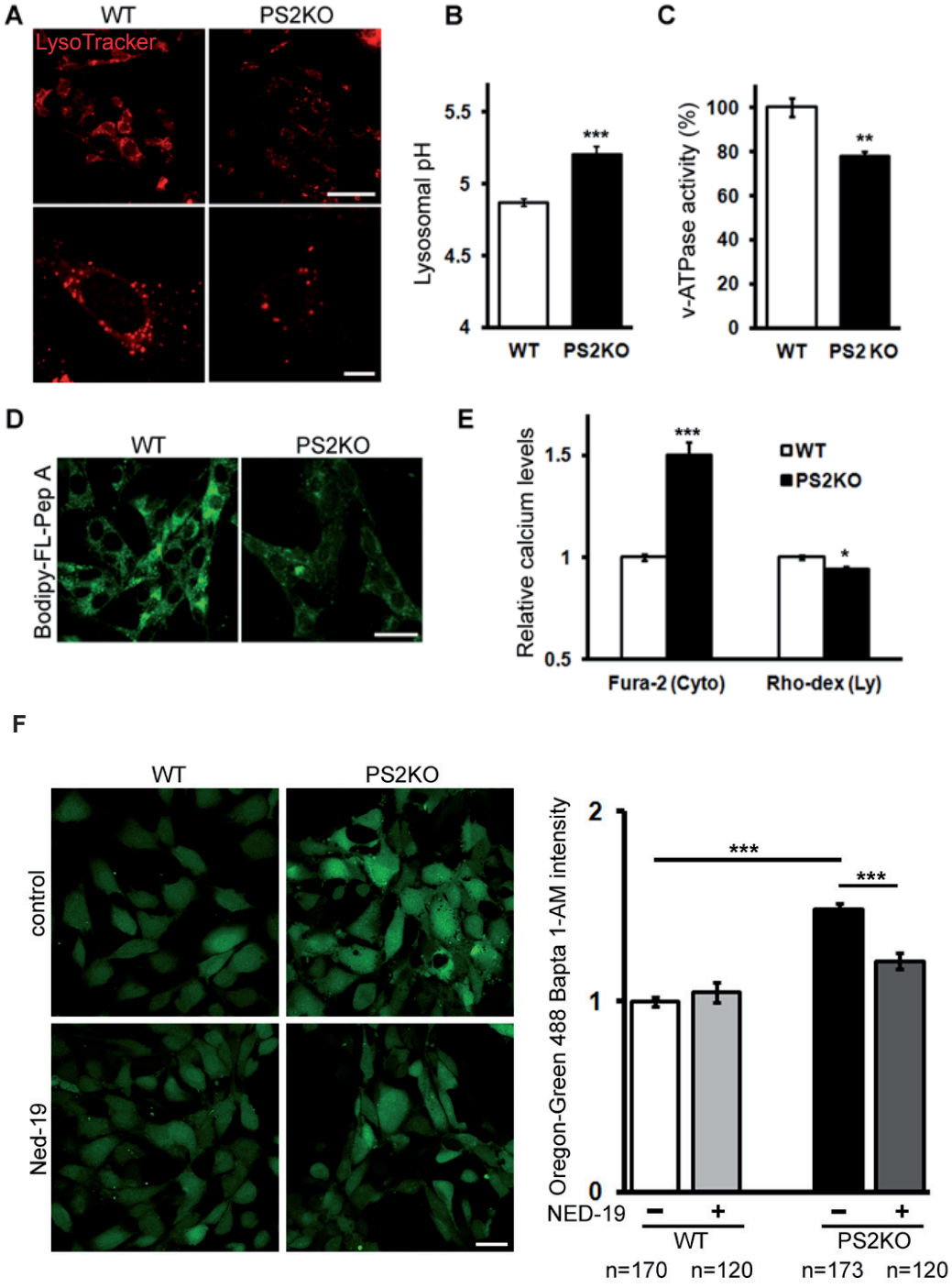
A
WT
PS2KO
LysoTracker
B
Lysosomal pH
5.5
5
4.5
4
***
WT
PS2KO
C
v-ATPase activity (%)
100
80
60
40
20
0
**
WT
PS2 KO
D
WT
PS2KO
Bodipy-FL-Pep A
E
Relative calcium levels
1.5
1
0.5
***
*
WT
PS2KO
Fura-2 (Cyto)
Rho-dex (Ly)
F
WT
PS2KO
control
Ned-19
Oregon-Green 488 Bapta 1-AM intensity
2
1
0
***
***
NED-19
−
+
−
+
WT
PS2KO
n=170
n=120
n=173
n=120

Figure 5: Lysosomal acidification and Ca^{2+} efflux impairment in PS2KO MEF cells

(A) Lysosomal acidification visualized by LysoTracker is reduced in PS2KO MEF cells. Scale bars 50, 10µm. (B) Lysosomal pH is increased in PS2KO MEF cells (n=12). (C) v-ATPase activity is reduced in PS2KO MEF cells (n=5). (D) In vivo CTSD activity is reduced in PS2KO MEF cells. Scale bars 20µm. (E) Lysosomal Ca^{2+} is reduced (WT: n=30; PS2KO n=28) and cytosolic Ca^{2+} (WT: n=30; PS2KO n=30) is elevated in PS2KO MEF cells. F. The cytosolic Ca^{2+} elevation induced by OGB-AM in untreated PS2KO MEF cells (Control; WT vs PS2KO) was reduced back to WT levels in the lysosomal NAADP dependent calcium channel inhibitor, Ned-19 treated PS2KO MEF cells (Ned-19; WT vs PS2KO). * $p<0.05$, ** $p<0.01$, *** $p<0.001$.

Figure 6

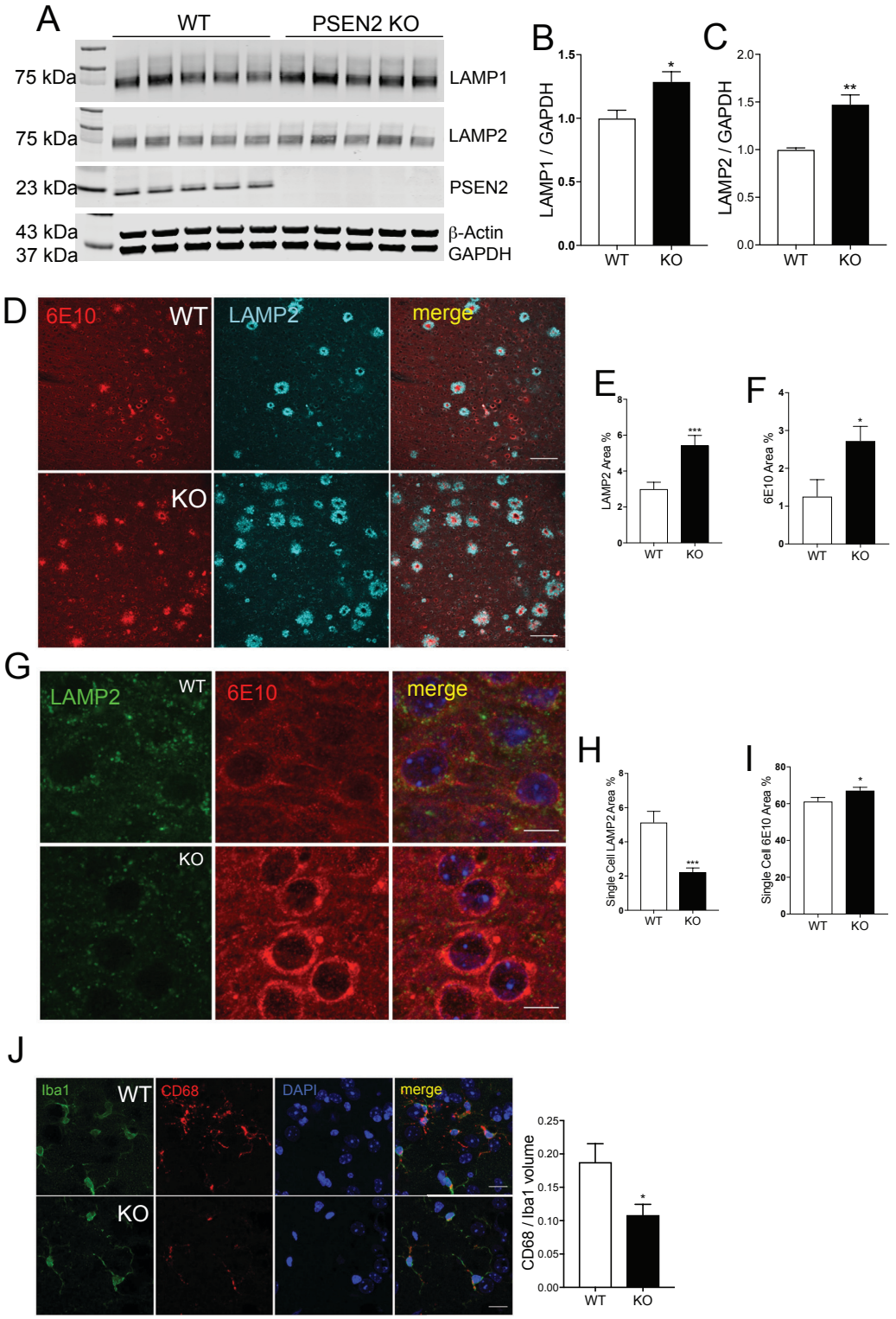
A
WT
PSEN2 KO
75 kDa
LAMP1
75 kDa
LAMP2
23 kDa
PSEN2
43 kDa
37 kDa
β-Actin
GAPDH
B
LAMP1 / GAPDH
WT
KO
C
LAMP2 / GAPDH
WT
KO
D
6E10
WT
LAMP2
merge
KO
E
LAMP2 Area %
WT
KO
F
6E10 Area %
WT
KO
G
LAMP2
WT
6E10
merge
KO
H
Single Cell LAMP2 Area %
WT
KO
I
Single Cell 6E10 Area %
WT
KO
J
Iba1
WT
CD68
DAPI
merge
KO
CD68 / Iba1 volume
WT
KO

Figure 6: Dysfunctional lysosomes in mice lacking PSEN2

A) Western blot analysis of lysates from cortex of wild-type AD and PSEN2 KO-AD mice. SDS soluble fractions of cortical samples were analyzed by western blotting with antibodies against Lamp1 and Lamp2. B & C) Graph showing quantification in A. D) 6E10 and Lamp2 antibody staining on brain slices of wild-type AD and PSEN2 KO-AD mice. E & F) Graph showing the quantification in D. G) 6E10 and Lamp2 antibody staining on brain slices of wild-type AD and PSEN2 KO-AD mice in areas devoid of plaques. H & I) Graph showing quantification in G. J) CD68 and Iba1 staining on brain slices of wild-type AD and PSEN2 KO-AD mice. CD 68 levels are significantly reduced in microglia from PSEN2 KO-AD mice compared to wild-type AD mice, indicating lower lysosomal levels in these microglia. * $p<0.05$, ** $p<0.01$, *** $p<0.001$.

Figure 7

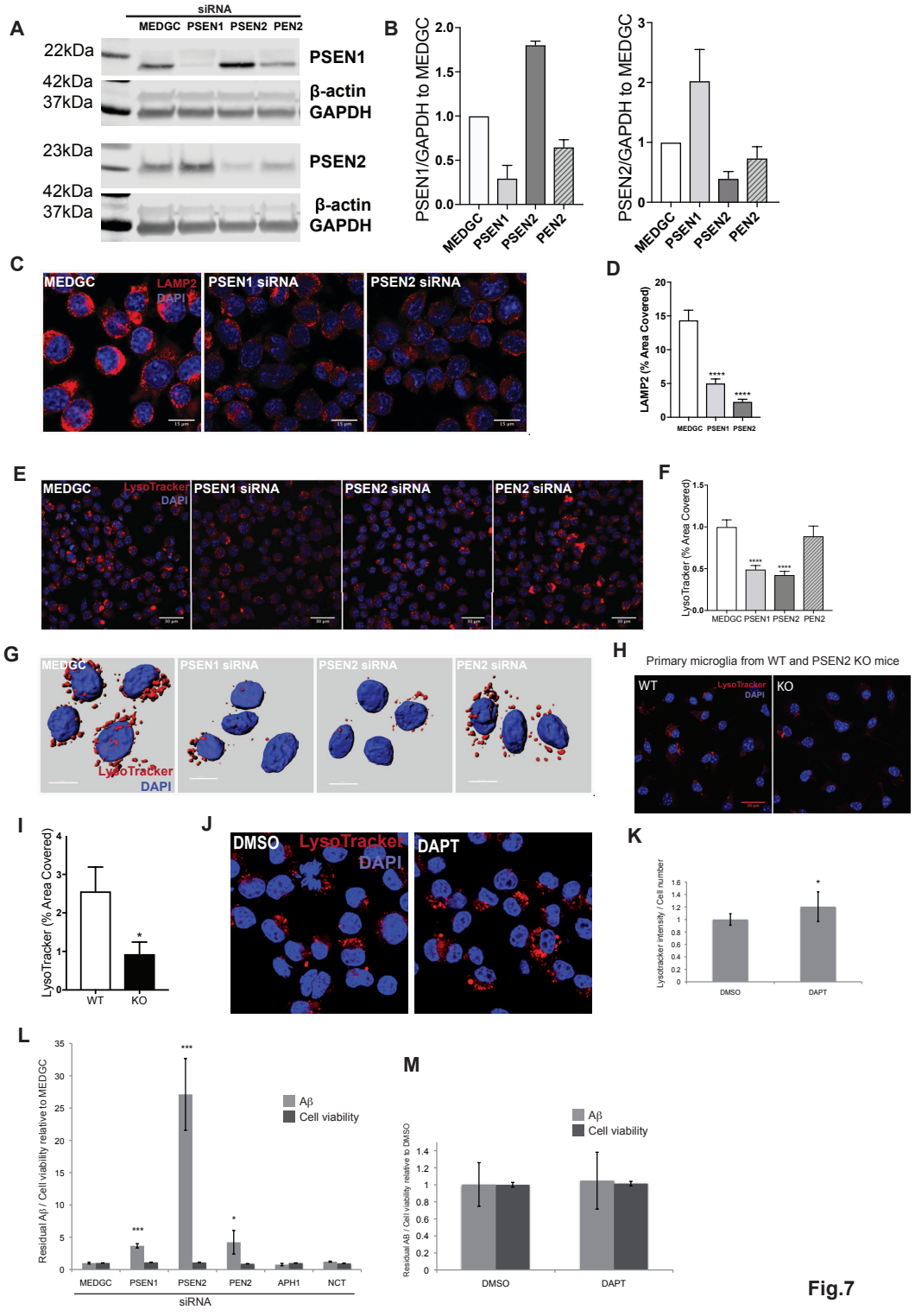

Fig.7

Figure 7: Impaired microglial clearance of amyloid upon PSEN2 depletion

A) Western blot showing confirmation of siRNA knockdown in BV microglia. BV2 microglia cells were transfected with control siRNA (MEDGC) or siRNA against PSEN1, PSEN2 or Pen2. After 65 hours the cells were lysed and the cell lysates were used for western blotting. B) Graph showing quantification for the western blot. C) LAMP2 immunostaining in BV2 microglia cells. BV2 microglia cells were transfected with control siRNA (MEDGC) or siRNA against PSEN1or PSEN2. After 65 hours, cells were PFA fixed, immunostained and processed for confocal imaging. D) Graph showing quantification for LAMP2 immunostaining in BV2 microglia cells. E) LysoTracker staining in BV2 microglia cells. BV2 microglia cells were transfected with control siRNA (MEDGC) or siRNA against PSEN1, PSEN2 or Pen2. After 48 hours, cells were incubated with LysoTracker Red DND-99 (red) for 1.5 hours and processed for confocal imaging. F) Graph showing quantification for LysoTracker staining in BV2 microglia cells. G) 3D reconstruction of LysoTracker puncta in BV2 microglia. BV2 microglia cells were transfected with control siRNA (MEDGC) or siRNA against PSEN1, PSEN2 or Pen2. After 48 hours, cells were incubated with LysoTracker Red DND-99 (red) for 1.5 hours and processed for confocal imaging. 3D reconstruction of LystoTracker puncta was performed by Imaris software. H) LysoTracker staining in primary microglia isolated from WT and PS2 KO mice. Cells were incubated with LysoTracker Red DND-99 (red) for 1.5 hours and processed for confocal imaging. I) Graph showing quantification in H. J & K) LysoTracker staining in BV2 microglia cells and graph showing quantification of the lysotracker signal. BV2 microglia cells were treated with DMSO or DAPT for 23 hours, cells were incubated with LysoTracker Red DND-99 (red) for 1.5 hours and processed for confocal imaging. A) Graph showing residual Aβ levels after Aβ clearance assay in BV2 microglia. BV2 microglia cells were transfected with control siRNA (MEDGC) or siRNA against PSEN1, PSEN2, PEN2, APH1 (a,b and c) and Nicastrin. After 48 hours, cells were incubated with 5 % serum containing conditioned medium from Hela sweAPP cells for 16 hours. Residual Aβ was measured by ECL assay. B) Graph showing residual Aβ levels after Aβ clearance assay in BV2 microglia. BV2 microglia cells were treated with DMSO or DAPT for 6 hours, cells were then incubated with 5 % serum containing conditioned medium (DMSO or DAPT) from Hela sweAPP cells for 16 hours. Residual Aβ was measured by ECL assay. * $p<0.05$, ** $p<0.01$, *** $p<0.001$.

Supplementary Figure 1 ***(This figure was part of Dr. Jitin Bali's PhD thesis)***

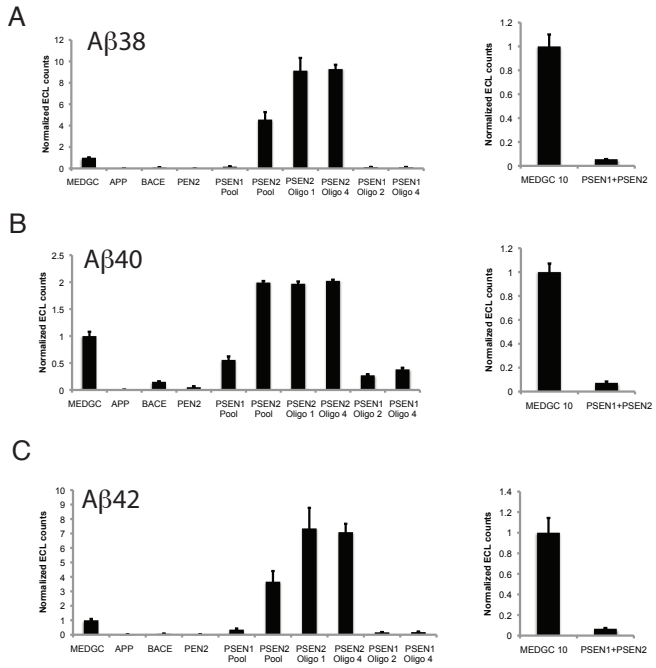

Supplementary Figure 1: PSEN2 deficiency increased all versions of the major Aβ species

HeLa-swe APP cells were transfected with individual siRNAs for PSEN1, PSEN2 and pooled siRNA against APP, BACE, PEN2, PSEN1, PSEN2 and PSEN1+2. The three different species of Aβ (38, 40 and 42) are increased upon PSEN2 silencing.

Supplementary Figure 2 ***(This figure was part of Dr. Jitin Bali's PhD thesis)***

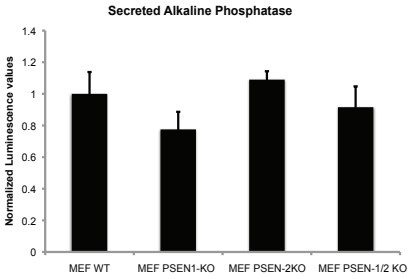

Supplementary Figure 2: PSEN2-loss does not impair secretion of secreted alkaline phosphatase (SEAP)

Graph showing SEAP levels. Different MEF cell lines (PSEN1KO, PSEN2KO, PSEN-1/2 KO) were transfected with pSEAP. 24 hours after transfection conditioned medium were assayed for SEAP levels.

Supplementary Figure 3 ***(This figure was part of Dr. Jitin Bali's PhD thesis)***

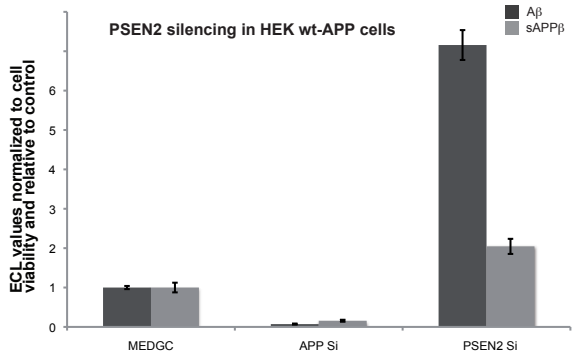

Supplementary Figure 3: PSEN2 silencing in HEK-wt APP cells leads to increased Aβ levels

Graph showing Aβ and sAPPβ levels. HEK-wt APP cells were transfected with siRNA against PSEN2 and APP. Conditioned medium were used to analyze Aβ (dark grey) and sAPPβ (light grey) levels by ECL assay.

Supplementary Figure 4

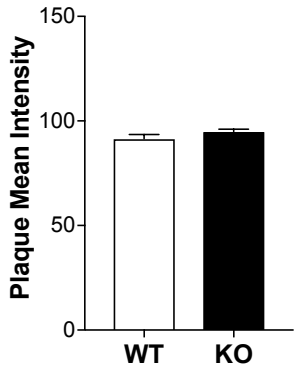

Supplementary Figure 4: Plaque mean intensity in wild-type AD and PS2KO-AD mice
Graph showing quantification of amyloid plaques measured by ThioS staining in wild-type Ad and PS2KO-AD mice.

Supplementary Figure 5

MEDGC Starved vs MEDGC Fed

	UP	DOWN
ATP6V0E1-Hs00859570_g1	2.34	0.43
ATP6V1H-Hs00977530_m1	2.00	0.50
CLCN7-Hs01126462_m1	1.70	0.59
CTSB-Hs00947433_m1	1.10	0.91
CTSD-Hs00157205_m1	1.19	0.84
HEXA-Hs00166843_m1	1.02	0.98
LAMP1-Hs00174766_m1	1.49	0.67
PSAP-Hs01551096_m1	4.64	0.22
NEU1-Hs00902543_g1	1.80	0.56
TPP1-Hs00166099_m1	1.58	0.63
GAPDH-Hs99999905_m1	1.00	1.00
GBA-Hs00164683_m1	1.44	0.70
PSMA1-Hs01027360_g1	1.58	0.63
UBE3A-Hs00166580_m1	1.51	0.66
UVRAG-Hs00163433_m1	1.09	0.92
SQSTM1-Hs01061917_g1	0.92	1.09
FOXO3-Hs00818121_m1	1.35	0.74
TFE3-Hs00232406_m1	1.72	0.58
MITF-Hs01117294_m1	1.43	0.70
TFEB-Hs00292981_m1	1.31	0.76
STAT3-Hs00374280_m1	1.94	0.52
HOXA9-Hs00266821_m1	130782.50	0.00
PSEN1-Hs00997789_m1	1.77	0.56
PSEN2-Hs01577197_m1	1.15	0.87

PSEN2 Si Starved vs PSEN2 Si Fed

	UP	DOWN
ATP6V0E1-Hs00859570_g1	1.57	0.64
ATP6V1H-Hs00977530_m1	1.45	0.69
CLCN7-Hs01126462_m1	1.91	0.52
CTSB-Hs00947433_m1	1.78	0.56
CTSD-Hs00157205_m1	1.91	0.52
HEXA-Hs00166843_m1	2.74	0.37
LAMP1-Hs00174766_m1	2.01	0.50
PSAP-Hs01551096_m1	3.25	0.31
NEU1-Hs00902543_g1	1.90	0.53
TPP1-Hs00166099_m1	3.20	0.31
GAPDH-Hs99999905_m1	1.00	1.00
GBA-Hs00164683_m1	1.53	0.65
PSMA1-Hs01027360_g1	1.56	0.64
UBE3A-Hs00166580_m1	1.55	0.64
UVRAG-Hs00163433_m1	1.87	0.53
SQSTM1-Hs01061917_g1	0.95	1.06
FOXO3-Hs00818121_m1	0.61	1.65
TFE3-Hs00232406_m1	1.69	0.59
MITF-Hs01117294_m1	2.10	0.48
TFEB-Hs00292981_m1	2.03	0.49
STAT3-Hs00374280_m1	2.64	0.38
HOXA9-Hs00266821_m1	11.67	0.09
PSEN1-Hs00997789_m1	1.26	0.79
PSEN2-Hs01577197_m1	1.59	0.63

Supplementary Figure 5: PSEN silencing does not impair expression of CLEAR network (lysosomal biogenesis) genes

HeLa-Swe APP cells were transfected with siRNA against PSEN2 or control (MEDGC). After 48 hours the medium was replaced with either nutrient rich (fed) or nutrient deprived (starved) medium. Cells were processed for RNA extraction followed by cDNA preparation. CLEAR network gene expression analysis was performed using. Fold change increase (green) or fold change decrease (red) for different genes are indicated.

Supplementary Figure 6

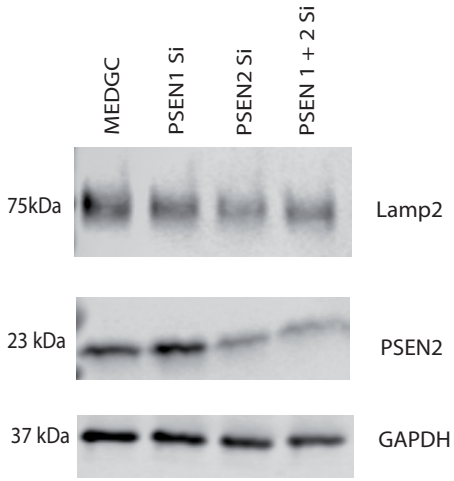

Supplementary Figure 6: PSEN silencing in mouse primary neurons reduces LAMP2 levels

Mouse primary neurons were transfected with siRNA against PSEN1, PSEN2 or PSEN1+2. Cell lysates were analyzed by western blot using antibody against LAMP2 and PSEN2. GAPDH was used as loading control

Supplementary Figure 7

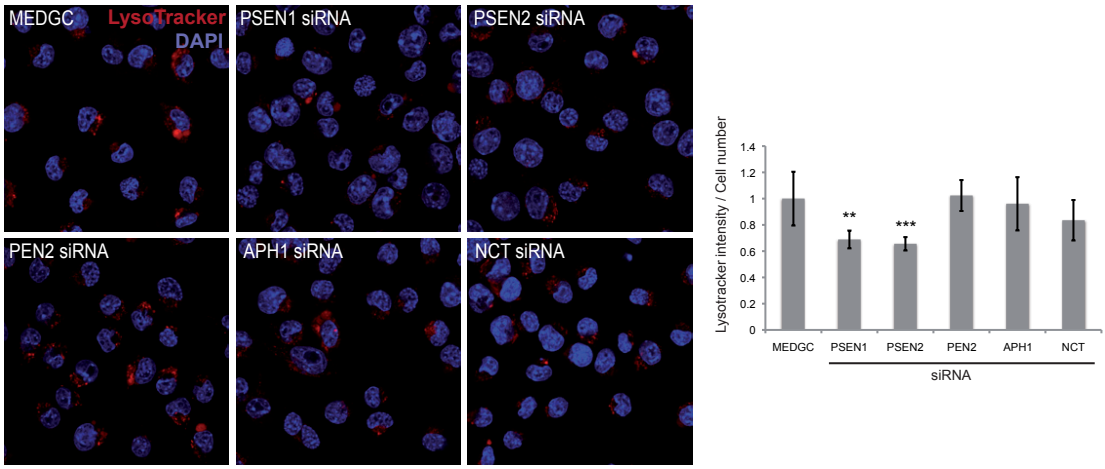

Supplementary Figure 7: LysoTracker staining in BV2 microglia cells and graph showing quantification of the lysotracker signal.

BV2 microglia cells were transfected with control siRNA (MEDGC) or siRNA against PSEN1, PSEN2 or PEN2. After 64 hours, cells were incubated with LysoTracker Red DND-99 (red) for 1.5 hours and processed for confocal imaging. * $p<0.05$, ** $p<0.01$, *** $p<0.001$.

Supplementary Figure 8

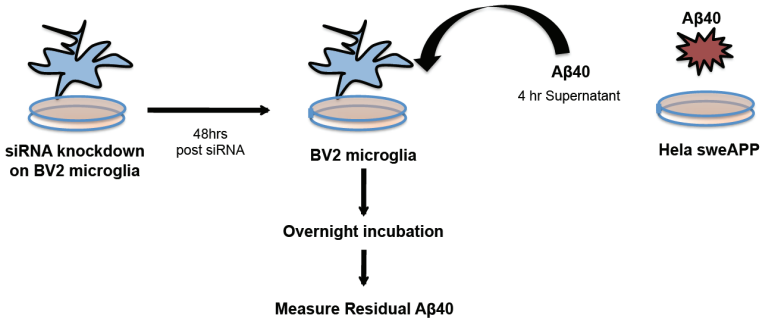

Supplementary Figure 8: Schematic representation of .Aβ clearance assay in BV2 microglia

Supplementary Figure 9:

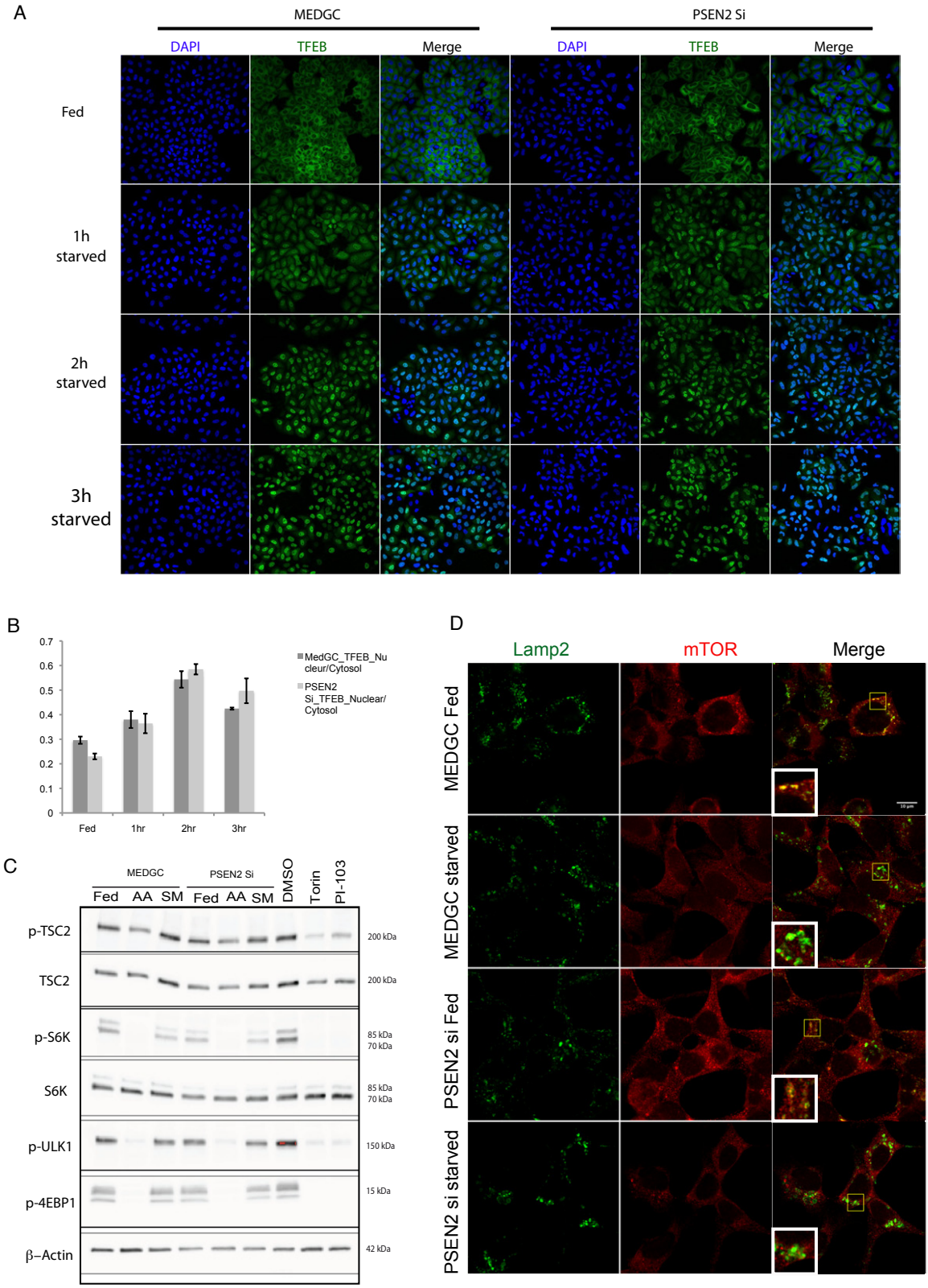

Supplementary Figure 9: PSEN2-loss dependent lysosomal deficiency is not due to defective mTOR/TFEB signaling

A) HeLa cells stably expressing TFEB-GFP were transfected with siRNA against PSEN2 or control (MEDGC). After 69 hours the medium was replaced with either nutrient rich (fed) or nutrient deprived (starved) medium for 1, 2 or 3 hours. Cells were fixed and processed for confocal imaging. DAPI (blue) is used to stain the nucleus. B) Graph showing levels of TFEB-GFP translocated into the nucleus (1hr, 2 hr, 3hr) relative to control (fed). C) HeLa-Swe APP cells were transfected with siRNA against PSEN2 or control (MedGC). Cells were incubated with either nutrient rich medium (NM), amino acid starved medium (AA) or serum starved medium (SM). Lysates were analyzed by Western Blot with antibody against phosphor/total TSC2, S6 kinase, ULK1, 4EBP1. Lysates from cells treated with either Torin or PI103 were used as controls. β-Actin was used as loading control. D) HeLa-Swe APP cells were transfected with siRNA against PSEN2 or control (MEDGC). 69 hours after transfection cells were incubated with either nutrient rich medium (Fed) or nutrient deficient medium (Starved) for 3 hours. Cells were fixed. Cells were stained with antibody against Lamp2 (green) or mTOR (red) and processed for confocal imaging.

Chapter 4

γ-Secretase Activating Protein (GSAP) does not specifically regulate γ-cleavage of APP but regulates APP levels in HeLa cells.

This chapter was published in two parts: (Udayar and Rajendran, Matters 2016 and Udayar and Rajendran, Matters Select 2016)

Part I

γ-secretase activating protein (GSAP) does not specifically affect the γ-secretase processing of APP

Vinod Udayar[a,b,c,d] and Lawrence Rajendran[a,d]

[a] *Systems and Cell Biology of Neurodegeneration,* [b] *Erasmus Mundus Neuroscience program,* [c] *Graduate programs of the Zurich Neuroscience Center, University of Zurich, Switzerland,* [d] *IREM, University of Zurich, Wagistrasse 12, 8952, Schlieren, Switzerland.*

Published in:

Matters, 2016 Feb; doi: 10.19185/matters.201511000002

Author contributions:

Vinod Udayar: Data curation, Data visualization, Formal analysis, Investigation, Methodology, Validation, Original draft, Review & editing.

Lawrence Rajendran: Conceptualization, Funding acquisition, Investigation, Project administration, Resources, Supervision, Original draft, Review & editing.

Abstract

Alzheimer's disease (AD) is characterized by the cerebral accumulation of β-amyloid (Aβ) peptide, which is generated by proteolytic processing of the amyloid precursor protein (APP) by β- and γ-secretases. γ-Secretase is an attractive therapeutic target for the treatment of AD; however, it also cleaves several other protein substrates including Notch. A recent study reported a novel γ-secretase activating protein (GSAP) that is processed from a holoprotein to a 16 kDa active form, which interacts with the γ-secretase complex to selectively regulate β-amyloid peptide generation from APP, without affecting Notch[1]. Since this finding implies that the GSAP processing might be an important target for AD, we tested if this finding could be reproducible. Here we show that processing of GSAP is not required for Aβ production, and rather than specifically regulating γ-secretase cleavage of APP, GSAP also regulated the levels of sAPPβ, the ectodomain shedded by the β-secretase processing of APP. Thus, our results caution the validity of GSAP as the γ-secretase-specific therapeutic target for Aβ production in AD.

Introduction

γ-Secretase is an attractive therapeutic target for the treatment of Alzheimer's disease (AD); however, it also cleaves several other protein substrates including Notch. γ-Secretase is a multimeric transmembrane protein complex composed of presenilin-1 (PS1)/presenilin-2 (PS2), Nicastrin, Aph-1, and Pen2[2]. Familial mutations in APP, PS1, or PS2 that increase the production of the amyloidogenic Aβ42 peptide have been associated with early-onset AD[3][4]. Thus, γ-secretase is an attractive therapeutic target for AD. However, γ-secretase inhibition affects the cleavage of physiologically important substrates such as Notch, and also the ε-cleavage of APP that releases the APP intracellular domain (AICD). The failure of recent clinical trials with γ-secretase inhibitors highlights the need for Aβ-specific inhibitors that spare the cleavage of Notch and the release of AICD[5][6][7]. Recent studies discovered that an anti-cancer compound, imatinib (also known as Gleevec), inhibited Aβ peptides without affecting AICD cleavage. In a hunt for the mechanism through which imatinib produced this effect, He et al. identified a novel γ-secretase activating protein (GSAP)[7]. The authors demonstrated that GSAP is synthesized as a holoprotein called pigeon homologue protein (PION) that is readily processed to a 16 kDa fragment. The authors further showed that this 16 kDa GSAP is the predominant form under steady-state conditions, which interacted with γ-secretase to modulate Aβ production. They also showed that overexpression of GSAP increased, whereas its silencing decreased, Aβ levels. Since this finding implies that the GSAP processing might be an important target for AD, we tested if this finding could be reproducible so that GSAP can be established as a reliable target for the treatment of AD.

Objective

Here we wanted to study if processing of GSAP is required for Aβ production, and if GSAP specifically affects the γ-secretase processing of APP.

Results and Discussion

Since GSAP has been shown to be processed to a 16 kDa fragment by an unknown protease and since this protease could be an ideal therapeutic target for AD[8], we intended to perform a protease RNA interference (RNAi) screen to identify the protease(s) responsible for the cleavage of GSAP. To establish conditions for detecting GSAP cleavage, we first expressed full-length GSAP (also called PION) in cells that produced robust amounts of Aβ[9]. Unexpectedly, we did not detect any 16 kDa cleavage product of GSAP/PION, and the full-length levels of GSAP/PION remained largely unaltered in all the cells that we tested, namely

N2a cells expressing the Swedish mutant of APP (N2a-695), HEK cells and HeLa cells expressing the Swedish mutant of APP (HeLa-swAPP) cells (Fig. 1A) in contrast to the findings of He et al. We used the GSAP construct that He et al. used but failed to see any cleavage of GSAP. We also used bioinformatics analysis to predict protease cleavage sites in GSAP and used the sequence of human GSAP as entry in Expassy's Peptide Cutter tool, a standard protease prediction online tool. First, there were only two enzymes that were predicted to cut GSAP once, but neither of them would liberate a 16 kDa fragment (Caspase 1 at residue 8 and Thrombin at residue 591) (data not shown). Second, even when we relaxed the number of times that the enzymes (and also chemicals) could cleave GSAP to up to 20 sites, there were no cleavage sites at the residue 733 predicted by He et al., to release a 16 kDa fragment, suggesting that GSAP is most likely not processed to a 16 kDa fragment by a cellular protease, one of the two core findings of He et al., i.e., GSAP is processed to a 16 kDa fragment that binds to γ-secretase and it is a γ-secretase activating protein, which implied that this protease could be a therapeutic target. Importantly, even in the absence of proteolytic processing of GSAP, the cells still produced robust amounts of Aβ suggesting that cleavage of GSAP is not essential for its putative γ-secretase-promoting activity (Fig. 1B).

To study the role of GSAP in APP processing and Aβ production, we silenced GSAP using a pool of four siRNAs and assayed for secreted Aβ and sAPPβ levels, the soluble fragment of APP that is generated after β-secretase-(BACE1)-mediated cleavage. As controls, we used siRNAs against APP, BACE1, Pen2, and a scrambled medium GC oligo (MedGC). RT-PCR analyses confirm efficient silencing of GSAP upon siRNA transfection (Fig. 1C). The measurements to monitor APP processing were performed using a multiplexed system to quantitatively measure both Aβ and sAPPβ levels from the sample[10]. This system allows one to investigate if a particular perturbation (via siRNAs or plasmid overexpression) affects at the level of β-cleavage of APP or at the level of γ-secretase/Aβ . As reported by He et al., we found that GSAP silencing significantly inhibited Aβ levels (Fig. 1D). However, we also found a similar decrease in sAPPβ levels (Fig. 1D). Since both the measurements come from the same samples and even from the same wells of the assay plates, the decrease in both sAPPβ and Aβ were not due to intermeasurement variations or use of different assays[10]. This decrease in both sAPPβ and Aβ was unexpected as it was claimed that GSAP regulated only γ-secretase cleavage of APP (He et al.). To ensure that our assay can recapitulate specific γ-secretase-affecting events, as a control, we silenced the expression of Pen2, a bona fide γ-secretase associated/activating protein[11], and found that it affected specifically Aβ levels without affecting sAPPβ levels (Fig. 1D). As additional controls, we silenced the

expression of APP and BACE1, which reduced both sAPPβ and Aβ levels as expected (Fig. 1D). siRNA-mediated silencing of genes works very efficiently in these cells ([12]Fig. 1C). Similar results were obtained when GSAP was silenced in HEK cells, which express wildtype APP (Fig. 1E). To rule out that the effect on sAPPβ was caused by off-target effects through siRNA silencing with pooled siRNAs, we silenced GSAP using four independent siRNA oligos individually and assayed for sAPPβ and Aβ levels. All individual siRNAs decreased both sAPPβ and Aβ, clearly demonstrating that GSAP regulates both sAPPβ and Aβ levels, and not just the γ-cleavage product, Aβ (Fig. 1F), as reported by He et al. The probability that all four oligos would work through an off-target is infinitesimally small and this clearly demonstrates that GSAP affects both Aβ and sAPPβ levels. Moreover, using the multiplexing system for measuring the peptides Aβ38, 40 and 42[12] we found that all three Aβ species were significantly reduced upon GSAP knockdown (Fig. 1G).

Conclusions

We show that GSAP is not processed to a 16 kDa fragment and it does not specifically alter γ-secretase cleavage of APP as claimed by He et al.

Limitations

One main limitation that we can think of is that our study used only cultured cells, but we used three different systems and found exactly the same result: that we could not replicate the He et al. studies, in line with the findings from Hussain et al.[1].

Conjectures

Since GSAP silencing also reduced the levels of sAPPβ in addition to Aβ, it could affect either the levels of APP or β-secretase (BACE) (in the case of β-secretase it could also affect the activity). In the next studies, we will follow up by studying whether GSAP regulated the levels/activity of APP/BACE1. If other labs are also interested, we invite them so that they can also investigate to know how GSAP affected sAPPβ and Aβ levels. We will provide the reagents we have used here.

Methods

cDNA constructs

For GSAP overexpression, mammalian expression vector pReceiverM07 with the full-length GSAP and a C-terminal-HA tag was purchased from Genecopoeia (same source as He et al.).

Cells

Hela-sweAPP and HEK-wtAPP cells are cultured and used as described 20. N2a-695-APP cells are a kind gift of Prof. G. Thinakaran, University of Chicago.

siRNA

siRNAs were purchased from Invitrogen (stealth siRNA).

siRNA transfection for HeLa-swAPP cells

RNAi silencing was performed in HeLa cells expressing the Swedish APP mutation (HeLa-swAPP). siRNAs were transfected with a final concentration of 5 nM using Oligofectamine (Invitrogen) as a transfection reagent at a concentration of 0.3 µl in a total volume of 100 µl following the manufacturer's instructions. Each siRNA transfection was performed in quadruplicate. After 24 h the transfection mix was replaced with fresh culture medium. 69 h after transfection, medium was again replaced with 100 µl fresh medium containing 10% Alamar Blue (AbD Serotec). Supernatants were collected and assayed for Aβ and sAPPβ, as described below. The cells were lysed with 50 µl lysis buffer (1% NP-40, 0.1% SDS and protease inhibitor cocktail tablet) for 20 min on ice.

siRNA transfection of HEK-wtAPP cells

Lipofectamine RNAiMAX (Invitrogen) was used as a transfection reagent. 24 h prior to transfection, cells were seeded at an initial seeding density of 3500 cells per well in a 96 well plate pre-coated with poly D lysine (Sigma Aldrich). siRNAs were transfected at a final concentration of 5 nM using 0.3 µl Lipofectamine RNAiMAX in a total volume of 100 µl. Each siRNA transfection was performed in quadruplicate. After 48 h the transfection mix was replaced with fresh medium containing 10% Alamar Blue. Supernatants were collected and assayed for Aβ and sAPPβ as described below. The cells were lysed with 35 µl lysis buffer for 20 min on ice.

Plasmid transfection

The plasmid transfection for GSAP/PION-HA was performed in HeLa-swAPP cells. Lipofectamine 2,000 (Invitrogen) was used as a transfection reagent. Cells were seeded in a 96 well plate at an initial seeding density of 6,000 cells per well 24 h prior to the transfection. 0.3 µg of plasmid DNA was transfected using 0.3 µl of Lipofectamine 2,000 in a total volume of 100 µl. Transfection mix was replaced after 3 h by fresh culture medium. 21 h after

transfection, medium was again replaced with fresh medium containing 10% Alamar Blue. 24 h after transfection, Alamar Blue measurements were taken. Supernatant was collected and assayed for Aβ and sAPPβ. The cells were lysed with 35 µl lysis buffer, incubated for 20 min on ice, and stored at -20°C.

Alamar Blue assay

For cell viability measurements using Alamar Blue, the medium of transfected cells (siRNA or plasmid) was replaced with normal medium containing 10% Alamar Blue. The final volume in each well was 100 µL. 3 h after medium change, cell viability was monitored using Fluoroscan Ascent Cf (Labsystems), with excitation wavelength 544 nm and emission at 590 nm. Cell viability was measured using the Alamar Blue assay (Serotec Ltd., Kidlington, Oxford, UK), where the absorbance was monitored at the end of the reaction (after 3 h) (Labsystems Multiscan MS UV visible spectrophotometer).

Electrochemiluminescence (ECL) detection of Aβ and sAPPβ

An electrochemiluminescence assay (Meso Scale Discovery, MD) was performed to determine the amount of secreted Aβ40 and sAPPβ in the cell culture medium. For the measurement of Aβ38, 40 and 42, triplex plates were used from conditioned supernatants collected for 12 h. Pre-coated plates were blocked with TBST (Tris Buffered Saline containing Tween), containing 3% Blocker A, for 1 h at room temperature on a shaker at 750 rpm. After washing, 10 µl of the cell culture supernatant was added to each well along with 10 µl of detection antibody followed by incubation for 2 h at room temperature on a shaker at 750 rpm. After washing, detection was performed in 35 µl of 2x MSDT read buffer and read with the Sector Imager 6000.

Western blotting

After 72 h of siRNA transfection, cells were lysed in buffer containing 1% NP-40 and 0.1% SDS and protease inhibitors (Roche). Equal amounts of the lysate (according to the protein content quantified by BCA assay; Pierce) were run on 4–12% BIS-TRIS gels (Invitrogen). The gel was blotted onto a nitrocellulose membrane (BioRad) and probed with the respective antibodies (anti-HA antibody: Roche diagnostics; GAPDH antibody: Meridian Science).

Real-time RT-PCR

Total RNA from cultured cells was isolated using TRIzol® Reagent (Life Technologies) following manufacturer's protocol. 1 μg of total RNA was used for reverse transcription with oligo-dT primer using the Superscript III first-strand synthesis system (Invitrogen) according to the manufacturer's protocol. Real-time PCR was performed using iTaqTM Universal SYBR® Green supermix (Bio-Rad) following manufacturer's instructions. Relative gene expression levels were calculated with the ΔΔCt method using GAPDH for normalization.

References

1. Ishrut Hussain, Julien Fabrègue, Laurence Anderes et al., The Role of γ-Secretase Activating Protein (GSAP) and Imatinib in the Regulation of γ-Secretase Activity and Amyloid-β Generation Journal of Biological Chemistry, 288/2012, pages 2521-2531 DOI: 10.1074/jbc.m112.370924

2. Dennis J. Selkoe, Michael S. Wolfe Presenilin: Running with Scissors in the Membrane Cell, 131/2007, pages 215-221 DOI: 10.1016/j.cell.2007.10.012

3. David R. Borchelt, Gopal Thinakaran, Christopher B. Eckman et al., Familial Alzheimer's Disease–Linked Presenilin 1 Variants Elevate Aβ1–42/1–40 Ratio In Vitro and In Vivo Neuron, 17/1996, pages 1005-1013 DOI: 10.1016/s0896-6273(00)80230-5

4. Karen Duff, Chris Eckman, Cindy Zehr et al., Increased amyloid-β42(43) in brains of mice expressing mutant presenilin 1 Nature, 383/1996, pages 710-713 DOI: 10.1038/383710a0

5. Corey R. Hopkins ACS Chemical Neuroscience Molecule Spotlight on ELND006: Another γ-Secretase Inhibitor Fails in the Clinic ACS Chemical Neuroscience, 2/2011, pages 279-280 DOI: 10.1021/cn2000469

6. Sanjay W. Pimplikar, Ralph A. Nixon, Nikolaos K. Robakis et al., Amyloid-Independent Mechanisms in Alzheimer's Disease Pathogenesis Journal of Neuroscience, 30/2010, pages 14946-14954 DOI: 10.1523/jneurosci.4305-10-2010

7. Kumar Sambamurti, Nigel H. Greig, Tadanobu Utsuki et al., Targets for AD treatment: conflicting messages from γ-secretase inhibitors Journal of Neurochemistry, 117/2011, pages 359-374 DOI: 10.1111/j.1471-4159.2011.07213.x

8.Peter St George-Hyslop, Gerold Schmitt-Ulms Alzheimer's disease: Selectively tuning γ-secretase Nature, 467/2010, pages 36-37 DOI: 10.1038/467036a

9. Lawrence Rajendran, Anja Schneider, Georg Schlechtingen et al., Efficient Inhibition of the Alzheimer's Disease β-Secretase by Membrane Targeting Science, 320/2008, pages 520-523 DOI: 10.1126/science.1156609

10. Vinod Udayar, Virginie Buggia-Prévot, Rita L. Guerreiro et al., A Paired RNAi and RabGAP Overexpression Screen Identifies Rab11 as a Regulator of β-Amyloid Production Cell Reports, 5/2013, pages 1536-1551 DOI: 10.1016/j.celrep.2013.12.005

11. Harald Steiner, Edith Winkler, Dieter Edbauer et al., PEN-2 Is an Integral Component of the γ-Secretase Complex Required for Coordinated Expression of Presenilin and Nicastrin Journal of Biological Chemistry, 277/2002, pages 39062-39065 DOI: 10.1074/jbc.c200469200

12. Jitin Bali, Ali Hashemi Gheinani, Sebastian Zurbriggen, Lawrence Rajendran Role of genes linked to sporadic Alzheimer's disease risk in the production of β-amyloid peptides Proceedings of the National Academy of Sciences, 109/2012, pages 15307-15311 DOI: 10.1073/pnas.1201632109

Figure 1

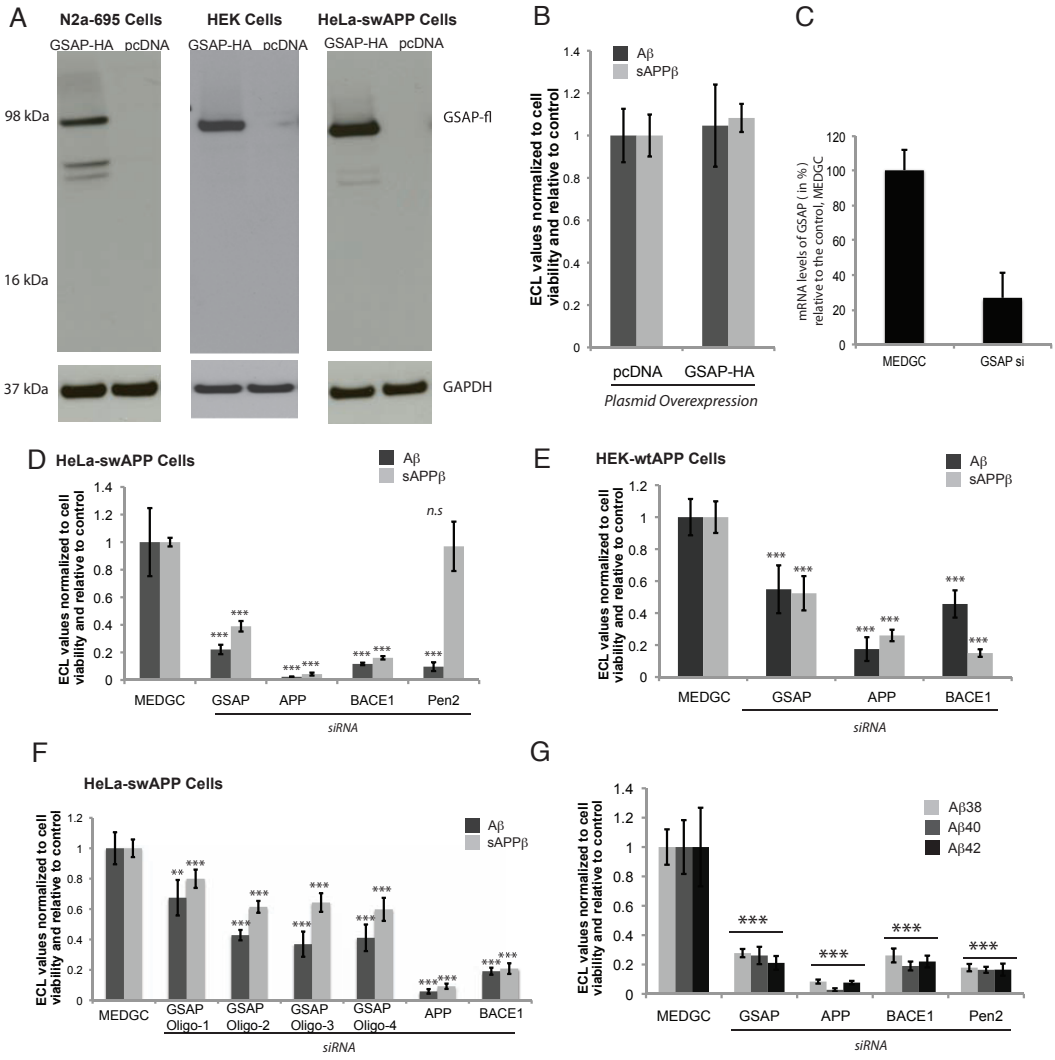
A
N2a-695 Cells
HEK Cells
HeLa-swAPP Cells
GSAP-HA pcDNA
GSAP-HA pcDNA
GSAP-HA pcDNA
98 kDa
16 kDa
37 kDa
GSAP-fl
GAPDH
B
Aβ
sAPPβ
ECL values normalized to cell viability and relative to control
pcDNA GSAP-HA
Plasmid Overexpression
C
mRNA levels of GSAP (in %) relative to the control, MEDGC
MEDGC
GSAP si
D
HeLa-swAPP Cells
Aβ
sAPPβ
n.s
ECL values normalized to cell viability and relative to control
MEDGC
GSAP
APP
BACE1
Pen2
siRNA
E
HEK-wtAPP Cells
Aβ
sAPPβ
ECL values normalized to cell viability and relative to control
MEDGC
GSAP
APP
BACE1
siRNA
F
HeLa-swAPP Cells
Aβ
sAPPβ
ECL values normalized to cell viability and relative to control
MEDGC
GSAP Oligo-1
GSAP Oligo-2
GSAP Oligo-3
GSAP Oligo-4
APP
BACE1
siRNA
G
Aβ38
Aβ40
Aβ42
ECL values normalized to cell viability and relative to control
MEDGC
GSAP
APP
BACE1
Pen2
siRNA

Figure 1. Full-length γ-secretase activating protein (GSAP) is not processed to a 16 kDa protein and its silencing leads to reduction in both β- and γ-secretase cleavage of APP

(A) Western blot analysis showing absence of the processed 16 kDa C-terminal fragment of GSAP: N2a-695 cells, HEK cells and HeLa-swAPP cells were transfected with either the pReceiverM07 construct expressing the full-length GSAP with a C-terminal-HA tag or pcDNA as the control plasmid and immunoblotted with anti-HA and anti-GAPDH antibodies. (B) Graph showing the levels of Aβ and sAPPβ after overexpression of GSAP-HA plasmids: HeLa-swAPP cells were transfected with pcDNA (negative control) or the plasmid expressing GSAP, and the supernatants were analyzed for sAPPβ and Aβ levels using an electrochemiluminescence (ECL)-based assay. (C) Graph showing GSAP knockdown efficiency: HeLa-swAPP cells were transfected with either MEDGC oligos (negative control) or siRNAs against GSAP and the knockdown efficiency was estimated by quantitative RT-PCR. (D) Graph showing the reduced levels of Aβ and sAPPβ after siRNA-mediated silencing of GSAP in Hela-swAPP cells: HeLa-swAPP cells were transfected with MedGC oligos (negative control) and with siRNA pools for silencing the expression of APP, BACE1, PEN2 and GSAP, and assayed for Aβ and sAPPβ using ECL. (E) Graph showing the reduced levels of Aβ and sAPPβ after siRNA-mediated silencing of GSAP in HEK-wtAPP expressing cells: HEK-wtAPP cells were transfected with MedGC oligos and siRNAs against APP, BACE1, and GSAP and assayed for Aβ and sAPPβ. (F) Graph showing the levels of Aβ and sAPPβ after siRNA-mediated silencing of GSAP using four different GSAP-specific siRNAs: HeLa-swAPP cells were transfected with MedGC oligos and siRNAs against APP, BACE1, and four different siRNAs against GSAP and assayed for Aβ and sAPPβ. (G) Graph showing the levels of Aβ38, Aβ40 and Aβ42 after siRNA-mediated silencing of GSAP: HeLa-swAPP cells were transfected with MedGC oligos and siRNAs against APP, BACE1, PEN2, and GSAP and assayed for Aβ38, Aβ40, and Aβ42. For Fig. 1D–1F and Fig. 1I–1K, $^{**}p < 0.05$, $^{***}p < 0.005$, n.s., not significant. All statistics are performed using a two-tailed t-test. Error bars indicate SD.

Part II

γ-Secretase activating protein (GSAP) does not specifically regulate γ-cleavage of APP but regulates APP levels in HeLa cells

Vinod Udayar[a,b,c,d] and Lawrence Rajendran[a,d]

[a] *Systems and Cell Biology of Neurodegeneration,* [b] *Erasmus Mundus Neuroscience program,* [c] *Graduate programs of the Zurich Neuroscience Center, University of Zurich, Switzerland,* [d] *IREM, University of Zurich, Wagistrasse 12, 8952, Schlieren, Switzerland.*

Published in:

Matters Select, 2016 Dec doi: 10.19185/matters.201611000002

Author contributions:

Vinod Udayar: Data curation, Data visualization, Formal analysis, Investigation, Methodology, Validation, Original draft, Review & editing.

Lawrence Rajendran: Conceptualization, Funding acquisition, Investigation, Project administration, Resources, Supervision, Original draft, Review & editing.

Abstract

Recently, it was shown that the γ-secretase activating protein (GSAP) regulates specifically the γ-cleavage of the β-amyloid precursor protein (APP), whose amyloidogenic processing is causatively linked to Alzheimer's disease (AD)[1]. This paper was contradicted by many groups refuting the reproducibility of the core findings; and recently, it was shown that GSAP did not specifically affect the γ-cleavage of APP but also that the levels of the β-cleaved product of APP (sAPPβ) was reduced in cells depleted of GSAP using siRNA[2]. Here we confirm these findings that GSAP silencing also reduced Aβ and sAPPβ levels but also showed, for the first time, that rather than specifically regulating γ-secretase cleavage of APP, GSAP regulates the levels of full-length APP, thus affecting the processing of APP by all three proteases, i.e., α-, β- and γ-secretases. This could explain why GSAP silencing reduces both Aβ and sAPPβ levels. Furthermore, imatinib, an anti-cancer drug that selectively reduces Aβ levels, which was shown to occur by inhibiting the GSAP-γ-secretase interaction, reduced Aβ levels also in the absence of GSAP. Thus, our results not only uncover a new aspect of GSAP function but also continue to caution the validity of GSAP as a specific therapeutic target for Aβ production in AD.

Introduction

GSAP was identified to be a specific regulator of γ-secretase cleavage of the amyloid precursor protein that is linked to Alzheimer's disease. This paper published in *Nature* in 2010[1] was refuted by several groups questioning the validity and reproducibility of the findings[2][3][4]. Recently, Udayar and Rajendran[2] showed that GSAP depletion did not only reduce Aβ but also reduced sAPPβ. Here we replicate these findings now but also show that silencing of GSAP reduced APP levels, thus explaining how GSAP could have regulated Aβ levels. These results question once again the validity of GSAP's specific role in γ-secretase cleavage of APP also uncover new insights into the role of GSAP in regulating APP levels.

Objective

To study the role of γ-secretase activating protein (GSAP) in regulating APP processing and to study the reproducibility of GSAP's role in specific γ-secretase cleavage of APP.

Results & Discussion

He et al.[1] showed that GSAP silencing specifically inhibited γ-cleavage of APP. This study was recently refuted by Udayar and Rajendran[2] showing that GSAP silencing did not specifically inhibit Aβ, but it also lowered the sAPPβ levels, which is a product of β-cleavage of APP and not γ-cleavage. To reproduce this finding, we silenced GSAP using a pool of four siRNAs and assayed for secreted Aβ and sAPPβ levels. As controls, we used siRNAs against APP, BACE1, Pen-2, and a scrambled medium GC oligo (MedGC). The measurements to monitor APP processing were performed using a multiplexed system to quantitatively measure both Aβ and sAPPβ levels from the sample[5]. We observed that GSAP silencing led to a decrease in both Aβ and sAPPβ levels, in agreement with the previously published finding[2] (Fig. 1A). To study how GSAP affected both Aβ and sAPPβ levels, we first examined APP processing by Western blotting with anti-APP C-terminus-specific antibody. Surprisingly, GSAP silencing dramatically decreased full-length APP levels (Fig. 1B) (see independent replicate data in supplementary information; Suppl. Fig. 1A). As a control, we used siRNAs against APP and found that it significantly reduced APP protein levels (Fig. 1B), as expected. To rule out that the reduction in APP was due to general cell toxicity or defective cell viability, we performed a number of controls. First, we analyzed the levels of a cellular protein, glyceraldehyde-3-phosphate dehydrogenase (GAPDH), and found these to be unchanged in GSAP-silenced cells (Fig. 1B; Suppl. Fig. 1A) in the same blot along with anti-APP antibody. Second, the levels of Nicastrin, another type 1 transmembrane protein, were

not affected in GSAP-silenced cells (Suppl. Fig. 1B). Third, cell viability measurements (of 20 replicates) by Alamar Blue™ from GSAP-silenced and scrambled oligo-treated control cells did not show any difference demonstrating that GSAP silencing did not induce any cell toxicity (Suppl. Fig. 1C). However, silencing Kif11, a kinesin involved in cell division, severely induced cell death, serving as a positive control for the cell toxicity assay measured by Alamar Blue (Suppl. Fig. 1C). Fourth, general morphological characterization showed no distinguishable effect of GSAP silencing on cell shape, structure, and number (Suppl. Fig. 1D). Fifth, release of the cytosolic protein, lactate dehydrogenase (LDH), was monitored to detect any membrane leakages or subtle cellular membrane defects. GSAP silencing did not affect the release of LDH (Suppl. Fig. 1E). We confirmed the efficiency of GSAP silencing by RT-PCR (Suppl. Fig. 1F). Together, our results conclusively show that GSAP silencing reduced full-length APP levels and thus altered both β- and γ-cleavage and not specifically γ-cleavage of APP or induced any cytotoxicity. To independently validate the effect of GSAP on APP levels and also to rule out any epitope-specific effects due to the use of the C-terminal antibody of APP that we used for Western blotting, we checked the cellular levels of APP using immunofluorescence with another anti-APP antibody, 6E10, that recognises the N-terminus of the Aβ domain. Again, silencing of GSAP substantially reduced APP levels (Fig. 1C) demonstrating that indeed GSAP regulates APP levels. Consistent with the observation that GSAP silencing reduces full-length APP levels, GSAP silencing also significantly reduced the levels of sAPPα, which is produced by the non-amyloidogenic (α-secretase) pathway (Fig. 1D). This reduction was not due to cell death, as the viability of GSAP-silenced cells was not affected (Fig. 1D; Suppl. Fig. 1). To rule out any off-target effects, we silenced GSAP using four different siRNAs singly and analyzed its effect on APP levels. We observed that each of the four siRNAs reduced APP levels individually (Suppl. Fig. 2A and Suppl. Fig. 2B), thus demonstrating the specificity of the observed effect of GSAP silencing on APP levels. Thus, GSAP regulates full-length APP levels and not specifically γ-secretase activity. To further validate our findings, we used yet another approach by using the anti-cancer drug, imatinib. Imatinib inhibits Aβ production, which was concluded to occur via binding to GSAP by blocking its activity[1]. Since our results indicate that GSAP does not specifically regulate the γ-secretase activity, we then asked whether imatinib could regulate γ-secretase activity in a GSAP-independent manner. Treatment of cells with imatinib indeed selectively decreased Aβ levels without affecting sAPPβ levels or cell viability, as has been previously shown by several laboratories[6][7][8](Fig. 1E; Suppl. Fig. 1G). However, while cells silenced with GSAP siRNA again showed a reduction in both Aβ

and sAPPβ levels, treatment with imatinib (10 mM[1], same concentration used in He et al.) caused a further significant and specific decrease in Aβ levels, suggesting that imatinib regulates Aβ levels independently of GSAP. Recent studies on imatinib and Aβ also fail to see an effect, further casting doubt that GSAP is an imatinib target[9][3]. We have tried to reproduce the results[1] using the cells, plasmids, experimental conditions, concentrations of inhibitors as identical as those employed by He et al.,[1] but we failed to reproduce many of their findings. Due to the unavailability of a working anti-GSAP antibodies, we were unable to look at the cleavage of endogenous GSAP. However, in large-set experiments, using RNAi against GSAP, we studied the functionality of the endogenous GSAP. The only one result that we can reproduce is the effect of GSAP on Aβ levels, which we discovered to be not due to the effect of GSAP on γ-secretase activity as claimed by He et al.,[1] but we have shown that this is rather due to GSAP's effect on APP.

Conclusions

These results conclusively shows that processing of GSAP is not necessary for Aβ production and that GSAP is inappropriately named as it affects Aβ levels via regulating the levels of full-length APP and not through activating the γ-secretase, as reported earlier[1]. Since APP and the fragments of APP have physiological functions[10], our work cautions the validity of GSAP as a therapeutic target for AD. This work also highlights the need for more efforts into reproducibility of the published data.

Limitations

It is largely a cell culture study.

Conjectures

With all the published data on this subject, it is clear that GSAP is not a specific activator of γ-secretase cleavage of APP and further characterization of GSAP function is needed. However, it will be interesting to pursue how GSAP silencing reduces APP levels. One possibility is that APP transcript levels are reduced or APP protein degradation is enhanced.

Methods

Cells

Hela-sweAPP are cultured and used as described[11].

siRNA

siRNAs were purchased from Invitrogen (stealth siRNA).

siRNA transfection for HeLa-swAPP cells

Cells were transfected with a final concentration of 5 nM using Oligofectamine (Invitrogen) as a transfection reagent at a concentration of 0.3 mL in a total volume of 100 mL following the manufacturer's instructions. Each siRNA transfection was performed in quadruplicate. After 24 h the transfection mix was replaced with fresh culture medium. 69 h after transfection, medium was again replaced with 100 mL fresh medium containing 10% Alamar Blue™ (AbD Serotec). Supernatants were collected and assayed for Aβ and sAPPβ, as described below. The cells were lysed with 50 mL lysis buffer (1% NP-40, 0.1% SDS and protease inhibitor cocktail tablet) for 20 min on ice.

Alamar Blue assay

For cell viability measurements using Alamar Blue, the medium of transfected cells (siRNA or plasmid) was replaced with normal medium containing 10% Alamar Blue. The final volume in each well was 100 mL. 3 h after the medium change, cell viability was monitored using Fluoroscan Ascent Cf (Labsystems), with excitation wavelength 544 nm and emission at 590 nm.

Electrochemiluminescence (ECL) detection of Aβ, sAPPβ, and sAPPα

An electrochemiluminescence assay (Meso Scale Discovery, MD) was performed to determine the amount of secreted Aβ40, sAPPα, and sAPPβ in the cell culture medium 10. For the measurement of Aβ38, 40 and 42, triplex plates were used from conditioned supernatants collected for 12 h. Pre-coated plates were blocked with Tris Buffered Saline containing Tween, containing 3% Blocker A, for 1 h at room temperature on a shaker at 750 rpm. After washing, 10 mL of the cell culture supernatant was added to each well along with 10 mL of detection antibody followed by incubation for 2 h at room temperature on a shaker at 750 rpm. After washing detection was performed in 35 mL 2X MSDT read buffer and read with the Sector Imager 6000.

Western blotting

After 72 h of siRNA transfection, cells were lysed in buffer containing 1% NP-40 and 0.1% SDS and protease inhibitors (Roche). Equal amounts of the lysate (according to the protein content quantified by BCA assay (Pierce)) were run on 4–12% BIS-TRIS gels (Invitrogen). The gel was blotted onto a nitrocellulose membrane (BioRad) and probed with the respective antibodies: anti-APP, C-terminal antibody: SIGMA (F3165-1MG); 6E10 anti-Aβ recognizing APP antibody: Covance; anti-Nicastrin antibody (2332-1): Epitomics; GAPDH antibody: Meridian Science.

Immunofluorescence

Cells were reverse-transfected either with MEDGC or siRNAs against APP or GSAP on chambered coverslides and 72 h later fixed, permeabilised, blocked and immunostained with 6E10 anti-APP antibody. The signal was visualised by the use of Alexa488 or Alexa546-coupled anti-mouse secondary antibody. Nuclei were visualised by DAPI staining.

Imatinib treatment

Cells were reverse-transfected either with MEDGC or siRNAs against GSAP, and 69 h later, cells were treated with DMSO or Imatinib (10 μM, Enzo Life Sciences) for 3 h. Treatment was done with culture medium containing 10% Alamar Blue. The final volume of culture medium in each well was 100 μL. After 72 h, cell viability was assessed by Alamar Blue assay, supernatants were collected and assayed for Aβ and sAPPβ.

Cell cytotoxicity assay

The cell cytotoxicity assay was carried out using the Cytotoxicity Detection Kit (Roche) by measuring the activity of released lactate dehydrogenase into the culture medium. The culture supernatant was collected from the cells (with and without Triton X-100 treatment). Samples were further diluted and processed according to manufacturers' protocol. The increase in amount of enzyme activity in the supernatant directly correlates with the amount of formazan formed, which is proportional to the number of lysed cells. Absorbance was measured at 492 nm with reference wavelength at 620 nm on a plate reader spectrophotometer.

Real-time RT-PCR

Total RNA from cells was isolated using TRI Reagent® (Sigma-Aldrich) following manufacturer's protocol. 1 μg of total RNA was used for reverse transcription with iScript™

cDNA synthesis kit (Bio-Rad) according to the manufacturer's protocol. Real-time PCR was performed using iTaq™ Universal SYBR® Green supermix (Bio-Rad) following manufacturer's instructions. Relative gene expression levels were calculated with the ΔΔCt method using GAPDH for normalization.

Funding Statement

L. R acknowledges the financial support from the Velux Foundation, the Swiss National Science Foundation grant, the Bangerter Stiftung, the Baugarten Stiftung and the Synapsis Foundation. L. R and V. U acknowledge the funding support from the European Neuroscience Campus of the Erasmus Mundus Program.

Acknowledgements

We thank G. Yu for the HeLa-swAPP cells.

Conflict of interest

The authors declare no conflicts of interest.

Ethics Statement

All the experiments were conducted according to the standard ethical guidelines. No fraudulence is committed in performing these experiments or during processing of the data. We understand that in the case of fraudulence, the study can be retracted by Matters.

References

1. Gen He, Wenjie Luo, Peng Li, Christine Remmers, William J. Netzer, Joseph Hendrick, Karima Bettayeb, Marc Flajolet, Fred Gorelick, Lawrence P. Wennogle, Paul Greengard. Gamma-secretase activating protein is a therapeutic target for Alzheimer's disease Nature, 467/2010, pages 95-98, DOI: 10.1038/nature09325

2. Vinod Udayar, Lawrence Rajendran. γ-Secretase Activating Protein (GSAP) does not specifically affect the γ-Secretase processing of APP Matters, 2015

3. Ishrut Hussain, Julien Fabrègue, Laurence Anderes, Solenne Ousson, Frédéric Borlat, Valérie Eligert, Sébastien Berger, Mitko Dimitrov, Jean-René Alattia, Patrick C. Fraering, Dirk Beher. The Role of γ-Secretase Activating Protein (GSAP) and Imatinib in the Regulation of γ-Secretase Activity and Amyloid-β Generation Journal of Biological Chemistry,288/2012, pages 2521-2531, DOI: 10.1074/jbc.m112.370924

4. Ishrut Hussain, Julien Fabrègue, Solenne Ousson, Aurelie Baguet, Stephane Genoud, Frederic Borlat, Bruno Antonsson, Dirk Beher, Characterization of endogenous and exogenous gamma-secretase activating protein (GSAP) expression in cells Alzheimer's & Dementia: The Journal of the Alzheimer's Association, 7/2011, page S387, DOI: 10.1016/j.jalz.2011.05.1118

5. Udayar Vinod, Buggia-Prévot Virginie, Guerreiro Rita L., *et al.,* A Paired RNAi and RabGAP Overexpression Screen Identifies Rab11 as a Regulator of β-Amyloid Production Cell Reports, 5/2013, pages 1536-1551, DOI: 10.1016/j.celrep.2013.12.005

6. Eisele Y. S., Baumann M., Klebl B., *et al.,* Gleevec Increases Levels of the Amyloid Precursor Protein Intracellular Domain and of the Amyloid-beta degrading Enzyme Neprilysin Molecular Biology of the Cell, 18/2007, pages 3591-3600, DOI: 10.1091/mbc.e07-01-0035

7. Netzer W. J., Dou F., Cai D et al., Gleevec inhibits β-amyloid production but not Notch cleavage Proceedings of the National Academy of Sciences, 100/2003, pages 12444-12449, DOI: 10.1073/pnas.1534745100

8. Sutcliffe J. Gregor,et al., Peripheral reduction of β-amyloid is sufficient to reduce brain β-amyloid: Implications for Alzheimer's disease Journal of Neuroscience Research, 89/2011, pages 808-814, DOI: 10.1002/jnr.22603

9. Olsson Bob, Legros Laurence, et al., Imatinib treatment and Aβ42 in humans Alzheimer's & Dementia: The Journal of the Alzheimer's Association, 10/2014, pages S374-S380, DOI: 10.1016/j.jalz.2013.08.283

10. Ulrike C. Müller, Hui Zheng Physiological Functions of APP Family Proteins Cold Spring Harbor Perspectives in Medicine, 2/2011, pages a006288-a006288, DOI: 10.1101/cshperspect.a006288

11. Jitin Bali, Ali Hashemi Gheinani, Sebastian Zurbriggen, Lawrence Rajendran Role of genes linked to sporadic Alzheimer’s disease risk in the production of β-amyloid peptides Proceedings of the National Academy of Sciences, 109/2012, pages 15307-15311, DOI: 10.1073/pnas.1201632109

Figure 1

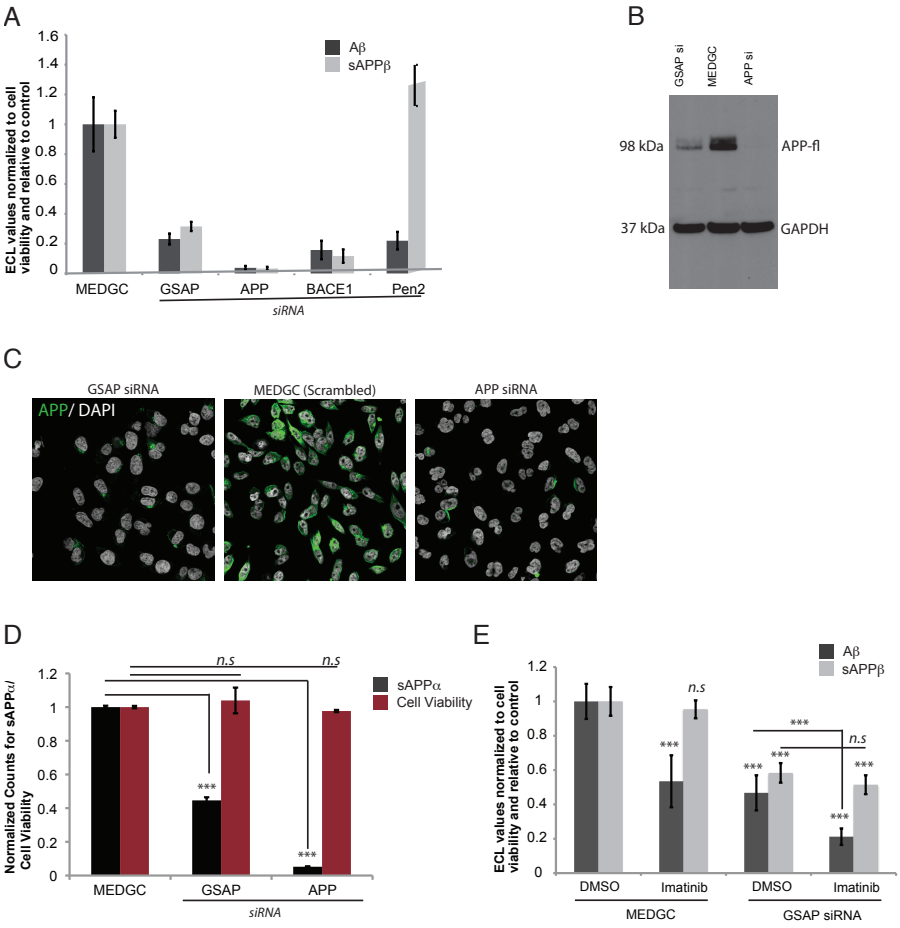
A
Aβ
sAPPβ
ECL values normalized to cell viability and relative to control
MEDGC
GSAP
APP
BACE1
Pen2
siRNA
B
GSAP si
MEDGC
APP si
98 kDa
APP-fl
37 kDa
GAPDH
C
GSAP siRNA
MEDGC (Scrambled)
APP siRNA
APP/ DAPI
D
n.s
n.s
sAPPα
Cell Viability
Normalized Counts for sAPPα/ Cell Viability
MEDGC
GSAP
APP
siRNA
E
Aβ
sAPPβ
n.s
n.s
ECL values normalized to cell viability and relative to control
DMSO
Imatinib
DMSO
Imatinib
MEDGC
GSAP siRNA

Figure 1. γ-secretase activating protein (GSAP) silencing leads to reduction in full-length APP levels and not specifically γ-secretase cleavage of APP

(A) Graph showing the reduced levels of Aβ and sAPPβ after siRNA-mediated silencing of GSAP in Hela-swAPP cells: HeLa-swAPP cells were transfected with MedGC oligos (negative control) and with siRNA pools for silencing the expression of APP, BACE1, PEN2, and GSAP, and assayed for Aβ and sAPPβ using ECL. (B) Western blot analysis showing full-length APP protein levels after siRNA-mediated silencing of GSAP in HeLa-swAPP cells: HeLa-swAPP cells were transfected with MedGC oligos and siRNAs against APP and GSAP and the cell lysates were probed for the protein levels of APP (C-terminus specific antibody) and GAPDH. (C) Immunofluorescence-based detection of APP levels after siRNA-mediated silencing of GSAP: HeLa-swAPP cells were transfected with MedGC oligos and siRNAs against APP and GSAP, and the cells were fixed and assayed for APP (green) using an APP-specific antibody (6E10). Nuclei (gray) were stained using DAPI. (D) Graph showing the levels of sAPPα and cell viability after siRNA-mediated silencing of GSAP: HeLa-swAPP cells were transfected with MedGC oligos and siRNAs against APP and GSAP and assayed for sAPPα and cell viability. (E) Graph showing the levels of Aβ and sAPPβ after siRNA-mediated silencing of GSAP followed by imatinib treatment: HeLa-swAPP cells were transfected with MedGC oligos or siRNA against GSAP followed by treatment with DMSO or imatinib (10 μM). * $p<0.05$, ** $p<0.01$, *** $p<0.001$, n.s., not significant. All statistics are performed using a two-tailed t-test. Error bars indicate SD.

Supplementary Figure 1

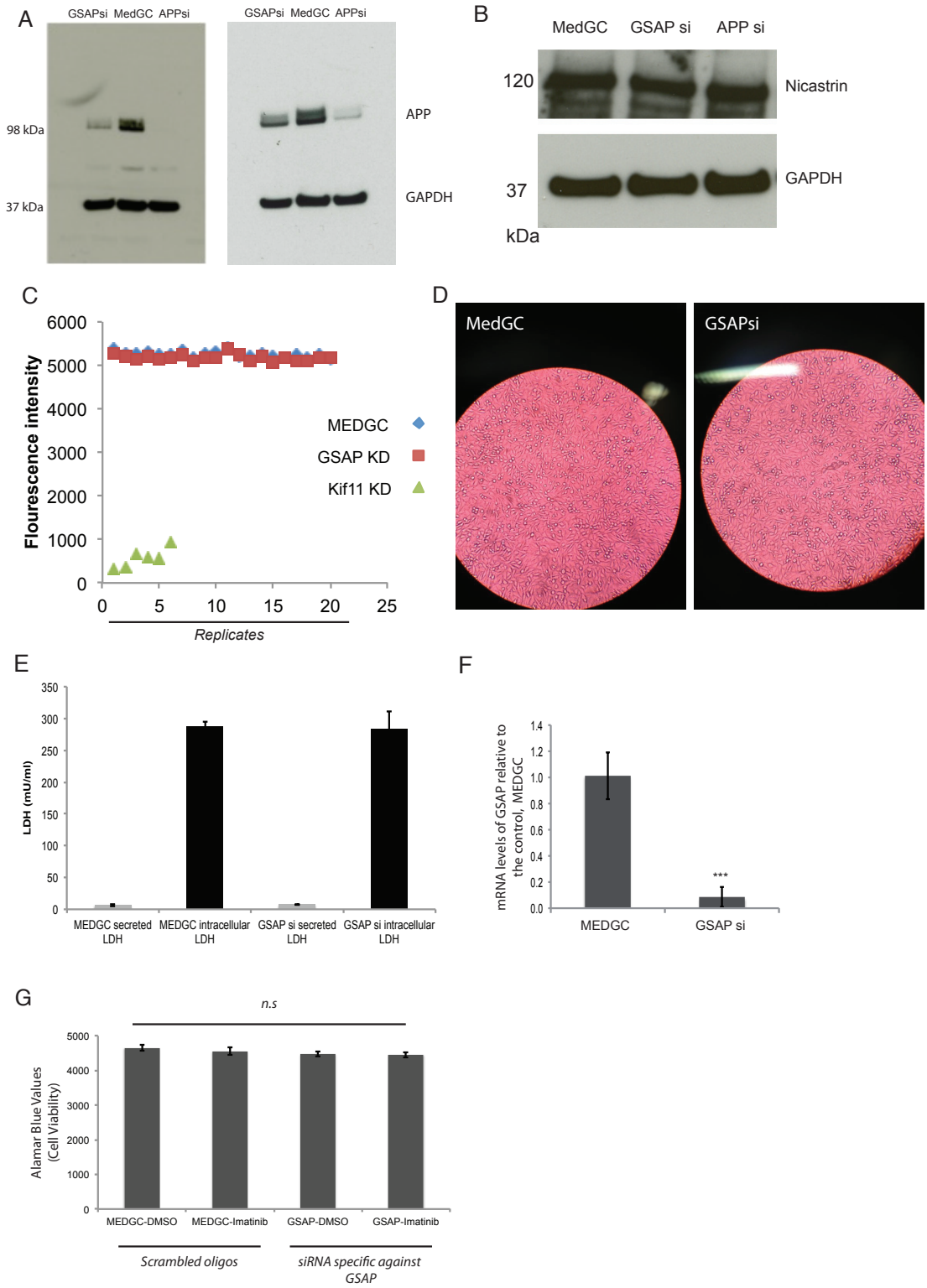

Supplementary Figure 1: A. Replicate Western blot analysis showing protein levels of APP are reduced in GSAP silenced conditions. HeLa-swAPP cells were transfected with either MedGC oligos or siRNAs against GSAP or APP and the cell lysates were probed for APP and GAPDH in the same blot. B. Western blot analysis showing protein levels of Nicastrin upon GSAP knockdown: HeLa-swAPP cells were transfected with either MedGC oligos or siRNAs against GSAP or APP and the cell lysates were probed for Nicastrin and GAPDH. C. Graph showing cell viability upon GSAP knockdown: HeLa-swAPP cells were transfected with MedGC oligos (20 replicates) or siRNAs against GSAP (20 replicates) or Kif11 (positive control, 6 replicates) and assayed for cell viability represented by the flourescence intensity upon metabolism of Alamar Blue by viable cells. D. Microscopy analysis of cell viability upon GSAP knockdown: Representative images of HeLa-swAPP cells after transfection with MedGC oligos or siRNAs against GSAP. E. Graph showing levels of secreted and intracellular LDH upon GSAP knockdown: HeLa-swAPP cells were transfected with MedGC oligos or siRNAs against GSAP and were assayed for the levels of secreted and intracellular LDH to assess cytotoxicity. F. Graph showing GSAP knockdown efficiency: HeLa-swAPP cells were transfected with either MEDGC oligos (negative control) or siRNAs against GSAP and the knockdown efficiency was analyzed by quantitative Reverse Transcriptase (RT)-PCR. G. Graph showing cell viability upon Imatinib treatment: HeLa-swAPP cells were transfected with MedGC oligos or siRNA against GSAP followed by treatment with DMSO or Imatinib (10 μM) and assayed for cell viability represented by the fluorescence intensity upon metabolism of Alamar Blue by viable cells. * $p<0.05$, ** $p<0.01$, *** $p<0.001$, n.s., not significant.

Supplementary Figure 2

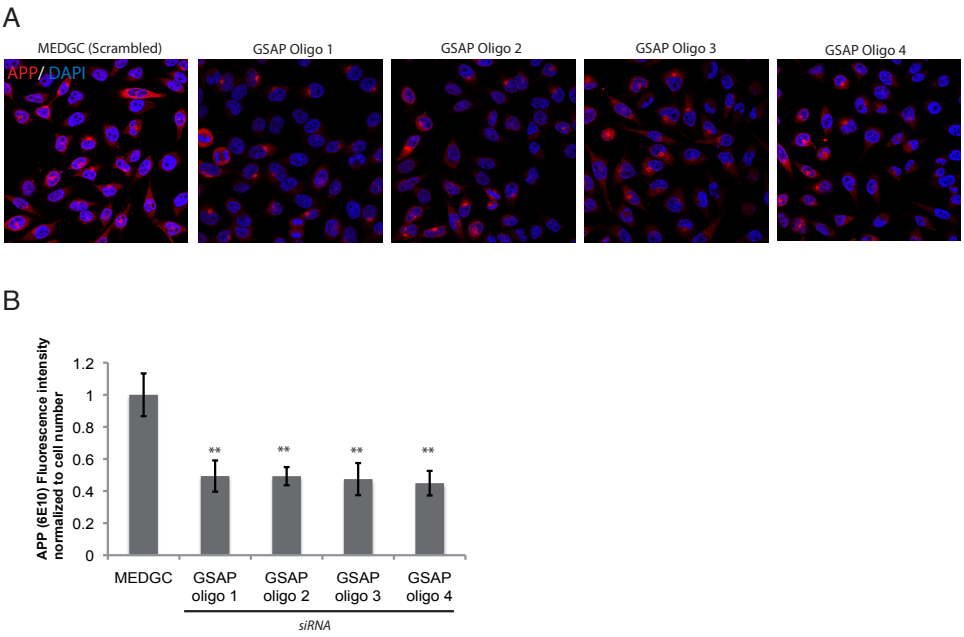

Supplementary Figure 2: A. Immunofluorescence based detection of APP levels after siRNA mediated silencing of GSAP with four different Oligos: HeLa-swAPP cells were transfected with MedGC oligos or four different siRNAs against GSAP, and the cells were fixed and assayed for APP (Red) using an APP specific antibody (6E10). Nuclei (Blue) were stained using DAPI. B. Graph showing quantification of APP levels after siRNA mediated silencing of GSAP with four different Oligos: The fluorescence signal were quantified using ImageJ software and normalized to the total cell number. * $p<0.05$, ** $p<0.01$, *** $p<0.001$.

Outlook

The main aim of this thesis was to create a cellular "roadmap" for membrane trafficking pathways that regulate Aβ metabolism, including its production and degradation. This work entailed both, the identification of trafficking regulators of Aβ as well as mechanistic characterization of the most interesting candidates. By focusing on Rab-GTPase family of proteins (60 in all) we were able to perform robust RNAi screens and validate the hit candidates in multiple cellular models. Using elegant cell and molecular biology techniques, we mechanistically characterized the top hits. By integrating our RNAi and experimental cell biology data, we established a "trafficking roadmap" for Aβ metabolism and identified novel regulators of Aβ levels. Majority of the works in this thesis were performed in cellular models and as a logical extension, one can test the relevance of these findings in animal models as well as their therapeutic potential. Below, I have discussed a few potential lines of investigation and strategies that stem out of this thesis.

We identified Rab11 as a novel positive regulator of Aβ production in cell lines and in mouse primary neurons. Rab11 silencing/dysfunction led to significant decrease in Aβ level. It will be interesting to see whether this effect of Rab11 depletion on Aβ production is also observed in mouse models of AD. General Rab11 knockout (ko) mice are embryonically lethal whereas brain-specific Rab11 ko (Nestin-cre-Rab11 ko) mice do not present overt brain abnormalities (Sobajima et al., 2014). One strategy would be to cross the brain-specific Rab11 ko mice with one of the many AD mouse models available and analyze amyloid status, neurodegeneration and behavior in these mice. According to our hypothesis, AD mice with brain-specific Rab11 deletion should have lower soluble Aβ and consequently lower amyloid plaques compared to control AD mice. This can then be complemented by behavioral studies to assess if reducing Aβ by depletion of Rab11 improved cognitive function in these mice. When designing such studies, one must consider that Rab11 has been previously implicated in the maintenance of spine morphology and function (Giorgini and Steinert, 2013). Taking this into account, an alternative strategy would be to use heterozygous brain-specific Rab11 knockout mice and cross it to AD mice. These could allow us to partly preserve the physiological functions of Rab11 and yet reduce the brain Aβ levels to a certain extent. This approach however, assumes that haploinsufficiency of Rab11 will sufficiently reduce Aβ levels while still maintaining physiological processes dependent on vesicle recycling. Nevertheless, both the above-mentioned approach can be tested to validate Rab11's role in regulating Aβ level in vivo. This is important as compared to the *in*

vitro models many more factors affect Aβ level in an organism. In vivo validation of Rab11's role in Aβ metabolism would allow us to design therapeutic strategies to lower Aβ in AD animal models.

Currently, there are no Rab11-specific inhibitors available and development of specific Rab inhibitors has been a long standing challenge. Watanabe and colleagues identified inhibitors that specifically target the geranylgeranylation of Rab proteins, a process that is critical for Rab function (Watanabe et al., 2008). However, these inhibitors are still not specific enough, though they are a step in the right direction. A promising approach to identify Rab11 specific inhibitors would be a screen for inhibitors of transferring receptor (TfR) recycling in cellular models. TfR is recycled from recycling endosomes to plasma membrane by the Rab11 pathway, very much the same way as BACE1 recycling. Using fluorescently-labeled TfR we have established TfR recycling assays that can be used for high-throughput screens for compounds that inhibit the recycling pathway. Once such an inhibitor(s) is identified, we can test if inhibiting the recycling pathway is a viable therapeutic option in AD.

In the second part of our study we identified the lysosomal pathway as a major route for intracellular Aβ degradation. Our data implicated the Rab7-regulated intracellular lysosomal pathway as an important route for Aβ degradation. We also identified PS2 as novel negative regulator of Aβ levels and showed that PS2 positively regulates Aβ degradation also by regulating the lysosomal pathway. It will be important to validate these finding in animal models of AD. We have validated our finding of PS2 depletion and increased Aβ in an AD mouse model and currently we are assessing whether this increase in Aβ and amyloid load leads to worsening of cognitive function in these mice. This would imply that boosting lysosomal function is a viable therapeutic option for AD. This leads to the question: Are there ways to boost lysosomal function in an organism? Indeed, there are inhibitors that can be used to stimulate the autophagy-lysosomal pathway. Rapamycin, a potent inhibitor of mammalian target of rapamycin (mTOR) is one such candidate. mTOR inhibition by rapamycin has been shown to activate the autophagy-lysosomal pathway. Studies on mice and other model systems have also demonstrated the beneficial effect of rapamycin on lifespan and aging (Cai and Yan, 2013; Harrison et al., 2009). However, we must thread with caution, as mTOR is the central regulator of many cellular pathways that are important for normal cellular function. Indeed, studies have shown that mTOR inhibition by rapamycin is detrimental (Lafay-Chebassier et al., 2006; Zhang et al., 2010).

Interestingly, there is an alternative approach to stimulate autophagy and lysosomal function that is non-invasive and has the potential to mitigate the pathology of protein accumulation. Our lab and others have shown that starvation/caloric restriction leads to an increase in clearance of amyloid through the autophagosome and lysosomal pathway. Our data from the PS2 study showed that starvation induced lysosomal degradation is dependent on PS2. This suggest that caloric restriction/starvation can boost lysosomal function and help clear amyloid in a PS2 dependent manner. Currently we are testing this hypothesis in PS2 knockout mice that have been crossed to ArcAD mice (Knobloch et al., 2007).

Our data on PS2 suggests that pan-inhibition of γ-secretase is a problematic approach as PS1 and PS2 have diametrically opposite roles in the regulation of Aβ levels. While PS1 is predominantly involved in the production of Aβ, PS2 is mostly involved in the clearance of Aβ. Pan inhibition by γ-secretase will also inhibit PS2-containing γ-secretase complexes and thereby interfere with Aβ degradation. Taking this into account, we can design strategies to target the γ-secretase inhibitors specfically to PS1 containing complexes. This would entail further research on understanding γ-secretase heterogeneity with respect to its subcellular localization and substrate specificity.

In line with our finding on the relevance of endo-lysosomal pathway in Aβ metabolism, recent late-onset AD (LOAD) GWAS studies have implicated the endosomal pathway in LOAD. Moreover, cholestrol metabolism and inflammation are two other major pathways that are implicated in these LOAD GWAS studies (Selkoe and Hardy, 2016). It will be interesting to study if and how these different pathways interact with each other in conferring disease risk. Cholestrol metabolism is intimately linked to endosomal processes such as endocytosis, vesicle recycling and lysosomal degradation. Inflammation is also known to regulate endosomal processes such as phagocytosis and exocytosis. Hence, an interactional network between these different pathways is plausible and could help us further unravel the molecular complexity of AD.

As mentioned before, early-onset (EOAD), which corresponds to less than 5% of the cases, is caused by autosomal dominant mutations that increase the overall production of Aβ. Both EOAD and LOAD (also called “sporadic” AD) are characterized by amyloid protein aggregates in the brain, which lead to synaptic dysfunction and neurodegeneration. Given that LOAD is not associated with strong disease-causing mutations, it likely arises from

distinct, and lesser-understood mechanisms such as amyloid clearance. My work has identified the cellular underpinnings of amyloid clearance, which could be the leading mechanism for LOAD. My work also shows the importance of lysosomal biogenesis and function in amyloid clearance and since lysosomal biogenesis is intrinsically coupled with nutrient sensing and assimilation, deliberations for therapy and prevention could be made.

Abbreviations

Aβ. *Amyloid- β*

ABC. *ATP-binding cassette*

AD. *Alzheimer's disease*

ADP. *Adenosine diphoshate*

Aph1. *Anterior pharynx-defective 1*

ApoE. *Apolipoprotein E*

APP. *Amyloid Precursor Protein*

BACE1. *β*-site amyloid precursor protein cleaving enzyme

BBB. *Blood–brain barrier*

BCB. *Blood CSF Barrier*

CAA. *Cerebral amyloid angiopathy*

CatB. *Cathepsin B*

CatD. *Cathepsin D*

CaMK II. *Calcium/calmodulin-dependent protein kinase II*

CBD. *Corticobasal degeneration*

CDK5. *Cyclin dependent protein kinase 5*

CR3. *Complement receptor 3*

CSF. *Cerebrospinal fluid*

CTF. *C-Terminal fragment*

Cx3cr1. *C-X3-C motif chemokine receptor 1*

EADI. *European Alzheimer Disease Initiative*

ECE. *Endothelin-converting enzyme 1*

EE. *Early endosome*

ELISA. *Enzyme-linked immunoabsorbant assay*

EOAD. *Early-onset Alzheimer's Disease*

ER. *Endoplasmic reticulum*

ERK. *Extracellular-signal-regulated kinase*

FAD. *Familial Alzheimer's Disease*

FTDP17. *Frontotemporal dementia with parkinsonism linked to chromosome 17*

FDA. *Food and Drug Administration*

GAPs. *GTPase activating proteins*

GEF. *GTP exchange factors*

GFP. *Green fluorescent protein*

GGA. *Golgi associated, Gamma adaptin ear containing, ARF Binding Protein 1*

GSAP. Gamma-*secretase activating*

GSK. *Glycogen synthase*

GTP. *Guanosine triphosphate Protein*

GWAS. *Genome-wide association study*

IDE. *Insulin-degrading enzyme*

ISF. *Interstitial fluid*

KO. *Knockout*

LDLR. *Low-density lipoprotein receptor*

LE. *Late endosome*

LOAD. *Late onset alzheimer's disease*

LRP1. *Lipoprotein receptor-related protein 1*

LTD. *Long-term depression*

LTP. *Long-term potentiation, Long-term potentiation*

MAP. *Mitogen-activated protein kinase*

MCI. *Mild cognitive impairment*

MMP. *Matrix-metalloproteinases*

MVB. *Multivesicular bodies*

MRI. *Magnetic resonance imaging*

NEP. *Neprilysin*

NFT. *Neurofibrillary tangle*

NMDA. *N-Methyl-D-aspartate*

p75NTR. *p75 neurotrophin*

PAR1. *Prader-Willi/Angelman region 1*

PET. *Positon emission tomography*

PHF. *Paired helical filament*

PiB. *Pittsburg compound-B*

PICALM. *Phosphatidylinositol binding clathrin assembly protein*

PKA. *Protein kinase A*

PP. *Protein phosphatases*

PS1. *Presenilin 1*

PS2. *Presenilin 2*

PSP. *Progressive supranuclear palsy*

RNAi. *RNA interference*

SAD. *Sporadic Alzheimer's disease*

SCARA. *Scavenger receptor A1*

siRNA. Small interfering RNA

SNAP25. *Synaptosomal-associated protein 25*

SNP. *Single-nucleotide polymorphism*

SorLA. *Sortilin related receptor 1*

Tg. *Transgenic*

TLR. *Toll-like receptor*

TREM2. *Triggering receptor expressed on myeloid cells 2*

UDP. *Uridine diphosphate*

VPS. *Vacuolar protein sorting-associated protein*

References

Acx, H., Serneels, L., Radaelli, E., Muyldermans, S., Vincke, C., Pepermans, E., Muller, U., Chavez-Gutierrez, L., and De Strooper, B. (2017). Inactivation of gamma-secretases leads to accumulation of substrates and non-Alzheimer neurodegeneration. EMBO Mol Med *9*, 1088-1099.

Albert, M.S., DeKosky, S.T., Dickson, D., Dubois, B., Feldman, H.H., Fox, N.C., Gamst, A., Holtzman, D.M., Jagust, W.J., Petersen, R.C.*, et al.* (2011). The diagnosis of mild cognitive impairment due to Alzheimer's disease: recommendations from the National Institute on Aging-Alzheimer's Association workgroups on diagnostic guidelines for Alzheimer's disease. Alzheimers Dement *7*, 270-279.

Alonso Adel, C., Mederlyova, A., Novak, M., Grundke-Iqbal, I., and Iqbal, K. (2004). Promotion of hyperphosphorylation by frontotemporal dementia tau mutations. J Biol Chem *279*, 34873-34881.

Alzheimer, A., Stelzmann, R.A., Schnitzlein, H.N., and Murtagh, F.R. (1995). An English translation of Alzheimer's 1907 paper, "Uber eine eigenartige Erkankung der Hirnrinde". Clin Anat *8*, 429-431.

Andersen, O.M., Reiche, J., Schmidt, V., Gotthardt, M., Spoelgen, R., Behlke, J., von Arnim, C.A., Breiderhoff, T., Jansen, P., Wu, X.*, et al.* (2005). Neuronal sorting protein-related receptor sorLA/LR11 regulates processing of the amyloid precursor protein. Proc Natl Acad Sci U S A *102*, 13461-13466.

Avila, J., Simon, D., Diaz-Hernandez, M., Pintor, J., and Hernandez, F. (2014). Sources of extracellular tau and its signaling. J Alzheimers Dis *40 Suppl 1*, S7-S15.

Baki, L., Marambaud, P., Efthimiopoulos, S., Georgakopoulos, A., Wen, P., Cui, W., Shioi, J., Koo, E., Ozawa, M., Friedrich, V.L., Jr.*, et al.* (2001). Presenilin-1 binds cytoplasmic epithelial cadherin, inhibits cadherin/p120 association, and regulates stability and function of the cadherin/catenin adhesion complex. Proc Natl Acad Sci U S A *98*, 2381-2386.

Bali, J., Gheinani, A.H., Zurbriggen, S., and Rajendran, L. (2012). Role of genes linked to sporadic Alzheimer's disease risk in the production of beta-amyloid peptides. Proc Natl Acad Sci U S A *109*, 15307-15311.

Bateman, R.J., Xiong, C., Benzinger, T.L., Fagan, A.M., Goate, A., Fox, N.C., Marcus, D.S., Cairns, N.J., Xie, X., Blazey, T.M.*, et al.* (2012). Clinical and biomarker changes in dominantly inherited Alzheimer's disease. N Engl J Med *367*, 795-804.

Bayer, T.A., Cappai, R., Masters, C.L., Beyreuther, K., and Multhaup, G. (1999). It all sticks together--the APP-related family of proteins and Alzheimer's disease. Mol Psychiatry *4*, 524-528.

Bednarski, E., and Lynch, G. (1996). Cytosolic proteolysis of tau by cathepsin D in hippocampus following suppression of cathepsins B and L. J Neurochem *67*, 1846-1855.

Bell, R.D., Sagare, A.P., Friedman, A.E., Bedi, G.S., Holtzman, D.M., Deane, R., and Zlokovic, B.V. (2007). Transport pathways for clearance of human Alzheimer's amyloid beta-peptide and apolipoproteins E and J in the mouse central nervous system. J Cereb Blood Flow Metab *27*, 909-918.

Ben Halima, S., Mishra, S., Raja, K.M.P., Willem, M., Baici, A., Simons, K., Brustle, O., Koch, P., Haass, C., Caflisch, A.*, et al.* (2016). Specific Inhibition of beta-Secretase Processing of the Alzheimer Disease Amyloid Precursor Protein. Cell Rep *14*, 2127-2141.

Benilova, I., Gallardo, R., Ungureanu, A.A., Castillo Cano, V., Snellinx, A., Ramakers, M., Bartic, C., Rousseau, F., Schymkowitz, J., and De Strooper, B. (2014). The Alzheimer disease protective mutation A2T modulates kinetic and thermodynamic properties of amyloid-beta (Abeta) aggregation. J Biol Chem *289*, 30977-30989.

Bentahir, M., Nyabi, O., Verhamme, J., Tolia, A., Horre, K., Wiltfang, J., Esselmann, H., and De Strooper, B. (2006). Presenilin clinical mutations can affect gamma-secretase activity by different mechanisms. J Neurochem *96*, 732-742.

Blennow, K. (2004). CSF biomarkers for mild cognitive impairment. J Intern Med *256*, 224-234.

Blennow, K., Hampel, H., Weiner, M., and Zetterberg, H. (2010). Cerebrospinal fluid and plasma biomarkers in Alzheimer disease. Nat Rev Neurol *6*, 131-144.

Braak, H., and Braak, E. (1991). Neuropathological stageing of Alzheimer-related changes. Acta Neuropathol *82*, 239-259.

Brinkmalm, A., Brinkmalm, G., Honer, W.G., Frolich, L., Hausner, L., Minthon, L., Hansson, O., Wallin, A., Zetterberg, H., Blennow, K.*, et al.* (2014). SNAP-25 is a promising novel cerebrospinal fluid biomarker for synapse degeneration in Alzheimer's disease. Mol Neurodegener *9*, 53.

Caceres, A., Potrebic, S., and Kosik, K.S. (1991). The effect of tau antisense oligonucleotides on neurite formation of cultured cerebellar macroneurons. J Neurosci *11*, 1515-1523.

Cai, Z., and Yan, L.J. (2013). Rapamycin, Autophagy, and Alzheimer's Disease. J Biochem Pharmacol Res *1*, 84-90.

Citron, M., Oltersdorf, T., Haass, C., McConlogue, L., Hung, A.Y., Seubert, P., Vigo-Pelfrey, C., Lieberburg, I., and Selkoe, D.J. (1992). Mutation of the beta-amyloid precursor protein in familial Alzheimer's disease increases beta-protein production. Nature *360*, 672-674.

Coppola, G., Chinnathambi, S., Lee, J.J., Dombroski, B.A., Baker, M.C., Soto-Ortolaza, A.I., Lee, S.E., Klein, E., Huang, A.Y., Sears, R.*, et al.* (2012). Evidence for a role of the rare p.A152T variant in MAPT in increasing the risk for FTD-spectrum and Alzheimer's diseases. Hum Mol Genet *21*, 3500-3512.

Crehan, H., Hardy, J., and Pocock, J. (2013). Blockage of CR1 prevents activation of rodent microglia. Neurobiol Dis *54*, 139-149.

Das, U., Scott, D.A., Ganguly, A., Koo, E.H., Tang, Y., and Roy, S. (2013). Activity-induced convergence of APP and BACE-1 in acidic microdomains via an endocytosis-dependent pathway. Neuron *79*, 447-460.

Das, U., Wang, L., Ganguly, A., Saikia, J.M., Wagner, S.L., Koo, E.H., and Roy, S. (2016). Visualizing APP and BACE-1 approximation in neurons yields insight into the amyloidogenic pathway. Nat Neurosci *19*, 55-64.

Daugherty, B.L., and Green, S.A. (2001). Endosomal sorting of amyloid precursor protein-P-selectin chimeras influences secretase processing. Traffic *2*, 908-916.

David, D.C., Layfield, R., Serpell, L., Narain, Y., Goedert, M., and Spillantini, M.G. (2002). Proteasomal degradation of tau protein. J Neurochem *83*, 176-185.

Dawson, H.N., Ferreira, A., Eyster, M.V., Ghoshal, N., Binder, L.I., and Vitek, M.P. (2001). Inhibition of neuronal maturation in primary hippocampal neurons from tau deficient mice. J Cell Sci *114*, 1179-1187.

De Felice, F.G., Velasco, P.T., Lambert, M.P., Viola, K., Fernandez, S.J., Ferreira, S.T., and Klein, W.L. (2007). Abeta oligomers induce neuronal oxidative stress through an N-methyl-D-aspartate receptor-dependent mechanism that is blocked by the Alzheimer drug memantine. J Biol Chem *282*, 11590-11601.

De Strooper, B. (2007). Loss-of-function presenilin mutations in Alzheimer disease. Talking Point on the role of presenilin mutations in Alzheimer disease. EMBO Rep *8*, 141-146.

de Wilde, M.C., Overk, C.R., Sijben, J.W., and Masliah, E. (2016). Meta-analysis of synaptic pathology in Alzheimer's disease reveals selective molecular vesicular machinery vulnerability. Alzheimers Dement *12*, 633-644.

Deane, R., Wu, Z., Sagare, A., Davis, J., Du Yan, S., Hamm, K., Xu, F., Parisi, M., LaRue, B., Hu, H.W.*, et al.* (2004). LRP/amyloid beta-peptide interaction mediates differential brain efflux of Abeta isoforms. Neuron *43*, 333-344.

Dejaegere, T., Serneels, L., Schafer, M.K., Van Biervliet, J., Horre, K., Depboylu, C., Alvarez-Fischer, D., Herreman, A., Willem, M., Haass, C.*, et al.* (2008). Deficiency of Aph1B/C-gamma-secretase disturbs Nrg1 cleavage and sensorimotor gating that can be reversed with antipsychotic treatment. Proc Natl Acad Sci U S A *105*, 9775-9780.

Dickey, C.A., Kamal, A., Lundgren, K., Klosak, N., Bailey, R.M., Dunmore, J., Ash, P., Shoraka, S., Zlatkovic, J., Eckman, C.B., *et al.* (2007). The high-affinity HSP90-CHIP complex recognizes and selectively degrades phosphorylated tau client proteins. J Clin Invest *117*, 648-658.

Ebneth, A., Godemann, R., Stamer, K., Illenberger, S., Trinczek, B., and Mandelkow, E. (1998). Overexpression of tau protein inhibits kinesin-dependent trafficking of vesicles, mitochondria, and endoplasmic reticulum: implications for Alzheimer's disease. J Cell Biol *143*, 777-794.

Eckman, E.A., and Eckman, C.B. (2005). Abeta-degrading enzymes: modulators of Alzheimer's disease pathogenesis and targets for therapeutic intervention. Biochem Soc Trans *33*, 1101-1105.

Eckman, E.A., Watson, M., Marlow, L., Sambamurti, K., and Eckman, C.B. (2003). Alzheimer's disease beta-amyloid peptide is increased in mice deficient in endothelin-converting enzyme. J Biol Chem *278*, 2081-2084.

Edbauer, D., Winkler, E., Regula, J.T., Pesold, B., Steiner, H., and Haass, C. (2003). Reconstitution of gamma-secretase activity. Nat Cell Biol *5*, 486-488.

Ehehalt, R., Keller, P., Haass, C., Thiele, C., and Simons, K. (2003). Amyloidogenic processing of the Alzheimer beta-amyloid precursor protein depends on lipid rafts. J Cell Biol *160*, 113-123.

Elliott, M.R., Chekeni, F.B., Trampont, P.C., Lazarowski, E.R., Kadl, A., Walk, S.F., Park, D., Woodson, R.I., Ostankovich, M., Sharma, P., *et al.* (2009). Nucleotides released by apoptotic cells act as a find-me signal to promote phagocytic clearance. Nature *461*, 282-286.

Falkevall, A., Alikhani, N., Bhushan, S., Pavlov, P.F., Busch, K., Johnson, K.A., Eneqvist, T., Tjernberg, L., Ankarcrona, M., and Glaser, E. (2006). Degradation of the amyloid beta-protein by the novel mitochondrial peptidasome, PreP. J Biol Chem *281*, 29096-29104.

Farris, W., Mansourian, S., Chang, Y., Lindsley, L., Eckman, E.A., Frosch, M.P., Eckman, C.B., Tanzi, R.E., Selkoe, D.J., and Guenette, S. (2003). Insulin-degrading enzyme regulates

the levels of insulin, amyloid beta-protein, and the beta-amyloid precursor protein intracellular domain in vivo. Proc Natl Acad Sci U S A *100*, 4162-4167.

Farris, W., Schutz, S.G., Cirrito, J.R., Shankar, G.M., Sun, X., George, A., Leissring, M.A., Walsh, D.M., Qiu, W.Q., Holtzman, D.M*., et al.* (2007). Loss of neprilysin function promotes amyloid plaque formation and causes cerebral amyloid angiopathy. Am J Pathol *171*, 241-251.

Fitz, N.F., Cronican, A.A., Saleem, M., Fauq, A.H., Chapman, R., Lefterov, I., and Koldamova, R. (2012). Abca1 deficiency affects Alzheimer's disease-like phenotype in human ApoE4 but not in ApoE3-targeted replacement mice. J Neurosci *32*, 13125-13136.

Frenkel, D., Wilkinson, K., Zhao, L., Hickman, S.E., Means, T.K., Puckett, L., Farfara, D., Kingery, N.D., Weiner, H.L., and El Khoury, J. (2013). Scara1 deficiency impairs clearance of soluble amyloid-beta by mononuclear phagocytes and accelerates Alzheimer's-like disease progression. Nat Commun *4*, 2030.

Fukumoto, H., Rosene, D.L., Moss, M.B., Raju, S., Hyman, B.T., and Irizarry, M.C. (2004). Beta-secretase activity increases with aging in human, monkey, and mouse brain. Am J Pathol *164*, 719-725.

Giorgini, F., and Steinert, J.R. (2013). Rab11 as a modulator of synaptic transmission. Commun Integr Biol *6*, e26807.

Gong, C.X., Singh, T.J., Grundke-Iqbal, I., and Iqbal, K. (1993). Phosphoprotein phosphatase activities in Alzheimer disease brain. J Neurochem *61*, 921-927.

Griciuc, A., Serrano-Pozo, A., Parrado, A.R., Lesinski, A.N., Asselin, C.N., Mullin, K., Hooli, B., Choi, S.H., Hyman, B.T., and Tanzi, R.E. (2013). Alzheimer's disease risk gene CD33 inhibits microglial uptake of amyloid beta. Neuron *78*, 631-643.

Guerreiro, R., Wojtas, A., Bras, J., Carrasquillo, M., Rogaeva, E., Majounie, E., Cruchaga, C., Sassi, C., Kauwe, J.S., Younkin, S*., et al.* (2013). TREM2 variants in Alzheimer's disease. N Engl J Med *368*, 117-127.

Gustke, N., Trinczek, B., Biernat, J., Mandelkow, E.M., and Mandelkow, E. (1994). Domains of tau protein and interactions with microtubules. Biochemistry *33*, 9511-9522.

Haass, C., Hung, A.Y., Selkoe, D.J., and Teplow, D.B. (1994). Mutations associated with a locus for familial Alzheimer's disease result in alternative processing of amyloid beta-protein precursor. J Biol Chem *269*, 17741-17748.

Hamano, T., Gendron, T.F., Ko, L.W., and Yen, S.H. (2009). Concentration-dependent effects of proteasomal inhibition on tau processing in a cellular model of tauopathy. Int J Clin Exp Pathol *2*, 561-573.

Hampel, H., Blennow, K., Shaw, L.M., Hoessler, Y.C., Zetterberg, H., and Trojanowski, J.Q. (2010). Total and phosphorylated tau protein as biological markers of Alzheimer's disease. Exp Gerontol *45*, 30-40.

Hanger, D.P., Anderton, B.H., and Noble, W. (2009a). Tau phosphorylation: the therapeutic challenge for neurodegenerative disease. Trends Mol Med *15*, 112-119.

Hanger, D.P., Seereeram, A., and Noble, W. (2009b). Mediators of tau phosphorylation in the pathogenesis of Alzheimer's disease. Expert Rev Neurother *9*, 1647-1666.

Harrison, D.E., Strong, R., Sharp, Z.D., Nelson, J.F., Astle, C.M., Flurkey, K., Nadon, N.L., Wilkinson, J.E., Frenkel, K., Carter, C.S.*, et al.* (2009). Rapamycin fed late in life extends lifespan in genetically heterogeneous mice. Nature *460*, 392-395.

He, X., Li, F., Chang, W.P., and Tang, J. (2005). GGA proteins mediate the recycling pathway of memapsin 2 (BACE). J Biol Chem *280*, 11696-11703.

Hebert, L.E., Scherr, P.A., Bienias, J.L., Bennett, D.A., and Evans, D.A. (2003). Alzheimer disease in the US population: prevalence estimates using the 2000 census. Arch Neurol *60*, 1119-1122.

Hebert, S.S., Serneels, L., Dejaegere, T., Horre, K., Dabrowski, M., Baert, V., Annaert, W., Hartmann, D., and De Strooper, B. (2004). Coordinated and widespread expression of

gamma-secretase in vivo: evidence for size and molecular heterogeneity. Neurobiol Dis *17*, 260-272.

Hemming, M.L., Elias, J.E., Gygi, S.P., and Selkoe, D.J. (2009). Identification of beta-secretase (BACE1) substrates using quantitative proteomics. PLoS One *4*, e8477.

Hickman, S.E., Allison, E.K., and El Khoury, J. (2008). Microglial dysfunction and defective beta-amyloid clearance pathways in aging Alzheimer's disease mice. J Neurosci *28*, 8354-8360.

Hoover, B.R., Reed, M.N., Su, J., Penrod, R.D., Kotilinek, L.A., Grant, M.K., Pitstick, R., Carlson, G.A., Lanier, L.M., Yuan, L.L.*, et al.* (2010). Tau mislocalization to dendritic spines mediates synaptic dysfunction independently of neurodegeneration. Neuron *68*, 1067-1081.

Hung, S.Y., and Fu, W.M. (2017). Drug candidates in clinical trials for Alzheimer's disease. J Biomed Sci *24*, 47.

Hutton, M., Lendon, C.L., Rizzu, P., Baker, M., Froelich, S., Houlden, H., Pickering-Brown, S., Chakraverty, S., Isaacs, A., Grover, A.*, et al.* (1998). Association of missense and 5'-splice-site mutations in tau with the inherited dementia FTDP-17. Nature *393*, 702-705.

Iliff, J.J., Wang, M., Liao, Y., Plogg, B.A., Peng, W., Gundersen, G.A., Benveniste, H., Vates, G.E., Deane, R., Goldman, S.A.*, et al.* (2012). A paravascular pathway facilitates CSF flow through the brain parenchyma and the clearance of interstitial solutes, including amyloid beta. Sci Transl Med *4*, 147ra111.

Ito, S., Ueno, T., Ohtsuki, S., and Terasaki, T. (2010). Lack of brain-to-blood efflux transport activity of low-density lipoprotein receptor-related protein-1 (LRP-1) for amyloid-beta peptide(1-40) in mouse: involvement of an LRP-1-independent pathway. J Neurochem *113*, 1356-1363.

Jonsson, T., Atwal, J.K., Steinberg, S., Snaedal, J., Jonsson, P.V., Bjornsson, S., Stefansson, H., Sulem, P., Gudbjartsson, D., Maloney, J.*, et al.* (2012). A mutation in APP protects against Alzheimer's disease and age-related cognitive decline. Nature *488*, 96-99.

Jonsson, T., Stefansson, H., Steinberg, S., Jonsdottir, I., Jonsson, P.V., Snaedal, J., Bjornsson, S., Huttenlocher, J., Levey, A.I., Lah, J.J., *et al.* (2013). Variant of TREM2 associated with the risk of Alzheimer's disease. N Engl J Med *368*, 107-116.

Kaether, C., Schmitt, S., Willem, M., and Haass, C. (2006). Amyloid precursor protein and Notch intracellular domains are generated after transport of their precursors to the cell surface. Traffic *7*, 408-415.

Kanatsu, K., Morohashi, Y., Suzuki, M., Kuroda, H., Watanabe, T., Tomita, T., and Iwatsubo, T. (2014). Decreased CALM expression reduces Abeta42 to total Abeta ratio through clathrin-mediated endocytosis of gamma-secretase. Nat Commun *5*, 3386.

Kester, M.I., Teunissen, C.E., Crimmins, D.L., Herries, E.M., Ladenson, J.H., Scheltens, P., van der Flier, W.M., Morris, J.C., Holtzman, D.M., and Fagan, A.M. (2015). Neurogranin as a Cerebrospinal Fluid Biomarker for Synaptic Loss in Symptomatic Alzheimer Disease. JAMA Neurol *72*, 1275-1280.

Kim, S.M., Mun, B.R., Lee, S.J., Joh, Y., Lee, H.Y., Ji, K.Y., Choi, H.R., Lee, E.H., Kim, E.M., Jang, J.H., *et al.* (2017). TREM2 promotes Abeta phagocytosis by upregulating C/EBPalpha-dependent CD36 expression in microglia. Sci Rep *7*, 11118.

Kinoshita, A., Fukumoto, H., Shah, T., Whelan, C.M., Irizarry, M.C., and Hyman, B.T. (2003). Demonstration by FRET of BACE interaction with the amyloid precursor protein at the cell surface and in early endosomes. J Cell Sci *116*, 3339-3346.

Klunk, W.E., Engler, H., Nordberg, A., Wang, Y., Blomqvist, G., Holt, D.P., Bergstrom, M., Savitcheva, I., Huang, G.F., Estrada, S., *et al.* (2004). Imaging brain amyloid in Alzheimer's disease with Pittsburgh Compound-B. Ann Neurol *55*, 306-319.

Knobloch, M., Konietzko, U., Krebs, D.C., and Nitsch, R.M. (2007). Intracellular Abeta and cognitive deficits precede beta-amyloid deposition in transgenic arcAbeta mice. Neurobiol Aging *28*, 1297-1306.

Koo, E.H., and Squazzo, S.L. (1994). Evidence that production and release of amyloid beta-protein involves the endocytic pathway. J Biol Chem *269*, 17386-17389.

Kouri, N., Carlomagno, Y., Baker, M., Liesinger, A.M., Caselli, R.J., Wszolek, Z.K., Petrucelli, L., Boeve, B.F., Parisi, J.E., Josephs, K.A.*, et al.* (2014). Novel mutation in MAPT exon 13 (p.N410H) causes corticobasal degeneration. Acta Neuropathol *127*, 271-282.

Kress, B.T., Iliff, J.J., Xia, M., Wang, M., Wei, H.S., Zeppenfeld, D., Xie, L., Kang, H., Xu, Q., Liew, J.A.*, et al.* (2014). Impairment of paravascular clearance pathways in the aging brain. Ann Neurol *76*, 845-861.

Kuhn, P.H., Koroniak, K., Hogl, S., Colombo, A., Zeitschel, U., Willem, M., Volbracht, C., Schepers, U., Imhof, A., Hoffmeister, A.*, et al.* (2012). Secretome protein enrichment identifies physiological BACE1 protease substrates in neurons. EMBO J *31*, 3157-3168.

Kvartsberg, H., Duits, F.H., Ingelsson, M., Andreasen, N., Ohrfelt, A., Andersson, K., Brinkmalm, G., Lannfelt, L., Minthon, L., Hansson, O.*, et al.* (2015). Cerebrospinal fluid levels of the synaptic protein neurogranin correlates with cognitive decline in prodromal Alzheimer's disease. Alzheimers Dement *11*, 1180-1190.

Lafay-Chebassier, C., Perault-Pochat, M.C., Page, G., Rioux Bilan, A., Damjanac, M., Pain, S., Houeto, J.L., Gil, R., and Hugon, J. (2006). The immunosuppressant rapamycin exacerbates neurotoxicity of Abeta peptide. J Neurosci Res *84*, 1323-1334.

Lai, A.Y., and McLaurin, J. (2012). Clearance of amyloid-beta peptides by microglia and macrophages: the issue of what, when and where. Future Neurol *7*, 165-176.

Lambert, J.C., Heath, S., Even, G., Campion, D., Sleegers, K., Hiltunen, M., Combarros, O., Zelenika, D., Bullido, M.J., Tavernier, B.*, et al.* (2009). Genome-wide association study identifies variants at CLU and CR1 associated with Alzheimer's disease. Nat Genet *41*, 1094-1099.

Lambert, J.C., Ibrahim-Verbaas, C.A., Harold, D., Naj, A.C., Sims, R., Bellenguez, C., DeStafano, A.L., Bis, J.C., Beecham, G.W., Grenier-Boley, B.*, et al.* (2013). Meta-analysis of 74,046 individuals identifies 11 new susceptibility loci for Alzheimer's disease. Nat Genet *45*, 1452-1458.

Lausted, C., Lee, I., Zhou, Y., Qin, S., Sung, J., Price, N.D., Hood, L., and Wang, K. (2014). Systems approach to neurodegenerative disease biomarker discovery. Annu Rev Pharmacol Toxicol *54*, 457-481.

Lee, V.M., Goedert, M., and Trojanowski, J.Q. (2001). Neurodegenerative tauopathies. Annu Rev Neurosci *24*, 1121-1159.

Leissring, M.A. (2008). The AbetaCs of Abeta-cleaving proteases. J Biol Chem *283*, 29645-29649.

Leissring, M.A. (2016). Abeta-Degrading Proteases: Therapeutic Potential in Alzheimer Disease. CNS Drugs *30*, 667-675.

Leissring, M.A., Farris, W., Chang, A.Y., Walsh, D.M., Wu, X., Sun, X., Frosch, M.P., and Selkoe, D.J. (2003). Enhanced proteolysis of beta-amyloid in APP transgenic mice prevents plaque formation, secondary pathology, and premature death. Neuron *40*, 1087-1093.

Lichtenthaler, S.F. (2011). alpha-secretase in Alzheimer's disease: molecular identity, regulation and therapeutic potential. J Neurochem *116*, 10-21.

Liu, S., Liu, Y., Hao, W., Wolf, L., Kiliaan, A.J., Penke, B., Rube, C.E., Walter, J., Heneka, M.T., Hartmann, T.*, et al.* (2012). TLR2 is a primary receptor for Alzheimer's amyloid beta peptide to trigger neuroinflammatory activation. J Immunol *188*, 1098-1107.

Louveau, A., Smirnov, I., Keyes, T.J., Eccles, J.D., Rouhani, S.J., Peske, J.D., Derecki, N.C., Castle, D., Mandell, J.W., Lee, K.S.*, et al.* (2015). Structural and functional features of central nervous system lymphatic vessels. Nature *523*, 337-341.

Luo, Y., Bolon, B., Kahn, S., Bennett, B.D., Babu-Khan, S., Denis, P., Fan, W., Kha, H., Zhang, J., Gong, Y.*, et al.* (2001). Mice deficient in BACE1, the Alzheimer's beta-secretase, have normal phenotype and abolished beta-amyloid generation. Nat Neurosci *4*, 231-232.

Maloney, J.A., Bainbridge, T., Gustafson, A., Zhang, S., Kyauk, R., Steiner, P., van der Brug, M., Liu, Y., Ernst, J.A., Watts, R.J.*, et al.* (2014). Molecular mechanisms of Alzheimer

disease protection by the A673T allele of amyloid precursor protein. J Biol Chem *289*, 30990-31000.

Marksteiner, J., Hinterhuber, H., and Humpel, C. (2007). Cerebrospinal fluid biomarkers for diagnosis of Alzheimer's disease: beta-amyloid(1-42), tau, phospho-tau-181 and total protein. Drugs Today (Barc) *43*, 423-431.

McGeer, P.L., Akiyama, H., Itagaki, S., and McGeer, E.G. (1989). Immune system response in Alzheimer's disease. Can J Neurol Sci *16*, 516-527.

Mecozzi, V.J., Berman, D.E., Simoes, S., Vetanovetz, C., Awal, M.R., Patel, V.M., Schneider, R.T., Petsko, G.A., Ringe, D., and Small, S.A. (2014). Pharmacological chaperones stabilize retromer to limit APP processing. Nat Chem Biol *10*, 443-449.

Meilandt, W.J., Cisse, M., Ho, K., Wu, T., Esposito, L.A., Scearce-Levie, K., Cheng, I.H., Yu, G.Q., and Mucke, L. (2009). Neprilysin overexpression inhibits plaque formation but fails to reduce pathogenic Abeta oligomers and associated cognitive deficits in human amyloid precursor protein transgenic mice. J Neurosci *29*, 1977-1986.

Mohr, S., Bakal, C., and Perrimon, N. (2010). Genomic screening with RNAi: results and challenges. Annu Rev Biochem *79*, 37-64.

Mueller-Steiner, S., Zhou, Y., Arai, H., Roberson, E.D., Sun, B., Chen, J., Wang, X., Yu, G., Esposito, L., Mucke, L.*, et al.* (2006). Antiamyloidogenic and neuroprotective functions of cathepsin B: implications for Alzheimer's disease. Neuron *51*, 703-714.

Mukrasch, M.D., Bibow, S., Korukottu, J., Jeganathan, S., Biernat, J., Griesinger, C., Mandelkow, E., and Zweckstetter, M. (2009). Structural polymorphism of 441-residue tau at single residue resolution. PLoS Biol *7*, e34.

Mullan, M., Crawford, F., Axelman, K., Houlden, H., Lilius, L., Winblad, B., and Lannfelt, L. (1992). A pathogenic mutation for probable Alzheimer's disease in the APP gene at the N-terminus of beta-amyloid. Nat Genet *1*, 345-347.

Muller, U.C., Deller, T., and Korte, M. (2017). Not just amyloid: physiological functions of the amyloid precursor protein family. Nat Rev Neurosci *18*, 281-298.

Naj, A.C., Schellenberg, G.D., and Alzheimer's Disease Genetics, C. (2017). Genomic variants, genes, and pathways of Alzheimer's disease: An overview. Am J Med Genet B Neuropsychiatr Genet *174*, 5-26.

Neve, R.L., Harris, P., Kosik, K.S., Kurnit, D.M., and Donlon, T.A. (1986). Identification of cDNA clones for the human microtubule-associated protein tau and chromosomal localization of the genes for tau and microtubule-associated protein 2. Brain Res *387*, 271-280.

Nilsson, P., Loganathan, K., Sekiguchi, M., Matsuba, Y., Hui, K., Tsubuki, S., Tanaka, M., Iwata, N., Saito, T., and Saido, T.C. (2013). Abeta secretion and plaque formation depend on autophagy. Cell Rep *5*, 61-69.

Nilsson, P., and Saido, T.C. (2014). Dual roles for autophagy: degradation and secretion of Alzheimer's disease Abeta peptide. Bioessays *36*, 570-578.

Nimmerjahn, A., Kirchhoff, F., and Helmchen, F. (2005). Resting microglial cells are highly dynamic surveillants of brain parenchyma in vivo. Science *308*, 1314-1318.

Ohno, M., Sametsky, E.A., Younkin, L.H., Oakley, H., Younkin, S.G., Citron, M., Vassar, R., and Disterhoft, J.F. (2004). BACE1 deficiency rescues memory deficits and cholinergic dysfunction in a mouse model of Alzheimer's disease. Neuron *41*, 27-33.

Pant, S., Sharma, M., Patel, K., Caplan, S., Carr, C.M., and Grant, B.D. (2009). AMPH-1/Amphiphysin/Bin1 functions with RME-1/Ehd1 in endocytic recycling. Nat Cell Biol *11*, 1399-1410.

Paolicelli, R.C., Bolasco, G., Pagani, F., Maggi, L., Scianni, M., Panzanelli, P., Giustetto, M., Ferreira, T.A., Guiducci, E., Dumas, L.*, et al.* (2011). Synaptic pruning by microglia is necessary for normal brain development. Science *333*, 1456-1458.

Paolicelli, R.C., Jawaid, A., Henstridge, C.M., Valeri, A., Merlini, M., Robinson, J.L., Lee, E.B., Rose, J., Appel, S., Lee, V.M.*, et al.* (2017). TDP-43 Depletion in Microglia Promotes Amyloid Clearance but Also Induces Synapse Loss. Neuron *95*, 297-308 e296.

Paresce, D.M., Ghosh, R.N., and Maxfield, F.R. (1996). Microglial cells internalize aggregates of the Alzheimer's disease amyloid beta-protein via a scavenger receptor. Neuron *17*, 553-565.

Pascale, C.L., Miller, M.C., Chiu, C., Boylan, M., Caralopoulos, I.N., Gonzalez, L., Johanson, C.E., and Silverberg, G.D. (2011). Amyloid-beta transporter expression at the blood-CSF barrier is age-dependent. Fluids Barriers CNS *8*, 21.

Pericak-Vance, M.A., Bebout, J.L., Gaskell, P.C., Jr., Yamaoka, L.H., Hung, W.Y., Alberts, M.J., Walker, A.P., Bartlett, R.J., Haynes, C.A., Welsh, K.A.*, et al.* (1991). Linkage studies in familial Alzheimer disease: evidence for chromosome 19 linkage. Am J Hum Genet *48*, 1034-1050.

Pfeil, A.M., Kressig, R.W., and Szucs, T.D. (2012). Alzheimer's dementia: budget impact and cost-utility analysis of a combination treatment of a cholinesterase inhibitor and memantine in Switzerland. Swiss Med Wkly *142*, w13676.

Prince, M., Ali, G.C., Guerchet, M., Prina, A.M., Albanese, E., and Wu, Y.T. (2016). Recent global trends in the prevalence and incidence of dementia, and survival with dementia. Alzheimers Res Ther *8*, 23.

Probst, A., Gotz, J., Wiederhold, K.H., Tolnay, M., Mistl, C., Jaton, A.L., Hong, M., Ishihara, T., Lee, V.M., Trojanowski, J.Q.*, et al.* (2000). Axonopathy and amyotrophy in mice transgenic for human four-repeat tau protein. Acta Neuropathol *99*, 469-481.

Prudencio, M., and Lehmann, M.J. (2009). Illuminating the host - how RNAi screens shed light on host-pathogen interactions. Biotechnol J *4*, 826-837.

Rajendran, L., Honsho, M., Zahn, T.R., Keller, P., Geiger, K.D., Verkade, P., and Simons, K. (2006). Alzheimer's disease beta-amyloid peptides are released in association with exosomes. Proc Natl Acad Sci U S A *103*, 11172-11177.

Rajendran, L., Schneider, A., Schlechtingen, G., Weidlich, S., Ries, J., Braxmeier, T., Schwille, P., Schulz, J.B., Schroeder, C., Simons, M.*, et al.* (2008). Efficient inhibition of the Alzheimer's disease beta-secretase by membrane targeting. Science *320*, 520-523.

Refolo, L.M., Sambamurti, K., Efthimiopoulos, S., Pappolla, M.A., and Robakis, N.K. (1995). Evidence that secretase cleavage of cell surface Alzheimer amyloid precursor occurs after normal endocytic internalization. J Neurosci Res *40*, 694-706.

Rogaeva, E., Meng, Y., Lee, J.H., Gu, Y., Kawarai, T., Zou, F., Katayama, T., Baldwin, C.T., Cheng, R., Hasegawa, H.*, et al.* (2007). The neuronal sortilin-related receptor SORL1 is genetically associated with Alzheimer disease. Nat Genet *39*, 168-177.

Rogers, S.L., and Friedman, R.B. (2008). The underlying mechanisms of semantic memory loss in Alzheimer's disease and semantic dementia. Neuropsychologia *46*, 12-21.

Rosseels, J., Van den Brande, J., Violet, M., Jacobs, D., Grognet, P., Lopez, J., Huvent, I., Caldara, M., Swinnen, E., Papegaey, A.*, et al.* (2015). Tau monoclonal antibody generation based on humanized yeast models: impact on Tau oligomerization and diagnostics. J Biol Chem *290*, 4059-4074.

Rovelet-Lecrux, A., Hannequin, D., Raux, G., Le Meur, N., Laquerriere, A., Vital, A., Dumanchin, C., Feuillette, S., Brice, A., Vercelletto, M.*, et al.* (2006). APP locus duplication causes autosomal dominant early-onset Alzheimer disease with cerebral amyloid angiopathy. Nat Genet *38*, 24-26.

Runz, H., Rietdorf, J., Tomic, I., de Bernard, M., Beyreuther, K., Pepperkok, R., and Hartmann, T. (2002). Inhibition of intracellular cholesterol transport alters presenilin localization and amyloid precursor protein processing in neuronal cells. J Neurosci *22*, 1679-1689.

Saido, T., and Leissring, M.A. (2012). Proteolytic degradation of amyloid beta-protein. Cold Spring Harb Perspect Med *2*, a006379.

Sannerud, R., Declerck, I., Peric, A., Raemaekers, T., Menendez, G., Zhou, L., Veerle, B., Coen, K., Munck, S., De Strooper, B.*, et al.* (2011). ADP ribosylation factor 6 (ARF6)

controls amyloid precursor protein (APP) processing by mediating the endosomal sorting of BACE1. Proc Natl Acad Sci U S A *108*, E559-568.

Schafer, D.P., Lehrman, E.K., Kautzman, A.G., Koyama, R., Mardinly, A.R., Yamasaki, R., Ransohoff, R.M., Greenberg, M.E., Barres, B.A., and Stevens, B. (2012). Microglia sculpt postnatal neural circuits in an activity and complement-dependent manner. Neuron *74*, 691-705.

Schneider, A., Rajendran, L., Honsho, M., Gralle, M., Donnert, G., Wouters, F., Hell, S.W., and Simons, M. (2008). Flotillin-dependent clustering of the amyloid precursor protein regulates its endocytosis and amyloidogenic processing in neurons. J Neurosci *28*, 2874-2882.

Schroeter, E.H., Ilagan, M.X., Brunkan, A.L., Hecimovic, S., Li, Y.M., Xu, M., Lewis, H.D., Saxena, M.T., De Strooper, B., Coonrod, A.*, et al.* (2003). A presenilin dimer at the core of the gamma-secretase enzyme: insights from parallel analysis of Notch 1 and APP proteolysis. Proc Natl Acad Sci U S A *100*, 13075-13080.

Schweers, O., Schonbrunn-Hanebeck, E., Marx, A., and Mandelkow, E. (1994). Structural studies of tau protein and Alzheimer paired helical filaments show no evidence for beta-structure. J Biol Chem *269*, 24290-24297.

Selkoe, D., and Kopan, R. (2003). Notch and Presenilin: regulated intramembrane proteolysis links development and degeneration. Annu Rev Neurosci *26*, 565-597.

Selkoe, D.J. (2001). Alzheimer's disease: genes, proteins, and therapy. Physiol Rev *81*, 741-766.

Selkoe, D.J., and Hardy, J. (2016). The amyloid hypothesis of Alzheimer's disease at 25 years. EMBO Mol Med *8*, 595-608.

Serrano-Pozo, A., Frosch, M.P., Masliah, E., and Hyman, B.T. (2011). Neuropathological alterations in Alzheimer disease. Cold Spring Harb Perspect Med *1*, a006189.

Seyhan, A.A., and Rya, T.E. (2010). RNAi screening for the discovery of novel modulators of human disease. Curr Pharm Biotechnol *11*, 735-756.

Shen, J., and Kelleher, R.J., 3rd (2007). The presenilin hypothesis of Alzheimer's disease: evidence for a loss-of-function pathogenic mechanism. Proc Natl Acad Sci U S A *104*, 403-409.

Shibata, M., Yamada, S., Kumar, S.R., Calero, M., Bading, J., Frangione, B., Holtzman, D.M., Miller, C.A., Strickland, D.K., Ghiso, J.*, et al.* (2000). Clearance of Alzheimer's amyloid-ss(1-40) peptide from brain by LDL receptor-related protein-1 at the blood-brain barrier. J Clin Invest *106*, 1489-1499.

Sierra, A., Abiega, O., Shahraz, A., and Neumann, H. (2013). Janus-faced microglia: beneficial and detrimental consequences of microglial phagocytosis. Front Cell Neurosci *7*, 6.

Silverberg, G.D., Mayo, M., Saul, T., Rubenstein, E., and McGuire, D. (2003). Alzheimer's disease, normal-pressure hydrocephalus, and senescent changes in CSF circulatory physiology: a hypothesis. Lancet Neurol *2*, 506-511.

Sims, R., van der Lee, S.J., Naj, A.C., Bellenguez, C., Badarinarayan, N., Jakobsdottir, J., Kunkle, B.W., Boland, A., Raybould, R., Bis, J.C.*, et al.* (2017). Rare coding variants in PLCG2, ABI3, and TREM2 implicate microglial-mediated innate immunity in Alzheimer's disease. Nat Genet *49*, 1373-1384.

Sinha, S., Anderson, J.P., Barbour, R., Basi, G.S., Caccavello, R., Davis, D., Doan, M., Dovey, H.F., Frigon, N., Hong, J.*, et al.* (1999). Purification and cloning of amyloid precursor protein beta-secretase from human brain. Nature *402*, 537-540.

Sjogren, M., Vanderstichele, H., Agren, H., Zachrisson, O., Edsbagge, M., Wikkelso, C., Skoog, I., Wallin, A., Wahlund, L.O., Marcusson, J.*, et al.* (2001). Tau and Abeta42 in cerebrospinal fluid from healthy adults 21-93 years of age: establishment of reference values. Clin Chem *47*, 1776-1781.

Sleegers, K., Brouwers, N., Gijselinck, I., Theuns, J., Goossens, D., Wauters, J., Del-Favero, J., Cruts, M., van Duijn, C.M., and Van Broeckhoven, C. (2006). APP duplication is

sufficient to cause early onset Alzheimer's dementia with cerebral amyloid angiopathy. Brain *129*, 2977-2983.

Small, S.A., and Gandy, S. (2006). Sorting through the cell biology of Alzheimer's disease: intracellular pathways to pathogenesis. Neuron *52*, 15-31.

Small, S.A., Kent, K., Pierce, A., Leung, C., Kang, M.S., Okada, H., Honig, L., Vonsattel, J.P., and Kim, T.W. (2005). Model-guided microarray implicates the retromer complex in Alzheimer's disease. Ann Neurol *58*, 909-919.

Sobajima, T., Yoshimura, S., Iwano, T., Kunii, M., Watanabe, M., Atik, N., Mushiake, S., Morii, E., Koyama, Y., Miyoshi, E*., et al.* (2014). Rab11a is required for apical protein localisation in the intestine. Biol Open *4*, 86-94.

Sontag, E., Hladik, C., Montgomery, L., Luangpirom, A., Mudrak, I., Ogris, E., and White, C.L., 3rd (2004). Downregulation of protein phosphatase 2A carboxyl methylation and methyltransferase may contribute to Alzheimer disease pathogenesis. J Neuropathol Exp Neurol *63*, 1080-1091.

Sperling, R.A., Aisen, P.S., Beckett, L.A., Bennett, D.A., Craft, S., Fagan, A.M., Iwatsubo, T., Jack, C.R., Jr., Kaye, J., Montine, T.J*., et al.* (2011). Toward defining the preclinical stages of Alzheimer's disease: recommendations from the National Institute on Aging-Alzheimer's Association workgroups on diagnostic guidelines for Alzheimer's disease. Alzheimers Dement *7*, 280-292.

Sperling, R.A., Laviolette, P.S., O'Keefe, K., O'Brien, J., Rentz, D.M., Pihlajamaki, M., Marshall, G., Hyman, B.T., Selkoe, D.J., Hedden, T*., et al.* (2009). Amyloid deposition is associated with impaired default network function in older persons without dementia. Neuron *63*, 178-188.

Stalder, M., Deller, T., Staufenbiel, M., and Jucker, M. (2001). 3D-Reconstruction of microglia and amyloid in APP23 transgenic mice: no evidence of intracellular amyloid. Neurobiol Aging *22*, 427-434.

Stefani, A., Bernardini, S., Panella, M., Pierantozzi, M., Nuccetelli, M., Koch, G., Urbani, A., Giordano, A., Martorana, A., Orlacchio, A.*, et al.* (2005). AD with subcortical white matter lesions and vascular dementia: CSF markers for differential diagnosis. J Neurol Sci *237*, 83-88.

Stenmark, H., and Olkkonen, V.M. (2001). The Rab GTPase family. Genome Biol *2*, REVIEWS3007.

Sun, L., Zhou, R., Yang, G., and Shi, Y. (2017). Analysis of 138 pathogenic mutations in presenilin-1 on the in vitro production of Abeta42 and Abeta40 peptides by gamma-secretase. Proc Natl Acad Sci U S A *114*, E476-E485.

Szaruga, M., Munteanu, B., Lismont, S., Veugelen, S., Horre, K., Mercken, M., Saido, T.C., Ryan, N.S., De Vos, T., Savvides, S.N.*, et al.* (2017). Alzheimer's-Causing Mutations Shift Abeta Length by Destabilizing gamma-Secretase-Abetan Interactions. Cell *170*, 443-456 e414.

Szodorai, A., Kuan, Y.H., Hunzelmann, S., Engel, U., Sakane, A., Sasaki, T., Takai, Y., Kirsch, J., Muller, U., Beyreuther, K.*, et al.* (2009). APP anterograde transport requires Rab3A GTPase activity for assembly of the transport vesicle. J Neurosci *29*, 14534-14544.

Tarasoff-Conway, J.M., Carare, R.O., Osorio, R.S., Glodzik, L., Butler, T., Fieremans, E., Axel, L., Rusinek, H., Nicholson, C., Zlokovic, B.V.*, et al.* (2015). Clearance systems in the brain-implications for Alzheimer disease. Nat Rev Neurol *11*, 457-470.

Tarawneh, R., D'Angelo, G., Crimmins, D., Herries, E., Griest, T., Fagan, A.M., Zipfel, G.J., Ladenson, J.H., Morris, J.C., and Holtzman, D.M. (2016). Diagnostic and Prognostic Utility of the Synaptic Marker Neurogranin in Alzheimer Disease. JAMA Neurol *73*, 561-571.

Tcw, J., and Goate, A.M. (2017). Genetics of beta-Amyloid Precursor Protein in Alzheimer's Disease. Cold Spring Harb Perspect Med *7*.

Terry, R.D., Masliah, E., Salmon, D.P., Butters, N., DeTeresa, R., Hill, R., Hansen, L.A., and Katzman, R. (1991). Physical basis of cognitive alterations in Alzheimer's disease: synapse loss is the major correlate of cognitive impairment. Ann Neurol *30*, 572-580.

Tesco, G., Koh, Y.H., Kang, E.L., Cameron, A.N., Das, S., Sena-Esteves, M., Hiltunen, M., Yang, S.H., Zhong, Z., Shen, Y.*, et al.* (2007). Depletion of GGA3 stabilizes BACE and enhances beta-secretase activity. Neuron *54*, 721-737.

Thies, E., and Mandelkow, E.M. (2007). Missorting of tau in neurons causes degeneration of synapses that can be rescued by the kinase MARK2/Par-1. J Neurosci *27*, 2896-2907.

Thorsell, A., Bjerke, M., Gobom, J., Brunhage, E., Vanmechelen, E., Andreasen, N., Hansson, O., Minthon, L., Zetterberg, H., and Blennow, K. (2010). Neurogranin in cerebrospinal fluid as a marker of synaptic degeneration in Alzheimer's disease. Brain Res *1362*, 13-22.

Tian, Y., Chang, J.C., Fan, E.Y., Flajolet, M., and Greengard, P. (2013). Adaptor complex AP2/PICALM, through interaction with LC3, targets Alzheimer's APP-CTF for terminal degradation via autophagy. Proc Natl Acad Sci U S A *110*, 17071-17076.

Tosto, G., and Reitz, C. (2013). Genome-wide association studies in Alzheimer's disease: a review. Curr Neurol Neurosci Rep *13*, 381.

Truman, L.A., Ford, C.A., Pasikowska, M., Pound, J.D., Wilkinson, S.J., Dumitriu, I.E., Melville, L., Melrose, L.A., Ogden, C.A., Nibbs, R.*, et al.* (2008). CX3CL1/fractalkine is released from apoptotic lymphocytes to stimulate macrophage chemotaxis. Blood *112*, 5026-5036.

Tucker, H.M., Kihiko, M., Caldwell, J.N., Wright, S., Kawarabayashi, T., Price, D., Walker, D., Scheff, S., McGillis, J.P., Rydel, R.E.*, et al.* (2000). The plasmin system is induced by and degrades amyloid-beta aggregates. J Neurosci *20*, 3937-3946.

Turner, A.J., and Nalivaeva, N.N. (2007). New insights into the roles of metalloproteinases in neurodegeneration and neuroprotection. Int Rev Neurobiol *82*, 113-135.

Udayar, V., Buggia-Prevot, V., Guerreiro, R.L., Siegel, G., Rambabu, N., Soohoo, A.L., Ponnusamy, M., Siegenthaler, B., Bali, J., Aesg*, et al.* (2013). A paired RNAi and RabGAP overexpression screen identifies Rab11 as a regulator of beta-amyloid production. Cell Rep *5*, 1536-1551.

Vassar, R., Bennett, B.D., Babu-Khan, S., Kahn, S., Mendiaz, E.A., Denis, P., Teplow, D.B., Ross, S., Amarante, P., Loeloff, R., *et al.* (1999). Beta-secretase cleavage of Alzheimer's amyloid precursor protein by the transmembrane aspartic protease BACE. Science *286*, 735-741.

Vassar, R., Kovacs, D.M., Yan, R., and Wong, P.C. (2009). The beta-secretase enzyme BACE in health and Alzheimer's disease: regulation, cell biology, function, and therapeutic potential. J Neurosci *29*, 12787-12794.

Velliquette, R.A., O'Connor, T., and Vassar, R. (2005). Energy inhibition elevates beta-secretase levels and activity and is potentially amyloidogenic in APP transgenic mice: possible early events in Alzheimer's disease pathogenesis. J Neurosci *25*, 10874-10883.

von Arnim, C.A., Spoelgen, R., Peltan, I.D., Deng, M., Courchesne, S., Koker, M., Matsui, T., Kowa, H., Lichtenthaler, S.F., Irizarry, M.C., *et al.* (2006). GGA1 acts as a spatial switch altering amyloid precursor protein trafficking and processing. J Neurosci *26*, 9913-9922.

Wake, H., Moorhouse, A.J., Jinno, S., Kohsaka, S., and Nabekura, J. (2009). Resting microglia directly monitor the functional state of synapses in vivo and determine the fate of ischemic terminals. J Neurosci *29*, 3974-3980.

Walter, L., Franklin, A., Witting, A., Wade, C., Xie, Y., Kunos, G., Mackie, K., and Stella, N. (2003). Nonpsychotropic cannabinoid receptors regulate microglial cell migration. J Neurosci *23*, 1398-1405.

Wang, Y., Cella, M., Mallinson, K., Ulrich, J.D., Young, K.L., Robinette, M.L., Gilfillan, S., Krishnan, G.M., Sudhakar, S., Zinselmeyer, B.H., *et al.* (2015). TREM2 lipid sensing sustains the microglial response in an Alzheimer's disease model. Cell *160*, 1061-1071.

Watanabe, M., Fiji, H.D., Guo, L., Chan, L., Kinderman, S.S., Slamon, D.J., Kwon, O., and Tamanoi, F. (2008). Inhibitors of protein geranylgeranyltransferase I and Rab geranylgeranyltransferase identified from a library of allenoate-derived compounds. J Biol Chem *283*, 9571-9579.

Weingarten, M.D., Lockwood, A.H., Hwo, S.Y., and Kirschner, M.W. (1975). A protein factor essential for microtubule assembly. Proc Natl Acad Sci U S A *72*, 1858-1862.

Weller, R.O., Subash, M., Preston, S.D., Mazanti, I., and Carare, R.O. (2008). Perivascular drainage of amyloid-beta peptides from the brain and its failure in cerebral amyloid angiopathy and Alzheimer's disease. Brain Pathol *18*, 253-266.

Wellington, H., Paterson, R.W., Portelius, E., Tornqvist, U., Magdalinou, N., Fox, N.C., Blennow, K., Schott, J.M., and Zetterberg, H. (2016). Increased CSF neurogranin concentration is specific to Alzheimer disease. Neurology *86*, 829-835.

Wen, L., Tang, F.L., Hong, Y., Luo, S.W., Wang, C.L., He, W., Shen, C., Jung, J.U., Xiong, F., Lee, D.H.*, et al.* (2011). VPS35 haploinsufficiency increases Alzheimer's disease neuropathology. J Cell Biol *195*, 765-779.

Willem, M., Garratt, A.N., Novak, B., Citron, M., Kaufmann, S., Rittger, A., DeStrooper, B., Saftig, P., Birchmeier, C., and Haass, C. (2006). Control of peripheral nerve myelination by the beta-secretase BACE1. Science *314*, 664-666.

Winblad, B., Amouyel, P., Andrieu, S., Ballard, C., Brayne, C., Brodaty, H., Cedazo-Minguez, A., Dubois, B., Edvardsson, D., Feldman, H.*, et al.* (2016). Defeating Alzheimer's disease and other dementias: a priority for European science and society. Lancet Neurol *15*, 455-532.

Wisniewski, T., Ghiso, J., and Frangione, B. (1997). Biology of A beta amyloid in Alzheimer's disease. Neurobiol Dis *4*, 313-328.

Wolfe, M.S. (2008). Inhibition and modulation of gamma-secretase for Alzheimer's disease. Neurotherapeutics *5*, 391-398.

Wong, E.S., Tan, J.M., Soong, W.E., Hussein, K., Nukina, N., Dawson, V.L., Dawson, T.M., Cuervo, A.M., and Lim, K.L. (2008). Autophagy-mediated clearance of aggresomes is not a universal phenomenon. Hum Mol Genet *17*, 2570-2582.

Xie, L., Kang, H., Xu, Q., Chen, M.J., Liao, Y., Thiyagarajan, M., O'Donnell, J., Christensen, D.J., Nicholson, C., Iliff, J.J., *et al.* (2013). Sleep drives metabolite clearance from the adult brain. Science *342*, 373-377.

Yamada, K., Holth, J.K., Liao, F., Stewart, F.R., Mahan, T.E., Jiang, H., Cirrito, J.R., Patel, T.K., Hochgrafe, K., Mandelkow, E.M., *et al.* (2014). Neuronal activity regulates extracellular tau in vivo. J Exp Med *211*, 387-393.

Yan, P., Hu, X., Song, H., Yin, K., Bateman, R.J., Cirrito, J.R., Xiao, Q., Hsu, F.F., Turk, J.W., Xu, J., *et al.* (2006). Matrix metalloproteinase-9 degrades amyloid-beta fibrils in vitro and compact plaques in situ. J Biol Chem *281*, 24566-24574.

Yan, R., Bienkowski, M.J., Shuck, M.E., Miao, H., Tory, M.C., Pauley, A.M., Brashier, J.R., Stratman, N.C., Mathews, W.R., Buhl, A.E., *et al.* (1999). Membrane-anchored aspartyl protease with Alzheimer's disease beta-secretase activity. Nature *402*, 533-537.

Young, J.E., Fong, L.K., Frankowski, H., Petsko, G.A., Small, S.A., and Goldstein, L.S.B. (2018). Stabilizing the Retromer Complex in a Human Stem Cell Model of Alzheimer's Disease Reduces TAU Phosphorylation Independently of Amyloid Precursor Protein. Stem Cell Reports *10*, 1046-1058.

Yu, W.H., Cuervo, A.M., Kumar, A., Peterhoff, C.M., Schmidt, S.D., Lee, J.H., Mohan, P.S., Mercken, M., Farmery, M.R., Tjernberg, L.O., *et al.* (2005). Macroautophagy--a novel Beta-amyloid peptide-generating pathway activated in Alzheimer's disease. J Cell Biol *171*, 87-98.

Yuyama, K., Yamamoto, N., and Yanagisawa, K. (2008). Accelerated release of exosome-associated GM1 ganglioside (GM1) by endocytic pathway abnormality: another putative pathway for GM1-induced amyloid fibril formation. J Neurochem *105*, 217-224.

Zahraoui, A., Touchot, N., Chardin, P., and Tavitian, A. (1989). The human Rab genes encode a family of GTP-binding proteins related to yeast YPT1 and SEC4 products involved in secretion. J Biol Chem *264*, 12394-12401.

Zetterberg, H., Blennow, K., and Hanse, E. (2010). Amyloid beta and APP as biomarkers for Alzheimer's disease. Exp Gerontol *45*, 23-29.

Zhan, Y., Paolicelli, R.C., Sforazzini, F., Weinhard, L., Bolasco, G., Pagani, F., Vyssotski, A.L., Bifone, A., Gozzi, A., Ragozzino, D.*, et al.* (2014). Deficient neuron-microglia signaling results in impaired functional brain connectivity and social behavior. Nat Neurosci *17*, 400-406.

Zhang, S., Salemi, J., Hou, H., Zhu, Y., Mori, T., Giunta, B., Obregon, D., and Tan, J. (2010). Rapamycin promotes beta-amyloid production via ADAM-10 inhibition. Biochem Biophys Res Commun *398*, 337-341.

Zhao, J., Fu, Y., Yasvoina, M., Shao, P., Hitt, B., O'Connor, T., Logan, S., Maus, E., Citron, M., Berry, R.*, et al.* (2007). Beta-site amyloid precursor protein cleaving enzyme 1 levels become elevated in neurons around amyloid plaques: implications for Alzheimer's disease pathogenesis. J Neurosci *27*, 3639-3649.

Zhao, Z., Sagare, A.P., Ma, Q., Halliday, M.R., Kong, P., Kisler, K., Winkler, E.A., Ramanathan, A., Kanekiyo, T., Bu, G.*, et al.* (2015). Central role for PICALM in amyloid-beta blood-brain barrier transcytosis and clearance. Nat Neurosci *18*, 978-987.

Zlokovic, B.V. (2004). Clearing amyloid through the blood-brain barrier. J Neurochem *89*, 807-811.

Zlokovic, B.V. (2011). Neurovascular pathways to neurodegeneration in Alzheimer's disease and other disorders. Nat Rev Neurosci *12*, 723-738.

Originality Report

This thesis was tested for plagiarism with Plagscan, from the access provided by University of Zurich. The prior published papers, bibliographies and materials and methods were removed before scan.

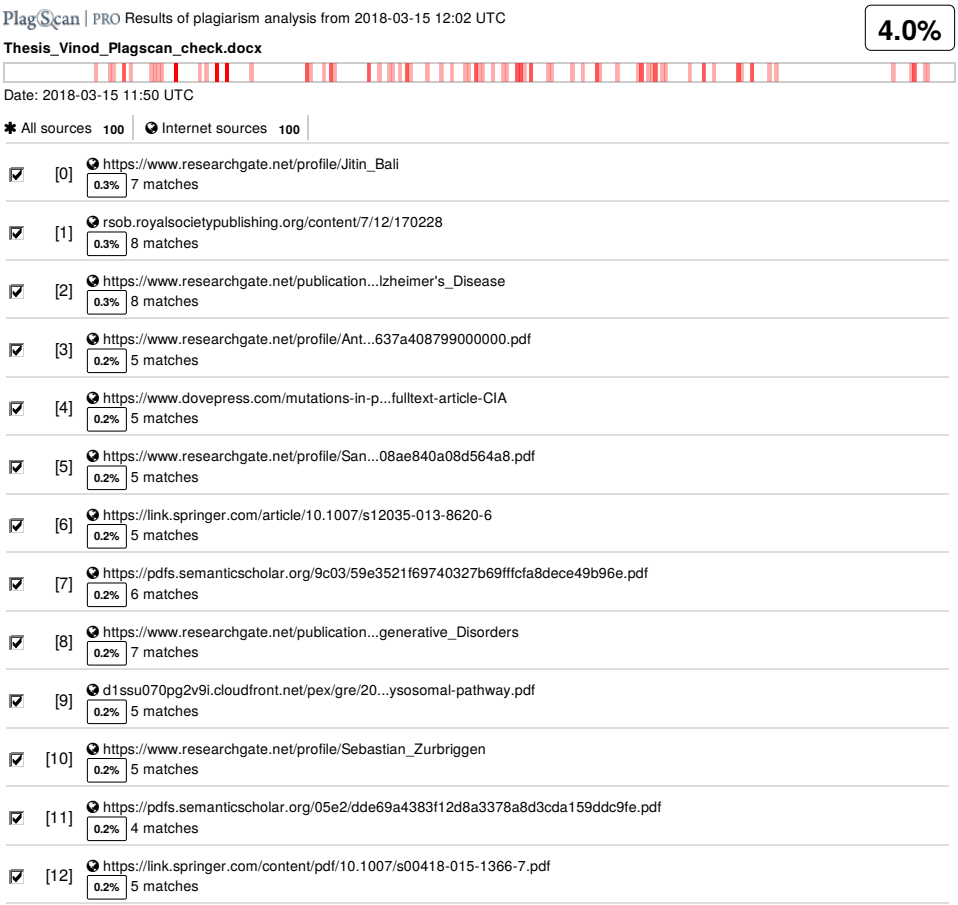

PlagScan | PRO Results of plagiarism analysis from 2018-03-15 12:02 UTC

4.0%

Thesis_Vinod_Plagscan_check.docx

Date: 2018-03-15 11:50 UTC

✱ All sources 100 | Internet sources 100

☑	[0]	https://www.researchgate.net/profile/Jitin_Bali	0.3% 7 matches
☑	[1]	rsob.royalsocietypublishing.org/content/7/12/170228	0.3% 8 matches
☑	[2]	https://www.researchgate.net/publication...lzheimer's_Disease	0.3% 8 matches
☑	[3]	https://www.researchgate.net/profile/Ant...637a408799000000.pdf	0.2% 5 matches
☑	[4]	https://www.dovepress.com/mutations-in-p...fulltext-article-CIA	0.2% 5 matches
☑	[5]	https://www.researchgate.net/profile/San...08ae840a08d564a8.pdf	0.2% 5 matches
☑	[6]	https://link.springer.com/article/10.1007/s12035-013-8620-6	0.2% 5 matches
☑	[7]	https://pdfs.semanticscholar.org/9c03/59e3521f69740327b69fffcfa8dece49b96e.pdf	0.2% 6 matches
☑	[8]	https://www.researchgate.net/publication...generative_Disorders	0.2% 7 matches
☑	[9]	d1ssu070pg2v9i.cloudfront.net/pex/gre/20...ysosomal-pathway.pdf	0.2% 5 matches
☑	[10]	https://www.researchgate.net/profile/Sebastian_Zurbriggen	0.2% 5 matches
☑	[11]	https://pdfs.semanticscholar.org/05e2/dde69a4383f12d8a3378a8d3cda159ddc9fe.pdf	0.2% 4 matches
☑	[12]	https://link.springer.com/content/pdf/10.1007/s00418-015-1366-7.pdf	0.2% 5 matches

Acknowledgements

As I walk towards an important personal milestone I would like to take a moment to express my gratitude and appreciation to several wonderful people that have helped me and made this journey a memorable one.

I begin by expressing my sincerest gratitude to my supervisor, Prof. Lawrence Rajendran. I cannot thank him enough for giving me the opportunity to come and do great science in a top-tier University. I would like to thank him for his constant support, mentorship and teaching. I value and appreciate his creative thoughts and deep scientific insights. These are qualities that I would like to cultivate as a scientist and I feel lucky to have got such an opportunity. Thank you so much Lawrie!

I would like to say thank you to my committee members, Prof Martin Schwab and Prof. Esther Stoeckli for their scientific advice and support. I would like to say thank you to Prof. Roger Nitsch and Prof. Christoph Hock for their advice and support. I would also like to say thank you to Dr. Cornelia Marty and Sebi Zurbriggen for all their help during the first years of my PhD. Thank you to all the members of IREM past and present alike. I also express my sincere gratitude to Dr. S. Vijayalakshmi for all her support and encouragement.

PhD would not have been as much fun if not for the support and company of my wonderful labmates, past and current. I would like to say special thank you to Gabi, Rosa, Saoussen, Mrityunjoy, Andrea, Fatma and Walther. You are the best labmates!

I would like to say a big thank you to all my friends for making this an enjoyable experience. Special thank you to Julian, Laura, Manuel, Patrick and Berni for the great friendship!

And last but never the least, I would like to express my love and gratitude to my family, my close friends and Anais. Thank you so much!

Curriculum vitae

Personal details

Name:	Vinod Udayar
Date of Birth:	October 20, 1986
Nationality:	Indian

Education

2002-2004	Higher Secondary school Certificate (HSC) G. N. Khalsa College, Mumbai, India
09/2004 - 05/2008	Bachelor of Technology in Biotechnology Specialization: Biochemistry, cell and molecular biology. YCMO University, Mumbai, India
08/2008 - 05/2010	Master of Technology in Biotechnology Specialization: Medical Biotechnology SRM University, Chennai, India Master thesis: Role of SPR3 in septogenesis in *E.ashbyii*
08/2011 – present	Doctoral Thesis, University of Zurich (Switzerland) Thesis: Membrane Trafficking Pathways in the Production and Clearance of the Alzheimer's Disease Aβ Peptide in Neurons and in Microglia